Mechanistic Insights Into Novel Cellular Therapy Strategies for The Treatment of Corneal Allograft Rejection

A thesis submitted to the National University of Ireland Galway as fulfilment of the requirement for the degree of

Doctor of Philosophy

By

Kevin Lynch B.A (Mod), M.Sc

Regenerative Medicine Institute (REMEDI),
College of Medicine, Nursing & Health Sciences,
National University of Ireland, Galway

Thesis Supervisors:

Professor Thomas Ritter

Dr Aideen Ryan

Date of Submission: 17/07/18

Table of Content

CONTENTS

Declaration

I declare that the work submitted presented herein describes work that was performed personally for this thesis. Where other individuals have aided has been stated appropriately. This work was performed between 2014 and 2018 at the Regenerative Medicine Institute, National University of Ireland, Galway. This work was supervised and mentored by Professor Thomas Ritter.

The work described within this thesis has not been submitted for degree, diploma or other qualification at any other University. I have no conflict of interest pertaining to the subject matter of this work.

Acknowledgments

Firstly, I would like to acknowledge both of my supervisors, Prof. Thomas Ritter and Dr Aideen Ryan. Thank you for giving me the opportunity to pursue a PhD and for mentoring and guiding my development as a researcher, for this I will always be grateful. I am looking forward to continuing our research and developing my skills further under your guidance and tutelage.

To Dr Oliver Treacy, who has contributed to every aspect of this study, I am eternally grateful for your time, advice and patience. Thank you for advising me when times were tough and for reassuring me in my times of doubt. You have been a true friend.

To Dr Nick Murphy, my bother in arms! Our non-PhD related intellectual debates over the years have made me reassess my thinking and how I approach breaking down an argument, a thought or an idea. I am a better person because of it, thank you.

To Dr Paul Lohan, for helping me every Friday for a whole year, for teaching me tissue culture, flow cytometry and many other techniques. Your willingness to help is a testament to who you are as a person. You've given me some of the best advice of the last four years. I've really appreciated it Paul, thank you.

To Dr Grace O'Malley! Your intelligence, humour and wit always made conversations interesting and entertaining. Thank you for listening to my endless droning about competitive gaming, mixed martial arts and their participants. (262 strong as of writing this!).

To Dr Serika Naicker, for the "lols and or bants", to Dr Tomas Griffin for being the devil's advocate, to Dr Joana Cabral, Dr Andreia Riberiro, Dr Nahidul Islam and Dr Conor Hennessy for your help, knowledge and support over the years. Your friendship has been invaluable. A special mention to both Niamh Leonard and Hannah Egan for helping me with all the undergrad students we had during the writing of this document.

To Prof. Matt Griffin, your insight and knowledge over the years has made me a significantly better researcher. Also, your enthusiasm for research has motivated me over the years, thank you.

To my friends, Andre, Colm, Liam, Mickey, Brenden, Sam, Aidan, Peter, Robert, Frankie, Steven, Keith, Danny, Taylor and Chris. Thank you for friendship over the years and showing me what is important in life. A special mention to Andre and Colm. To Andre, thank you for the years of music, you are an incredible mind and your outlook on life always inspires me. Now that I have a bit of free time we can finally write that album. To Colm, my oldest friend of 26 years, I have considered you my brother since we were children, thank you for all your advice, we've been through a lot together and have grown because of it. Thanks brother.

Thank you to my family, to my mother Marie, my father Michael, my two bothers Conor and Ciaran. To my sister in law Michelle and the three kids Cara, Oran and Rian! A special mention to Michelle, who always keeps me updated on the kids via whatsapp during my busy times.

To Niamh, my best friend and my partner of 12 years, to whom this work is dedicated to. I don't know where I would be without you. I look forward to the years to come, the home we will build and the family we will create. To put it perfectly, "You're my safe harbour in an endless stormy sea. You're my shady willow on a sunny day. You're sweet music in a distant room. You're unexpected cake on a rainy day. You're my bright penny on the roadside, you are worth more than the moon on the long night walk. You are sweet wine in my mouth, a song in my throat and laughter in my heart." Thank you.

Finally, to Niamh's parents Geraldine and Matthew, thank you so much for all the help you have given me over the years, it has been much appreciated.

Abstract

It has previously been demonstrated by our lab that tolerogenic dendritic cells (tDCs) prolong corneal allograft survival. This study revealed that tDCs had significantly higher levels of sialic acid on the cell surface compared to immature DCs (iDCs). The first part of this work focused on investigating how the generation of tDCs by dexamethasone changed the glycosylation profile of tDCs. Dendritic cellular therapies and dendritic cell vaccines show promise for the treatment of autoimmune diseases, the prolongation of graft survival in transplantation and in educating the immune system to fight cancers. Cell surface glycosylation plays a crucial role in the cell-cell interaction, uptake of antigens, migration, and homing of DCs. Glycosylation is known to change with environment and the functional state of DCs. tDCs are commonly generated using corticosteroids including dexamethasone, however, to date little is known on how corticosteroid treatment alters glycosylation and what functional consequences this may have. Here, we present a comprehensive profile of rat bone marrow derived dendritic cells, examining their cell surface glycosylation profile before and after Dexa treatment as resolved by both lectin microarrays and lectin-coupled flow cytometry. We further examine the functional consequences of altering cell surface glycosylation on immunogenicity and tolerogenicity of DCs. Dexa treatment of rat DCs leads to profoundly reduced expression of markers of immunogenicity (MHC I/II, CD80, CD86) and pro-inflammatory molecules (IL-6, IL-12p40, iNOS) indicating a tolerogenic phenotype. Moreover, by comprehensive lectin microarray profiling and flow cytometry analysis we show that sialic acid (Sia) is significantly up regulated on tDCs after Dexa treatment and that this may play a vital role in the therapeutic attributes of these cells. Interestingly, removal of Sia by neuraminidase treatment increases the immunogenicity of iDCs and also leads to increased expression of pro-inflammatory cytokines while tDCs are protected from this increase in immunogenicity. These findings may have important implications in strategies aimed at increasing tolerogenicity where it is advantageous to reduce immune activation over prolonged periods. These findings are also relevant in therapeutic strategies aimed at increasing the immunogenicity of cells, for example, in the context of tumour specific immunotherapies.

It has previously been demonstrated by our lab that the i.v. infusion of allogeneic MSCs prolong corneal allograft survival, however, syngeneic MSCs fail to do so. The

second part of this study focused on the optimisation of a pre-activation strategy to enhance the immunomodulatory properties of syngeneic MSCs. While TNF-α + IL-1β MCSs showed enhanced potency *in vitro*, they were not successfully in prolonging corneal allograft survival. It was determined that TGF-β1 pre-activated MSCs (TGF-β MSCs) were the most potently immunosuppressive. TGF-β MSCs potently suppress both $CD4^+$ and $CD8^+$ proliferation, increase the numbers of Tregs in co-cultures and significantly modulated MHC I, MHC II, CD80 and CD86 on activated macrophages. Further characterisation of TGF-β MSCs demonstrated increased expression of CD73 on the cell surface with increases in mRNA for *ptgs2* (*Cox2*) and in addition increased levels of PGE2 were detected in the supernatants of T lymphocyte co-cultures. As a result, TGF-β MSCs were chosen for *in vivo* administration.

The third part of this study focused on how *in vitro* pre-activated TGF-β MSCs prolonged rejection free survival of corneal allografts after administration. TGF-β MSC treated animals presented with a survival rate of 70% (n=13) compared to 25% (n=14) in the untreated MSC group. Prolongation of graft survival was associated with; (i)increased Treg populations in the draining lymphocyte nodes (DLNs) and lungs of TGF-β MSC treated animals, (ii) increases in regulatory B cell populations in the DLNs and spleens of TGF-β MSC treated animals and (iii) decreases in APC populations in the DLNs, lungs and spleens of TGF-β MSC treated animals. Finally, we confirmed that TGF-β MSCs mediated their effects via canonical SMAD2/3 signalling, that the potent immunosuppressive effects mediated by TGF-β MSCs was contact dependent and that CD73 and more significantly PGE2 (via EP4) play a vital role in TGF-β MSC mediated immunosuppression of T lymphocytes.

In summary, this study demonstrates that TGF-β enhances the ability of syngeneic MSCs to prolong corneal allograft survival. *In vivo*, TGF-β MSC therapy was associated with increased proportion of regulatory cells which resulted in prolongation of graft survival. The results in this study point toward PGE2 as the main mediator of TGF-β MSC immunosuppression. Therefore, this study identifies the anti-inflammatory cytokine TGF-β as a pre-activation strategy to enhance syngeneic MSC therapy in the treatment of allogeneic tissue transplantation.

List of Figures

Chapter 1:

Chapter 2:

Chapter 3:

List of Tables

Abbreviations

αMSH	α-Melanocyte-stimulating hormone
ACAID	Anterior chamber associated immune deviation
ACK	Ammonium chloride potassium
ANOVA	Analysis of variance
APC	Antigen presenting cell
AH	Aqueous humour
BMDM	Bone marrow derived macrophage
BSA	Bovine serum albumin
CFSE	Carboxyfluorescein succinimidyl ester
CFU-F	Colony forming unit fibroblast
CGRP	Calcitonin gene-related peptide
CsA	Cyclosporine A
CTL	Cytotoxic T lymphocyte
DA	Dark Agouti
DAMP	Danger associated molecular pattern
dLN	Draining lymph node
DPBS	Dulbecco's phosphate buffered saline
DTH	Delayed type hypersensitivity
DC	Dendritic cell
EDTA	Ethylenediaminetetraacetic acid
ELISA	Enzyme-linked immunosorbent assay
eNOS	Endothelial nitric oxide synthase

FACS	Fluorescence-activated sorting
FMO	Fluorescence minus one
GAPDH	Glyceraldehyde 3-phosphate dehydrogenase
GM-CSF	Granulocyte-macrophage colony-stimulating factor
GPI	Glycosylphosphatidylinositol
GvHD	Graft versus host disease
HBSS	Hank’s balanced salt solution
HCL	Hydrogen chloride
HGF	Hepatocyte growth factor
HLA	Human leukocyte antigen
HO	Heme oxygenase
HSV	Herpes simplex virus
ICAM-1	Intercellular Adhesion Molecule 1
iDC	Immature Dendritic Cell
IDO	Indoleamine-pyrrole 2,3-dioxygenase
IFN-γ	Interferon gamma
IL-1RA	Interleukin-1 receptor antagonist
IL-1β	Interleukin-1 beta
iNOS	Inducible nitric oxide synthase
I.v.	Intravenous
KO	Knock out
LB	Luria broth
LPS	Lipopolysaccharide

mDC	Mature dendritic cell
MDSCs	Myeloid-derived suppressor cells
MFI	Median fluorescent intensity
MHC	Major histocompatibility complex
MIF	Macrophage migration inhibitory factor
MMP	Metalloproteinase
mRNA	Messenger RNA
MSC	Mesenchymal stem cell
NK	Natural killer cell
NKT	Natural killer T cell
nNOS	Neuronal nitric oxide synthase
NO	Nitric oxide
PAMPs	Pattern associated molecular pattern
PD-1	Programmed cell death protein
PDL1	Programmed death ligand 1
PGE2	Prostaglandin E2
PI	Propidium iodide
POD	Post-operative day
RMA	Robust Multi-array Average
RFI	Relative fluorescent intensity
RFS	Rejection free survival
SCID	Severe combined immunodeficiency
SEM	Standard error mean

SIA	Sialic Acid
SLE	Systemic lupus erythematosus
SMT	S-methylisothiourea
tDC	Tolerogenic dendritic cell
TCM	T cell media
TCR	T cell receptor
TGF-β MSC	TGF-β stimulated MSCs
TGFβ	Transforming growth factor β
Th1	Type 1 T helper cell
Th2	Type 2 T helper cell
TLR	Toll like receptor
TOR	Timepoint of rejection
Treg/s	Regulatory T cell
TNF-α	Tumour necrosis factor alpha
TNF-α + IL-1β MSC	TNF-α/IL-1β stimulated MSC
TRAIL	TNF-related apoptosis-inducing ligand
TSG-6	Tumor necrosis factor-inducible gene 6 protein
VCAM-1	Vascular adhesion molecule 1
VEGF	Vascular endothelial growth factor

Chapter One:

Introduction

1.1 The Cornea

1.1.1 Anatomy and Function of The Cornea

The cornea is a transparent layer positioned at the anterior part of the eye. The cornea has two main functions, firstly it acts as a physical barrier to foreign particles or pathogenic microbes and secondly it is essential for focusing light onto the retina at the posterior part of the eye producing the image [1, 2].

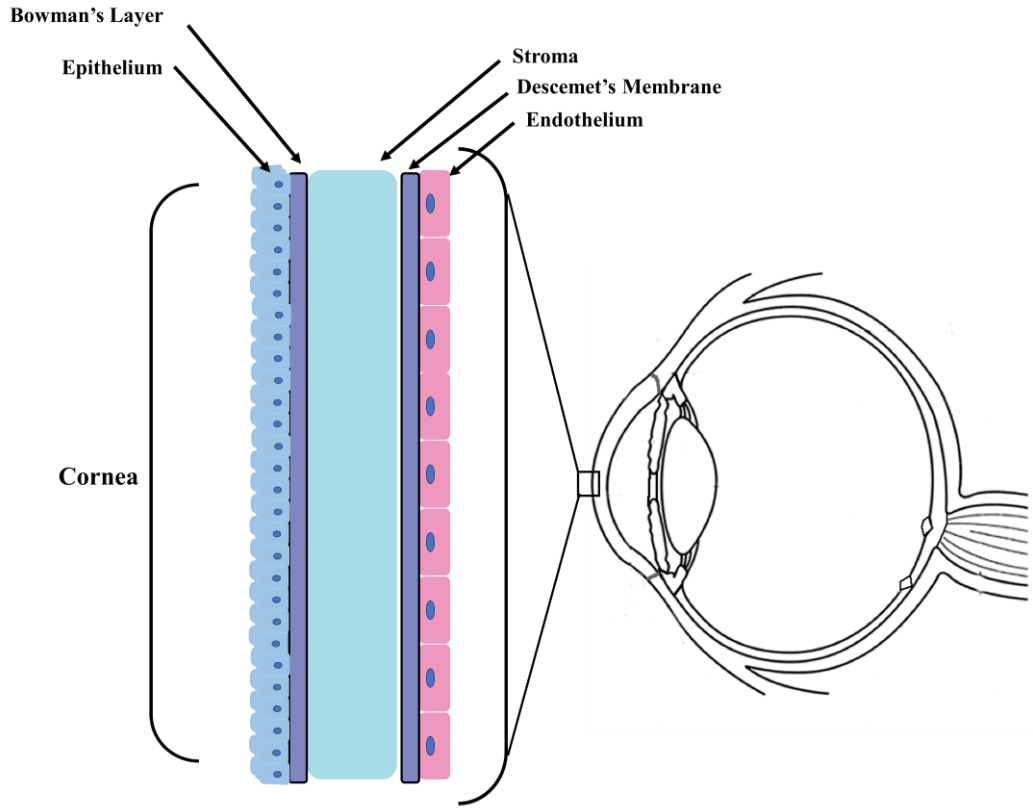

Figure 1.1: Anatomy of the eye and cornea. |

As demonstrated in **Figure 1.1** the cornea consists of five different layers, three cellular layers known as the epithelium, the stroma and endothelium and two membrane layers known as the Bowman's layer and Descemet's membrane [2, 3]. The epithelium sits atop the Bowman's layer and here it acts as a physical barrier to the outside environment, as a result, its cells are constantly proliferating to replace damaged and dying cells. A tear film containing both IgA and lysozyme is present in the epithelium to protect the cells from microbes, but also to provide factors which are known to aid the proliferation and repair of the epithelial layer [1, 4, 5]. As mentioned, Bowman's layer lies under the epithelium layers, is acellular, and it consists solely of

irregularly ordered collagen fibres. The next layer of the cornea is the stroma, that lies between two acellular membranes and is formed of tightly packed aligned collagen. As a result of the thick collagen fibres, the stroma is the thickest layer of the cornea and houses keratocytes, cells capable of repair following insult or injury. The Descemet's layer, which lies on top of the endothelium is secreted by the endothelial monolayer. The endothelial monolayer is the final layer of the cornea, is made up of a single layer of polygon-shaped cells which form the barrier between the cornea and the anterior chamber of the eye. The endothelial layer is vital to the maintenance of corneal function as it supplies nutrients from the aqueous humour and it also protects the stroma from damage by pumping out excess stromal fluid. This process which is very important after surgery due to post-operative inflammation [2-4, 6, 7]. The endothelium does not have the ability to regenerate and has been shown not to have mitotic capabilities *in vivo*. This can result in dysfunctional fluid regulation. Donor epithelium, stroma and endothelium are all susceptible to immune rejection after transplantation. However, it is worth noting that the epithelial layer can be restored by the recipient's cells and treatment of the graft with topical corticosteroids can alleviate stromal damage. However, due to the attributes of the endothelium damage caused by immune rejection cannot be repaired making the latter the most susceptible during transplantation [1, 7-9].

1.1.2 Immune Privilege of the Eye

The eyes, like the brain and testes are well-defined immune privileged organs [10-16]. Immune privilege was first coined by Medawar in 1948 upon discovering that skin allografts transplanted to the eye or the brain did not undergo immune-mediated rejection [17]. An immune privileged tissue is one that can be transplanted to an allogeneic recipient and can survive for extended periods of time without immunosuppressive intervention [18]. As stated previously, the endothelium does not have the ability to regenerate, this also applies to the retina, therefore preservation and protection of the ocular tissues is essential for preserving vision. Ocular inflammatory processes in response to ocular damage or infection may lead to damage of the endothelium or the retina leading to blindness. Therefore, the microenvironment of the eye must be held in a state of homeostasis where immune-mediated inflammation responses are controlled to limit damage to these vital tissues and maintain optimum vision [4, 19]. The maintenance of immune privilege has been widely studied and it is

now accepted that immune privilege of the cornea is a complex process involving physiological, anatomical and immunological processes [20]. Maintenance of immune privilege is achieved by inhibition of both the afferent and efferent arms of the immune system which will be discussed in detail below.

1.1.3 Maintenance of Immune Privilege in the Cornea

Blockade of the afferent arm of the immune system is vital in maintaining immune privilege of the cornea. The avascular structure of the cornea plays a vital role in its immune privilege. The avascular status reduces the presence of antigen presenting cells (APCs) and thus, antigen presentation by the lymphatic drainage pathway. The lack of blood vessels inhibits effector cell infiltration as they are unable to migrate to the cornea [21]. Both of these characteristics are particularly relevant in human/mouse corneal transplantation, exemplified by reduced success rates in transplantations where pre-existing or secondary neovascularization was present before the transplant [21, 22]. The epithelial cells of the cornea play a vital role in maintaining the avascular structure due the expression of vascular endothelial growth factor receptor 1 (VEGFR-1) which sequesters vascular endothelial growth factor A (VEGF-A) a pro-angiogenic factor. The keratocytes and corneal epithelial cells also sequester vascular endothelial growth factor C (VEGFR-C), a factor which promotes lymphangiogenesis by expressing vascular endothelial growth factor receptor 2 (VEGFR-2) [23, 24]. Endostatin is another anti-angiogenic factor which is expressed in the cornea and it is known to prevent both lymphangiogenesis and hemangiogenesis contributing to the immune privilege of the cornea [21]. As mentioned, the migration of APCs is restricted in the cornea due to its avascular nature and as a result there are very few bone marrow derived APCs present in the cornea [25, 26]. Not only this, but resident Langerhans cells and stromal DCs have been shown to have an immature phenotype lacking expression of major histocompatibility complex II (MHC II) and co-stimulatory molecules CD80 and CD86 [27].

The immune privileged status of the cornea is further protected by the blood-ocular barrier. This consists of the blood-aqueous barrier and the blood-retinal barrier. The blood-aqueous barrier is located at the anterior of the eye and the blood-retinal barrier is located at the posterior of the eye. Both cell barriers consist of tight junctions located between epithelial cells and endothelial cells, and immune cells are required to pass through them in order to gain access to the eye [28, 29]. The cells that make up these

barriers constitutively express CD86 which binds cytotoxic T-lymphocyte antigen (CTLA)-4 on the surface of T lymphocytes resulting in the inhibition of interferon-gamma (IFN-γ) production, inhibition of T lymphocyte proliferation and the induction of the regulatory T lymphocyte (Treg) phenotype. This was demonstrated by the reversal of inhibition of T lymphocyte proliferation and activation in CD86 or CTLA4 knockout animal models [30].

Blockade of the efferent arm is also vital in maintaining the immune privilege status of the cornea. Griffith *et al* [31] demonstrated that there are multiple ocular cells, including both corneal epithelium and endothelium, that express first apoptosis signal ligand (FasL), which is a ligand that induces apoptosis in cells which have the corresponding receptor Fas. Griffith *et al* also demonstrated that both neutrophils and activated T cells are susceptible to induced apoptosis via FasL expressed on ocular cells [31]. The importance of FasL has been demonstrated by experiments where approximately 50% of the corneal grafts from donor mice that express FasL on both corneal epithelium and endothelium experienced long-term survival [32-34] whereas rejection occured in 89–100% of the corneal grafts donated from FasL knockout mice [32-34]. Two other inhibitory factors that are expressed on the cells of the cornea are programmed death ligand-1 (PD-L1), and tumour necrosis factor-related apoptosis inducing ligand (TRAIL) [31, 35, 36] These inhibitory factors interact with receptors on the surface of effector $CD4^+$ T lymphocytes leading to the inhibition of T lymphocyte proliferation, IFN-γ production and induction of apoptosis [35, 37].

One of the pioneering observations in ocular immunology made by Medawar *et al* was that the introduction of foreign antigen into the eye where an established effector immune response was already active does not elicit a further inflammatory response [17, 33]. This is partially due to the ocular microenvironment itself and it is partially mediated by soluble molecules present in the aqueous humour. The aqueous humour is a transparent plasma-like fluid which is secreted from the ciliary epithelium lining and it occupies both the anterior and posterior chambers of the eye [38]. The aqueous humour's immunomodulatory environment consists of many different factors such as transforming growth factor beta (TGF-β), FasL, macrophage migration inhibitory factor (MIF), vasoactive intestinal peptide (VIP), CD59, and complement regulatory protein (CRP) which can inhibit complement-mediated cytolysis [4, 10, 39, 40].

Each of the different molecules of aqueous humour target different cells of the immune response and different activities [14, 15]. For example, factors such as the neuropeptide α-melanocyte-stimulating hormone (α-MSH) and TGF-β2 can induce $CD4^+FoxP3^+$ Tregs in the aqueous humour mainly through the activation of suppressive APCs that convert effector T lymphocytes to Tregs [14, 15, 41-43]. Considering that an effector response is already active in these studies and that these effector populations are being re-educated to suppressive populations, it could be said that immune privilege is maybe more than just suppressing inflammation and elucidating as to how this balance is maintained could be exploited to induce tolerance via cellular therapies.

Kaplan *et al* demonstrated that the introduction of allogeneic MHC-mismatched tumour cells into the anterior chamber of the eye resulted in subsequent skin graft acceptance in mice. Mice that received said tumour cells under the skin before undergoing skin transplantation rejected both the injection of cells and rejected 100% of the skin grafts [44, 45]. This induction of tolerance was termed anterior chamber-associated immune deviation (ACAID) as it was considered a deviation from the expected hypersensitivity immune response [15]. ACAID-like responses have also been reported when foreign antigen is placed in the subretinal space or the vitreous [46-48]. ACAID is antigen specific as it inhibits the activation of antigen specific T lymphocytes that are reactive to the injected antigen. This antigen specificity is dependent on $F4/80^+$ macrophages of the spleen [49, 50]. Interestingly, this effect can be mimicked *in vitro*, if aqueous humour or TGF-β2 is cultured with macrophages in the presence of antigen, the macrophages can be converted into tolerogenic APCs [51-54]. After antigen uptake, the APCs in the ocular microenvironment leave the eye and migrate towards the marginal zones of the spleen, where multiple cell interactions occur [15]. The APCs form cell clusters with $CD4^+$, $CD8^+$ and natural killer T cells (NKT) [55], but also with B lymphocytes that are capable of taking the antigen directly from the APCs and presenting it themselves [56]. The APCs stimulate the NKT cells to secrete chemokine (C-C motif) ligand 5 (CCL5), this in turn attracts $CD8^+$ lymphocytes and results in the induction and expansion of antigen-specific suppressor CD8+ T lymphocytes [55, 57] and these cells have been shown to prevent rejection of the graft [58-60].

In summary, the immune privileged status of the eye is maintained by a combination of physical barriers; the presence of immunosuppressive molecules within the aqueous humour that modulate resident immune cells; and finally, by ACAID, which induces systemic tolerance to ocular antigens.

1.2 Cornea Transplantation (Penetrating Keratoplasty)

Corneal transplantation was first proposed in 1797, but over a century passed before the first human corneal transplant was successfully performed by Eduard Zirm in 1905. The cornea is the most commonly transplanted tissue in humans with 100,000 procedures being carried out each year. Historically, penetrating keratoplasty was used to treat corneal injuries such as corneal burns, infections and trauma. However, fewer patients today require corneal transplantation for these reasons due to the development of antibiotics and antiviral treatments. Corneal transplantation today is mainly used to treat corneal blindness as a result of keratoconus, re-grafting due to failed grafts, bullous keratopathy and corneal dystrophy [61-64]. There are multiple host and donor risk factors to consider before transplantation, as the presence of risk factors will determine the outcome of the graft. Some of these include; the presence of stromal blood vessels in the recipient's cornea (high-risk), post-surgery corneal neovascularization, pre-operative glaucoma, past graft rejection episodes, ocular inflammation, herpes simplex keratitis, neurotrophic keratopathy or the presence of an anterior synechiae [65-69].

1.2.1 Corneal Allograft Rejection

Under normal conditions, the avascular nature of the cornea provides an immune privileged environment. For this reason, corneal transplantation is among the most successful organ transplantations in first-time 'low-risk' graft recipients. Low-risk patients experience a success rate of approximately 90% in the first two years post-transplant without a need for corticosteroid intervention or human leukocyte antigen (HLA) matching [68, 70, 71]. Disruption to this immune privilege can occur if there is an increase in pro-inflammatory, angiogenic and lymphangiogenic factors. This will lead to a response from the recipient's immune system to the donor graft. This is the case in high-risk patients where pre-existing neovascularisation, a vascularised corneal bed or a previous history of graft rejection is present. In these patients up to 70% of

grafts will fail [72]. In these cases, the recipient's immune system rejects the donor corneal button stimulating an immune response consisting of both innate and adaptive cells/mediators. The induction phase of corneal allograft rejection occurs when the recipient becomes sensitised to donor antigens. APCs orchestrate this process by presenting donor antigen to naïve T cells in draining lymph nodes (DLNs) [68, 73]. Antigen can be presented by the direct or indirect pathway. The direct antigen presentation pathway is mediated by presentation of donor antigens to naïve T lymphocytes via donor APCs through foreign MHC II recognition. This results in the expansion and proliferation of alloreactive T effector cells [68, 74]. The indirect pathway of antigen presentation is mediated by recipient APCs migrating to the cornea where they uptake antigen, process the antigen on the way to the lymph node and present the antigen to naïve T lymphocytes. This also results in the expansion and proliferation of alloreactive T effector cells [68, 74]. Originally it was thought that the induction of graft rejection was exclusively mediated by the indirect pathway of antigen presentation [68, 75]. In the two decades since, a lot of experimental evidence indicates that both the direct and indirect pathways are important in the induction of graft rejection, especially in high-risk patients where the immune privilege has been compromised [76-81].

Graft rejection is a complex process and antigen presenting cells play a vital role in the rejection event [82]. The importance of APCs was demonstrated in experiments where APCs were depleted using clodronate liposomes. In both a model of rat and mouse corneal transplantation, animals with depleted APCs experienced increased graft survival [83, 84]. Experiments completed in immunocompromised mice added a small bit of clarity to their role. These experiments demonstrated that APCs could not alone induce graft rejection and that when $CD4^+$ lymphocytes from graft rejecters were adoptively transferred to APC depleted mice, they were able to induce rejection. This demonstrated that while APCs cannot solely initiate graft rejection, they mediate induction of the afferent phase of graft rejection [84].

There are several anatomically distinct subsets of APCs located in the anterior structure of the eye [77]. Both macrophages and $MHCII^+$ DCs located within the iris and the trabecular meshwork are perfectly located to uptake soluble antigen released from the endothelium of the corneal graft [77, 85]. Macrophages located in the iris have demonstrated antigen uptake and the ability to stimulate T lymphocytes by local

presentation of antigen [86, 87]. There are resident populations of DCs in the cornea from both epithelial and stromal origin [26, 88] and these are vital in modulation of corneal immunogenicity [27, 89]. In the non-inflamed cornea these resident DCs display an immature phenotype being $MHCII^+$ low or negative. However if an inflammatory event occurs as is the case in corneal transplantation, this DC population has been reported to activate, upregulating MHCII, co-stimulatory molecules and increase in number [26, 88, 90, 91]. Other DC populations have been identified in recent years adding another layer of complexity to corneal allograft rejection [92].

Corneal antigen presentation can occur in several different anatomical locations, the DLNs being of primary importance. When GFP positive corneas were transplanted into wild-type mice, GFP^+ cells were detected in the DLNs 6 hours after transplantation. These cells were shown to have allo-stimulatory capabilities after maturation [68, 93]. In the rejection process the lymph nodes act as the priming centre for T lymphocyte activation and allo-sensitisation driving the "expression" phase of graft rejection [68, 93], inevitably leading to destruction of the graft. In experiments investigating the importance of the DLNs in corneal rejection, cervical lymphadenectomy (lymph node removal) was performed on high-risk BALB/c mice before corneal transplantation. It was demonstrated that 100% of high-risk mice rejected their grafts when the DLNs were present. However after removal, 92% graft survival was observed supporting the importance of the DLNs in the rejection process regardless of the pre-operative risks [94]. Allo-sensitisation and activation of T lymphocytes leads to the secretion of multiple cytokines and chemokines that facilitates the expansion and migration of these alloreactive T lymphocytes to the cornea, that is mediated by multiple adhesion molecules [68]. The initial damage caused to the cornea and surrounding tissue during transplantation leads to the secretion of both Interleukin 1 (IL-1) and tumour necrosis factor alpha (TNF-α). This inflammatory event begins the process of immune mediated damage to the graft. This cytokine/chemokine secretion is heightened in high-risk grafts. Essential cytokines/chemokines known to mediate this process include monocyte chemotactic protein-1 (MCP-1), chemokine C-C motif ligand 2 (CCL2), CCL5, MIP-1α and MIP-1β (CCL4) [68, 73, 95-97].

Once activated and expanded alloreactive T lymphocytes migrate to the cornea where they will recognise and respond to donor MHC antigens. There are multiple different

subpopulations of T lymphocytes and in recent years and each of these populations have been shown to play a role in graft rejection or survival.

$CD4^+$ T-helper lymphocytes are the main mediators of corneal graft rejection [82]. While the role of $CD8^+$ cytotoxic lymphocytes remains somewhat controversial [98-100] there is evidence to support their role in graft rejection [101-104]. $CD4^+$ Th1 cells, a subpopulation of $CD4^+$ T-helper cells, are largely considered to be the primary effector cells in corneal graft rejection [74, 84]. $CD4^+$ Th1 effector cells secrete lymphotoxin (TNF-β), IFN-γ and IL-2. IL-2 is vital for sustaining T and B lymphocyte proliferation and activation while IFN-γ activates APCs such as macrophages and upregulates MHCII in the microenvironment where it is secreted [68].

Yamada et al. observed that if the allo-immune response was shifted to a Th2 phenotype it enhanced the survival of corneal allografts in a high-risk model of murine corneal transplantation [105]. Due to this study it was thought that a Th2 phenotype would be desirable, however, more recent studies [106, 107] have found that if graft recipients previously suffered with allergic conjunctivitis, a disease that leads to an elevated Th2 phenotype, they rejected their grafts at accelerated rates, demonstrating a role for Th2 cells in corneal allograft rejection.

The role of Th17 populations in corneal allograft rejection is still unclear and some consider their roles in the rejection process to be somewhat limited [68]. Interestingly, experiments carried out in a murine model of corneal transplantation have demonstrated that if there is an increased expression of Th17 cells in the early stages of corneal graft rejection this leads to an increased Th1 response in the later stages of the rejection process [108]. Also, Chen *et al* observed improved graft survival using blocking antibodies to IL-17 [109]. Contrastingly. studies completed using IL-17 knockout mice demonstrated no increase in survival of grafts [108]. This is thought to be a result of the onset of a Th2 response due to the lack of IL-17. The emerging Th2 cells then mediate rejection of the graft [68, 109, 110].

The complexity of the rejection process results in controversy regarding clear roles for each of the $CD4^+$ subsets. It is clear however that these cells mediate the destruction of the graft and therefore cellular therapies that result in the balance of Th1/Th2/Th17 responses is crucial for corneal allograft survival [111].

The induction of regulatory immune populations is desirable to circumvent the rejection process. Regulatory T lymphocytes (Tregs) are a population of $CD4^+$ lymphocytes that make up about 5-10% of the $CD4^+$ subset. The inducement of this subset is highly sought after in therapies for transplantation rejection. Tregs have shown efficacy in prolonging allograft survival not only in corneal transplantation [112] but in models of bone marrow [113], skin [113], cardiac [113], liver [114], and kidney [115] transplantation also. It was recently demonstrated that functional Tregs in the DLNs were responsible for allograft survival in a mouse model of cornea transplantation [112]. This reiterates the importance of the lymph nodes role not only in rejection of the graft but also to the induction of tolerance of the graft.

To summarise, the induction phase of corneal rejection is initiated by APCs presenting alloantigen via the indirect pathway to T lymphocytes. This can occur in the sub-ocular space, the conjunctiva and in other areas of the eye but the crucial location is the DLNs. This results in the activation and expansion of $CD4^+$ effector T lymphocytes which then migrate to the cornea and cause delayed type hypersensitivity (DTH) responses and inevitably graft rejection. Antigen can be presented to $CD8^+$ lymphocytes via the direct pathway of presentation but evidence would suggest that this is not the predominant mechanism of graft rejection (**Figure 1.2**). Also, Tregs in the DLNs can suppress graft rejection by modulating the immune response in an antigen specific manner which has been shown to be important for graft acceptance.

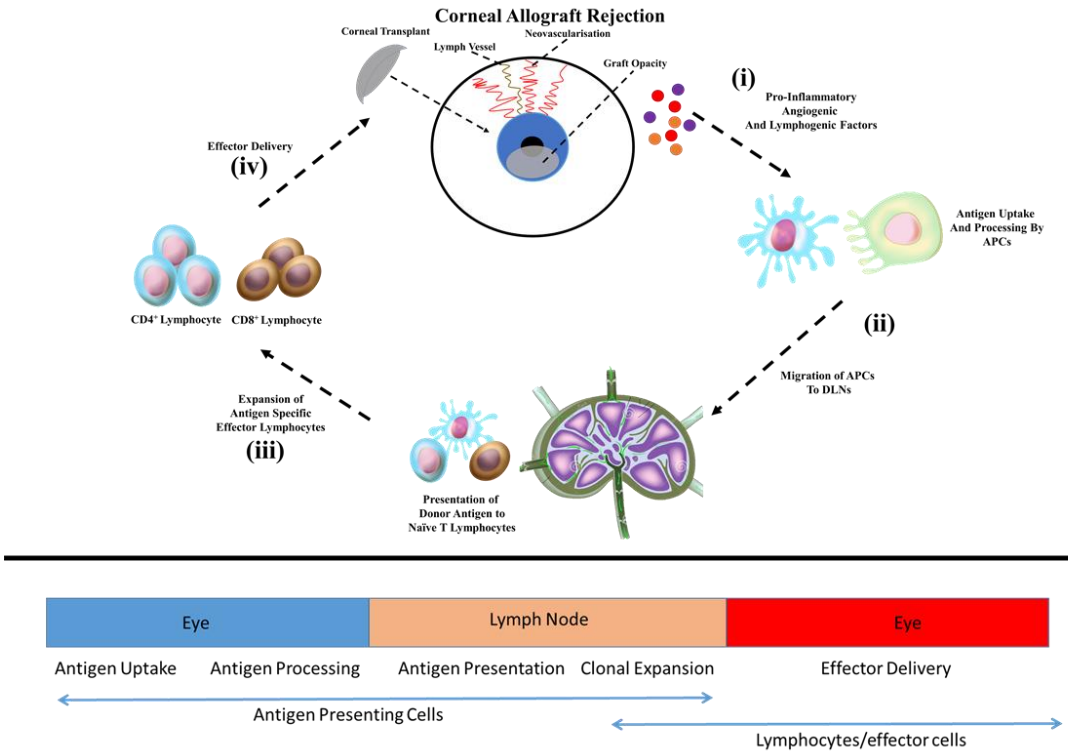

Figure 1.2 Schmatic of Corneal Allograft Rejection Process. (i) Following corneal transplantation there is an upregulation of pro-inflammatory cytokines, pro-angiogenic factors, adhesion molecules and lymphogenic factors which result in the infiltration of immune cells and the formation of new blood and lymphatic vessels in the cornea. (ii) MHC II positive APCs leave the cornea via the newly formed lymphatic vessels and migrate towards the DLNs. APCs present alloantigen's to naïve conventional T lymphocytes. (iii) Alloreactive T lymphocytes undergo clonal expansion and develop into $CD4^{+}IFN\text{-}\gamma^{+}$ cells and $CD8^{+}$ cytotoxic lymphocytes. (iv) Effector alloreactive $CD4^{+}IFN\text{-}\gamma^{+}$ cells and $CD8^{+}$ cytotoxic lymphocytes migrate through blood vessels and mount a DTH response versus the allogeneic corneal graft which inevitably results in rejection of the tissue

1.2.2 Advantages and Disadvantages of Current Therapies for Corneal Allograft Rejection

Topical corticosteroids are the frontline treatment in managing post-operative inflammation and prevention of acute graft rejection both in low and high-risk patients. Prednisolone is the preferred drug of choice and it is applied daily [116]. In cases of severe endothelial rejection patients can be directed to apply topical corticosteroids hourly [68]. However, continued topical use of corticosteroids can lead to glaucoma, impaired wound healing and keratitis [68].

Systemic corticosteroids are used in cases of severe endothelial graft rejection. Intravenous dexamethasone is routinely administered and this has been shown to

reverse graft rejection in up to 72% of cases when used in combination with topical treatments [117]. As with topical treatments, systemic dexamethasone treatment is associated with negative effects such as diabetes, weight gain and osteoporosis [68].

Calcineurin inhibitors such as Cyclosporine A and Tacrolimus are used in high-risk patients. However, multiple different groups have investigated the benefits of Cyclosporine A use and the results are conflicting [68]. A randomised clinical trial published in 2008 showed no additional benefit of using Cyclosporine A in the treatment of acute corneal rejection [118]. Contrarily, a study in paediatric patients showed short term efficacious benefits using Cyclosporine A compared to situations where it was not used. In this study, no long-term graft survival benefits were noted [119]. The side effects of administering Cyclosporine A long-term include nephrotoxicity, hepatotoxicity, bone marrow toxicity and systemic hypertension [120]. For these reasons it is usually only given when corticosteroids treatment is not optimal. Tacrolimus is another calcineurin inhibitor and its negative side effects and mechanism of action are similar to Cyclosporine A. Both topical [121] and systemic administration [122, 123] of Tacrolimus has proved beneficial in reversal of acute graft rejection in high-risk patients.

Antimetabolites like mycophenolate mofetil (MMF) inhibit DNA synthesis in lymphocytes. Randomised clinical trials [124, 125] have shown that MMF has therapeutic efficacy in the treatment of graft rejection in high-risk patients. Negative effects of taking MMF include gastrointestinal disorders, anaemia, leukopenia, and increased risk of infections [126, 127].

While the prognosis for low-risk patients is excellent due to long term survival with minimal or no systemic immunosuppressants needed, this is not the case for high-risk patients. High-risk patients generally must take multiple immunosuppressive drugs and as listed above this comes with a plethora of negative side effects. This is not ideal and is hard to justify in a non-life-threatening disorder. Therefore, we propose that alternative treatments that induce a state of immune non-responsiveness to the graft while having none of the negative effects associated with systemic immunosuppressive drugs would be desirable.

In recent years both DC and mesenchymal stromal cell (MSC) therapy has been researched as a method to prolong corneal allograft survival. To date several studies

have demonstrated efficacy with both cell preparations with varying reports of success and mechanism of action. In the following sections I will discuss the biology and characteristics of these cell types to highlight that which makes them appealing therapies in transplantation and in the treatment of other inflammatory diseases.

Dendritic Cells

1.3.1 DC Biology and Function in the Immune System

DCs were discovered 45 years ago by Steinman and Cohn [128] and it is now very well established that they are a key component of the immune system and in immune regulation. Among other features, DCs are responsible for priming the T lymphocyte specific responses to infection or foreign antigens and they achieve this through pathogen-recognition receptors (PRRs). Depending on DC maturation state, they can function differently in immune responses. Dendritic cell precursors develop from hematopoietic stem cells in the bone marrow. These cells have the capacity to migrate to tissues, secondary lymphoid organs and sites of potential infection via blood and there they develop into immature dendritic cells (iDCs) [129-132]. iDCs then act as sentinels and monitor the environment in these peripheral tissues utilising toll-like receptors (TLRs). TLRs can recognise a vast range of evolutionally conserved bacterial molecules such as LPS and CpG islands [131, 133-135]. As iDCs start to mature after antigen uptake they begin to migrate towards the lymph nodes or T lymphocyte zones. In transit the iDCs decrease the uptake of antigen and start to increase major histocompatibility complexes so that they can prime the antigen specific T lymphocyte response [131, 136-138].

DCs are a heterogeneous population and have many differentiation/maturation states [139] which will not be the focus of this thesis. To simplify, DCs can be divided into two main functional subpopulations based on phenotype and function, plasmacytoid DCs (pDCs) and conventional DCs (cDCs). pDCs are recruited to control pathogenic infections and produce large amounts of type I interferon in response to antigen. Contrastingly, cDCs are tissue specific and many different subtypes of cDC reside in the tissue in an immature state. Here they recognise both bacterial and viral components [140]. Briefly, cDCs can be divided into two main subsets which can be

phenotypically defined by the expression of CD8α and/or CD103 and CD11b expression. Both populations can be found in the lymph nodes, spleen and bone marrow but also in non-lymphoid tissue also [141]. Acquired immunity is primed by cDCs as they initiate the primary T lymphocyte responses to foreign antigens, contrastingly, naïve T lymphocytes are not stimulated by pDCs but it has been reported that pDCs can differentiate into cDC-like cells after they have been activated thus acquiring the ability to present antigen to T lymphocytes [142]. The Th1/Th2 T helper lymphocyte populations also seem to have preference as to which DC subset activates them, with the Th1 response having preference for cDCs and the Th2 response being partial to pDC activation with each subset of DC having differences in which TLRs they express [142].

DCs have evolved many different mechanisms to recognise and internalize antigens including receptor-mediated endocytosis, micropinocytosis and phagocytosis. Receptor-mediated endocytosis occurs when antigen binds specifically to certain PRRs such as C-type lectins. After recognition, antigen is endocytosed and taken in by the cell [143]. Micropinocytosis involves the non-specific internalization of large quantities of fluid-phase solute and this process is actin dependent and once antigen is taken up it is then processed for presentation to T lymphocytes [144, 145]. Phagocytosis concerns the uptake of large particles such as cell debris from apoptosis or necrosis, bacteria and viruses. These processes will lead to the maturation if the sampled proteins are antigenic [144].

1.3.2 Tolerogenic DC (tDC) Generation and Functions

While DCs are highly specialised professional APCs and are paramount in regulating immune responses, they also maintain the balance between tolerance and immunity. DCs have been extensively investigated as a potential cellular therapy as they have been shown to induce or re-establish tolerance. They promote both central and peripheral tolerance by multiple different mechanisms including the induction of Tregs, inhibition of memory T lymphocyte responses, T lymphocyte anergy and clonal deletion [146]. As mentioned previously, the current immunosuppressive drug regimen come with heavy negative side effects which are difficult to justify. The ability of DCs to promote tolerance has gained considerable interest within the field of transplant immunology as they could potentially offer a side effect free alternative.

Numerous different methods to generate tDCs have been developed and the safety of both un-manipulated DCs and tDCs has been demonstrated in humans via several multiple phase I clinical trials [147, 148]. Considering their potent ability to generate Tregs and the safety of human administration the potential of tDCs being used in the clinic is feasible.

tDCs display an immature phenotype characterised by low expression of MHCI, MHCII, CD80 and CD86. They also have a modified secretome, secreting higher levels of anti-inflammatory cytokines and lower levels of pro-inflammatory cytokines. If tDCs present antigen without sufficient co-stimulation it results in T lymphocyte anergy, this also drives the differentiation of Tregs *in vitro* and *in vivo* [146]. Typically, the stimulation of the T cell receptor (TCR) leads to activation of nuclear factor of activated T cells (NFAT), inducing a transcriptional response which orchestrates T lymphocyte activation [149]. Intriguingly, the mechanism of how insufficient co-stimulation results in a transcriptional cascade that favours Treg induction and differentiation is still largely unknown [150].

The secretome profile of tDCs is important in their ability to induce tolerance. Anti-inflammatory cytokines such as interleukin-10 (IL-10) and transforming growth factor-beta (TGF-β) are typically secreted by tDCs. IL-10 has been shown to be paramount in multiple different settings [151-153] in tDC regulatory functions and TGF-β has been shown to be vital in the induction of tolerance demonstrated convincingly in transgenic mice by the ablation of the TGF-β activating integrin αvβ8 (Itgb8) which leads to colitis and resulting autoimmunity [154]. In addition to the secretome, tDCs have several cell surface molecules that contribute to tolerance induction. These include the expression of FASL [155] and TRAIL [156] which cause the induction of lymphocyte apoptosis. They also express inhibitory Ig-like transcripts [157], programmed cell death (PD-L1) ligand 1 and 2 (PD-L2) [158, 159] which regulate lymphocyte proliferation and differentiation and cytotoxic T-lymphocyte-associated protein 4 (CTLA-4) [160] which competes with CD28 binding preventing co-stimulation and dampening the TCR signalling responses. Not only this, tDCs can also regulate the metabolic state of cells by the secretion of both heme oxygenase-1 (HO-1) and indoleamine 2-3 dioxygenase (IDO). HO-1 converts heme to carbon monoxide, free iron, and biliverdin, this overall reduces the amount of functional haemoglobin resulting in reduced DC immunogenicity [161]. IDO limits the amount

of free tryptophan by converting it to N-formylkynurenine, tryptophan is a vital amino acid needed for T lymphocyte proliferation [162]. Furthermore, tDCs produce retinoic acid and can shed CD25. Retinoic acid is capable of inducing Treg differentiation [163]. CD25 that has been shed from tDCs can sequester free IL-2, therefore restricting IL-2 in the environment and controlling T lymphocyte proliferation [164].

iDCs express a phenotype that meets the optimal requirement for tolerance induction, that is they express low levels of co-stimulatory markers and they don't secrete pro-inflammatory cytokines, however, they are not maturation resistant, as such they may be unstable, and the threat is that they may switch to immunogenic DCs under inflammatory conditions. For this reason, many different protocols to generate tDCs have been developed. A common method is to genetically modify iDCs to stability express immunomodulatory molecules. To date human iDCs have been modified to express FasL [165], PD-L1 and TRAIL [166, 167], IDO [168], IL-10 and TGF-β [166, 167]. These studies have reported the successful induction of T lymphocyte apoptosis, suppression of effector T lymphocytes or general immunosuppression.

Non-genetic modifications involve the treatment of DCs with immunosuppressive drugs including acetylsalicylic acid, rapamycin, cyclosporine or corticosteroids such as dexamethasone. It has been shown by us and others that dexamethasone treatment of iDCs leads to the generation of a maturation resistant tDC exhibiting low levels of MHC II, CD80 and CD86 while also increasing IL-10 both a mRNA and protein level [169, 170].

Recently, we demonstrated that dexamethasone generated tDCs were capable of prolonging allograft survival in a model of rat corneal transplantation. One interesting observation from this study was that tDCs expressed higher levels of sialic acids than their iDC counter-part. Little is known about how sialic acid contributes to the immunogenicity or tolerogenicity of tDCs. In the next section, the importance of glycosylation, focusing particularly of sialic acid will be discussed.

1.4 Glycosylation: Importance of Sialic Acid in DC Function

Glycosylation is a vital post-translational event which is essential in cell-cell interactions, correct protein transport, protein function and the migratory attributes of cells. Taking this into consideration, concerning immunity, one would assume that an

immune cell's glycosylation state would be of vital importance in determining that immune cell's fate. The ever-increasing evidence in the literature would suggest that all immunological studies should consider glycosylation. This being the case, there is still a gap in knowledge with regards to how exactly glycosylation is contributing to the overall immune response. Currently little information exists on how DC glycosylation patterns change after tDC generation and what consequences, if any this may have on their tolerogenicity or immunogenicity.

Sialic acids (Sias) are ubiquitous terminal end monosaccharides which are expressed on virtually all cell surfaces and their presence or absence have been heavily implicated in the regulation of immune cell function. DCs are very important players in the boundary between adaptive and innate immunity and have a complex glycocalyx which has been implicated in DCs cell-cell interaction. The manner in which DCs are glycosylated is paramount in initiating an immune response, may it be anti or pro inflammatory. Structures that contain Sias terminal residues are important in virtually all DC functions such as antigen uptake, DC migration and the DCs ability to activate resting T cells i.e. the method in which a T lymphocyte and DC interact at the MHC / TCR boundary. Taking this into consideration one can comfortably state that Sias plays a role in DC cell function and this may imply that Sias could potentially be targeted and manipulated for therapeutic benefits.

As mentioned, glycosylation is one of the most vital and most frequent form of post translational modification and it is involved in the function of many immune associated molecules. Some of these functions include but are not limited to protein folding and molecular trafficking to the cell surface [171-173]. Also glycosylation has been implicated in the stability of proteins in steady state and protection from proteolysis [174]. All immune cells are coated by a complex conglomerate of glycans to make up the cell's glycocalyx., one such component are Sias. Sias are a broad family of negatively charged carbon monosaccharides that are exposed to the cellular microenvironment and they are involved in communication and in cellular defence [175]. Sias have long been implicated in being important for the overall immune system to function. It has been suggested that Sias can play important roles in both acting as a recognisable molecule for cellular interactions but also as a biological shield preventing receptors on cells recognising their ligands [144]. Large amounts of Sias on the cell surface of immune cells will result in an overall negative charge. This

can have biophysical effects, such as the repulsion of cells from each other and hence have an effect on cellular interactions [176]. As mentioned Sias can mask or stealth a cell, this could have implications in pathogen-host interactions but also in allogeneic DC cell vaccines or therapies and this attribute of Sias could potentially be a clinical target. If one could somehow manipulate the content and composition of the cell's glycocalyx to contain more Sias, one could potentially apply this to transplantation biology or cellular therapy treatments. Interestingly, certain lectins can only recognise their corresponding glycan in the absence of Sias. If N-glycans are heavily sialylated they cannot be recognised by galectins [177].

1.4.1 Pattern Recognition

Siglecs contribute to the immune system by the recognition of Sias on their target molecules, thus allowing recognition of the antigen which leads to maturation and activation of the DC. Siglecs are broken up into two different categories even though there is little structural difference between them. These are the CD33-related siglecs, comprising of Siglecs 3, 5, 6, 7, 8, 9, 10, 11 and 14. The second group consists of sialoadhesin (Siglec-1 or CD169), MAG (Siglec-4) and Siglec-2 (CD22) [178]. Sias can be α(2-3), α(2-6) or α(2-8) linked to glycans and even though all siglecs only recognise sialylated molecules they can discriminate between the differences in linkages [178]. To date, of all of the siglecs family members, 13 of them have been identified on immune cells as critical components to the correct functioning of the immune system. DCs are one such immune population. A point of note is that siglecs are barely detectable on T cells, thus highlighting their importance in DC/antigen presenting cell biology [178]. The fact that Sias are also present at high numbers on pathogenic microbes indicates the multifunctional potential of siglecs [179].

1.4.2 Endocytosis

Endocytosis the process by which DCs uptake particles from their microenvironment by engulfing them has been shown to be regulated by Sias content on the cell. When surface sialylated glycans expressed during human DC generation were analysed, it was shown that α2-3-sialylated O-glycans, and α2-6- and α2-3- sialylated N-glycans are present in monocytes and their expression increases during mo-DC differentiation. When surface Sia is removed by neuraminidase (an enzyme that cleaves Sias linkages) DC endocytic capacity was decreased [180]. Both macropinocytosis and phagocytosis have also been shown to be directly affected by the removal of Sias from DC cell

surface, decreasing and increasing respectively [181]. In experiments using sialyltransferase (ST6Gal-I and ST3Gal-I) deficient mice similar results were seen [182]. Sialyltransferases are conserved enzymes responsible for the transfer of Sias to nascent oligosaccharide [183]. Compiling the information from these experiments, the removal of, or in the case of the knock-downs, the absence of Sias from DCs facilitates the maturation of monocyte derived dendritic cells (iDCs). These papers also note a significant increase in both co-stimulatory (CD80/86) and presentation machinery (MHC I/II) after the removal of Sias. In this case, the documented decreases in endocytosis would make sense, as when DCs mature their endocytosis ability decrease. This being the case, there is also a documented increase in phagocytosis which is conflicting. Mature DCs continue to uptake antigens via phagocytosis and receptor-mediated endocytosis. Although, never to the same levels of immature DCs, the authors suggest this could be a reason for the confliction [144, 181, 182, 184-186]. Noting that sialidase treatment of DCs increases phagocytosis, Cabral *et al* conducted a follow up study where they asked the question whether the noted increase in phagocytosis was a result of cytoskeleton rearrangements prompted by the treatment? And if yes, was this cdc42 and Rac1 dependent? When DCs were treated with sialidase in the presence of *E. coli*, a disruption of the cytoskeleton was noted, however, the authors stated after further experimentation that this disruption was not cdc42 and Rac1 GTPase dependent and therefore concluded that the increases in phagocytosis is not due to increased cytoskeleton dynamics [181]. This being the case the group did state that changes in phagocytosis seemed to be dependent on the presence of bacterial Sias highlighting again the importance of Siglecs [181].

1.4.3 Migration

Migration is another characteristic of DCs that can somewhat be attributed to the functionality of Sias. During migration or extravasation DCs need to interact with the endothelium and this is dependent on either molecules present on the DCs or on the endothelium. Some of these molecules include selectins 1 and 2 [187] which are a form of CLR. Selectins recognise and bind tertasaccharide that contains fucose and/or Sias and in this recognition the main element that is vital are sialyl-Lewis x (SLe^x) structures [144]. Selectins have been long established as vital for leukocyte rolling and transmigration. These molecules have been identified and studied in neutrophils [188], lymphocytes [189] and iDCs [190, 191]. In a study carried out by Silva *et al* [192],

were they highlighted that most iDC based vaccines do not reach their maximum efficacy due to the reduced migratory capacity of these cells. They investigated what role SLe^x structures had in selectin binding. The results suggest that SLe^x structures are vital in the binding of iDCs to selectins on TNF-α activated endothelial cells, again in these experiments neuraminidase was used to cleave Sias on the iDCs, thus disrupting the SLe^x structures [192]. The same group also interestingly showed that sialidase treatment disrupted iDCs tethering to purified P-, L- and E selectins under flow conditions, highlighting how important Sias seem to be in migration of iDCs [192]. Studies have implicated a role of sialic acid in meditating the stopping of cells on the endothelium, i.e. to facilitate chemokine receptor arrest of the cells [144, 193]. Preliminary unpublished results from Paula A. Videira's laboratory suggest that sialic acid is somehow important in the migratory capacity of DCs towards the lymph nodes.

1.4.4 T-Cell Interactions

In classic studies carried out by Boog *et al* [194] it was shown that MHC I molecules are present to a greater extent on DCs when compared to other antigen presenting cell (APC) populations, and that Sias are present at a lower level on MHC I molecules isolated from DCs when compared to the other APC populations. Based on the results obtained, the group suggested that Sias may have a negative impact on DC antigen presentation and this was possibly due to Sias interfering with ability of MHC I to load peptides [144, 194]. In line with this, results from our lab where iDCs isolated from Dark Agouti rats were treated with neuraminidase showed increased immunogenicity when co-cultured in allogeneic mixed lymphocyte reactions. There are many different scenarios as to why this may occur, some of which are mentioned above. Interestingly, experiments carried out in our lab and others [182] have seen a pro-inflammatory mRNA profile (IL-6, IL-1β and TNF-α) in these cells after treatment. This could be one such reason as to why increases in activation and proliferation are seen. Host tolerance has been implicated to be partially mediated by Siglecs as tolerogenic immature iDCs have high levels of Sias and this is also the case for regulatory T cells [144, 195]. Again, results generated from our lab have shown that immature iDCs have an overall higher glycosylation when compared to OX62+ (CD103) cells isolated from the spleen, Sias are significantly upregulated on these cells indicating that Sias could have a role to play in tolerogenicity.

Considering the ubiquitous nature of Sias one should not be surprised at their vital roles in DC function. While several aspects of how sialic acids contribute to DC biology have been covered here, there are many different areas in which sialic acids play interesting roles that space did not permit a discussion. For example, how sialylated structures have been implicated in DC/tumour cell interactions or the importance of sialyation on cluster of differentiation (CD) molecules. While sialic acids were predominately discussed, there is a vast amount of literature implicating glycosaminoglycans, galactose and fucose in immunity, once again highlighting the importance of glycosylation in immune biology. There are still large gaps in knowledge regarding how sialic acids functions and what systemic implication they have in immunity, however this being said, the importance of glycosylation is beginning to become more apparent with more information being reported. Discovering this role could be clinically relevant in many different areas, for example as highlighted, in DC based vaccines, if the alteration of the sialic acid profile of these cells could increase the migratory capacity of DCs one could see an increase in efficiency of treatment. Another example is in the context of cellular therapy or transplantation biology. Sialic acids have been shown to function in masking or hiding cells from the immune system. While its doubtful that changes in sialic acid alone would be sufficient in masking therapeutic allogeneic cells from the immune system, it is not implausible to assume that manipulating the glycocalyx to a more "unrecognisable" phenotype that maybe the therapeutic cells could have a longer life span to administer their therapeutic effects before clearance by the recipient's immune system. A summary of the roles of Sia in DC biology is presented in **Figure 1.3** below. Most of research done to date in DCs has been in monocyte derived or bone marrow derived DCs. In the following chapters we highlight the importance of sialic acid in the regulating immunogenicity and tolerogenicity of iDCs and tDCs by modulation of cell surface glycosylation by dexamethasone treatment.

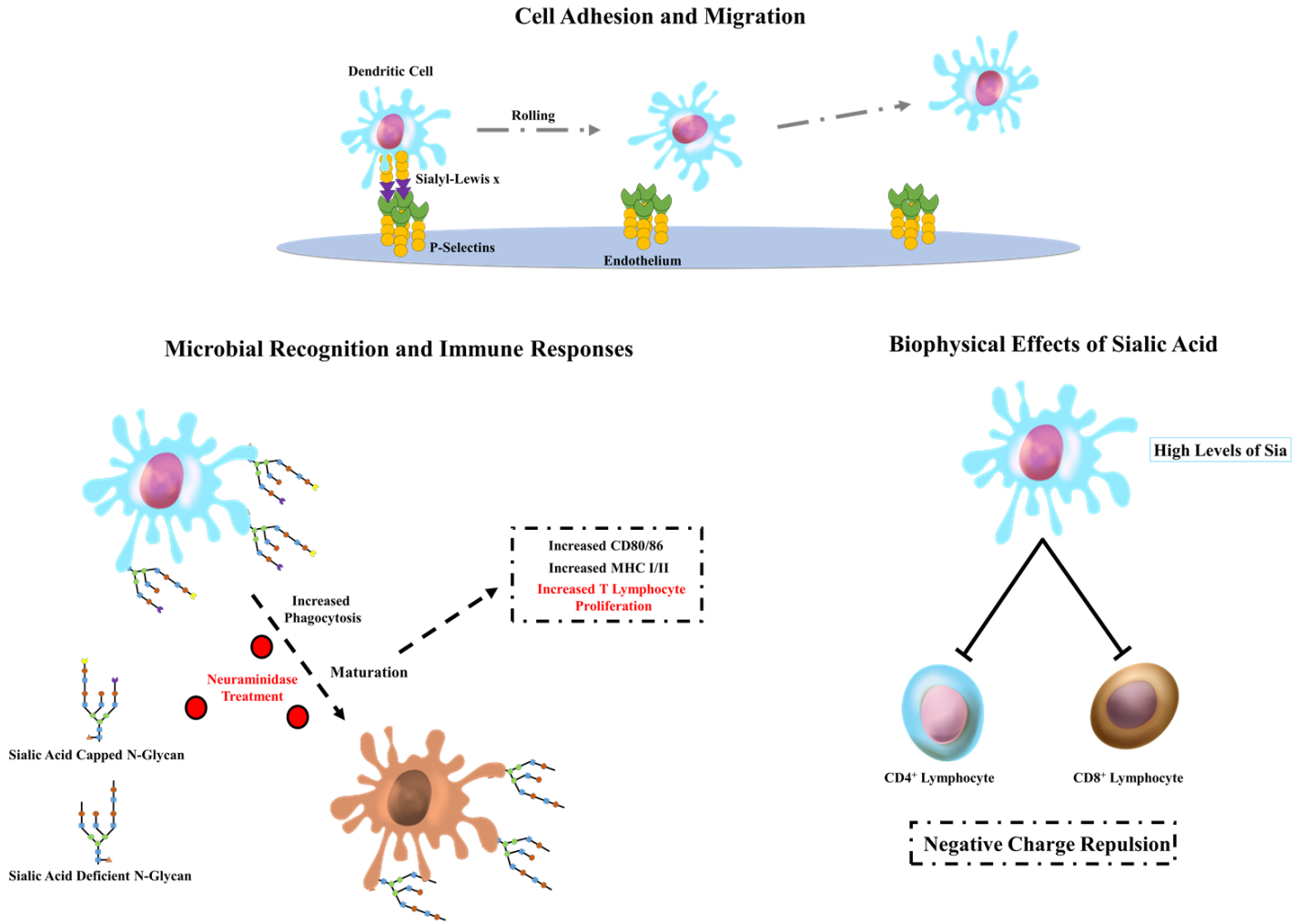

Figure 1.3 Sia is important in DC function. Glycans that contain sialic acid are important in modulating processes like cell adhesion, microbial recognition, DC maturation, phagocytosis, biophysical repulsion, and T cell proliferation either directly or indirectly.

1.5 Mesenchymal Stromal Cells

1.5.1 Introduction

Shortly after the discovery of haematopoietic stem cells (HSCs), mesenchymal stomal/stem cells (MSCs) were discovered by Friedenstein et al, who reported that stromal cells from the bone marrow compartment could form bone, fat, and cartilage following heterotopic transplantation in mice [196]. It was subsequently shown that a subset of fibroblast-like cells which were termed colony forming unit fibroblasts (CFU¬Fs) could be isolated and expanded from the bone marrow due to the cells being plastic adherent [197]. Further studies demonstrated that CFUFs had the ability to proliferate while still maintaining their ability to differentiate to osteocytes, chondrocytes and adipocytes in vitro [198], this was interpreted to mean that these cells were multipotent and self-renewing in vivo and therefore stem like in nature, thus the term mesenchymal stem/stromal cell [199-201]. Since their initial discovery MSCs have been isolated from numerous tissues including umbilical cord, adipose tissue, muscle, dental pulp and lung [197, 202]. Despite the considerable amount of research since their discovery a pan MSC marker has yet to be discovered, as a result, definition still largely depends on plastic adherence. Due to potential contamination with haematopoietic cells but also due multiple different isolation methods the International Society for Cellular Therapy (ISCT) set out the minimal criteria to define a MSC, these include: adherence to plastic in standard cell culture conditions, expression of cell surface markers CD90, CD73, CD105 and lack of expression of CD45, CD34, CD14 or CD11b, CD79α or CD19 and MHC surface molecules and they need to demonstrate multilineage potential, differentiating to osteogenic, adipogenic and chondrogenic lineage [203].

Due to their multi-lineage potential and the ease of their isolation and expansion, MSCs are ideally positioned to be promising therapeutic cells in the treatment of inflammatory diseases. In fact, MSCs have shown reparative efficacy in multiple pre-clinical models including myocardial infarction, hepatic failure, renal failure, wound healing, retinal degeneration, osteoarthritis and stroke [197]. In recent years, it has been demonstrated that MSCs deliver their therapeutic effects mainly via their immunosuppressive properties. In this section I will discuss important aspects regarding MSC biology and identify aspects that are still unclear. I will discuss well

established properties of MSCs cultured *in vitro* and focus on how these properties could potentially be exploited for use in cellular therapies especially in the context of corneal allograft rejection.

1.5.2 Immunomodulatory Attributes of MSCs

The immunomodulatory effects of MSCs were described in 2002, experiments by Di Nicola *et al* and Bartholomew *et* al demonstrated that bone-marrow-derived MSCs suppressed T lymphocyte proliferation [198, 199]. Until publication of both studies, scientists hoped to exploit MSCs for their multipotentiality and reparative functions but these studies indicated the potential use of MSCs for regulation of immune cells and as a result we now have a vast amount of information regarding immunoregulatory functions of MSCs. In the following text I will discuss the current knowledge in how MSCs modulate the many different cells that are reported to contribute to corneal allograft rejection (summarised in **Figure 1.4**).

Innate Immunity

DCs: As mentioned previously, DCs are a vital component of the corneal rejection process. Following maturation, DCs present antigen to naïve T lymphocytes, activation of naïve T lymphocytes is facilitated by upregulation of co-stimulatory molecules, engagement of either MHC I or MHC II and release of proinflammatory cytokines. Maturation of both monocyte-derived and haematopoietic progenitor derived DCs has been shown to be inhibited by MSCs *in vitro* [200-202], moreover, Nauta *et al* [202] observed that MSCs convert DCs to a tolerogenic phenotype and this was mediated by soluble factors. Also, matured DCs co-cultured with MSCs have decreased expression of MHC II, CD80, CD86 and decreased levels of interlukin-12 (IL-12), TNF-α and IFN-γ with increased level of IL-10 secreted from pDCs [200, 203-207].

Macrophages: Similarly, in co-culture experiments where MSCs have been incubated with macrophages, decreased levels of MHC II, CD86, TNF-α and IFN-γ were observed with the effects being partially mediated by soluble factors such as PGE2. Not only this but MSC educated macrophages confer protection in graft-versus-host disease [208-212].

Natural Killer (NK) Cells: NK cells are an important cell type in innate immunity and studies have shown that NK cells can discriminate between self and non-self-tissues, playing a key role in the initiation of adaptive immune responses to the graft [213]. MSCs have been shown to downregulate NKp30 and natural-killer group 2, member D (NKG2D), thus inhibiting the cytotoxic activity of resting NK cells. The function and activation of NK cells is tightly regulated by these cell-surface receptors where their engagement can result in either activation or inhibitory signals [207, 214]. NK cells proliferate *in vitro* in the presence of IL-2 and IL-15, these cells are strongly cytotoxic and secrete IFN-γ. When co-cultured with MSCs, levels of proliferation, cytotoxic capabilities and levels of IFN-γ all decrease significantly [207, 214, 215].

Neutrophils: Neutrophils are a component of the innate immune system that typically kill microorganisms. Once activated by bacterial components neutrophils undergo respiratory burst and produce neutrophilic extracellular traps [207]. In solid organ transplantation neutrophils are typically the first leukocyte to infiltrate the transplanted graft [216]. While they have long thought not to play an important role in graft rejection recent evidence points towards a role in stimulation of angiogenesis and direct interactions between neutrophils and other leukocytes have been shown to promote allo-immunity [216]. Via secreted IL-6 MSCs have been reported to reduce respiratory burst and apoptosis in activated neutrophils [207]

Adaptive Immunity

B Cells: While T lymphocytes are the main effector cells responsible for destruction of the graft, B cells and B cell related products can contribute substantially to graft rejection/destruction. *In vitro* studies investigating the relationship between B cells and MSCs are conflicting and opposing results have been reported, although this could be a result of different culturing systems used and the reagents that were used for stimulation of the B cells [217-220]. Studies from Corcione *et al* [218] and Augello *et al* [217] have both convincingly demonstrated that MSCs inhibit B cell proliferation, differentiation into plasma cells and antibody secretion via MSC secreted factors. However, Traggiai *et al* [220] and Rasmusson *et al* [221] demonstrated that MSCs aid B cell proliferation, differentiation and antibody secretion. To date, more evidence has been collected to suggest that MSCs do in fact have inhibitory effects on B cells [222, 223]. MSCs have been shown to also alter the expression of chemokine receptors on

B cells in a PD-L1 contact dependent fashion [217, 218]. Considering that B cell responses are heavily dependent on T lymphocytes and T lymphocytes are heavily modulated by MSCs both *in vitro* and *in vivo*, the opposing *in vitro* B cell results may not be relevant *in vivo* if correct.

Regulatory B Cells (Bregs): In a kidney and liver transplant cohort, transplant tolerant patients had increased numbers of B cells and B cell related genes in peripheral blood when compared to patients who were on immunosuppressant regiments or to healthy controls [224, 225]. Interestingly, increases in immature and naive B cells have been related to tolerance in a model of islet allograft survival in nonhuman primates [226]. *In vitro,* MSCs have been shown to increase the proliferation of IL-10 secreting Bregs [227-229] and there is evidence of a IL-10 secreting B cell population which is known to be downregulated in autoimmune decreases [230]. Not only this but there is preliminary evidence for this IL-10 population in immunosuppressive free kidney transplant patients [231, 232]. If MSCs can increase this Breg population *in vivo* they may be able to contribute to prolongation of graft survival.

T Lymphocytes: Once T lymphocytes become activated they expand releasing pro-inflammatory cytokines and in the case of $CD8^+$ lymphocytes initiate cytotoxicity which will inevitably mediate graft destruction. As mentioned previously, early experiments by Di Nicola *et al* found that MSCs could inhibit the proliferation of T lymphocytes that had been stimulated by allogeneic peripheral blood lymphocytes, DCs or phytohemagglutinin (PHA). They showed that this inhibition was contact-independent and could be reversed using antibodies against TGF-β1 [199]. Since this study, MSCs have been shown to inhibit T lymphocytes under many different activation conditions including polyclonal mitogens, allogeneic cells or in an antigen specific fashion [198, 203, 219, 233-239]. Although many studies have been carried out since the early experiments, the mechanism of MSC T lymphocyte immunosuppression is still only partially understood with the mechanism being multifactorial. Both contact dependent and contact independent mechanism have been reported. Some of the soluble mediators initially need cell-cell contact to be secreted.

PD-L1 on MSCs is one such reported cell-cell contact mechanism, PD-L1 has been shown to directly inhibit T cell proliferation [217]. The receptor for PD-L1 is PD-1 and it is expressed on activated T cells, B cells, NK cells, T cells and myeloid cells.

Upon interaction with PD-L1 and PD-L2, PD-1 inhibits both the proliferation and effector function of T cells and also inhibits antibody production of B cells [240]. Interestingly, IFN-γ increases the expression of PD-L1 on MSCs and recently it was shown that PD-L1 and PD-L2 can be secreted from MSCs and this is one of their mechanisms of T lymphocyte suppression [241]

In work carried out by Meisel *et al*, indoleamine 2,3-dioxygenase (IDO) was described as being important in MSC-mediated T lymphocyte suppression, this result has been corroborated by others [234, 242]. However, this observation is human and non-human primate applicable and not the case in rodents [243]. Interestingly, when Chinnadurai *et al* [244] blocked IDO release from MSCs they noted a restoration of T lymphocyte proliferation but observed no such changes in IFN-γ secretion, the research group implicated that PD-L1 and PD-L2 suppressed T lymphocyte function.

Nitric oxide (NO) seems to be the main mediator of T lymphocyte suppression in rodents and IDO appears to be dispensable [236, 243]. Sato *et al* reported that Stat5 activation is paramount in T lymphocyte activation and that in the presence of MSCs, phosphorylation of Stat5 is absent. They reported that NO secreted from MSCs is responsible. Interestingly, when they used IDO and TGF-β neutralizing antibodies they did not see a reverse in effect, when inducible nitric oxide synthase (iNOS) inhibitors or PGE2 inhibitors were used they did see restoration in proliferation of lymphocytes [237].

Regulatory T Lymphocytes (Tregs): The relationship between MSCs and Tregs in the suppression of the allo-response is of interest in transplant biology. The two main MSC derived factors that are thought to induce Tregs are PGE2 and TGF-β [245, 246]. TGF-β is vital for the initiation and maintenance of forkhead box P3 (FoxP3) expression and also the suppressive nature of Tregs [247, 248]. PGE2 is an immunomodulatory lipid that is known to inhibit conventional T lymphocyte mitogenesis and block the production of IL-2, which is needed for T lymphocyte survival and proliferation [249, 250]. Not only this, PGE2 induces FoxP3 gene expression and modulates Treg function in human CD4+ T cells [251]. Also, PGE2 has been reported to encourage IL-10 production from macrophages [252, 253]. Both TGF-β and PGE2 are constitutively secreted by MSCs, especially in cytokine rich environments. Ge *et al* demonstrated using a renal allograft model that frequencies of

$CD4^+$ $CD25^+$ $FOXP3^+$ Tregs were increased in the spleen and in the allograft of MSC treated recipients compared to untreated animals [254].

While there are numerous suggested mechanisms responsible for MSC suppressive effects, there is definitive evidence to show that MSCs inhibit both the innate and adaptive arms of the allo-response, increasingly so in the presence of cytokines, in particular IFN-γ, TNF-α and IL-1β [236, 242]. **Figure 1.4** below summarises all the known methods by which MSCs exert their immunosuppressive effects on the cells of the immune system. In the next section I discuss the potential of pre-activating MSCs before use *in vivo* in order to immune their efficacy.

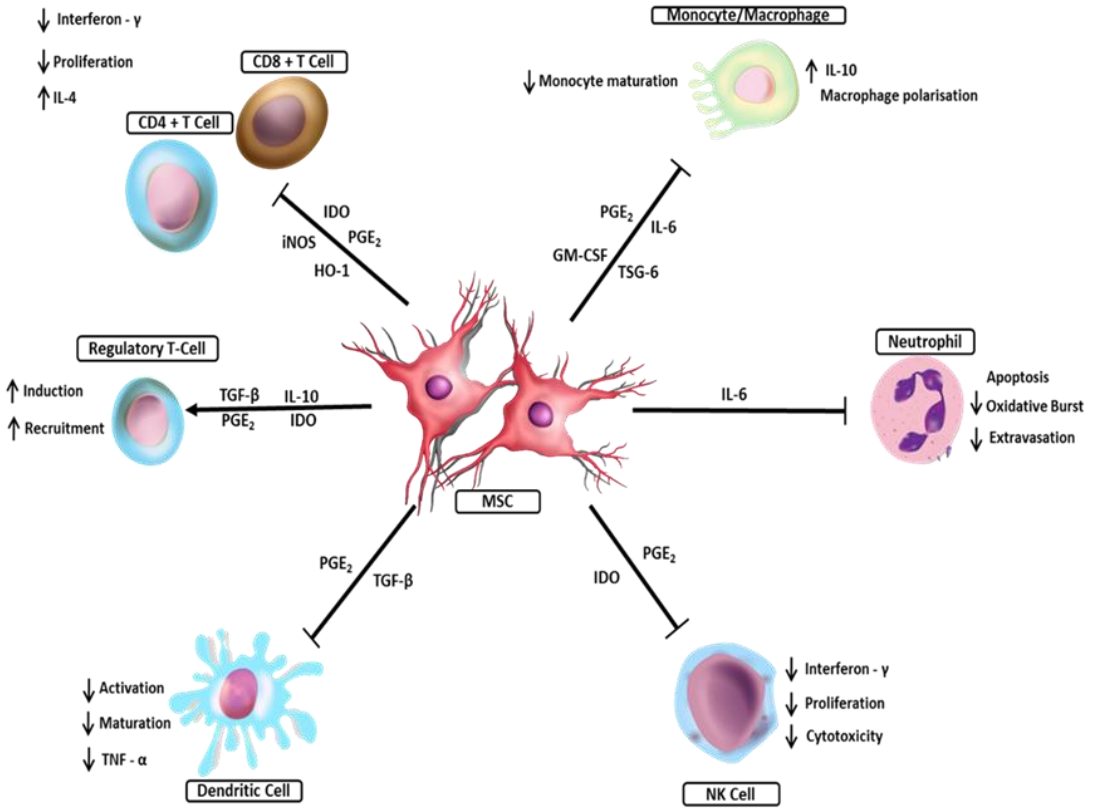

Figure 1.4 Proposed mechanisms of MSC interaction with immune cells. MSCs respond to local environmental cues and communicate with immune cells from both the innate and adaptive immune system through the secretion of immunoregulatory molecules. Via the secretion of interleukin-6 (IL-6), MSCs reduce neutrophil oxidative burst potential, decrease extravasation and increase apoptosis. MSCs prevent monocyte/macrophage maturation or shift it towards a tolerogenic phenotype, MSCs derived prostaglandin E2 (PGE_2), interleukin-6 (IL-6) and GM-CSF are key factors in this effect. Tumour necrosis factor-inducible gene 6 (TSG-6) decreases nuclear factor kappa-light-chain-enhancer of activated B cells (NF-κB) signalling and reduces the secretion of pro-inflammatory cytokines by inflammatory macrophages. Many different soluble and cell contact-dependent molecules have been accredited to MSC inhibition of both CD4+ and CD8+ T-cell activation and proliferation *in vitro*. These molecules can act via antigen presenting cells or on T-cells directly and include but are not limited to prostaglandin E2 (PGE_2), the tryptophan depleting molecule Indoleamine 2,3-dioxygenase (IDO), inducible nitric oxide synthase (iNOS) and heme oxygenase (HO-1), a molecule shown to be important in MSC-mediated suppression of allo-activated T lymphocyte. MSC have been shown to induce and recruit regulatory T lymphocytes via transforming growth factor beta 1 (TGF-β1), Indoleamine 2,3-dioxygenase (IDO), prostaglandin E2 (PGE_2) and the anti-inflammatory Interleukin-10 (IL-10). MSCs mediate their suppressive effects on dendritic cells via prostaglandin E2 (PGE_2) and transforming growth factor beta 1 (TGF-β1), resulting in decreased levels of CD80, CD86, MHCI, MHCII and secreted tumour necrosis factor-α (TNF-α). MSC limit NK cell cytolysis, inhibit proliferation and decrease the secretion of interferon – γ [62].

Pre-Activation / Licensing of MSCs

As previously described and summarised in **Figure 1.4**, MSCs have the capability to become potent regulators of immune cells. In steady state conditions MSCs reside in perivascular spaces surrounding almost every region of the body where they are thought to maintain tissue homeostasis by sensing tissue damage and then acting to promote tissue repair and healing after insult [255, 256]. MSCs become increasingly immunomodulatory once exposed to pro-inflammatory microenvironments (IFN-γ, TNF-α and IL-1β) [236, 250], not only this, it is also reported that pro-inflammatory environments enhance MSC homing capabilities and up-regulates their chemokine secretion. This allows MSCs to enter sites of inflammation and subsequently recruit immune cells to their locality where they can exert their immunomodulatory effects [236]. This phenomenon was first described by Krampera *et al*, they reported that IFN-γ secreted from activated T lymphocytes and NK cells was essential for MSC-mediated immunomodulation of both T lymphocytes and NK cells. They also reported that this effect was IDO mediated [242]. A corroborating report from Ren *et al* demonstrated that IFN-γ in combination with TNF-α, IL-1α or IL-1β increased the T lymphocyte suppressive effect of MSCs and they observed that this effect was reversible in the presence of neutralising antibodies to the pro-inflammatory cytokines . Ren *et al* also reported in the same study that IFN-γ receptor-deficient MSCs had no ability to suppress T lymphocyte proliferation in their co-culture systems showing the importance of pro-inflammatory stimulus for MSC-T lymphocyte suppression [236]. Also, these IFN-γ receptor-deficient MSCs lost the ability to prevent graft versus host disease (GvHD) in mice when compared to wild type MSCs. Activation of MSCs via pro-inflammatory microenvironments has been shown *in vivo*. In human GvHD, MSCs were administered either in an inflammatory (efferent phase) or non-inflammatory (at the time of bone marrow transplant) microenvironment [257-259]. MSCs administered at the time of the efferent phase of GvHD showed therapeutic efficiency while the MSCs administered at the time of the marrow transplant did not

Taken together these studies would suggest that the pre-activation of MSCs is beneficial in increasing their therapeutic efficacy as the MSCs would be actively secreting their immunomodulatory molecules on administration.

1.5.3 Therapeutic Application of MSCs in Corneal Transplantation

There is a plethora of data available on the therapeutic effects of MSCs in vivo [260]. To date, only small numbers studies have investigated the ability of MSCs to modulate corneal allograft survival. Most reports have shown positive results, which is encouraging, however as different MSC application strategies (time point of injection, cell number/number of injections, route of injection, MSC source, MSC pre-activation) have been employed in various animal models it is difficult to compare and validate the results.

MSCs ability to promote graft survival has been attributed to their modulation of the recipient immune system, altering the Th1/Th2 balance, expanding Foxp3 Tregs, polarizing macrophages and inhibiting intra-graft infiltration of antigen presenting cells. More in depth analysis is required to elucidate the mechanism of MSC-immunomodulation in vivo [62].

Regarding organ/tissue transplantation, first reports on beneficial effects of MSC therapy date back to 2002 when Bartholomew *et al* [198] reported that infusion of donor-derived baboon MSC ($20x10^6$ /kg bodyweight on day 0) led to a modest but significant prolongation of survival of MHC-mismatched donor and third-party skin grafts in baboons.

Even before MSCs were tested as a therapeutic agent to prolong corneal allograft survival, they were investigated for their potential to improve corneal injury following alkali burn [261, 262]. Oh *et al* [261] demonstrated that either local application (200 µl of $2x10^6$ MSC solution) of MSC isolated from Fischer rats or 200 µl MSC conditioned medium applied either once or daily for 3 consecutive days resulted in a reduction of corneal inflammation and neovascularization in a Sprague-Dawley rat corneal injury model. Moreover, a reduction of proinflammatory cytokines IL-2 and IFN-γ and an increase in anti-inflammatory cytokines IL-10, TGF-β1 and thormobospondin-1 in corneal tissue was reported. Interestingly, while the results with MSC conditioned medium were encouraging indicating paracrine therapeutic effects by molecules secreted from MSC in this model, the topical application of MSC onto the ocular surface was superior [261].

Recent work on the use of MSCs to modulate corneal graft survival is summarised in Table 1.1. In 2012, Jia *et al.* [263] reported that MSC treatment prolonged corneal

allograft survival in a rat corneal transplant model. The authors demonstrated that post-transplant i.v. injection of $5x10^6$ MSCs (days 0, 1 and 2) in Lewis rats receiving Wistar corneal transplants prolonged corneal allograft survival which could be further extended by co-application of Cyclosporine A. Further, the authors claim that i.v. injection of MSCs increased the ratio of $CD4^+$ $CD25^+$ $FoxP3^+$ cells compared with $CD4^+$ cells in the draining lymph nodes and increased production of anti-inflammatory cytokines (IL-4 and IL-10) and reduced proinflammatory cytokine (IL-2 and IFN-γ) secretion in lymphocytes isolated from MSC-treated animals. This report indicated that allogeneic MSCs have the potential to modulate corneal graft survival, but the time point of injection seems to be critical for the outcome of transplant survival. In 2012, Oh *et al* [264] also reported that human MSC injection prolongs corneal allograft survival claiming that human MSC application prevents early inflammation and late rejection in transplanted graft recipients. As previously investigated by this group, the beneficial effects of human MSCs were tested this time in a mouse corneal transplant model. Two peri-transplant i.v. injections of $1x10^6$ human MSCs at day 1 and day 0 (which were more effective than a single d0 injection) decreased early surgically-mediated inflammation but also reduced the activation of APCs in the cornea and in the lymph nodes. Consequently, immune rejection was prevented, and graft survival was prolonged. The authors did not find evidence for engraftment of human MSCs [262]. Mechanistically, the authors found that human MSCs were trapped in the lungs of treated animals wherein they became activated and secreted TSG-6, which, in turn, modulated the early inflammatory response and attenuated graft rejection. We have shown in the past [265] in a rat model of corneal transplantation that syngeneic MSCs administered at days +7 and 0 did not prolong corneal allograft survival despite reducing inflammatory cell populations in the corneal graft; however, no increase in Tregs cells were observed in the organs of treated animals. Moreover, these results support other reports from the literature that MSC need to be immune-activated to exert their therapeutic effects. In 2011, Duijvestein *et al* [266] reported that mouse MSCs treated with IFN-γ (500 U/ml) have enhanced immunosuppressive properties in murine colitis models compared with untreated MSCs. In addition, induced nitric oxide synthase (iNOS), one of the key molecules involved in MSC mediated immunosuppression in rodents, was found to be up-regulated following treatment with IFN-γ which also resulted in enhanced inhibition of T cell proliferation [266].

1.6 Research Hypotheses and Aims of Research

1.6.1 Research Hypotheses

1) Sialyation is important in regulating immunogenicity and tolerogenicity of iDCs and tDCs.

2) Pre-activation of MSCs prior to administration *in vivo* will stimulate their immunomodulatory properties enabling them to prolong corneal allograft survival.

1.6.2 Aims of Research

Chapter 3:

- To profile the glycocalyx of dexamethasone generated tDCs.
- To identify if sialic acid is important in the ability of iDCs and tDCs to regulate T lymphocytes *in vitro*.

Chapter 4 + 5:

- To identify a cytokine pre-treatment strategy that enhances MSCs immunomodulatory phenotype and properties.
- To characterise the enhanced MSC phenotype, identify mechanism of immune modulation and select a pre-treatment strategy to administer *in vivo*.
- To establish a fully allogeneic MHC mismatched corneal transplant model in mouse.
- To identify an efficacious strategy for *in vivo* administration of pre-treatmented MSCs to prolong corneal allograft survival.
- To evaluate the in vivo immunomodulatory properties of pre-activated MSCs.

Paper	Source	Recipient Species (Xeno-, allo- or syn- geneic)	Normal (NR) or High Risk (HR) Model	Route (Timing of Administration)	Number of MSC Per Injection (Number per kg body weight)	Outcome	Mechanism of action
Oh et al.[264]	Human BM MSC	BALB/c Mouse **(Xenogeneic)**	NR	IV administration (d-1) IV administration (d-1, d0)	$1x10^6$ MSC **($58.8x10^6$/kg)**	hMSCs through TSG-6 reduced the surgery induced inflammation prolonging allograft survival in a dose-dependent manner	hMSC treatment reduced IL-6, IL-1β and IL-12 levels and infiltrating APCs in the cornea and dLN subsequently inhibiting the adaptive CD4+ and CD8+ T cell immune response The effect was mediated by TSG-6 as demonstrated by TSG-6 siRNA knock down and recombinant TSG-6 IV administration
Ko et al. [267]	Human BM MSC	BALB/c Mouse **(Xenogeneic)**	NR	IV administration (d-7, d-3)	$1x10^6$ MSC **($58.8x10^6$/kg)**	hMSCs prolong allograft survival by enriching a population of regulatory myeloid cells in the lung mediated by TSG-6	hMSCs in a TSG-6 dependent manner induced a MHC class $II^+B220^+CD11b^+$ population of myeloid cells in the lung which remained in circulation for up to 7 days post MSC administration This specific myeloid cell population suppressed T cell proliferation in vitro and could prolong allograft survival when adoptively transferred
Fuentes Julian et al. [268]	Human AD MSC Rabbit AD MSC	New Zealand White Rabbit **(Xenogeneic)** **(Syngeneic)**	NR + HR	NR – SI administration (d0) HR – IV administration (d-7, d0, d3, d14)	NR/HR – $2x10^6$ MSC **($0.666x10^6$/kg)**	SI in the NR model and IV injection in the HR model lead to more rapid allograft rejection compared to controls	SI or IV administration of hAD-MSC or rAD-MSC lead to an increase in corneal edema and a higher number of infiltrating CD45+ leukocytes which could be attributed to MSCs production of inflammatory cytokines IL-6 and IL-8
Omoto et al. [269]	BALB/c Mouse BM MSC GFP^+C57BL/6 Mouse BM MSC	BALB/c Mice C57BL/6 Mice **(Syngeneic)**	NR	IV administration (d0) IV administration (d0, d7)	$1x10^6$MSC **($47.62x10^6$/kg)**	BALB/c MSC prolong allograft survival in a C57BL/6 host in a dose dependent manner	IV administered MSCs migrated to the transplanted cornea, conjunctiva and draining lymph nodes where they suppressed the maturation of CD11c+MHC II+ APCs, consequently inhibiting DCs direct and indirect allo-sensitization of CD4+ T cells

Jia et al. [263]	Wistar Furth Rat BM MSC	Lewis Rat **(Allogeneic)**	NR	IV administration (d-3, d-2, d-1) IV administration (d0, d1, d2)	$5x10^6$MSC **($25x10^6$/kg)**	Allograft survival was prolonged by post-surgical but not pre-surgical MSC administration Co administration of MSCs with low dose CsA (1mg/kg) accelerated graft rejection while administration with 2mg/kg CsA prolonged allograft survival	Post-operative MSC administration inhibited T cell proliferation both i*n vitro* and *in vivo* decreasing expression of Th1 associated cytokines IFN-γ and IL-2 and increasing Th2 associated IL-4, while expanding CD4+CD25+Foxp3+ regulatory T cells
Treacy et al.[265]	Lewis Rat BM MSC Wistar Furth Rat BM MSC Dark Agouti Rat BM MSC	Lewis Rat **(Syngeneic)** **(Allogeneic)**	NR	IV administration (d-7, d0)	$1x10^6$ MSC **($3.95x10^6$/kg)**	MSCs derived from allogeneic sources (WF BM MSC and DA BM MSC) significantly prolonged allograft survival while recipient derived (syngeneic) Lewis BM MSC failed to prolong allograft survival	Allo-MSC inhibited the intra-graft infiltration of CD3+CD8+CD161+ NKT cells, CD11b/c+ APCs, CD4+CD25+ activated T cells and CD45RA+ B cells, while also expanding a population of CD4+CD25+Foxp3+ splenic regulatory T cells DTH experiment demonstrated allo-MSC specifically inhibit corneal donor alloantigen sensitization

Table 1.1 The application strategy and major findings from the most recent MSC therapy in cornea transplantation studies. IV, intravenous; SI, stromal injection; NR, normal risk; HR, high risk; MSC, mesenchymal stromal/stem cell; BM, bone marrow derived; dLN, draining lymph node.

Chapter Two:

Methods

2.1 Introduction

Herein lies the detailed descriptions of all the techniques, materials and methods used in examining MSC and BMDC biology. The reader is referred to this chapter for detailed descriptions of the individual techniques discussed in later chapters.

2.2Animal Strains and Ethical Approval

2.2.1 Murine Strains

All mice used in experiments were accommodated in an accredited animal housing facility under a license granted by the Department of Health, Ireland, and were approved by the Animals Ethics Committee of the National University of Ireland, Galway. 8 to 14-week-old female BALB/c, BALB/c C.Cg-Foxp3^{tm2Tch}/J and C57BL/6J mice were purchased from Envigo. Experimental animals were housed in a specific pathogen-free facility and fed a standard chow diet.

2.2.2 Rat Strains

All rats used in experiments were accommodated in an accredited animal housing facility under a license granted by the Department of Health, Ireland, and were approved by the Animals Ethics Committee of the National University of Ireland, Galway. Bone marrow used in the generation of BMDCs was isolated from male Dark Agouti (DA, RT-1^{avl}) rats at 8-14 weeks of age. For the allogeneic T lymphocyte co-cultures, male Lewis (LEW, RT-1^{l}) rats served as a source of lymphocytes, isolated from both the cervical and mesenteric lymph nodes and spleen. DA and LEW rats were obtained from Envigo. Experimental animals were housed in a specific pathogen-free facility and fed a standard chow diet.

2.3 Murine Cell Isolation

2.3.1 MSC Isolation

Mice were euthanised by CO_2 inhalation and the femur and tibia were removed, cleaned of connective tissue and placed in MSC medium, MEM-α (Biosciences-Gibco) supplemented with 10% heat inactivated FBS (Fisher – Hyclone or Sigma), 10% equine serum (Fisher – Hyclone) and 1% penicillin/streptomycin (Sigma). The heat inactivated FBS was pre-screened to ensure it supported MSC growth and differentiation. The epiphysis of each bone was cut, and cells were flushed out with culture medium using a 30.5-gauge needle. Clumps were removed by filtering through

a 70µm mesh filter. Cells were then centrifuged at 400 x g for 5 minutes, re-suspended in 25ml culture medium and plated at a density of $9x10^5$ per cm^2 in a T175. Cells were incubated at 37ºC, 21% O_2, 5% CO_2 (Normoxic) or 37ºC, 5% O_2, 5% CO_2 (Hypoxic) and non-adherent cells were removed 24 hours later. This process was repeated 3 times per week until cells reached confluency. At this point trypsin was added and incubated at 37ºC for 5 minutes. Culture medium was added to neutralise trypsin. Cells no longer adhering to the flask were removed, centrifuged and re-plated. Characterisation was carried out at passage 4.

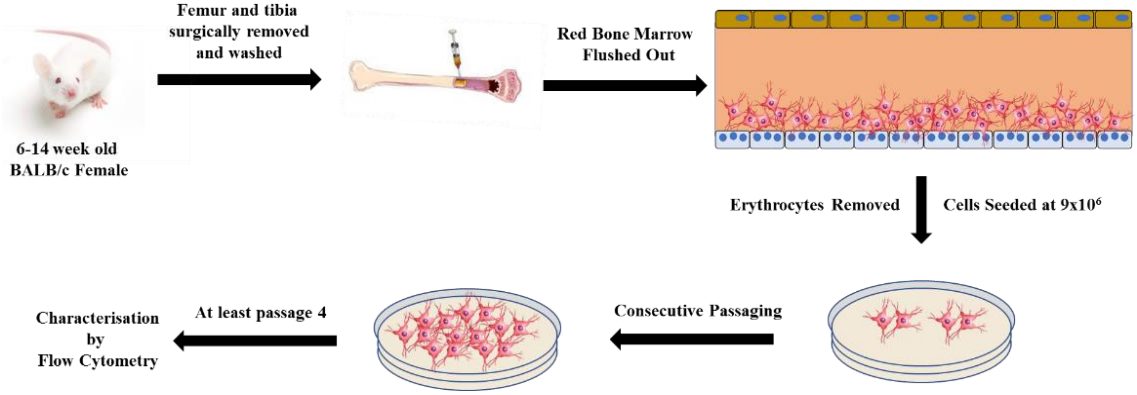

Figure 2.1 Isolation and generation of mouse BALB/c MSCs.

2.3.2 Macrophage Isolation

Mice were euthanised by CO_2 inhalation and the femur and tibia were removed, cleaned of connective tissue and placed in macrophage culture medium. Macrophage medium consisted of 65% complete medium and 35% L929-conditioned medium. Complete medium: RPMI 1640 (Lonza) supplemented with 10% FBS (Sigma), 1% sodium pyruvate, 1% non-essential amino acids, 1% L-glutamine, 1% penicillin/streptomycin (all Sigma) and 0.01% β-mercaptoethanol (Sigma). L929-conditioned medium: DMEM medium (Lonza), 10% FBS (Sigma) and 1% penicillin/streptomycin (Sigma) collected from 3-day cultures of L929 cell lines which produce M-CSF. The epiphysis of each bone was cut, and cells were flushed out with macrophage medium using a 30.5-gauge needle. Clumps were removed by filtering through a 70µm mesh filter. Cells were then centrifuged at 400 x g for 5 minutes, red blood cells were removed using ACK buffer and the cells were centrifuged at 400 x g for 5 minutes. The cells were re-suspended at $2.25x10^6$ cells/ml in macrophage medium and plated at a density of $4.5x10^6$ per well of a 6 well plate. Cells were incubated at 37ºC, 5% CO_2, changing the medium every two days. This process was

repeated for 6 days. Trypsin was added for 10-12 mins at 37°C to detach the macrophages from the plates. Culture medium was added to neutralise trypsin. Cells no longer adhering to the plates were removed and counted. If stimulated macrophages were required, IFN-γ (100u/ml) was added on day 6 for 24 hours followed by LPS (10ng/ml) stimulation for 4 hours.

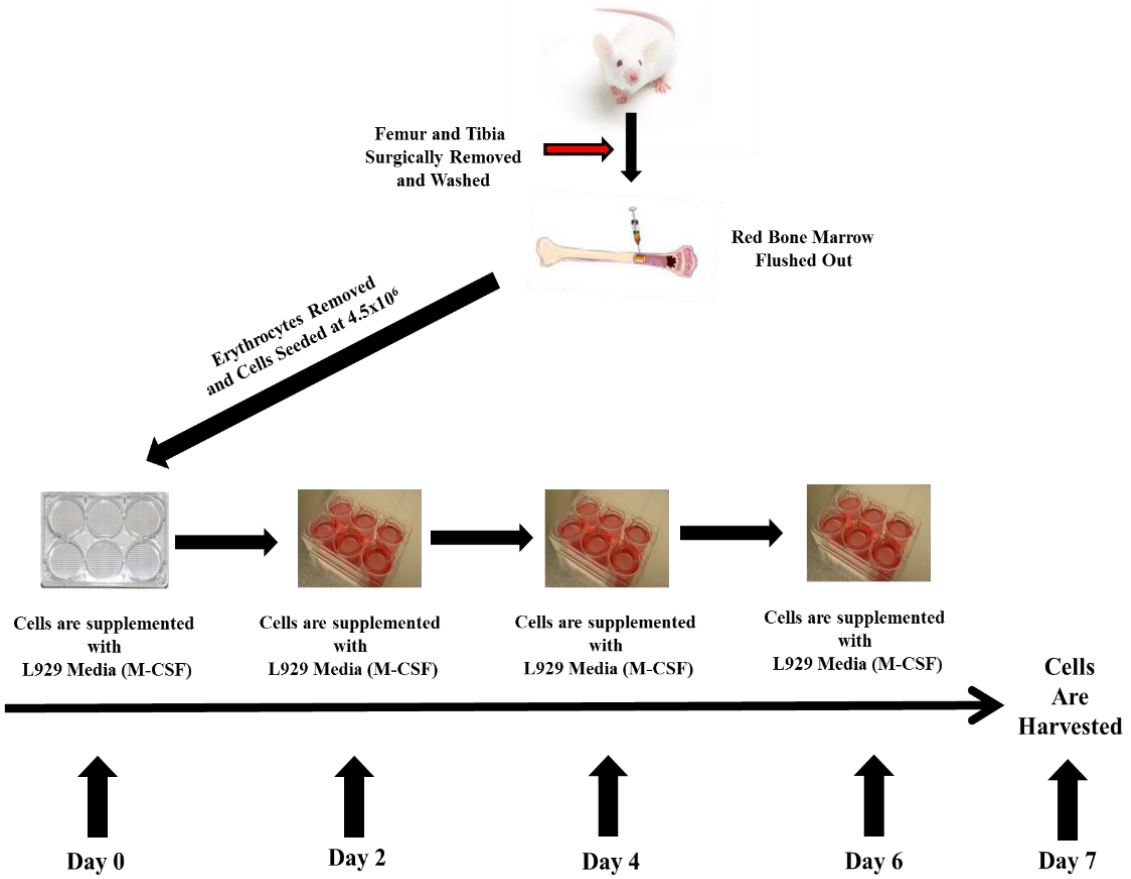

Figure 2.2 Isolation and generation of mouse BALB/c macrophages.

2.4 Rat Cell Isolation

2.4.1 Isolation and Generation of iDCs and tDCs.

iDCs were generated using an adapted version of the protocol which has been previously described ([169]). Briefly, on day 0, male DA rats of the specified age were sacrificed, and the tibia and femur were surgically removed post-mortem. The epiphyses were cut, and the bone marrow was flushed from the long bones with a syringe/needle combination. The erythrocytes were removed from the suspension by lysis using a standard red blood cell lysis buffer (Sigma). After erythrocyte lysis, the cells were washed in RPMI-1640 (Gibco) medium supplemented with 10% FBS, 2 mmol/L L-glutamine, 100 mmol/L nonessential amino acids, 1 mmol/l sodium

pyruvate, 100 U/mL penicillin, 100 µg/mL streptomycin, and 55 µmol/L β-mercaptoethanol (Sigma). Cells were resuspended at a concentration of 1.5 x 10^6/mL and plated at a concentration of 4.5 x 10^6 per well of a 6 well plate. The culture medium was supplemented with 5 ng/mL rat GM-CSF (Invitrogen) and 5 ng/mL rat IL-4 (Peprotech). Cells were incubated under standard cell culture conditions (37 °C at 5% CO_2) and, on the 3rd day of culture, half of the medium from each well was harvested and cells were resuspended in fresh medium supplemented with rat GM-CSF and IL-4 and added back into the culture. On the 5th day, the supernatant was exchanged with fresh supplemented growth medium to remove dead granulocytes and lymphocytes. In experiments requiring tDCs, Dexa (Sigma-Aldrich) was added to the culture at 10^{-6} mol/L at this point. On the 7th day of culture half of the medium was again removed and replaced with fresh supplemented medium (Dexa was added as required). To generate mDCs, LPS (1 µg/mL; Sigma-Aldrich) was added 24 hours before the cells were cultured. Cultures were maintained until day 10 and then gently pipetted off the bottom of the wells for the *in vitro* assays.

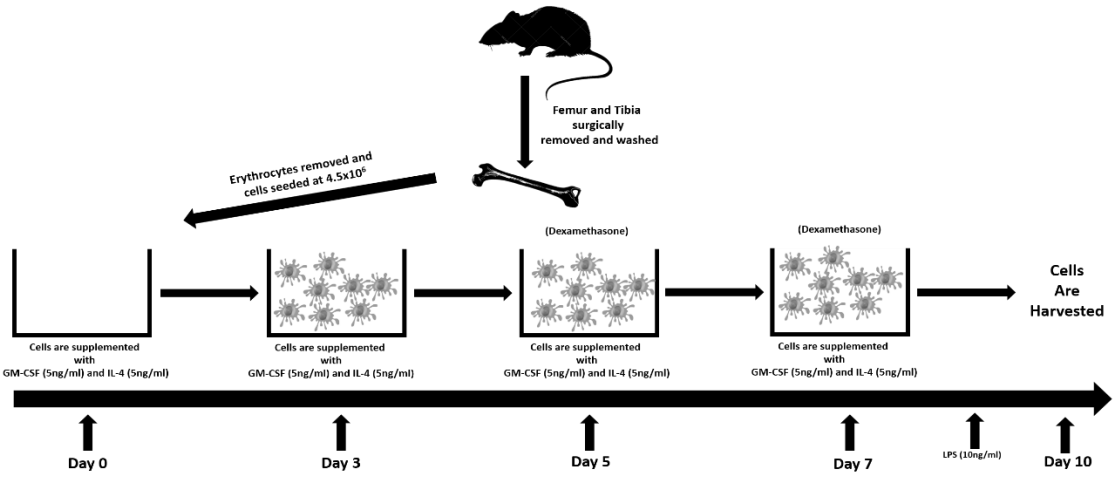

Figure 2.3 Isolation and generation of rat DA BMDCs.

2.5 MSC Differentiation, Characterisation and Pre-activation Strategy.

2.5.1 Adipogenesis

To differentiate MSCs to adipocytes, 2x10^5 MSCs were plated in each well of a 6 well plate in 2ml of MSC medium. Cells were incubated at 37ºC, 5% CO_2 until confluency was reached. Once confluent, MSC medium was removed and replaced with 2ml per well of adipogenic induction medium (see table 2.1). Control wells received standard

MSC medium. Medium was changed on day three and replaced with adipogenic maintenance medium (see table 2.2). Again, control wells received standard MSC medium. Medium was changed every three days for a total of three cycles of induction and maintenance medium. The last addition of maintenance medium was left on the cells for 5 days. After 5 days, the maintenance medium was removed. PBS was used to wash the MSCs twice and then the MSCs were fixed in 10% neutral buffered formalin for at least 30 mins at room temperature. After fixation the formalin was removed and the MSCs were washed with distilled water. A working stock of Oil Red O (Sigma) was prepared by adding six parts Oil Red O to four parts distilled water and then this working solution was then added to both control and test wells. The wells were lightly agitated by swirling left to right, to ensure maximum coverage. This was then incubated for five minutes at room temperature. The Oil Red O stain was then removed and 60% isopropanol (Sigma) was added to each well to remove excess Oil Red O. The Isopropanol was then removed, and the wells were washed with distilled water. Hematoxylin was diluted at a ratio of 1:5 in distilled water and added at 500µl to each well and allowed to stand for 1 minute. Wells were then washed in warm tap water and covered with 500µl of dH_2O for images to be taken on an inverted light microscope. To process the MSCs for absorbance measurements, 500µl of 99% isopropanol (Sigma) was added to each well to strip the stain from the MSCs. This was repeated two times and all the isopropanol was collected. The tubes were spun at 500 x g for 5 mins. 200µl of this solution was then added to a 96-well flat bottom plate in triplicate. Absorbance was measured at 520nm on a Wallac1410 plate reader (Perkin Elmer). Results were plotted as mean absorbance.

Reagent	Volume (for 100ml)	Final Concentration
DMEM (High glucose)	87.6ml	
Dexamethasone 1mM	100µl	**1µM**
Insulin 1mg/ml	1ml	**10µg/ml**
Indomethacin 100mM	200µl	**200µM**
500mM MIX	100µl	**500µM**
Penicillin/streptomycin	1ml	**100U/mL penicillin** **100µg/mL streptomycin**
FBS	10ml	**10%**

Table 2.1. Adipogenic induction medium recipe.

Reagent	Volume (for 100ml)	Final Concentration
DMEM (High glucose)	88ml	
Insulin 1mg/ml	1ml	**10µg/ml**
Penicillin/streptomycin	1ml	**100U/mL penicillin** **100µg/mL streptomycin**
FBS	10ml	**10%**

Table 2.2. Adipogenic maintenance medium recipe.

2.5.2 Osteogenesis

To differentiate MSCs to osteocytes, $2x10^5$ MSCs were plated in each well of a 6 well plate in 2ml of MSC medium. The cells were incubated at 37°C, 5% CO_2 until the cells were confluent. Once the MSCs were confluent, the MSC medium was removed and it was replaced with osteogenic medium (see table 2.3). Control wells received standard MSC medium. Medium was changed every 2 days and replaced with either control MSC medium or osteogenic medium. Observing the condition of the monolayer, cells were harvested between 10 and 17 days. The monolayer can become detached from the plate, if this occurs, harvest the cells before they reach this point. The osteogenic potential of the cells was assayed by Alizarin Red Staining.

Reagent	Volume (for 100ml)	Final Concentration
Iscoves MEM	77.5ml	
Dexamethasone 1mM	10µl	**100nM**
Ascorbic acid 2-P 10mM	0.5ml	**50µM**
β glycerophosphate 1M	2ml	**20mM**
L-thyroxine	50µl	**50ng/ml**
FBS	9ml	**9%**
Equine serum	9ml	**9%**
L-glutamine	1ml	**2mM**

Table 2.3 Osteogenic Medium recipe.

2.5.3 MSC Characterisation

MSCs were characterised as plastic adherent with a capacity for tri-lineage differentiation and having the presence or absence of the antigens reported by The International Society for Cellular Therapy in their definition. Surface antigen

characterisation was carried out by flow cytometry. Positive antigens included CD90. CD73, CD105, SCA-1 and CD44. Negative antigens included CD45, CD11b, CD11c, MHC II, CD80 and CD86 (All eBioscience).

2.5.4 MSC Licensing/Pre-activation

Pre-activation of MSCs was carried out using three pro-inflammatory cytokines (IFN-γ, TNF-α and IL-1β) (All Peprotech) and one anti-inflammatory cytokine (TGF-β) (Bio-Techne). All cytokines were used at 50ng/ml. MSCs were seeded at 50,000 cells/ml in a T175 in 20ml of MSC medium. The cells were given 24 hrs to adhere in either hypoxic or normoxic conditions, depending on the experiment. After this incubation time, pro-inflammatory cytokines were added alone or in combination (figure 2.4). TGF-β was only added alone. After addition of the cytokine, the MSCs were incubated for 72 in hypoxia or normoxia. The cells were then washed twice with 10ml of PBS. 5ml of trypsin was added and the cells were incubated for 5 mins at 37^{o}C. Trypsin was neutralised by adding 10ml of FBS containing medium. The MSCs were then washed twice in PBS and counted before used in subsequent experiments.

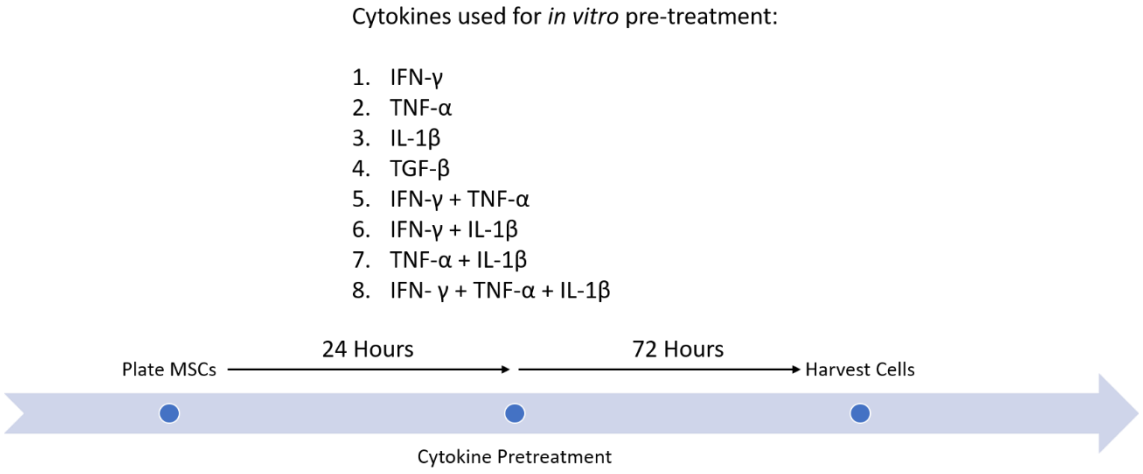

Figure 2.4 Protocol for MSC pre-activation.

2.6 In vitro Assays

2.6.1 Enzyme-linked Immunosorbent Assay (ELISA)

Supernatants from various *in vitro* assays and mixed lymphocyte reaction experiments were analysed using Ready-SET-Go! ® ELISA kits (Affymetrix-eBioscience). Nunc MaxiSorp™ 96-well flat-bottom plates (ThermoFisher Scientific) were coated with 50µl/well of capture antibody diluted in coating buffer (according to manufacturer's

instructions), sealed and incubated overnight at 4ºC. The plate was then aspirated and washed (175µl) 3 times in ELISA wash buffer (1 x PBS with 0.05% Tween-20) with time given for soaking (1 minute) between washes. The plate was then blotted on tissue paper to remove any residual buffer. Once the buffer was removed, the plates were blocked with ELISA diluent (according to manufacturer's instructions) for 1 hour at room temperature. The plate was then aspirated and washed once in ELISA wash buffer. The standards were diluted in ELISA diluent according to manufacturer's instructions and 50µl was put into the appropriate wells. 2-fold serial dilutions were performed of the top standards to make the standard curve for a total of 8 points. 50µl of test sample was added to the appropriate wells. The plate was sealed and left at 4ºC overnight to insure maximal sensitivity. The plate was then aspirated and washed (175µl) 5 times in ELISA wash buffer. 50µl of detection antibody (diluted according to manufacturer's instructions) was added to the wells and incubated at room temperature for 1 hour. The plate was then aspirated and washed (175µl) 5 times in ELISA wash buffer. 50µl of Avidin-Horse radish peroxidase was added to the wells and was incubated at room temperature for 30 minutes. The plate was then aspirated and washed (175µl) 5 times in ELISA wash buffer, in this step the wells were allowed soak for 2 minutes between washes. 50µl of Tetramethylbenzidine substrate solution was added to each well and the plate was incubated at room temperature for 15 minutes. 50µl of 2N sulfuric acid was added after the 15 minutes to stop the reaction. The plate was then read at 450 and 570nm on a Wallac 1420 plate reader (Perkin Elmer).

2.6.2 Griess Assay

A Griess assay was used to quantify the nitric oxide levels in cell culture supernatants. 2µl of Griess assay standard was added to 998µl of appropriate cell culture medium to create a 100µM which served as the 1st standard. Six 2-fold serial dilutions of 1st standard in appropriate cell culture media was carried out to create standards and cell culture media alone served as a blank. 100µl of standard or sample was added to each well of a 96-well flat bottom plate. Griess Solution A and Griess Solution B were mixed at a ratio of 1:1 to make up Griess assay working solution. 100µl of Griess assay working solution was added to wells of 96-well plate. The absorbance was read at 540nm on a plate reader.

2.6.3 DQ OVA Assay

Cells from various *in vitro* assays and sources were seeded in a 96-well round bottom plate at a concentration of $1x10^5$ cells/250µl in appropriate cell culture medium. DQ OVA (Molecular Probes, Invitrogen) was added to the cells at a final concentration of 50µg/ml. Cells were collected at various time points. The cells were washed in PBS and resuspended in FACS buffer for flow cytometry analysis.

2.6.4 RNA-isolation and RT-PCR

RNA was exacted from iDCs, tDCs, mDCs, and ntDCs on day 10 using Bioline Isolate II RNA mini kits according to manufacturer's protocols. All cDNA was produced using RevertAid^{TM} H Minus Reverse Transcriptase (ThermoFisher Scientific) with random primers. For primer sequences of, GAPDH, TNF-α, IL-12p40, iNOS IL-10, IDO, IL-6, and IL-1β see Table 2.4. All samples were normalized to expression of the house-keeping gene GAPDH and made relative to iDCs. All quantitative real-time PCR was performed according to the standard program using a real-time PCR system (StepOne Plus, Applied Biosystems, ThermoFisher Scientific).

Gene	Forward	Reverse	Probe
iNOS	TTCCCATCGCTCCGCTG	CCGGAGCTGTAGCACGCA	AACACAGTAATGGCCGACCTGATGTTGC
IDO	CAGGTTACAGCGCCTGGCAC	TCGCAGTAGGGAACAGCAAT	ACATCACCATGGCGTATGTGTGGAA
IL-10	GAAGACCCTCTGGATACAGCTGC	TGCTCCACTGCCTTGCTTTT	CGCTGTCATCGATTTCTCCCCTGTGA
IL-6	TCAACTCCATCTGCCCTTCAG	AAGGCAACTGGCTGGAAGTCT	AACAGCTATGAAGTTTCTCTCCGCA
IL-1β	AACAGCAATGGTCGGGACATA	CATTAGGAATAGTGCAGCCATCTTTA	TTGACTTCACCATGGAACCCGTGTCTT
GAPDH	NM_017008.4 (Thermo Fisher Scientific, Waltham, MA)		
IL-12p40	NM_022611.1 (Thermo Fisher Scientific, Waltham, MA)		
TNF-α	NM_012675.3 (Thermo Fisher Scientific, Waltham, MA)		

Table 2.4 Forward and reverse primer information for rat RT-PCR

2.6.5 T Lymphocyte Co-Cultures

2.6.5.1 Suppression Assays

On the morning of the assay, lymph nodes and spleens were harvested from animals and single cell suspensions were obtained by mechanical disruption of the tissue. This was achieved by passing it through a 40µm cell strainer in RPMI 1640 (Fisher-Lonza) supplemented with 10% FBS (Sigma), 1% sodium pyruvate, 1% non-essential amino acids, L-glutamine, 1% penicillin/streptomycin (all Sigma) and 0.01% β-

mercaptoethanol. Lymphocyte proliferation was assayed by staining the cells with CellTrace™ Violet (CTV) (Invitrogen) according to manufacturer's instructions. Lymphocytes ($1x10^6$) were stained with 1µl of CTV in 1ml of PBS for 20 minutes in the dark with gentle agitation every 5 minutes. The staining process was terminated by adding 4mls of FBS containing culture medium. The FBS will soak up any remaining CTV in the solution. The lymphocytes were then washed twice in PBS. Lymphocytes were then activated using CD3/CD28 Mouse T-Activator Dynabeads® (Life Technologies). $2x10^5$ CTV stained lymphocytes were placed into well of a 96-well round bottom plate. MSCs or DCs were placed into the wells at different ratios (1:10, 1:20, 1:50, 1:100) and the culture was placed into an incubator for 3/4 days at 37 °C following which T-cell proliferation and activation were assayed by flow cytometry. Anti-CD3/CD28 bead stimulated T cells alone served as positive controls in all T cells immunosuppression assays and unstimulated T cells in the absence of anti-CD3/CD28 beads served as negative controls.

2.6.5.2 Immunogenicity Assays

Lymphocytes were isolated from the spleen and lymph nodes of LEW rats. Lymphocytes were washed with phosphate-buffered saline and stained in pre-warmed (37°C) CellTrace™ Violet (CTV) phosphate-buffered saline staining solution (Invitrogen) as per manufacturer's instructions. For positive controls 2×10^5 CTV-stained lymphocytes were stimulated at a 1:1 ratio with anti-rCD3/anti-rCD28-labeled beads in supplemented RPMI 1640 media. Test wells did not receive anti-rCD3/anti-rCD28-labeled beads. Assays were incubated at various BMDC: T-cell ratios in a humidified incubator for 4/5 days at 37 °C following which T-cell proliferation and activation were assayed by flow cytometry (mAbs CD3-PE, CD4-APC and CD8α-PE-Cy7; Biolegend). T-cell proliferation, activation, and differentiation were analysed using a FACS Canto II.

2.6.5.3 Inhibitor Co-Cultures

For SMAD 2 inhibition, SB431542 (Cell Signalling, #14775S) was used at 10 µM two hours prior to treatment with TGF-β. To inhibit CD73 activity Adenosine 5′-(α, β-methylene) diphosphate (AMP) (Sigma M3763) was added to T lymphocyte co-cultures at a final concentration of 100 µM. The selective EP1 antagonist (SC-51322) and selective EP4 antagonist (L-161,982) (Both Cayman Chemicals, Ann Arbor, MI, USA) were used in T lymphocyte to assay the importance of EP/PGE2 signalling. The

EP1 antagonist was used at a final concentration of 1mM and the EP4 antagonist was used at a final concentration of 1mM.

2.6.5.3 Analysis of Proliferation and Activation

After the incubation period, medium was removed from the wells and stored at -80ºC for further analysis. The cells were washed twice in FACs buffer (PBS supplemented with 1% FBS and 0.05% sodium azide). Cells were incubated with CD8a-APC (Biolegend) or CD4-PE-Cy7 (Biolegend) for 10 minutes at 4ºC. Cells were washed twice in FACS buffer and proliferation was measured using a FACSCanto® II cytometer (Becton Dickinson). Data was analysed using FlowJo® v10 software (TreeStar Inc.).

2.7 Flow Cytometry

2.7.1 General Cell Surface Antigen Staining

Cells were prepared for flow cytometry as follows. Cells were washed and trypsinised or were isolated from tissue and resuspended in a single cell suspension of FACs buffer. Cells were counted and seeded in a 96-well V-bottom plate. Cells were then centrifuged at 800 x g (lymphocytes, splenocytes and lung tissue) or 400 x g (all other cells) or for 5 minutes. Surface molecules were stained with flow cytometry antibodies for 15 minutes at 4°C in 50µl FACS buffer. Cells were washed with FACS buffer three times and resuspended in 100µl of FACS buffer and transferred to a FACS tube for analysis. For lectin couple flow cytometry, the lectins listed in table 2.10 were biotinylated. PE or APC tagged streptavidin was used as secondary antibodies to allow visualization by flow cytometry.

2.7.2 Viability Staining

Cells were first prepared as described in section 2.7.1. Once resuspended in 100µl of FACS buffer, viability dyes such as SYTOX blue or SYTOX AADvanced was added. The FACS tube was vortexed and cells incubated at 4°C for 20 minutes in the dark prior to analysis by flow cytometry. Cells were incubated with a 1% bleach solution as a positive control for cell death.

2.7.3 Intracellular Cytokine Staining for Flow Cytometry

Brefeldin A (0.6µg/ml) was added to the culture 6 hours before harvesting the cells. This stops the secretion of the cytokines into the supernatant. Following this

incubation period, the cells were harvested and centrifuged at 400 x g for 5 minutes. The supernatant was carefully removed from the cells and stored at -80ºC for further analysis. If surface stains were being used in combination with intracellular stains they were added at this point, following the protocol described in section 2.7.1. After surface staining the cells are washed 3 times. 100µl paraformaldehyde (2%) was added to the cells for 10 minutes to fix the cells. Cells were washed three times with 100µl of FACs buffer and centrifuged at 400 x g for 5 minutes. The supernatant was carefully discarded using a pipette and 100ul of permeabilization buffer (0.5% Saponin in 1% BSA/PBS) was added along with the intracellular antibody of interest or an isotype control. Following 15 minutes of incubation in the dark at room temperature the cells are washed 3 times in FACs buffer and centrifuged again at 400 x g. The cells were then resuspended in 100µl of FACs buffer and ran on a FACSCanto® II cytometer (Becton Dickinson).

2.7.4 Flow Cytometry Analysis of Mouse Tissue

Several polychromatic flow cytometry panels were used to identify immune cell populations of interest. After the cells were prepared as discussed in section 2.10.5 the cells were staining according to section 2.7.1 with the following panels **(Table 2.9**).

CD4+ T Cells					**CD8+ T Cells**		
Antigen	Fluorochrome	Catalog Number			Antigen	Fluorochrome	Catalog Number
CD3	FITC	100204			CD3	FITC	100204
CD69	PE	104508			CD69	PE	104508
Sytox	PerCP	S10349			Sytox	PerCP	S10349
CD44	PE-CY7	103030			CD44	PE-CY7	103030
CD4	APC	100412			CD8	APC	100712
CD25	BV421	102034			CD25	BV421	102034
CD62L	BV410	104441			CD62L	BV410	104441
FoxP3	GFP	N/A					
TH T Cell Subset					**B Cells**		
Antigen	Fluorochrome	Catalog Number			Antigen	Fluorochrome	Catalog Number
CD3	FITC	100204			CD19	FITC	152404
CCR6	PE	129804			CD5	PE	100608
CD4	PE-CY7	100422			CD24	PE-CY7	101822
CCR4	APC	131212			CD45.2	APC	109814
CXCR3	BV421	126522			Sytox	PerCP	S10349
Sytox	PerCp	S10349					
Neutrophils/NK Cells					**Antigen Presenting Cells**		
Antigen	Fluorochrome	Catalog Number			Antigen	Fluorochrome	Catalog Number
GR1	PE	108408			CD11b	FITC	108910
CD49b	PE-Cy7	108922			CD11c	FITC	117306
CD115	BV410	135513			MHC I	PE-CY7	
Sytox	PerCP	S10349			MHC II	APC-Strep	115003
					CD86	BV421	104726
					CD80	BV510	105040
					CD69	PE	104508
					Sytox	PerCP	S10349

Table 2.9 Flow cytometry panels used in immune cell distribution experiments. All antibodies were purchased from Biolegend™.

2.8 Rat BMDC Lectin Micro-Array Profiling

2.8.1 Membrane protein extraction and labelling

Membrane proteins were extracted from iDCs, tDCs, niDCs and ntDCs using a commercial protein extraction kit (Mem-Per®, Thermo Fisher Scientific). Proteins recovered from 10^6 cells were labelled with 100 µg (10 mg/mL in DMSO) Alexa Fluor® succinimidyl ester 555 dye (Thermo Fisher Scientific) as per the manufacturer's instructions. Labelled protein was separated from unconjugated dye with Bio-Gel® P6 (Bio-Rad Laboratories, Dublin, Ireland).

2.8.2 Lectin microarray construction and sample interrogation

Lectin microarrays were constructed essentially as described previously in [270]. Forty-four lectins (see table 2.5) sourced from multiple vendors were diluted to 0.5 mg/mL in PBS supplemented with 1 mM of respective haptenic sugar to maintain binding site integrity (see table 2.5) and printed on Nexterion® H (Schott, Mainz, Germany) functionalized glass substrates using a sciFLEXARRAYER S3 non-contact spotter (Scienion, Berlin, Germany). During printing, relative humidity and

temperature were maintained at 62% (+/- 2%) and 20 °C, respectively. Following printing, slides were incubated in a humidity chamber overnight at 20 °C to ensure completion of covalent conjugation. Unoccupied functional groups were deactivated by 1 h incubation with 100 mM ethanolamine in 50 mM sodium borate, pH 8. Finished slides were washed with PBS with 0.05% Tween-20 (PBS-T) three times for 3 min and once with PBS for 3 min, centrifuged dry (450 x *g*, 5 min), and stored at 4 °C with desiccant until use.

Labelled cellular proteins were incubated with finished microarrays following extensive optimization as described in [270]. All processes were carried out with limited light exposure. Samples were applied to microarrays using an eight-well gasket slide and incubation cassette system (Agilent Technologies, Cork, Ireland). 70 µL of each labelled glycoprotein at 0.5 mg/mL, in incubation buffer (TBS-T; Tris-buffered saline (TBS; 20 mM Tris-HCl, 100 mM NaCl, pH 7.2, supplemented with 1 mM $CaCl_2$ and 1 mM $MgCl_2$) with 0.05% Tween®-20), was applied to each well of the gasket. A total of 18 technical replicates were carried out for iDC and tDC profiling (encompassing samples of 5 biological replicates). Each microarray slide was loaded into a cassette with an accompanying gasket slide and placed in a rotating incubation oven (23 °C, approximately 4 rpm) for 1 h. Incubation cassettes were disassembled under TBS-T, and microarrays were washed in a Coplin jar twice in TBS-T for 2 min each and once with TBS for 2 min. Microarrays were dried by centrifugation (450 x *g*) and imaged immediately using an Agilent G2505B microarray scanner at 5 µm resolution (532 nm laser, 100% laser power, 90% PMT).

2.8.3 Microarray data extraction and analysis

Data extraction and analysis was performed essentially as previously described [270, 271]. In brief, raw intensity values were extracted from high-resolution *.tif files using GenePix Pro v6.1.0.4 (Molecular Devices, Berkshire, UK) and a proprietary *.gal file (containing feature spot addresses and identities) using adaptive diameter (70–130%) circular alignment based on 230 mm features. Numerical data were exported as text to Excel (Version 2010, Microsoft, Dublin, Ireland). Local background-corrected median feature intensity data (F543median-B543) was analysed. The median value, derived from data from six replicate spots per subarray, was handled as a single data point for graphical and statistical analyses.

Lectin microarray intensity values were normalized to the median total intensity value for all features across all subarrays. The significance of difference between relative intensity data (*p<0.05, **p<0.01, ***p<0.001, ****p<0.0001) was evaluated for each set of replicates on a lectin-by-lectin basis using a standard Student's t-test (two-tailed, two sample unequal variance). Unsupervised, hierarchical clustering of lectin binding data was performed with Hierarchical Clustering Explorer v3.0 (http://www.cs.umd.edu/hcil/hce/hce3.html). For clustering analysis, previously normalized data was imported directly and clustered with the following parameters: no pre-filtering, complete linkage, Euclidean distance. Principal component analysis (PrCA) of previously normalized and pre-filtered data (those lectins which demonstrated $p < 0.01$ or better in the above t-tests, 15 in total) was performed using Minitab version 16.1.1 (Minitab, Inc., State College, PA, USA).

No	Abbreviation	Origin	Species	Common name	Major Ligand(s)	Printed in	Supplier
1	AIA, Jacalin	Plant	*Artocarpus integrifolia*	Jack fruit lectin	Gal, Gal-β-(1,3)-GalNAc (sialylation tolerant)	Gal	EY Labs
2	RPbAI	Plant	*Robinia pseudoacacia*	Black locust lectin	Gal, GalNAc	Gal	EY Labs
3	PA-I	Bacteria	*Pseudomonas aeruginosa*	Pseudomonas lectin	Gal, Gal derivatives	Gal	Sigma Aldrich
4	SNA-II	Plant	*Sambucus nigra*	Sambucus lectin-II	Gal/GalNAc	Gal	EY Labs
5	SJA	Plant	*Sophora japonica*	Pagoda tree lectin	β-GalNAc	Gal	EY Labs
6	DBA	Plant	*Dolichos biflorus*	Horse gram lectin	GalNAc	Gal	EY Labs
7	GHA	Plant	*Glechoma hederacea*	Ground ivy lectin	GalNAc	Gal	EY Labs
8	SBA	Plant	*Glycine max*	Soy bean lectin	GalNAc	Gal	EY Labs
9	VVA-B4	Plant	*Vicia villosa*	Hairy vetch lectin	GalNAc	Gal	EY Labs
10	BPA	Plant	*Bauhinia purpurea*	Camels foot tree lectin	GalNAc/Gal	Gal	EY Labs
11	WFA	Plant	*Wisteria floribunda*	Japanese wisteria lectin	GalNAc/sulfated GalNAc	Gal	EY Labs
12	ACA	Plant	*Amaranthus caudatus*	Amaranthin	Sialylated/Gal-β-(1,3)-GalNAc	Lac	Vector Labs
13	ABL	Fungi	*Agaricus bisporus*	Edible mushroom lectin	Gal-β-(1,3)-GalNAc, GlcNAc	Lac	EY Labs
14	PNA	Plant	*Arachis hypogaea*	Peanut lectin	Gal-β-(1,3)-GalNAc	Gal	EY Labs
15	GSL-II	Plant	*Griffonia simplicifolia*	Griffonia/Bandeiraea lectin-II	GlcNAc	GlcNAc	EY Labs
16	sWGA	Plant	*Triticum vulgaris*	Succinyl WGA	GlcNAc	GlcNAc	EY Labs
17	DSA	Plant	*Datura stramonium*	Jimson weed lectin	GlcNAc	GlcNAc	EY Labs
18	STA	Plant	*Solanum tuberosum*	Potato lectin	GlcNAc oligomers	GlcNAc	EY Labs
19	LEL	Plant	*Lycopersicum eculentum*	Tomato lectin	GlcNAc-β-(1,4)-GlcNAc	GlcNAc	EY Labs
20	NPA	Plant	*Narcissus pseudonarcissus*	Daffodil lectin	α-(1,6)-Man	Man	EY Labs
21	GNA	Plant	*Galanthus nivalis*	Snowdrop lectin	Man-α-(1,3)-	Man	EY Labs
22	HHA	Plant	*Hippeastrum hybrid*	Amaryllis agglutinin	Man-α-(1,3)-Man-α-(1,6)-	Man	EY Labs
23	ConA	Plant	*Canavalia ensiformis*	Jack bean lectin	α-linked Man, Glc, GlcNAc	Man	EY Labs
24	Lch-B	Plant	*Lens culinaris*	Lentil isolectin B	Man, core fucosylated, agalactosylated biantennary *N*-glycans	Man	EY Labs
25	PSA	Plant	*Pisum sativum*	Pea lectin	Man, core fucosylated trimannosyl *N*-glycans	Man	EY Labs
26	WGA	Plant	*Triticum vulgaris*	Wheat germ agglutinin	NeuAc/GlcNAc	GlcNAc	EY Labs
27	MAA	Plant	*Maackia amurensis*	Maackia agglutinin	Sialic acid-α-(2,3)-Gal(NAc)	Lac	EY Labs
28	SNA-I	Plant	*Sambucus nigra*	Sambucus lectin-I	Sialic acid-α-(2,6)-Gal(NAc)	Lac	EY Labs
29	CCA	Animal	*Cancer antennarius*	California crab	*O*-acetylated sialic acids	Lac	EY Labs
30	PHA-L	Plant	*Phaseolus vulgaris*	Kidney bean leukoagglutinin	tri-/tetra-antennary β-Gal/Gal-β-(1,4)-GlcNAc	Lac	EY Labs
31	PCA	Plant	*Phaseolus coccineus*	Scarlet runner bean lectin	GlcNAc in complex oligosaccharides	Lac	Sigma Aldrich
32	PHA-E	Plant	*Phaseolus vulgaris*	Kidney bean erythroagglutinin	biantennary, bisecting GlcNAc, β-Gal/Gal-β-(1,4)-GlcNAc	Gal	EY Labs
33	RCA-I/120	Plant	*Ricinus communis*	Castor bean lectin I	Gal-β-(1, 4)-GlcNAc	Gal	Vector Labs
34	CPA	Plant	*Cicer arietinum*	Chickpea lectin	Complex oligosaccharides	Lac	EY Labs
35	CAA	Plant	*Caragana arborescens*	Pea tree lectin	Gal-β-(1, 4)-GlcNAc	Lac	EY Labs
36	ECA	Plant	*Erythrina cristagalli*	Cocks comb/coral tree lectin	Gal-β-(1, 4)-GlcNAc oligomers	Lac	EY Labs
37	AAL	Fungi	*Aleuria aurantia*	Orange peel fungus lectin	Fuc-α-(1,6)- and Fuc-α-(1,3)-linked	Fuc	Vector Labs
38	LTA	Plant	*Lotus tetragonolobus*	Lotus lectin	Fuc-α-(1,3)-, Fuc-α-(1→6)- and Fuc-α-(1→2)-linked	Fuc	EY Labs
39	UEA-I	Plant	*Ulex europaeus*	Gorse lectin-I	Fuc-α-(1,2)-linked	Fuc	EY Labs
40	EEA	Plant	*Euonymous europaeus*	Spindle tree lectin	Terminal α-linked Gal	Gal	EY Labs
41	GSL-I-B4	Plant	*Griffonia simplicifolia*	Griffonia/Bandeiraea lectin-I	Terminal α-linked Gal	Gal	EY Labs
42	MPA	Plant	*Maclura pomifera*	Osage orange lectin	Terminal α-linked Gal	Gal	EY Labs
43	VRA	Plant	*Vigna radiata*	Mung bean lectin	Terminal α-linked Gal	Gal	EY Labs
44	MOA	Fungi	*Marasmius oreades*	Fairy ring mushroom lectin	Terminal α-linked Gal	Gal	EY Labs

Table 2.10 Table listing the common names, abbreviations, origins and major ligands of the lectins used in iDC and tDC lectin microarray

2.9 Mouse MSC RNA Sequencing

2.9.1 Preparing cells for RNA Sequencing

MSCs were plated at $1x10^5$ cells per well of a 6 well plate and placed into an incubator at 37^{o}C. The cells were given 24 hours to adhere to the wells and to recover. After this period, TNF-α, IL-1β or TGF-β was added to the MSCs at 50ng/ml. The MSCs were incubated with the cytokines for 72 hours. After this time period, the cells were scraped off the bottom of the wells and lysed using lysis buffer from the Bioline Isolate II RNA mini kits (Qiagen) according to manufacturer's protocols. RNA was then extracted according to manufacturer's instructions and stored at -80^{o}C until shipping.

2.9.2 Experiment Workflow

RNA Sequencing (RNASeq) was performed on several MSC groups that were either untreated, pro-inflammatory cytokine treated or TGF-β MSC treated (**Table 2.9**).

Group Name	**Samples in Group**
MSC	MSC1/MSC2/MSC3
TGF-β MSC	TGF-β MSC1/TGF-β MSC2/TGF-β MSC3
TNF-α MSC	TNF-α MSC 1/ TNF-α MSC2/ TNF-α MSC3
TNF-α + IL-1β MSC	TNF-α + IL-1β MSCs 1/TNF-α + IL-1β MSCs 2/TNF-α + IL-1β MSCs 3

Table 2.11 RNASeq group information.

RNASeq was carried out by the sequencing company ArrayStar^{TM}. Briefly, total RNA samples were quantified using a Nanodrop and qualified by agarose gel electrophoresis. The mRNA was then enriched by oligo(dT) magnetic beads or the total RNA was depleted of rRNAs by rRNA removal kits if the RNA sample was degraded. ArrayStar^{TM}. used Illumina kits for the RNA-seq library preparation, which included procedures of RNA fragmentation, random hexamer primed first strand cDNA synthesis, dUTP based second strand cDNA synthesis, end-repairing, A-tailing, adaptor ligation and library PCR amplification. Finally, they prepared RNA-seq libraries by using the Agilent 2100 Bioanalyzer and the samples were quantified by

the qPCR absolute quantification method. The sequencing was performed using Illumina Hiseq 4000.

2.10 Development and Optimisation of Corneal Transplantation in Mice

2.10.1 Mouse corneal transplantation

A fully allogeneic major histocompatibility complex class I/II disparate mouse model of corneal transplantation was established for these studies (figure 2.5). Female BALB/c C.Cg-Foxp3^{tm2Tch}/J mice served as recipients of female C57BL/6J grafts leading to approximately 68% rejection in untreated animals (32% spontaneous acceptance). All animals were 8-14 weeks old, sourced from Envigo and were housed in a specific pathogen-free facility and fed a standard chow diet.

2.10.2 Surgical procedure

All animal surgeries were performed by a fully trained and qualified surgeon. For induction, animals were placed in an anaesthesia box connected to an isoflurane vaporizer and pre-filled with a mixture of oxygen and isoflurane (5% anaesthetic in 2 L/min medical oxygen). For surgical anaesthesia, a mixture of ketamine (90mg/kg) and xylazine (7.5mg/kg) was injected intraperitoneal under isoflurane anaesthesia. Deep anaesthesia was achieved when limb withdrawal and eye reflexes were abolished. Depth of anaesthesia was monitored by the breathing pattern of the animals. Donor animals were humanely euthanised by CO_2 asphyxiation and corneas were excised using a 2 mm trephine and a small angled scissors. Recipient animals were transferred to a heated operating table which maintained a body temperature of 37^{o}C during the surgery. Tetracaine drops were administered along with pupil dilating drops. The recipient graft bed was prepared by marking the central cornea with a 1.5 mm trephine followed by excision of the corneal tissue using a small angled scissors. The donor cornea was then sutured onto the recipient eye with a continuous looped suture. The recipient eye was kept moist throughout the surgery using sterile saline. Once the graft was in place and sutured, Atropine drops and antibiotic ointment containing chloramphenicol were applied to the ocular surface. The eyelids were sutured closed to prevent the animals from scratching the graft. These were removed two days after the surgery. Following surgery, transplanted animals were placed in

clean cages, on heating pads. Animals remained in the recovery cage until fully awake, which was determined by observing normal inquisitive behaviour.

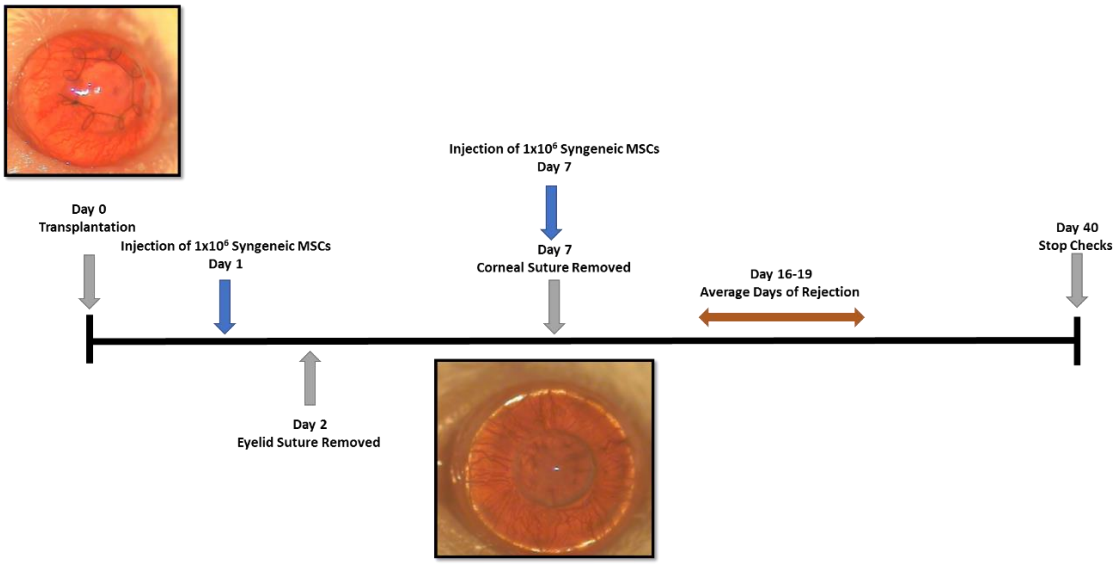

Figure 2.5 Schematic of mouse corneal transplantation and injection strategy.

2.10.3 Post-operative monitoring of transplanted animals

Post-surgery animals were anaesthetised and inspected under an operating microscope every 2/3 day and the status of the graft was assessed. Corneal opacification, oedema and progression of neovascularisation was recorded, and images were taken. Animals with surgical complications were excluded from the study and euthanized by CO_2 inhalation. Graft transparency was used as the primary indicator of rejection and this was evaluated every 2/3 days and graded on a scale of 0-3 (**Figure 2.6**). Neovascularization was also evaluated and calculated based on the number of quaternary segments of donor corneas in which the vessels were present and scored between 0 and 4 (**Figure 2.7**), with 4 indicating that there were blood vessels present in all 4 segments. Grafts were considered rejected if they had an opacity scoring of 2 or above.

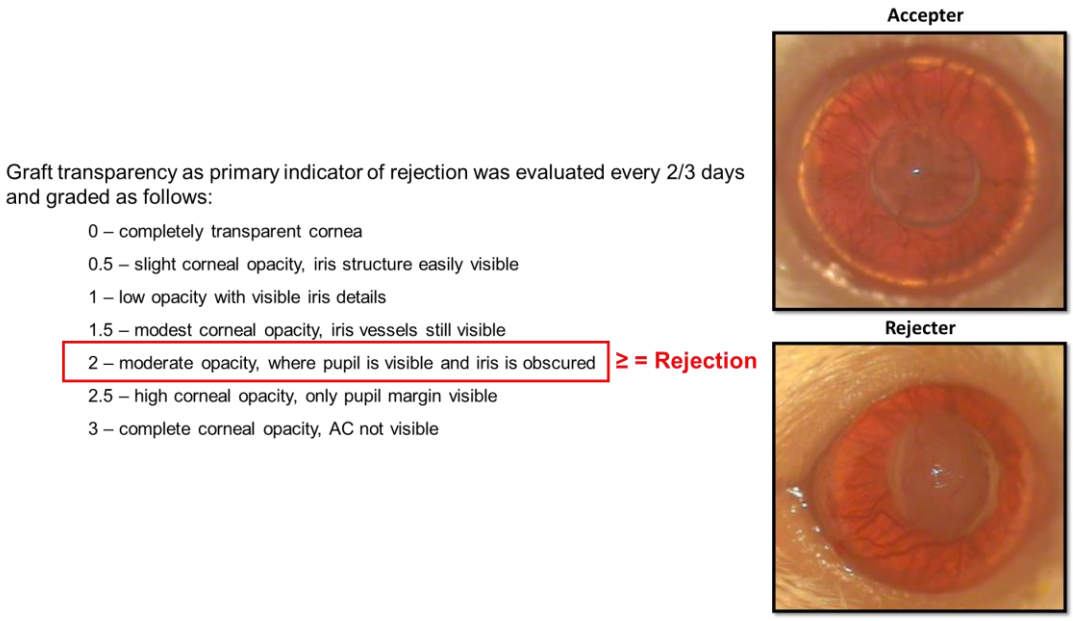

Figure 2.6. Corneal opacity grading.

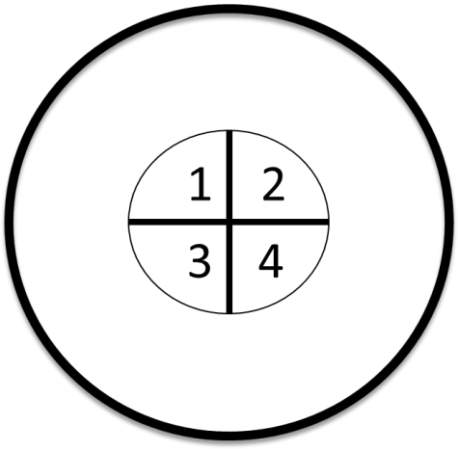

Figure 2.7 Neovascularization scoring.

2.10.4 Intravenous administration of MSCs

MSCs were isolated and expanded from BALB/c mice as described in Section 2.3.1 and where appropriate were pre-activated with either pro-inflammatory cytokines TNF-α and IL-1β or TGF-β as described in Section 2.5.4. MSCs were washed in DPBS (x3) and filtered through a 40µm filter before administration. Mice were given some time to relax after taking them out of their cages and then were placed into a cylindrical restraining devise. $1x10^6$ cells in 100µl of PBS were injected i.v. through the lateral tail vein using a 30.5G needle. Mice were monitored for 25-30 minutes before returning them back to their cages.

2.10.5 Isolation of Mouse Tissues for Analysis

Mice were humanely sacrificed by CO_2 asphyxiation followed by cervical dislocation. The ipsilateral submandibular lymph node was excised by first spraying the fur of the mouse with 70% ethanol and then cutting away the fur and making an incision along the length of the neck. Once submandibular lymph node was identified, it was grasped with a forceps and the fat was cut away with a scissors as previous described by us [265] and others [272]. The lymph node was stored in DPBS in a 15ml tube at 4°C. To isolate the spleen, again the body of the mouse was sprayed with 70% ethanol and the fur was cut away on the left side of the body. Then an incision was made on the left side of the body midway between the front and back legs. The spleen was identified by its deep red colour and district shape, using some scissors and forceps the adjacent fat was cut away. The spleen was stored in PBS in a 15ml tube at 4°C. To isolate and harvest the lung, the skin was removed from the chest cavity. An incision was made to open the body cavity at the bottom of the rib cage. The rib cage was cut on the left and right side of the body up towards the shoulder to expose the lungs and heart. Holding the trachea with some forceps the tissue connecting the lung to the diaphragm was cut away. The blood vessels and connecting tissue between the heart and lung were removed and the lung was excised. The lung was stored in a 50ml tube at 4°C.

Single cell suspensions of the lymph node and spleen were easily generated by passing the organs through a 40µm cell strainer. The lung needs to be enzymatically digested first before passing through a cell strainer. The lung was cut into 1mm pieces in a petri dish using some forceps and a scalpel. The remnants of the trachea and bronchioles were removed with the help of some forceps and a scalpel. The 1mm pieces were washed in at least 3mls of Hank's Balanced Salt Solution (HBSS). The lung is then placed into a 15ml tube in 3mls of HBSS and collagenase IV was added to the tube to a final concentration of 200U/ml. DNase I was also added to a final concentration of 200U/ml. The tube was incubated at 37°C for 2 hours at 150rpm. After this incubation the lung, like the spleen and lymph node is passed through a 40µm filter with a 1ml syringe plunger in 5mls of DPBS and stored on ice. The single cell suspensions are then centrifuged at 800 x g for 5 minutes. The red blood cells in both the lung and spleen suspensions were lysed using ACK buffer for 5 minutes on ice. After the lysis, the cells in all suspensions were counted and seeded in the wells of a 96-well plate for

flow cytometry staining as described in section 2.7.4. Remaining cell suspension was centrifuged, and the supernatant removed, and the pellets stored at -80°C for RNA isolation followed by RT-PCR analysis as described in section 2.6.4.

Material	**Supplier Code**	**Manufacturer/Supplier**
Vannas scissors: 8 cm, 45°angle	500260	World Precision Instruments
Dumont #7 curved student forceps	91197-00	World Precision Instruments
Iris scissors	500216	World Precision Instruments
Iris forceps	15915	World Precision Instruments
Colibri forceps w/ needle holder	G-18950	Geuder AG, Germany
3 mm Elliot trephine	custom made	Geuder AG, Germany
2.5 mm Elliot trephine	G-17155	Geuder AG, Germany
toothed forceps; model Bonn; tip width 0.3mm	11084-07	Fine Science Tools, UK
Halsey micro needle holder	12075-14	Fine Science Tools, UK
suture tying forceps	18025-10	Fine Science Tools, UK
10-0 ETHILON polyamid monofilament suture	W1770	Ethicon, UK
6-0 Coated Vicryl	W9752	Ethicon, UK
BD Visispear, eye sponges	581089	BD Biosciences, UK
	Ophthalmic Surgery Pharmaceuticals	
1% Atropine single dose units		Chauvin Pharmaceuticals
1% Tropicamide single dose units		Chauvin Pharmaceuticals

2.5% Phenylephrine single dose units		Chauvin Pharmaceuticals
1% Tertacaine single dose units		Chauvin Pharmaceuticals
Chloramphenicol antibiotic ointment		
Balance salt solution (BSS®)	0065082650	Alcon, UK
Isoflurane		
Medical oxygen		BOC Gases, Ireland

Table 2.12. Surgical Materials.

2.8 Statistical Analysis

All statistical analysis was performed using GraphPad Prism software (La Jolla, USA). Data was presented as mean ± SEM. Student's t test (paired/unpaired) one/two tailed was used for direct comparison between two samples *in vitro*. One-way ANOVA was used for multiple comparison tests both *in vitro* and *in vivo* followed by Tukey's post-test. *In vivo* data was confirmed to come from a Gaussian distribution by applying the Kolmogorov-Smirnov test for normality. Kaplan-Meier survival analysis was used for analysis of allograft survival and log-rank (Mantel Cox) test applied. Significance was denoted as: *$p \leq 0.05$, **$p \leq 0.01$ and ***$p \leq 0.001$.

Chapter Three:

Regulating Immunogenicity and Tolerogenicity of Bone Marrow-Derived Dendritic Cells through Modulation of Cell Surface Glycosylation by Dexamethasone Treatment

3.0 Chapter Experimental Design

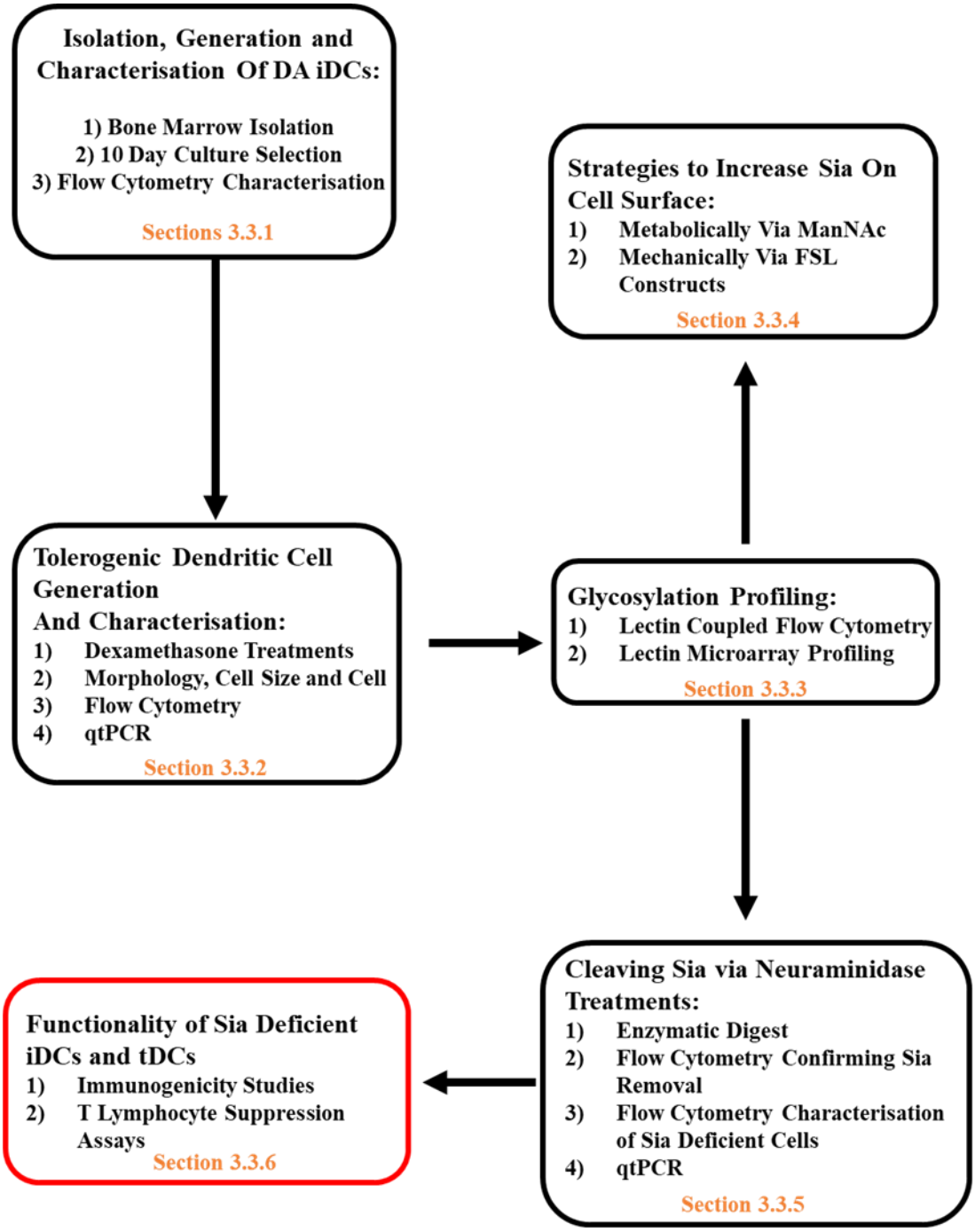

Schematic overview of chapter experimental design | A schematic presenting the sequence and progression of experiments described in this chapter.

3.1 Introduction

Dendritic cells (DCs) are professional antigen presenting cells which are a component of the innate immune system which induce adaptive immune responses [273]. DCs were first described by Steinman and Cohn in 1973 [128] and were subsequently identified to be potent activators of the immune system when employed in mixed lymphocyte reactions (MLRs) [274]. DCs are a heterogeneous population classified in different subsets dependent on the origin [275]. DCs have been extensively investigated for potential use as a cellular therapy due to their ability to maintain peripheral tolerance, which is of importance in the field of transplantation and autoimmunity. Since mature DCs are potent activators of the T-cell responses, pharmacological approaches have been used to maintain DCs in a maturation resistant state [276-278]. The glucocorticoid dexamethasone (Dexa) has been widely used in this context [279-282]. Glucocorticoids are potent immunosuppressive drugs that are used in clinical regimens to treat both Th1 and Th2 mediated inflammatory diseases including allograft rejection [283]. Dexa is known to exert potent effects on many immune cells including DCs [169, 279]. It has been consistently described in the literature that Dexa has inhibitory effects on the development of immature DCs (iDCs) [276, 279, 283, 284] and that it also impairs LPS (TLR4) stimulation of DCs which would otherwise lead to their maturation (mDCs) [285-287]. In addition to this, Dexa treated DCs have a reduced capacity to activate naïve T lymphocytes by interfering with Signals 1-3 important for T-cell activation [287].

In the context of transplantation, pre-clinical experiments suggested the potential therapeutic use of both donor and recipient derived tolerogenic dendritic cells to prevent organ graft rejection [288]. In a rat model, we have recently shown that pre-treatment of donor DCs with Dexa ex-vivo prevents the maturation of DCs and prolongs rat corneal allograft survival upon injection in corneal transplant recipients [169]. However, the mechanisms of how tolerogenic dendritic cells engage with other immune cells and exert their immunomodulatory effects are not completely understood. Despite this, tolerogenic dendritic cells have been already tested in humans suffering from various diseases. As of this writing, there are currently 8 tolerogenic DC cell therapies listed in Phase I/II clinical trials for treatment of autoimmune disease and graft rejection (clinicaltrials.gov. April 2017, search for key

words tolerogenic dendritic cells) which highlights the importance and urgency of understanding the mechanisms associated with the therapeutic effect.

Glycosylation is one of the most vital and frequent forms of post-translational modification and is involved in the function of many immune associated molecules. Some of the functions of glycosylation include, but are not limited to, protein folding and molecular trafficking to the cell surface [171-173, 289, 290]. Glycosylation has also been implicated in the stability of proteins and protection from proteolysis [174]. All immune cells are coated by a glycocalyx composed of a complex assortment of oligosaccharides (glycans), of which one frequent terminal component is sialic acid (Sia). Sias are a broad family of negatively-charged, 9-carbon monosaccharides that are exposed to the cellular microenvironment and are involved in communication and in cellular defence [175]. It has been reported that a typical somatic cell surface presents millions of Sia molecules [291] and also that they have long been noted to be important in immune cell behaviour [292]. It has been suggested that Sias can play important roles in both acting as a recognisable molecule for cellular interactions but also as a biological shield preventing receptors on cells recognising their ligands [144]. Large amounts of Sias on the cell surface of immune cells will result in an overall negative charge, which can have biophysical effects, such as the repulsion of cells from each other and subsequently disrupting cellular interactions [176].

Since immune cell interactions form the basis of immune responses, glycosylation is therefore likely to play a major role in dictating these responses. However, there is a significant knowledge gap as to how glycosylation modulates immune responses. Currently little information exists on how DC glycosylation patterns change after Dexa treatment. In this chapter we present a comprehensive profile of bone marrow derived dendritic cells (BMDCs), examining their cell surface glycosylation before and after Dexa treatment as resolved by both lectin microarrays and lectin-coupled flow cytometry.

In this work, the composition of the glycocalyx of both iDCs and tDCs was altered using neuraminidase (sialidase) treatment and the functional consequences in immunogenicity and inhibition of T-cell proliferation were observed. We show that Sia is upregulated on tDCs contributing to the tolerogenic state of tDCs. However, removal of Sia leads to increased stimulatory activity of iDCs leading to enhanced T-

cell activation and proliferation. These findings have important implications in strategies aimed at increasing tolerogenicity where it is advantageous to reduce immune activation over prolonged periods. These findings are also relevant in therapeutic strategies aimed at increasing the immunogenicity of cells, for example, in the context tumour specific immunotherapies.

3.2 Hypothesis and Objectives

3.2.1 Hypothesis

iDCs and tDCs have significant differences in glycosylation profiles and that these differences have a role to play in their therapeutic benefits. If we were to have a better understanding of the relationship between glycosylation and therapeutic efficacy, we could modulate cells in such a way as to exploit this, leading to a more efficacious cell therapy.

3.2.2 Objectives

- Profile iDCs and tDCs and to characterise them functionally in immune assays.
- Analyse the differences in glycosylation between iDCs and tDCs.
- After identification of the key changes in glycosylation, modulate the more significantly important glycans and study the functional consequences.

3.3 Results

3.3.1 Isolation, ex *vivo* Generation and Characterisation of iDCs

To generate iDCs, bone marrow was flushed from the long bones of the tibia and femur of DA rats and cultured in medium supplemented with GM-CSF, IL-4 and Dexa (for tDCs) as required (**Figure 3.1A**). This method of differentiation is well established and has been used by us [169] in the past and by others [293, 294]. By day 4, cell aggregates are visible and by day 8 these aggregates have grown considerably in size (**Figure 3.1B**). On day 10, iDCs were analysed by flow cytometry by gating according to size and granularity, followed by live/dead discrimination based on Sytox negative cells (live). After single cell selection, cells were selected by CD11b/c (APC) and CD45 (FITC) positivity (**Figure 3.1C**). The positivity of the classical DC markers expressed by iDCs were examined; these included lymphocyte common antigen CD45, antigen presentation molecules MHCI and MHC II, co-stimulatory molecules CD80 and CD86 and phagocytosis associated CD47 and SIRPα (**Figure 3.1D**). HIS36, a macrophage marker was also used to assess the level of contaminating macrophages (**Figure 3.1D**). HIS36 was very lowly expressed on the iDC preparations indicating a very pure iDC population [295, 296].

3.3.2 Generation and Characterisation of Tolerogenic DCs (tDCs) and Stimulated DCs (mDCs).

Dexa treatment of iDCs is reported to generate tolerogenic DCs (tDCs) [297]. iDCs were supplemented with Dexa on day 5 and day 7 to generate tDCs as described (**Figure 3.1A**). As Dexa has been consistently described in the literature to have inhibitory effects on the development of immature DCs and that it also impairs LPS (TLR4) stimulation of DCs which would otherwise lead to their maturation (mDCs), iDCs and tDCs were stimulated with LPS (10ng/ml) on Day 9. tDC generation did not result in any significant changes in cell size (**Figure 3.2(i)**) but the number of cells harvested from wells that were treated with Dexa was significantly lower than that of wells that were Dexa-free (**Figure 3.2(ii)**). This may be due to Dexa induced apoptosis of the DCs, which has been reported by other groups [298]. While lower numbers of cells were obtained from tDC wells, after harvesting and washing of the cells no significant changes in viability was noted (**Figure 3.2(iii)**).

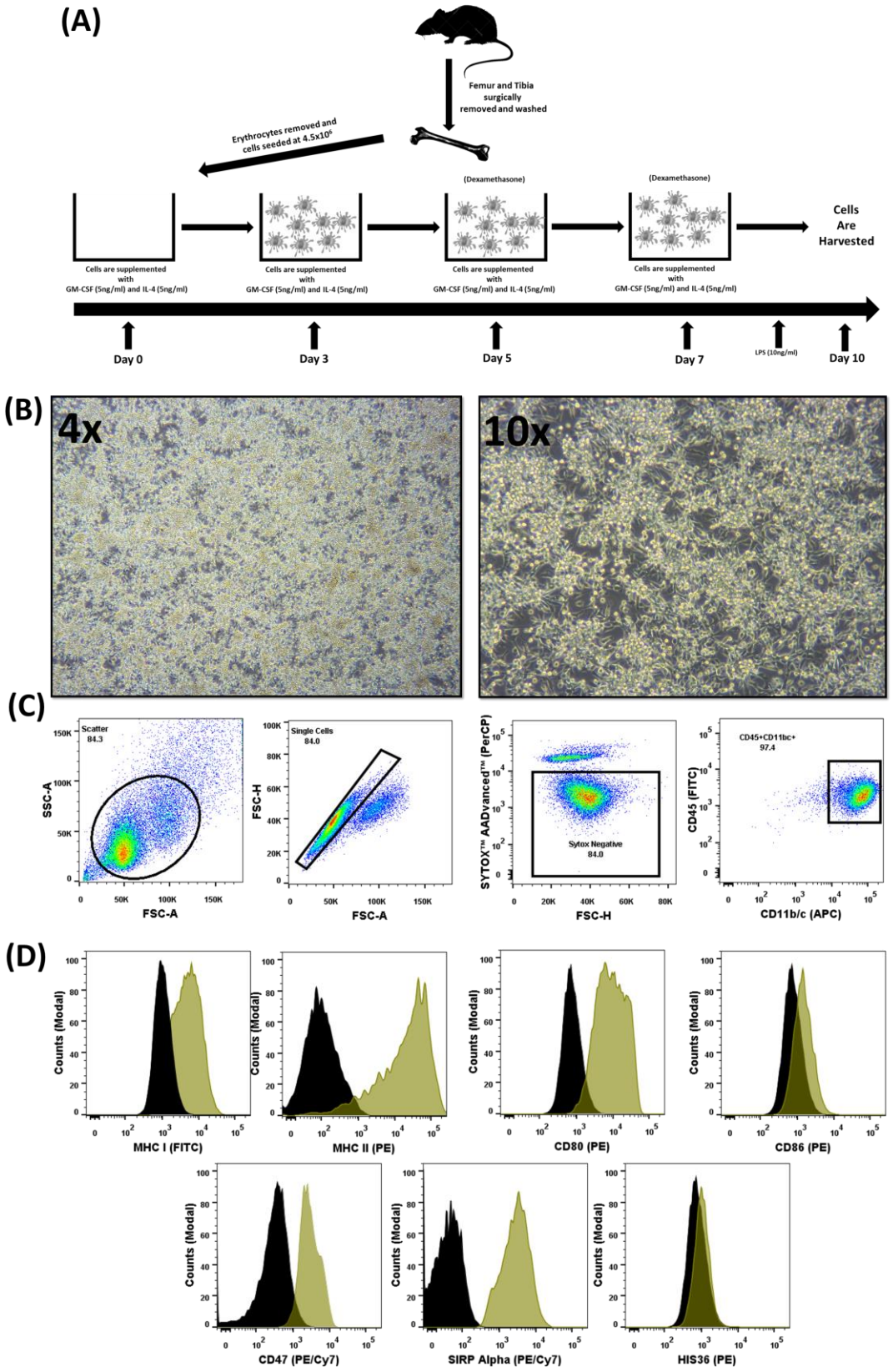

Figure 3.1 Isolation, generation and characterisation of immature DCs (iDCs). | (A) Bone marrow was flushed from the femur and tibia of 8-14-week-old DA rats and cultured in IL-4

and GM-CSF culture media for 10 days. (B) Brightfield microscopy images of iDC culture on day 10 (C) Representative gating strategy. Cells were selected according to size and granularity, followed by live/dead discrimination based on Sytox negative cells (live). After single cell selection, cells were selected by CD11b/c (APC) and CD45 (FITC) positivity. (D) Representative flow cytometry analysis histograms for the cell surface expression (Black = control (unstained cells), mustard = iDCs) of MHCI, MHC II, CD80, CD86, CD47, SIRPα and HIS36. (*n*=3).

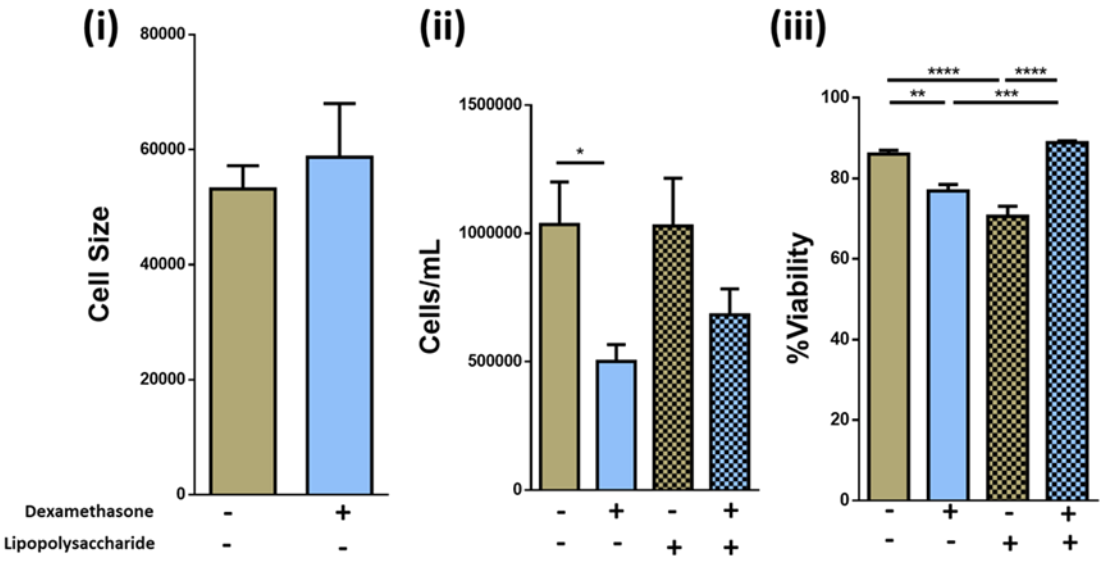

Figure 3.2 Effect of tDC generation on morphology, yield and viability. | Changes in cell size (*n*=3) (i), the number of cells harvested (*n*=8) (ii) and viability of iDCs to tDCs (*n*=4) (iii) was compared. Error bars: mean +/- SEM *p<0.05, **p<0.01 ***p<0.001 ****p<0.0001 one-way ANOVA, Tukey's multiple comparisons test

We also analysed the expression levels of the costimulatory molecules CD80/CD86 and the major histocompatibility complex class I and II molecules (MHCI/II) as an indicator of the maturation status of generated iDCs and tDCs (**Figure 3.3A**). The expression levels of CD80, CD86, MHC I, and MHC II indicate that the iDCs display a semi-mature phenotype. However, when the cells were treated with Dexa, a significant reduction in the expression level of MHC II was observed with no changes in MHC I (**Figure 3.3A**). To mature iDCs or tDC in vitro, LPS was added to the cultures (10 ng/mL) for 24h. A significant increase in both CD80/CD86, MHC I and MHC II as noted. However, tDCs following LPS treatment showed significantly reduced expression levels of CD80/CD86 and MHC I/II molecules compared to stimulated iDCs indicating a phenotype that is maturation resistant. iDC and tDC populations were also assessed for expression of pro- and anti-inflammatory markers with and without Dexa-treatment by qRT-PCR (**Figure 3.3B**).

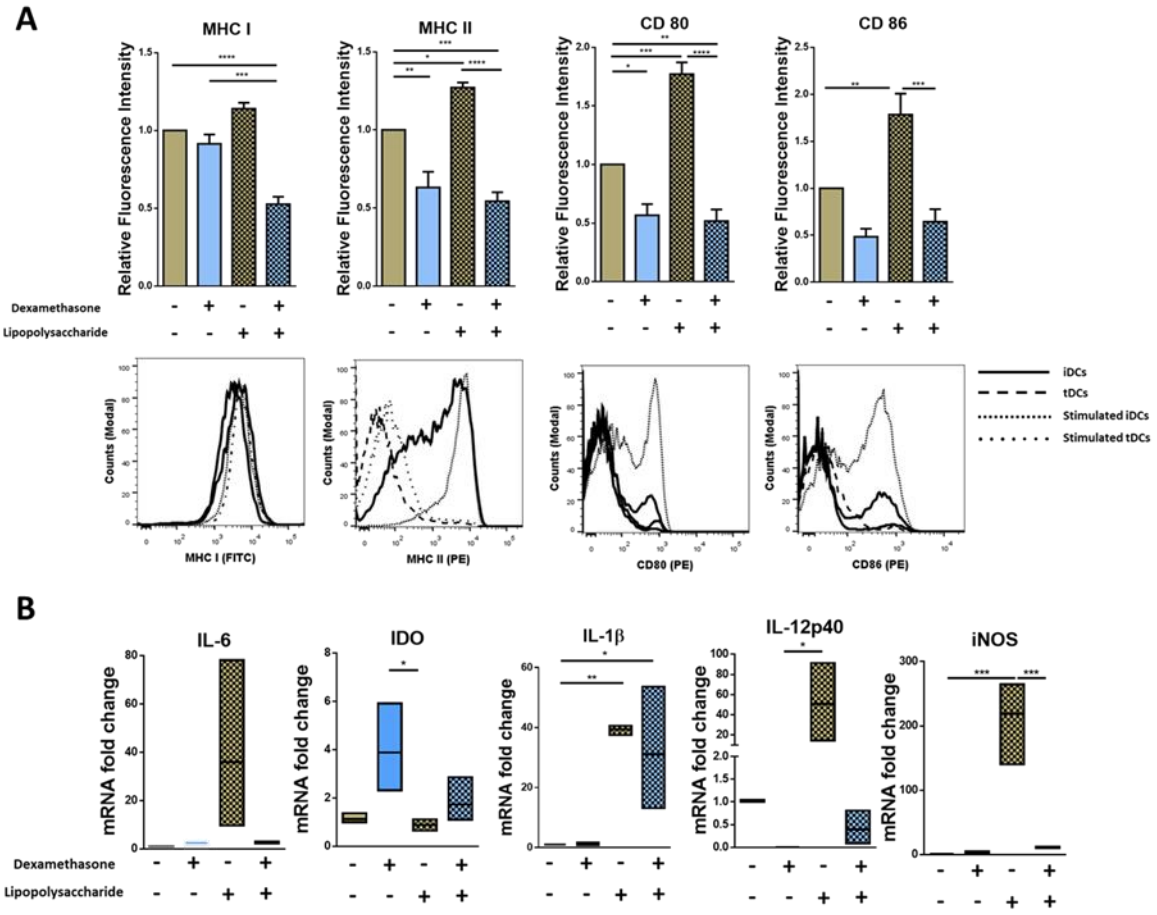

Figure 3.3 Characterisation of tolerogenic DCs (tDCs), and stimulated DCs (mDCs). | (A) Both immature DCs (iDCs) and tDCs were analysed by flow cytometry for their cell surface expression of MHC I (FITC), MHC II (PE), CD 80 (PE) and CD 86 (PE). Representative histograms and bar charts displaying relative fluorescence intensity (RFI) for flow cytometric analysis of DC cell surface (*n=4*). Median fluorescence intensities were established relative to iDCs. (B) The mRNA expression of interleukin 6 (IL-6), Indoleamine 2,3-dioxygenase (IDO), interleukin 1 beta (IL-1β), inducible nitric oxide synthase (iNOS), and IL-12p40 was analysed in iDCs and tDCs. Normalized to GAPDH and fold change relative to iDCs. Error bars: mean ± SEM *p < 0.05, **p < 0.01, ***p < 0.001, ****p < 0.0001 one-way ANOVA, Tukey's multiple comparisons test.

Results indicate that LPS stimulation of iDCs leads to an increase in mRNA expression of pro-inflammatory molecules such IL-6, IL-12p40, and iNOS. In contrast, tDCs are less sensitive to TLR4 stimulation compared to mDCs, indicated by no observed increases in IL-6, IL-12-p40, and iNOS after LPS treatment. Higher levels of IDO mRNA, which is a known marker in tolerogenic cells, is present in LPS-treated tDCs when compared to mDCs. Interestingly, IL-1β mRNA expression does not seem to be regulated by Dexa, as LPS stimulation leads to a profound increase, which cannot be blocked by Dexa. All together these data indicate that Dexa treatment of iDCs leads to the generation of a tolerogenic DC phenotype with reduced expression of markers

of immunogenicity and reduced expression of pro-inflammatory molecules but increases in immunoregulatory molecules.

3.3.3 tDC Generation Modulates the Glycocalyx, Significantly Increasing Levels of α2-6-Linked Sia

Changes in DC glycocalyx after induction of tolerogenic phenotype have not been investigated to date. To address this knowledge gap, lectin microarray profiling of proteins extracted from the membranes of iDCs and tDCs and lectin-coupled flow cytometry of intact iDCs and tDCs was undertaken.

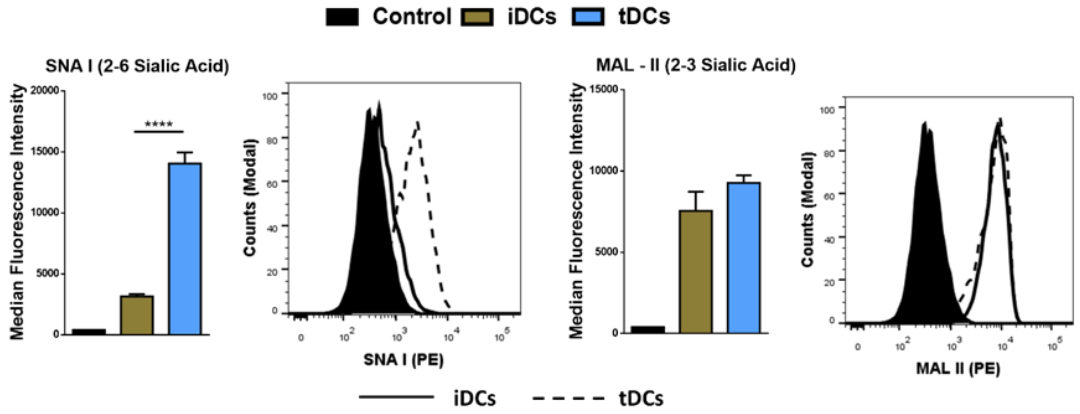

Figure 3.4 tDC generation leads to significant increases in α2-6 -linked sialic acid. | Both iDCs and tDCs were analyzed by flow cytometry for their expression of α2-3-linked Sia (MAL-II) and α2-6-linked Sia (SNA-I) (n = 3). Streptavidin controls were used for non-specific fluorescence. Representative histograms and bar charts displaying median fluorescence intensity (MFI) for flow cytometric analysis of DC cell surface. Error bars: mean ± SEM *p < 0.05, **p < 0.01, ***p < 0.001, ****p < 0.0001 one-way ANOVA, Tukey's multiple comparisons test.

Using lectins specific to Sia residues, we assayed the changes in both α2-3-linked Sia (MAL-II) and α2-6-linked Sia (SNA-I) using lectin-coupled flow cytometry. Significant increases in SNA-I was observed after Dexa treatment, this increase was not observed for MAL-II (**Figure 3.4**). To confirm this result, but to also investigate other glycosylation changes on the surfaces of these cells, lectin microarrays (**Lectin names and abbreviations in Table 2.8, chapter 2**) were performed. Comparisons of all lectin microarray replicate profiles were made by unsupervised hierarchical clustering. This clustering approach revealed two major clusters with separation at 53% minimum similarity (**Figure 3.5A**).

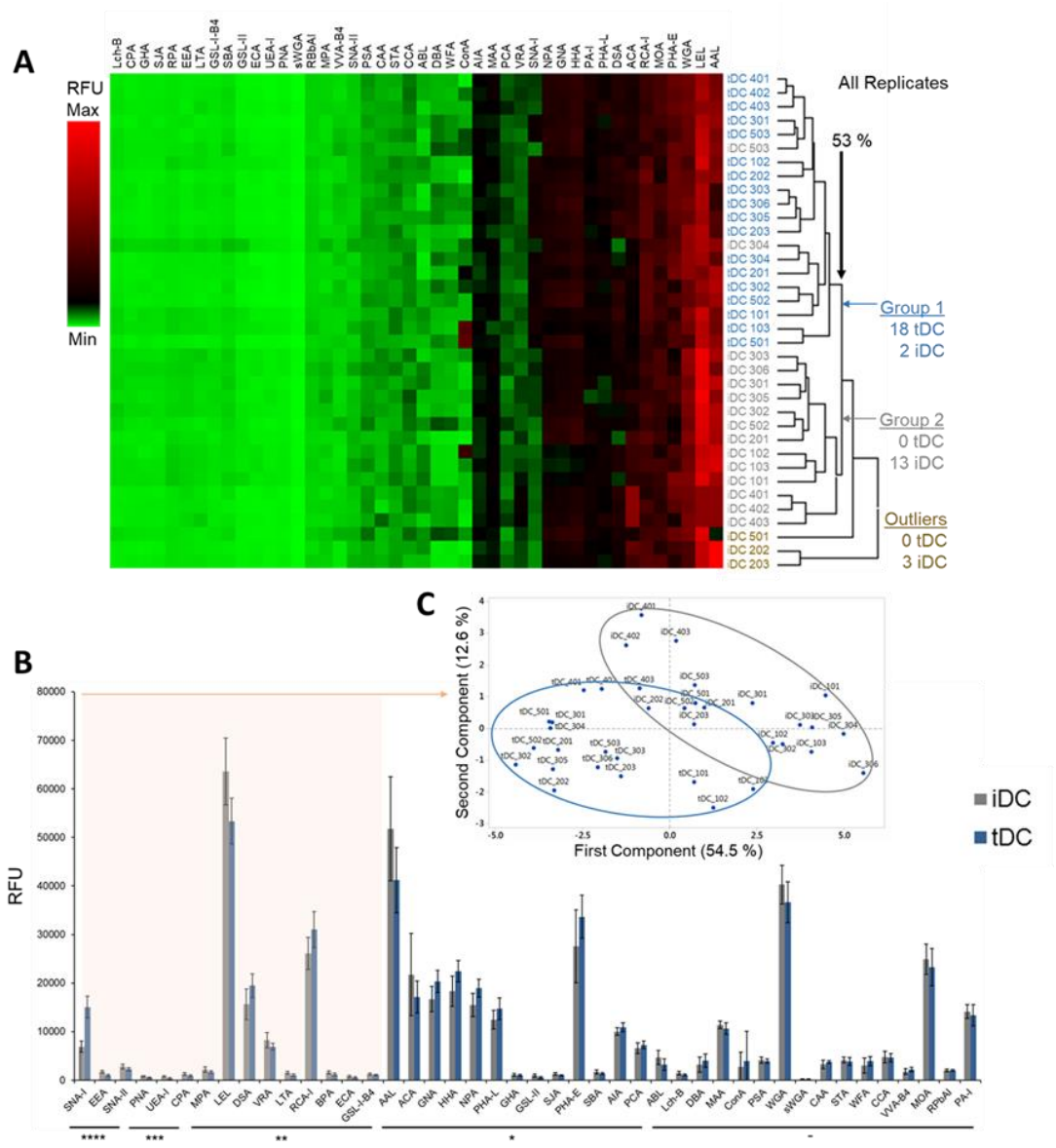

Figure 3.5 Tolerogenic DC (tDC) generation leads to pronounced changes in glycosylation. | (a) Unsupervised, hierarchical clustering of previously normalized lectin data (all replicates) was performed with the following parameters: no pre-filtering, complete linkage, Euclidean distance. **(B)** Median responses (n = 18) for iDC and tDC glycoproteins at 44 lectins, *$p < 0.05$, **$p < 0.01$, ***$p < 0.001$, ****$p < 0.0001$. Error bars: median ± average deviation. **(c)** Principal component analysis performed using the 15 lectins, which demonstrated significant signal changes (all $p < 0.01$) and the resulting division of replicate profiles into distinct groups containing predominantly immature DCs (iDCs) (gray border) or tDCs (blue border) with minimal overlap.

With the complete linkage method employed, two untreated iDC replicates were placed into the tDC group while only three of the iDC replicates, two from biological set 2 and one from set 5 (**Figure 3.5A**), showed outlier behaviour and were excluded from the major cluster containing the balance of the iDC replicate data. However, the well-defined separation of the clear majority of the iDC and tDC replicates into two

groups (**Figure 3.5A**, Group 1 and 2) supports the solidity of the subtle profile differences and also the high level of reproducibility for the lectin profiling method in distinguishing membrane glycoprotein samples from iDCs and tDCs. Median values obtained from normalized lectin microarray profile data (n = 18) for iDCs and tDCs were broadly similar with only small, but significant, differences in intensities noted at a subset of the lectin panel (**Figure 3.5B**). The general profiles of tDC glycoproteins remained similar to those of iDCs across lectin features. Furthermore, the lectin profiles displayed no obvious signs of cell stress as evidenced by a lack of elevation of signals suggesting increased endoplasmic reticulum and proximal Golgi-associated glycan structures (i.e., increased evidence of high mannose structures). However, SNA-I showed a consistent intensity increase with tDC surface glycoproteins ($p = 2 \times 10{-}10$) relative to iDCs, which is in line with previous findings from our group. PrCA performed using the 15 lectins, which demonstrated $p < 0.01$ (SNA-II, BPA, PNA, DSA, LEL, SNA-I, RCA-I, CPA, ECA, LTA, UEA-I, EEA, GS-I-B4, MPA, and VRA) revealed a division of replicate lectin profiles dominated by distinct groups containing iDCs or tDCs with minimal overlap and further reinforced the ability of these lectins to distinguish untreated iDCs from tDCs (**Figure 3.5C**).

In short, these lectin microarray profiles demonstrate that the glycocalyxes of the iDC and tDCs are distinct. These changes were validated using lectin-coupled flow cytometry as stated above. The increase in SNA-I binding suggests an increase in quantity or better accessibility to α2-6-linked with no significant change suggested for α2-3-linked Sia.

3.3.4 ManNAc sugar supplementation does not increase 2-6 linked Sia

As stated previously, Sia is an essential terminal sugar on the glycan moieties of many functional and structural glycoproteins. A key intermediate in the biochemical process to form sialic acid is the monosaccharide, ManNAc, which is formed by the bifunctional enzyme UDP- N-acetylglucosamine. ManNAc is an intermediate in the formation of the 9-phosphate of Sia (**Figure 3.6**). At this point, Sia is either modified to form other Sias or is activated in the cell nucleus to form the nucleotide CMP-Sia. This is normally the last step in the biosynthesis of a wide range of glycoproteins which are found in all human tissues [299].

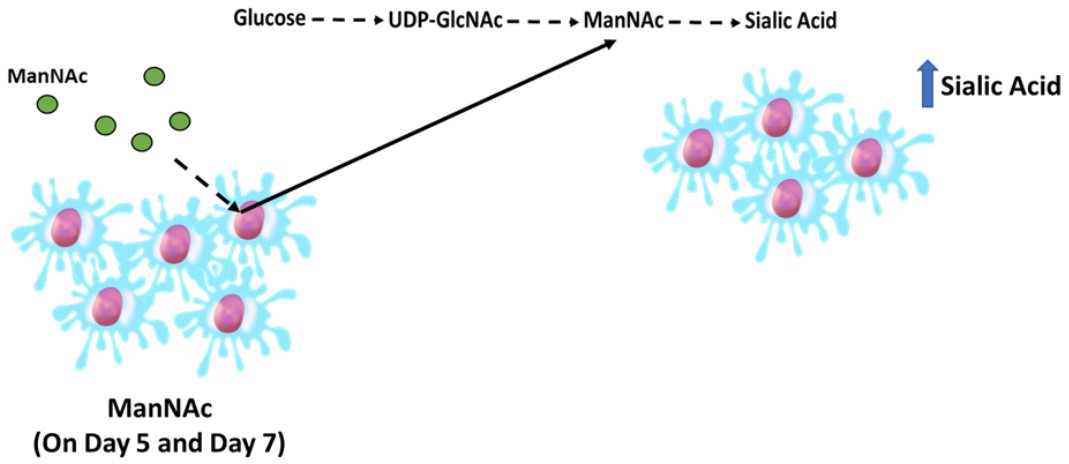

Figure 3.6 Schematic of ManNAc treatments | ManNAc at varying concentrations (0.1mM, 1mM, 5mM, 10mM and 20mM) was supplemented to the media at day 5 and day 7 of culture.

Considering the significant increases in 2-6-linked Sia observed in both lectin coupled flow cytometry and the lectin microarrays after Dexa treatment, we wanted to study the functional consequences of an increase in Sia independent of Dexa treatment. Synthesis of Sia was encouraged by adding the precursor sugar N-acetylmannosamine (ManNAc) to the media during culturing in hope to naturally increase cell surface Sia. ManNAc was added on day 5 and day 7 of the culture and on day 10 the cells were analysed by both lectin microarray and flow cytometry. Membrane proteins were extracted from iDCs and iDCs treated with the various concentrations of ManNAc and analysed by lectin microarray as previously described. 2-6-linked Sia did not significantly increase after ManNAc treatment except in the cases of the 1mM and 20mM (**Figure 3.7 A**). To verify this result, lectins specific to Sia residues were used to analyse the cells via flow cytometry. Similar to the microarray results, ManNAc did not significantly increase 2-6-linked Sia (**Figure 3.7 B**).

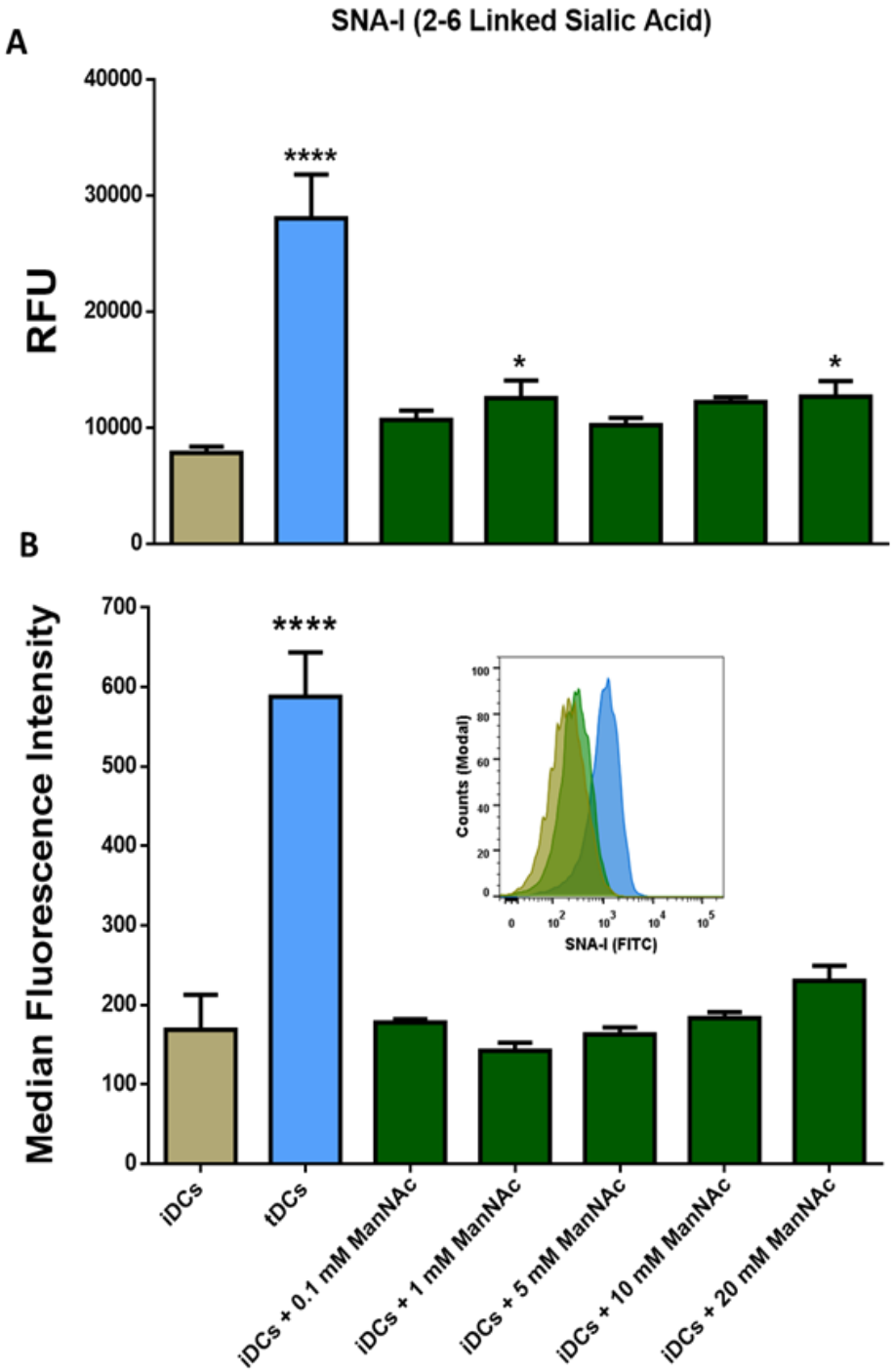

Figure 3.7 ManNAc treatment failed to increase 2-6-linked Sia significantly on iDCs. | ManNAc at varying concentrations (0.1mM, 1mM, 5mM, 10mM and 20mM) was supplemented into the media at day 5 and day 7 of culture. (A) ManNAc treated cells were analysed by lectin microarray for modulation of 2-6-linked Sia. (B) Day 10 ManNAc treated cells were analysed by flow cytometry for modulation of 2-6-linked Sia. Error bars: mean +/- SEM *p<0.05, **p<0.01 ***p<0.001 ****p<0.0001 one-way ANOVA, Tukey's multiple comparisons test. Test samples were compared to iDCs.

3.3.5 Neuraminidase Treatment of iDCs and tDCs Modulates Levels of α2-6-Linked Sia and Alters Expression Levels of Immunogenicity Markers

ManNAc treatment did not significantly increase Sia after addition to the media. Subsequently, we tried to increase Sia content by mechanically inserting 2-6, Sia using lipid tail constructs (data not shown) to no avail. Considering that Sia has long been reported to be important in DC biology [144] and the dramatic increase observed after Dexa treatment (**Figures 3.4 and 3.5C**), we cleaved Sia using neuraminidase to study phenotypical and functional changes upon removal.

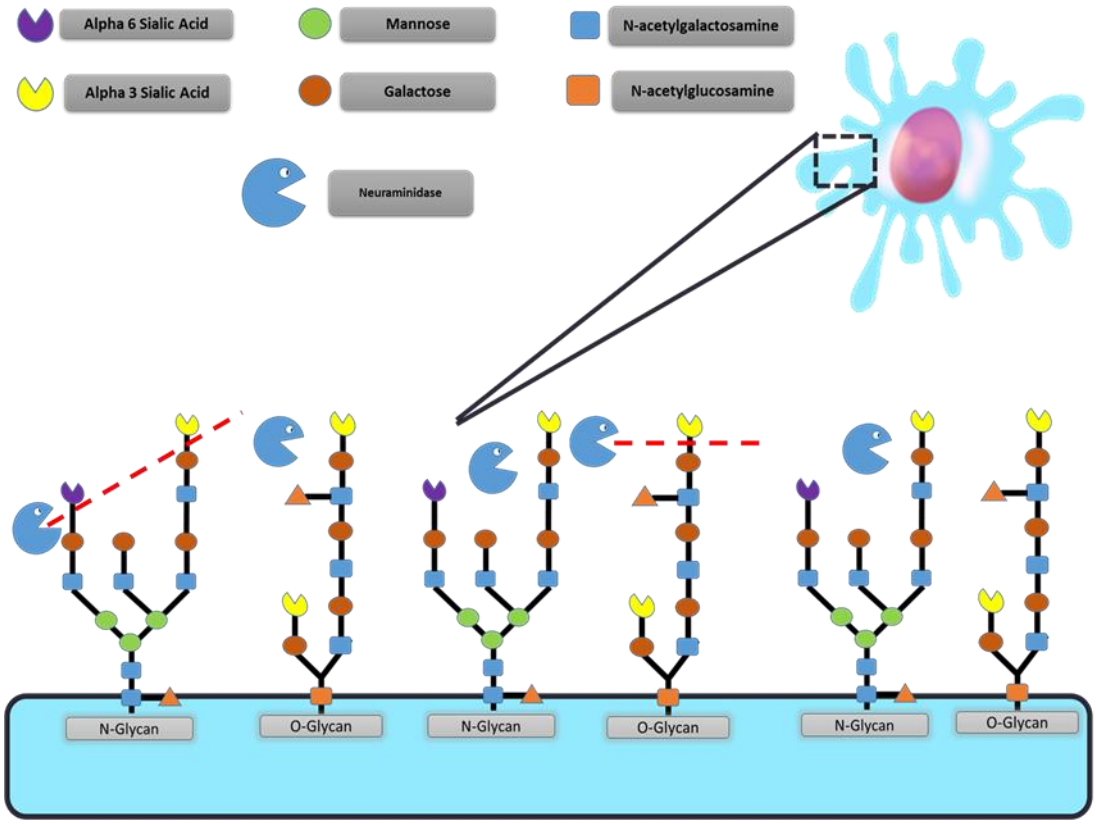

Figure 3.8 Schematic of enzymatic digestion of sialic acid from the cell surface of DCs. | iDCs or tDCs were treated with neuraminidase for 90 min at 37°C to cleave Sia residues on the surface.

iDCs and tDCs were treated with neuraminidase (designated niDC and ntDC, respectively) (**Figure 3.8**) and lectin binding profiles for SNA-I and MAL-II were analysed using flow cytometry (**Figure 3.9**). Both niDCs and ntDCs showed a significant reduction in SNA-I binding intensities (**Figure 3.9 (i + iii))** and trend decreases in MAL-II binding intensities (**Figure 3.9 (ii + iv))** suggesting the successful removal of α2-6-linked and α2-3-linked Sia, respectively.

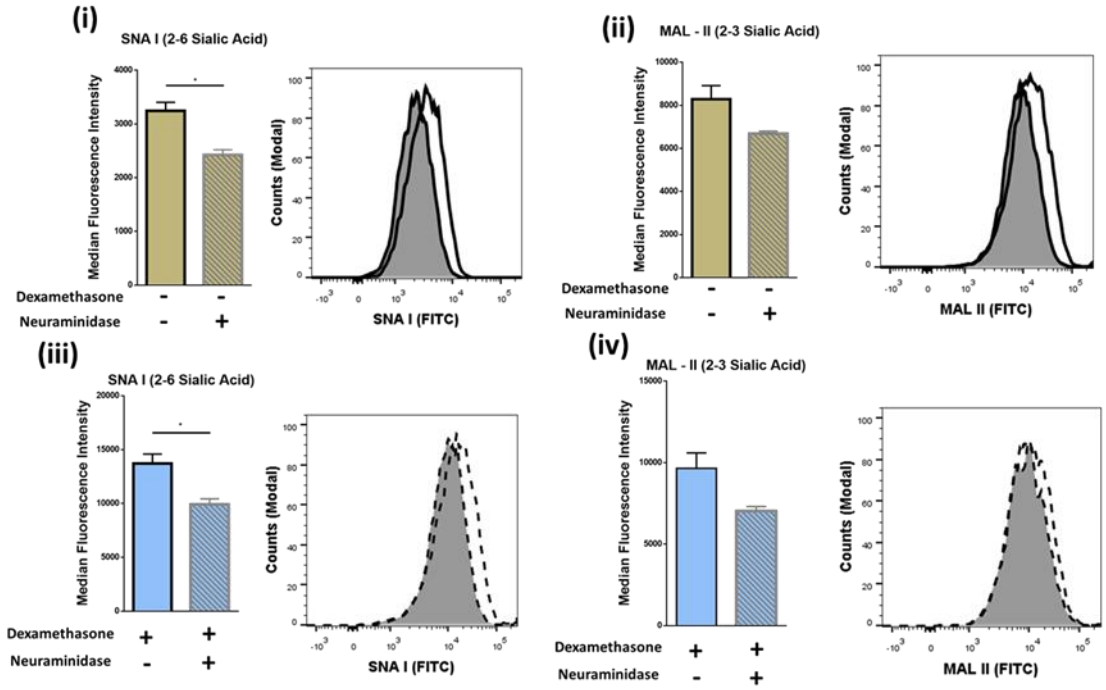

Figure 3.9 Neuraminidase treatment of immature DCs (iDCs) and tolerogenic DCs (tDCs) decreases levels of α2-6-linked Sia significantly. | α2-6-linked Sia (SNA-I) (i) and α2-3-linked Sia (MAL-II) (ii) was measured on iDCs and niDCs after neuraminidase treatment (n = 3). α2-6-linked Sia (SNA-I) (iii) and α2-3-linked Sia (MAL-II) (iv) was measured on tDCs and ntDCs after neuraminidase treatment (n = 3). Representative histograms and bar charts displaying median fluorescence intensity (MFI) for flow cytometric analysis of DC cell surface. Error bars: mean ± SEM *p < 0.05, **p < 0.01, ***p < 0.001, ****p < 0.0001 one-way ANOVA, Tukey's multiple comparisons test. Data sets with two groups were analysed using an unpaired t-test.

Based on these results, we further investigated if the removal of Sia resulted in a detectable increase of the expression of MHC I, MHC II, CD80, and CD86 immunogenicity markers after treatment with neuraminidase. niDCs (**Figure 3.10**) had small but significant increases in MHC II and CD86 expression when compared to iDCs. MHC I showed a trend increase in expression on niDCs compared to iDCs, and there was no change in CD80 expression after treatment with neuraminidase. ntDCs (**Figure 3.10**) displayed a significant increase in both MHC I and MHC II with no changes in CD80 and a trend increase in CD86 after neuraminidase treatment.

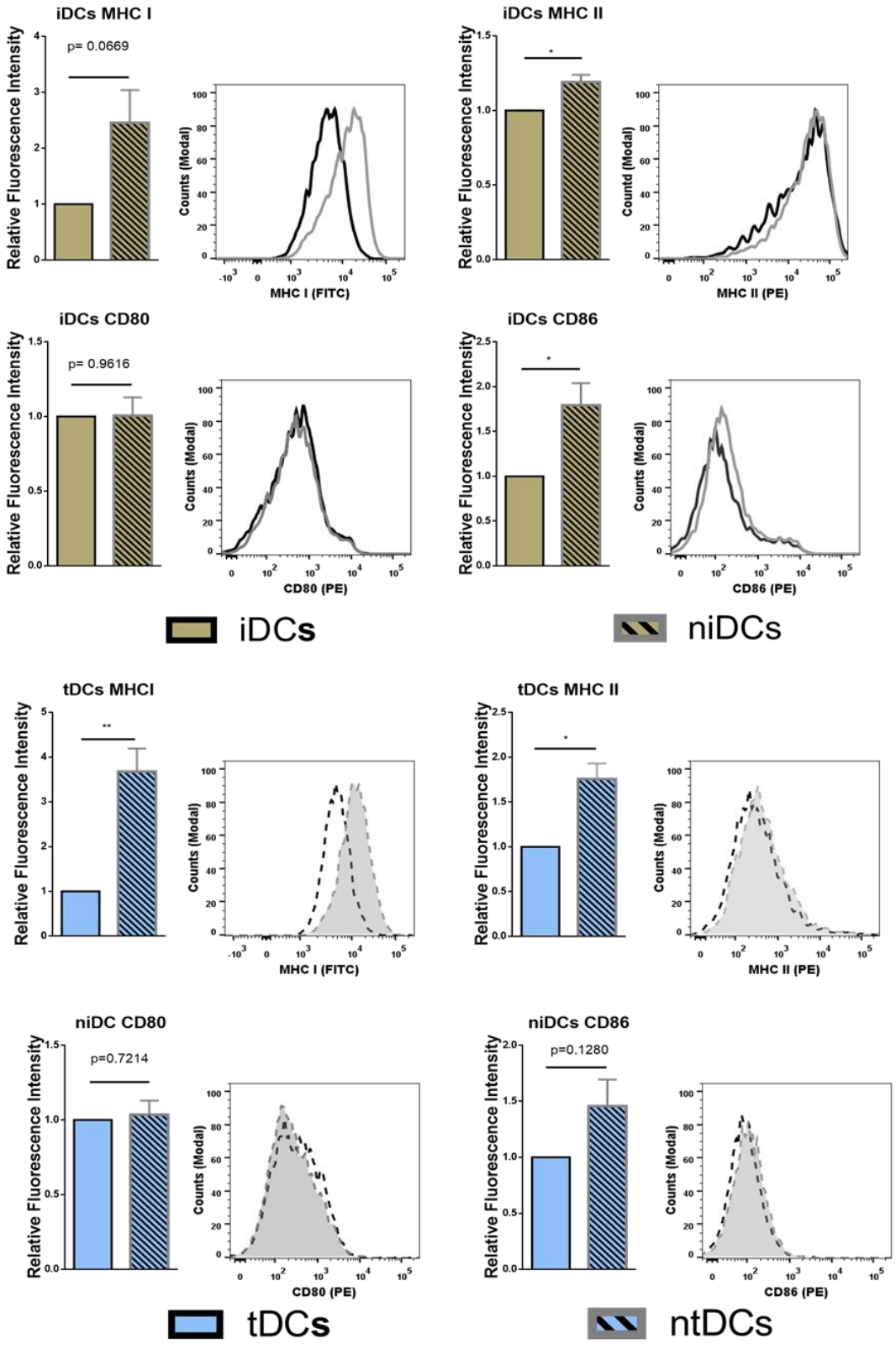

Figure 3.10 Neuraminidase treatment of immature DCs (iDCs) and tolerogenic DCs (tDCs) significantly alters phenotype. | Both iDCs and tDCs were analysed by flow cytometry for their expression of MHC I (FITC), MHC II (PE), CD 80 (PE), and CD 86 (PE) after neuraminidase treatments. Representative histograms and bar charts displaying relative fluorescence intensity (RFI) for flow cytometric analysis of DC cell surface. Median

fluorescence intensities were established relative to iDCs in the case of niDCs and tDCs in the case of ntDCs. Error bars: mean ± SEM *$p < 0.05$, **$p < 0.01$, ***$p < 0.001$, ****$p < 0.0001$ one-way ANOVA, Tukey's multiple comparisons test. Data sets with two groups were analyzed using an unpaired *t*-test.

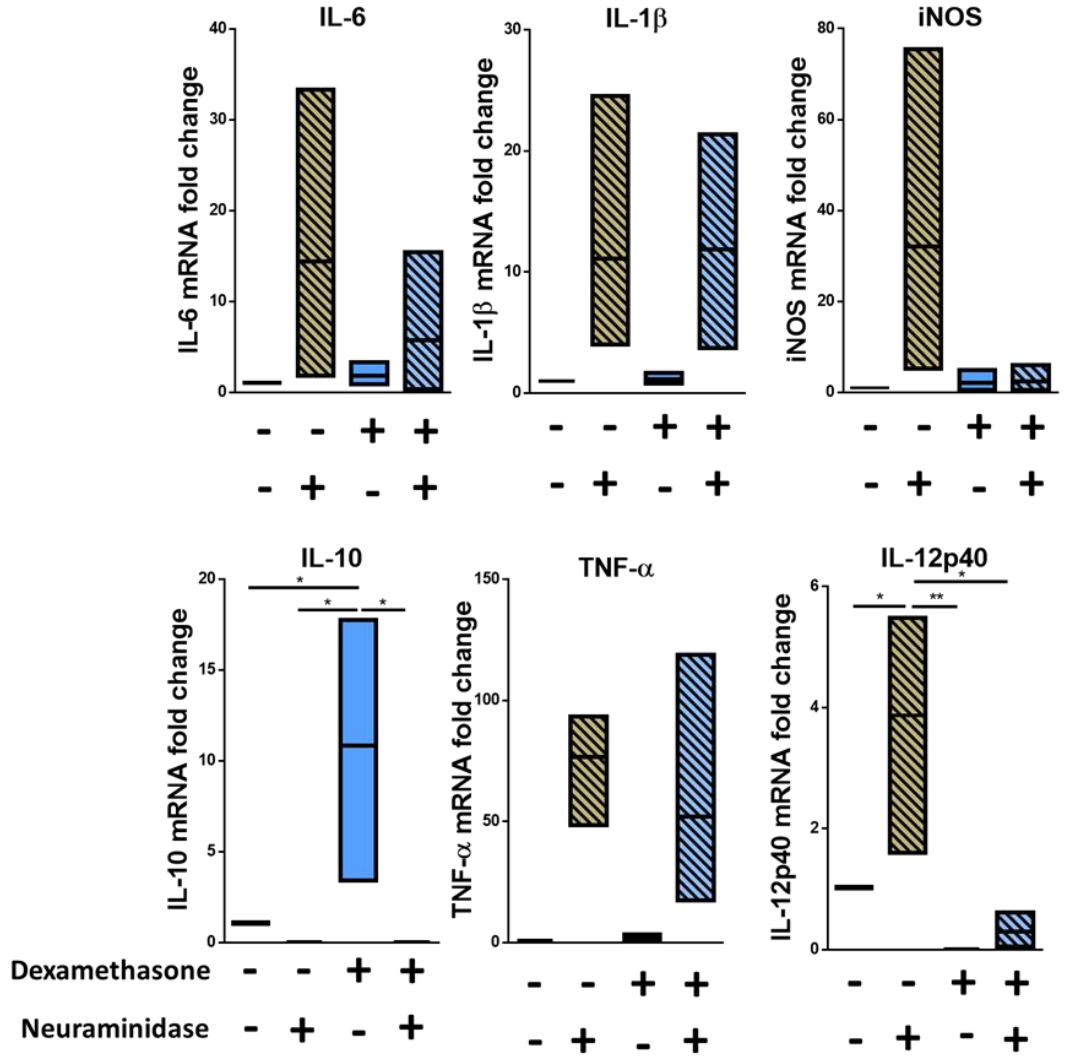

Figure 3.11 Neuraminidase treatment of immature DCs (iDCs) and tolerogenic DCs (tDCs) significantly altered mRNA expression. | The mRNA expression of interleukin 6 (IL-6), interleukin 1 beta (IL-1β), inducible nitric oxide synthase (iNOS), tumour necrosis factor alpha (TNF-α), interleukin subunit beta (IL-12p40), and interleukin 10 (IL-10) was analysed in iDCs, niDCs, tDCs, and ntDCs. Normalized to GAPDH and fold change relative to iDCs. Error bars: mean ± SEM *$p < 0.05$, **$p < 0.01$, ***$p < 0.001$, ****$p < 0.0001$ one-way ANOVA, Tukey's multiple comparisons test. Data sets with two groups were analysed using an unpaired *t*-test.

niDC and ntDC populations were also assessed for expression of pro- and anti-inflammatory markers by qRT-PCR (**Figure 3.11**). Although there was some sample-to-sample variation, our data indicate that neuraminidase treatment of iDCs leads to dramatic increases in pro-inflammatory mRNA expression of IL-6, IL-1β, iNOS,

TNF-α, and IL-12-p40. However, ntDCs were protected from this strong increase in pro-inflammatory cytokine expression in the case of iNOS and IL-12-p40, but mRNA levels of IL-6, IL-1β, and TNF-α were increased. Interestingly, levels of anti-inflammatory IL-10 are lost after neuraminidase treatment in both iDCs and tDCs. In summary, these results indicate that neuraminidase treatment reduces Sia on the cell surface of both iDCs and tDCs and leads to the stimulation of pro-inflammatory cytokine mRNA expression, which can be largely inhibited by Dexa treatment.

3.3.6 Neuraminidase Treatment Alters Immunomodulatory Properties of iDCs and tDCs

Considering that the removal of Sia altered the immunogenic phenotype of both iDCs and tDCs, we further analysed the effects of neuraminidase treatment on iDCs and tDCs through *in vitro* allogeneic coculture experiments. iDCs or tDCs from DA rats were treated with neuraminidase and cocultured with allogeneic lymphocytes. The immunogenic potential or the ability of niDCs and ntDCs to induce the proliferation and/or the activation of allogeneic lymphocytes was analysed by T-cell proliferation assays (**Figure 3.12**).

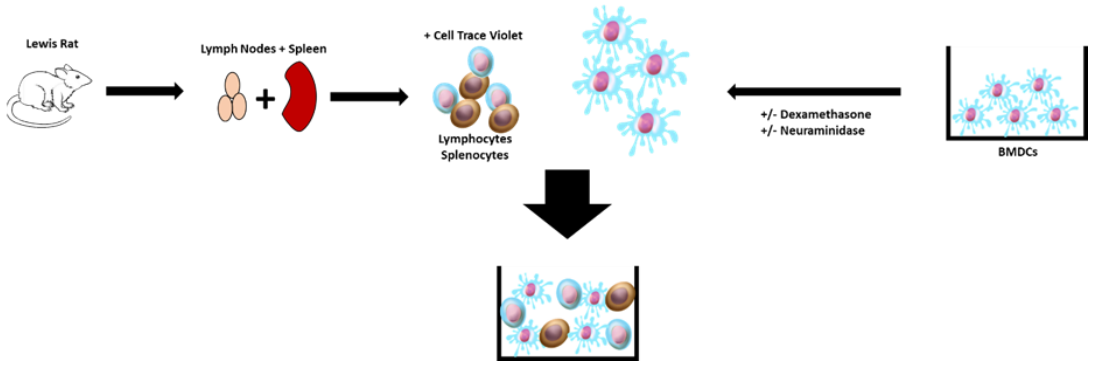

Figure 3.12 Schematic representation of experimental design. | DA iDCs, niDCs, tDCs, and ntDCs were placed in cocultures for 5 days with allogeneic LEW lymphocytes isolated from the spleen and lymph nodes.

Responder LEW rat T cells were analysed based on their co-expression of CD3+CD4+ or CD3+CD8+. Proliferation of lymphocytes was measured using CellTrace^{TM} Violet (CTV) (**Figure 3.13)** and activation of lymphocytes was measured using CD25 as an activation marker. DA iDCs (**Figure 3.14(i)**) and tDCs (**Figure 3.14(ii)**) did not induce an allogeneic response as indicated by a lack of changes in LEW CD3+CD4+ or CD3+CD8+ T cell proliferation when compared to unstimulated lymphocytes alone. Additionally, we observed no significant changes in CD3+CD4+CD25 or CD3+CD8+CD25 expression (data not shown) supporting our data on reduced

immunogenicity of iDCs and tDCs. However, niDCs (**Figure 3.14(i)**) significantly stimulated both CD3+CD4+ and CD3+CD8+ T cell proliferation when compared to both unstimulated lymphocyte controls and iDCs. This indicates the importance of Sia in the maintenance of an iDCs phenotype.

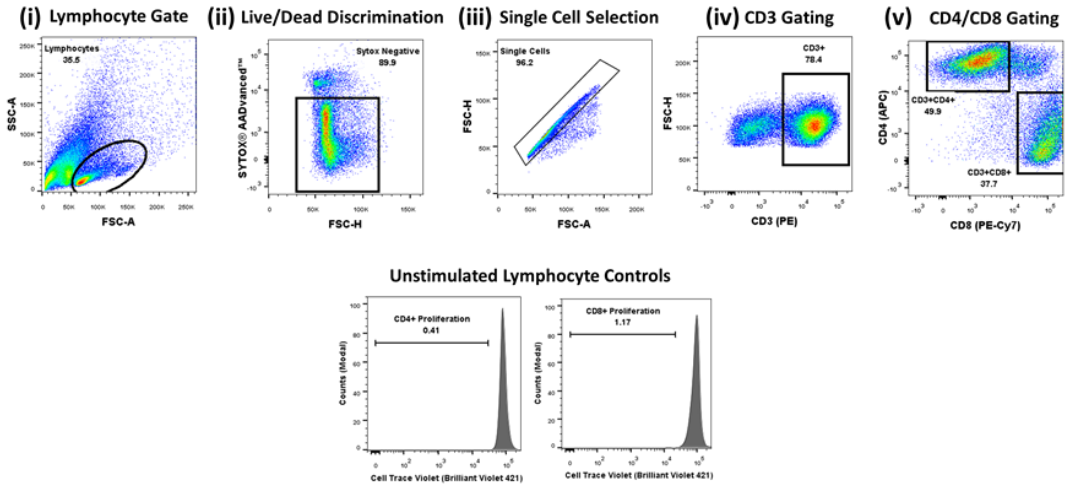

Figure 3.13 Representative gating strategy for analysis of immunogenicity assays. | Cells were selected according to size and granularity (i) followed by live/dead discrimination based on Sytox AADvanced™ negative cells (live) (ii). After single cell selection (iii) cells were selected by CD3 (PE) positivity (iv). Further selected by CD4 (APC) and CD8 (PE-CY7) and proliferation was measured by successive generations of CellTrace™ Violet positive cells.

While ntDCs show a trend increase to stimulate $CD3^{+}CD8^{+}$ T cells there were no significant changes noted **(Figure 2.14(ii)).** To eliminate the possibility of cell death as a potential cause of this increase in proliferation we assessed cell death using Sytox Blue. We observed iDCs have less cell death after neuraminidase treatment than tDCs **(Figure 3.15)** enabling us to exclude this possibility.

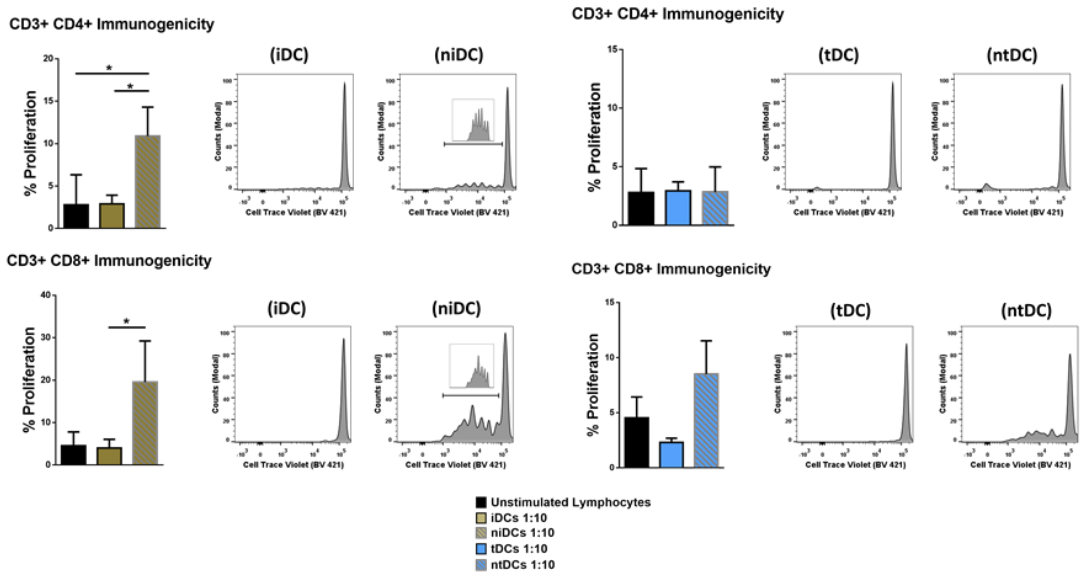

Figure 3.14 Neuraminidase treatment alters immunogenic properties of immature DCs (iDCs) and tolerogenic DCs (tDCs). | The ability of iDCs, niDCs, tDCs, and ntDCs to stimulate allogeneic LEW T-cells was analysed using unstimulated splenocytes/lymphocytes as a negative control (n = 3). (i) Representative histograms and bar charts displaying CD4+ and CD8+ T cell proliferation following a 5-day coculture with iDCs and niDCs. (ii) Representative histograms and bar charts displaying CD4+ and CD8+ T cell proliferation following a 5-day co-culture with tDCs and ntDCs. Error bars: mean ± SEM *p < 0.05, **p < 0.01, ***p < 0.001, ****p < 0.0001 one-way ANOVA, Tukey's multiple comparisons test.

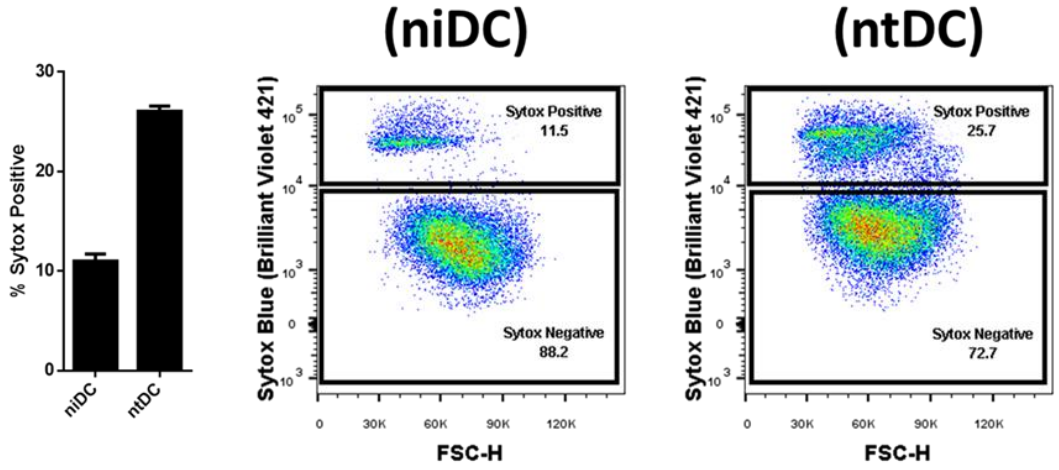

Figure 3.15 Resultant cell death due to neuraminidase treatment of iDCs and tDCs | Both iDCs and tDCs were treated with neuraminidase for 90 mins. These cells were then washed and placed into culture for 48 hours. Cells were prepared for flow cytometry as previously described and stained with the live/dead indicator Sytox blue (n=1, technical replicate of 2).

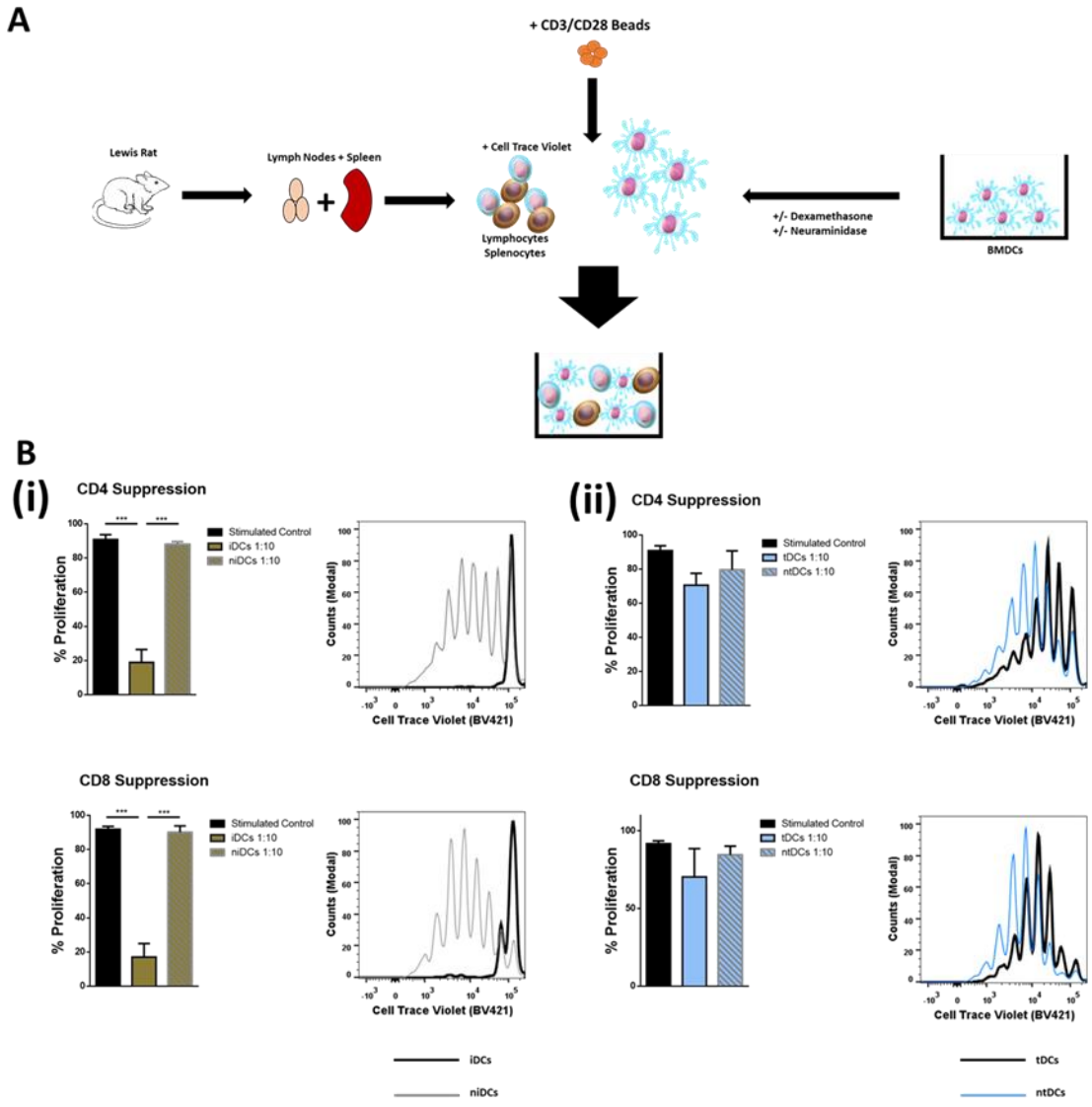

Figure 3.16 Neuraminidase treatment alters T-cell suppression properties of immature DCs (iDCs) and tolerogenic DCs (tDCs). | To test the T-cell suppression properties of iDCs, niDCs, tDCs, and ntDCs, they were placed into stimulated MLR cultures for 4 days. Splenocytes/lymphocytes were stimulated with CD3/CD28 beads. **(a)** Schematic representation of experimental design. DA iDCs, niDCs, tDCs, and ntDCs were placed in cocultures for 4 days with CD3/CD28-stimulated allogeneic LEW lymphocytes isolated from the spleen and lymph nodes. **(B)** The ability of iDCs, niDCs, tDCs, and ntDCs to suppress CD3/CD28 stimulated allogeneic T-cells was analyzed using stimulated splenocytes/lymphocytes as a positive control. Error bars: mean ± SEM *$p < 0.05$, **$p < 0.01$, ***$p < 0.001$, ****$p < 0.0001$ one-way ANOVA, Tukey's multiple comparisons test. (i) Representative histograms and bar charts displaying stimulated CD4+ and CD8+ T cell proliferation following a 4-day coculture with iDCs and niDCs. (ii) Representative histograms and bar charts displaying stimulated CD4+ and CD8+ T cell proliferation following a 4-day coculture with tDCs and ntDCs.

Finally, we investigated if niDCs and ntDCs can regulate the proliferation of stimulated T cells. LEW T cells were labelled with CTV, stimulated with CD3/CD28 labelled beads and co-cultured with niDCs and ntDCs (**Figure 3.16A**) and $CD3^+CD4^+$ and $CD3^+CD8^+$ proliferation was measured by flow cytometry. Neuraminidase treatment completely abrogates the T cell inhibitory effect of iDCs leading to full restoration of T cell proliferation (**Figure 3.16A (i))**. Interestingly, Dexa treatment is not sufficient to enable iDCs to inhibit the proliferation of activated T cells as no differences were observed between tDCs and ntDCs (**Figure 3.16B (ii)**).

In summary, these data indicate that the removal of Sia from iDCs increases the immunogenicity by its ability to stimulate CD4 and CD8 T cell proliferation which can be prevented by Dexa treatment. In contrast, neuraminidase treatment completely restores the proliferation of polyclonally activated T cells which cannot be prevented by Dexa treatment.

3.4 Discussion

Organ transplantation is often considered as the only therapeutic option for patients with life-threatening organ disease and is now performed on a routine basis. Due to incompatibilities between donor and recipient MHC-molecules, patients are required to take immunosuppressive drugs to prevent the destruction of the transplanted organ by the recipient's immune system. Immunosuppressive drug regimens are associated with severe side effects long term [300-302]. As a result, alternative immunosuppressive treatment strategies have been researched and developed including the use of therapeutic DCs in the treatment of autoimmune diseases and in the prevention of allograft rejection. DCs promote central and peripheral tolerance through various mechanisms, such as T cell anergy, inhibition of memory T cell responses and clonal deletion amongst others [146]. These characteristics form the basis of the use of DCs in the induction of tolerance. iDCs even have displayed the ability to convert naïve conventional T cells to regulatory T cells (Tregs) both *in vitro* [303, 304] and *in vivo* [305]. As shown here, and as shown by others, iDCs in non-inflammatory conditions display a poor immunogenic phenotype. One of the major barriers for use of iDCs in cellular therapies is that they respond to inflammatory stimuli, exemplified here by TLR4 (LPS) stimulation. In the context of autoimmunity and transplantation, iDCs are bound to encounter inflammatory environments if employed in therapeutic regiments. A potential solution to overcome this is the use of tDCs, which are maturation resistant.

Using tDC cellular therapies for the treatment of organ transplantation looks promising [306]. tDCs are now routinely generated using different induction protocols, including the use of corticosteroids such as Dexa [282, 284, 285, 287, 307] and in fact we have recently shown in a rat model of corneal transplantation that Dexa generated tDCs significantly prolonged allograft survival without the need for additional immunosuppression [169]. In this chapter, we generate tDCs using Dexa and we characterise their maturation resistant phenotype by analysing the expression of the immunogenicity markers MHCI, MHCII, CD80 and CD86 before and after TLR4 stimulation. We also analyse the expression of several immunomodulatory cytokine mRNAs. Dexa generated, maturation resistant, tDC have been well characterised by us [169, 297] and by other groups [287]. However, to our knowledge little is known on how Dexa induction of tDCs may affect the glycosylation profile of

these cells and what functional consequences this may have. Glycosylation changes are not routinely assayed but are likely to play crucial roles in iDC and tDC biology.

We describe here for the first time, using both lectin microarray and flow cytometry, that generation of tDCs by Dexa treatment leads to significant alterations in the cell surface glycosylation profile when compared to iDCs. We noted highly significant changes in lectin binding for α2-6-linked Sia (SNA-I) with no significant changes in lectin binding for α2-3-linked Sia (MAL-II). Interestingly, Jenner *et al* [308] when comparing human iDCs with iDCs matured with a cytokine cocktail (IL-6, IL-1β, TNF-α and prostaglandin E2) noted decreased α2-6-linked Sia with no changes in α2-3-linked Sia on the more immunogenic DC. This study also showed that Tregs have higher levels of α2-6-linked Sia when compared to activated conventional T cells. This suggests a possible link between α2-6-linked Sia content and tolerogenicity, where the increased α2-6-linked Sia may potentially serve as ligands for inhibitory sialic acid binding proteins (Siglecs) on the surface of effector cells [308]. In fact, hyper-sialylated antigens loaded onto dendritic cells were recently shown to impose a regulatory program in the DCs. This resulted in the inducement of Tregs via Siglec-E and the inhibition of effector T cells [309].

Looking more closely at the lectin microarray analysis, other differences in lectin profiles observed here also hint at significant changes in the total abundance or potential branching alterations of underlying oligosaccharide structures, particularly *N*-acetyllactosamine (LacNAc), which may have occurred because of Dexa treatment. The relationship of responses among the fifteen lectins (SNA-II, BPA, PNA, DSA, LEL, SNA-I, RCA-I, CPA, ECA, LTA, UEA-I, EEA, GS-I-B4, MPA and VRA) which demonstrated the most significant differences between untreated iDCs and tDCs may hold further clues as to the nature of these variations in the glycocalyx and it is possible that a portion of such variations exist among the membrane glycolipid structures as well as membrane proteins which were analysed here. With extracted glycoproteins, only one of the three lectins on the microarray which has been reported to be indicative of Sia presence, SNA-I, demonstrated a significant intensity increase for tDCs. This was also demonstrated by lectin coupled flow cytometry showing how highly regulated Sia metabolism is in DCs. However, responses at lectins which bind to structures which are the most frequent attachment points for sialylation, those which bind to galactose (Gal) or *N*-acetylgalactosamine (GalNAc) (SNA-II, BPA, PNA) and

those which bind to the associated disaccharide Type II LacNAc (RCA-I, CPA, ECA) or poly-LacNAc (LEL), are particularly interesting because the expected relationship of higher SNA-I binding and simultaneously lower Gal/GalNAc and LacNAc lectin binding did not consistently hold true across the lectin microarray profiles for DCs. The binding profiles and behaviour of SNA-I and MAL-II in these experiments strongly infer quantitative differences between iDC and tDC surface Sia content, however absolute quantitation will ultimately require chromatographic (e.g. HPLC) or chromatography-conjugated mass spectrometric analysis (LC-MS).

Because of the reported importance of Sias in DC pattern recognition [179, 308], endocytosis, phagocytosis [180, 182, 183, 310], antigen presentation [311], migration [144, 189, 191, 192, 312] and T cell interactions [144, 194]. But also, considering that α2-6-linked Sia was the most significantly increased change after tDC generation by Dexa, we choose to investigate Sia's importance in iDC and tDC immunogenicity in an allogeneic setting which would have potential implications in iDC and tDC cellular therapies.

Initially, we attempted to naturally increase the abundance of cell surface Sia by supplementing the culture media with the monosaccharide ManNAc. This method has been used by others to increase the activity, performance and yield of recombinant human proteins produced by cells by increasing Sia on these glycoconjugates [313, 314]. ManNAc was fed to iDCs at varying concentrations on day 5 and day 7 of culture and analysed by microarray and flow cytometry. 2-6-linked Sia did not significantly increase after ManNAc supplementation when analysed by flow cytometry. The second lowest concentration (1mM) and the highest concentration (20mM) showed significant increases on the lectin microarray. Considering the slight increase observed and that the difference in concentrations where we observed significance were so far apart we concluded that the small significant increases were biologically insignificant.

Our second attempt to increase 2-6-linked Sia on the surface of the iDCs involved using Function Spacer Lipid constructs (FSLs). FSLs are a technology developed by Kode Technology, they are water dispersible bio-surface engineering constructs that can be used to engineer the surface of cells. In short, they allow us to spontaneously and stably incorporate Sia moieties into the iDCs membranes using lipid tails [315,

316]. The FSL constructs failed to increase Sia on the surface of iDCs (data not shown).

Considering our lack of success in trying to naturally or mechanically increase Sia on the surface of iDCs, we decided to remove it and study the functional consequences. For this we removed Sia from the surface of the cells by enzymatic digestion using neuraminidase (sialidase). These experiments showed that Sia is involved in maintaining the tolerogenic phenotype of both iDCs and tDCs, as removal of Sia resulted in an increase in immunogenicity markers and increases in pro-inflammatory TH1 mRNA transcripts notably IL-6, IL-1β, iNOS (iDCs only), TNF-α and IL-12p40 (iDCs only) with significant decreases in anti-inflammatory or tolerogenic IL-10. In experiments where neuraminidase treated human monocyte derived DCs were cultured with ovalbumin [182] or *Escherichia coli [310]* there were reported increases in immunogenicity markers and cytokine gene expression also. Here we show that even after Dexa treatment and tDC generation the removal of Sia from the cell surface results in increases in both cell surface immunogenicity markers and TH1 pro-inflammatory cytokine gene expression, underpinning the importance of Sia in a non-immunogenic phenotype.

In the context of allogeneic cell therapy for the treatment of autoimmune diseases and in the prevention of allograft rejection it is important that the cell therapy itself does not elicit a deleterious immune response. In unstimulated allogeneic co-cultures using LEW responder lymphocytes, we show that iDCs and tDCs are non-immunogenetic and do not elicit either $CD3^+CD4^+$ nor $CD3^+CD8^+$ proliferation. This attribute makes them ideal candidates in DC cellular therapies. We show that removal of Sia from iDCs is sufficient enough to stimulate the allogeneic responders, again showing the importance of Sia in a non-immunogenic phenotype. This may indicate that the removal of Sia uncaps underlying structures which are then recognized as a signal for T-cell proliferation or that the Sias may act as ligands for inhibitory Siglecs on the surface of effector cells and once removed, this inhibitory effect is lost. Sia removal of tDCs did not induce $CD3^+CD4^+$ proliferation but we noted a trend increase in $CD3^+CD8^+$ proliferation. Interestingly, this indicates that, despite the increase of immunogenicity markers and the transcript increase in several pro-inflammatory mRNAs, Dexa treatment of iDCs was sufficient to keep the cells, at least partially, in a non-immunogenic state.

In CD3/CD28 stimulated (hyper stimulated) allogeneic co-cultures using LEW responder lymphocytes, we show that iDCs had an impressive ability to suppress stimulated allogeneic lymphocytes. Sia is critical in maintaining this suppressive ability as when it was absent we observed complete restoration of T cell proliferation for both $CD3^+CD4^+$ and $CD3^+CD8^+$ populations. These results are supported by the fact that Crespo *et al* [182] showed increased T-lymphocyte proliferation in autologous mixed lymphocyte cultures using human monocyte-derived DCs where the lymphocytes were stimulated with tetanus toxoid, inactivated with mitomycin C and co-cultured with neuraminidase monocyte-derived DCs. Interestingly, we showed that tDCs do not have the ability to suppress hyper stimulated allogeneic lymphocytes to the same extent as iDCs. Sia removal had little effect on tDCs suppressive ability and did not exaggerate proliferation. Together these experiments highlight that the tolerogenic properties between iDCs and tDCs are not inherently the same and understanding these characteristics and limitations will inform us on how to optimise therapy strategies.

The findings outlined here could also have numerous implications for our understanding of DC phenotype and function in the tumour microenvironment. Efficient induction of anti-tumour responses requires that DCs in the tumour undergo proper maturation and activation [317]. Understanding DC activation is important both in terms of their role in regulating immune responses locally in the tumour microenvironment [318], and also their use in ex vivo cellular and vaccination strategies to induce tumour specific immune responses.

In the context of tumour vaccination strategies using DCs, the required response is to induce tumour-specific effector T cells that can eliminate tumour cells specifically and that can induce immunological memory to control tumour relapse. Our findings suggest that Dexa, a common component of chemotherapy regimens, could suppress DC maturation and activation, their ability to present antigen [319], as well as their ability to induce T cell proliferation and activation. Interestingly, our data indicates that these potent Dexa induced effects could be somewhat reversed in the presence of a neuraminidase, suggesting a key role for sialylation in Dexa generated tDCs. Removal of sialic acid has also previously been shown to increase tumour antigen specific T cell responses [311] . Our data also shows that as well as a more potent ability to induce CD8+ T cell activation. In terms of modulating the tumour

microenvironment directly, local delivery targeted approaches using sialyltransferase inhibitors delivered either to the tumour or the local lymph nodes could be exploited. In terms of ex vivo generated DCs for either cellular therapy or in vaccination strategies, treatment of DCs with sialyltransferase inhibitors could be sufficient to allow efficient priming of T cells systemically. As DCs provide an essential link between innate and adaptive immunity, these findings could have important implications in our understanding of the suppressive mechanisms within the tumour microenvironment that hinder adaptive anti-tumour immune responses and potential mechanisms by which they could be overcome.

Together, these results highlight the importance of Sia's in DC biology, especially in the context of iDC allogeneic cellular therapy. While the precise implications of increased or decreased Sia expression on iDCs and tDCs remain to be elucidated *in vivo*, we show here strong evidence that supports a function of Sia in the therapeutic aspects of DC cellular therapies. Identification of the molecular mechanisms and factors which are regulated by Sia's are important to exploit this phenomenon in the clinic. This study points towards the potential of DC surface sialylation as a therapeutic target to improve and diversify DC-based therapies and treatments. In the context of disease, cell glyco-engineering could have positive implications in the treatment of autoimmunity, DC-based vaccines, the tumour microenvironment and transplant biology.

3.5 Summary: Limitations and Further Studies

In this chapter, the data confirm the hypothesis that iDCs and tDCs have significant differences in glycosylation profiles and that these differences have a role to play in their therapeutic benefits. However, all work in this chapter has been discussed in an *in vitro* context. To confidently conclude that 2-6-linked Sia plays an important role in the therapeutic efficacy of iDCs and tDCs we would need to test these cells in an appropriate model. As stated previously, we have recently shown that both iDCs and tDCs can prolong corneal allograft survival in an allogeneic model of corneal transplantation. It would be interesting to cleave 2-6-linked Sia from both cell populations and inject them in the same manner and study if they can still prolong survival.

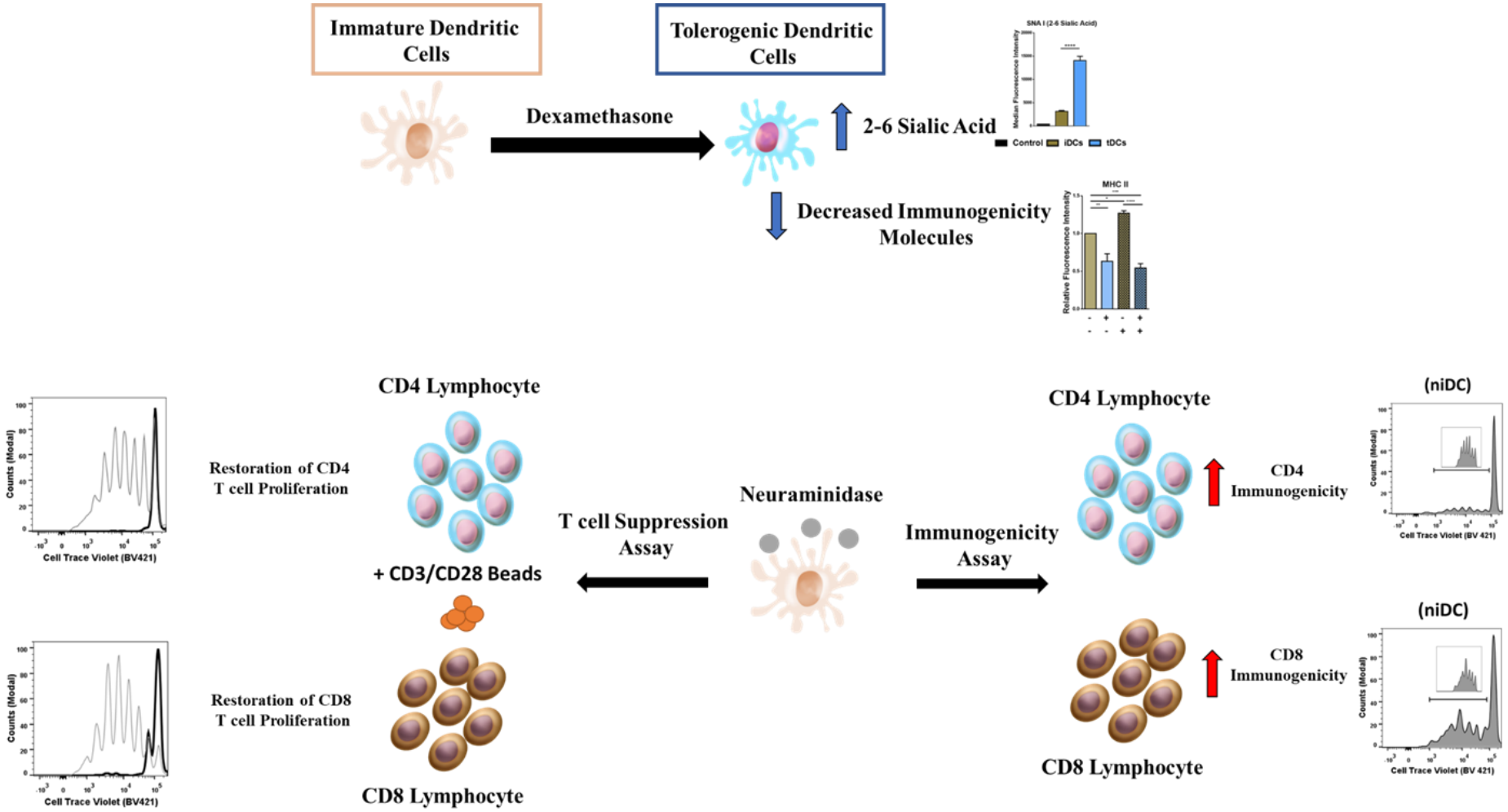

Figure 3.17. Graphical summary of significant results discussed in chapter 3

We used neuraminidase to cleave Sia from the surface of iDCs and tDCs. Two potential questions that arise with this method are: is the harsh treatment by the neuraminidase activating the iDCs indirectly? And the other question is what of glycoconjugates that are synthesised inside the cell and secreted afterwards? The neuraminidase would not be able to cleave the Sia on these conjugates. A potential solution to both questions is to use a sialyltransferase inhibitor such as 3Fax-Peracetyl Neu5Ac (SI). This SI is cell permeable and acts on the enzymes responsible for capping proteins and lipids with Sia. While the SI was not readily available at the beginning of our study, it is widely available now. Preliminary results (data not shown) using this SI show that it efficiently and significantly down regulates Sia on the surface of the cells without effecting proliferation rates or cell viability. It is a less harsh way of achieving a Sia deficient cell. It would be interesting to repeat this study using this SI and see if the results indicating the importance of α2-6-linked Sia on iDC cell surface would be replicated. A graphical summary of the more significant results presented and discussed in this chapter is found above (**Figure 3.17**)

Chapter Four:

Elucidating the Immunomodulatory Potential of Pre-Activated MSCs *in vitro* and Investigating *in vivo* Efficacy

4.0 Chapter Experimental Design

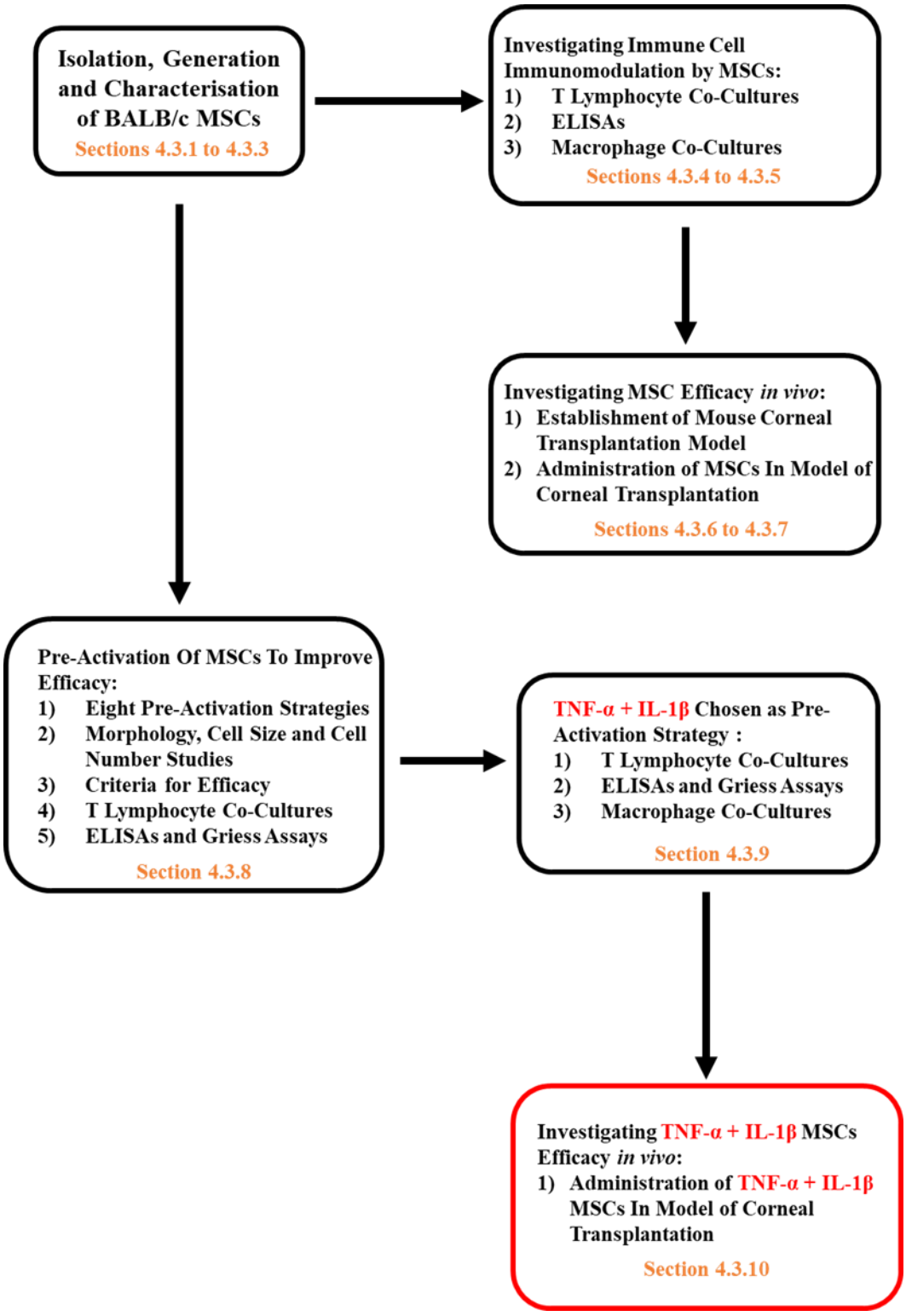

Schematic overview of chapter experimental design | A schematic presenting the sequence and progression of experiments described in this chapter.

4.1 Introduction

MSCs can be isolated from multiple different tissues, including bone marrow, muscle, fat, placenta, and umbilical cord. They were initially identified by their tri-lineage differentiation potential into mesenchymal tissues such as bone and adipose tissue [196, 320]. They are defined by their proliferative capacity, multilineage potential and their plastic adherence [321]. In steady state conditions MSCs reside in perivascular spaces surrounding almost every region of the body where they are thought to maintain tissue homeostasis by sensing tissue damage and then acting to promote tissue repair and healing after insult [255, 256]. The inflammatory environment of damaged tissue is what activates MSCs allowing them to become potent immune regulators. Intravenously infused MSCs become trapped in the lung and migrate to a variety of organs, prioritising inflamed tissues [320]. Here they become activated due to the inflammatory environment and via both contact dependent and contact independent mechanisms exert their immunosuppressive properties [320]. This information promoted the idea that MSC-mediated suppression of immune cells is not innate and that the pre-activation of MSCs before *in vivo* administration could promote their efficacy. This has been demonstrated using pro-inflammatory cytokines such as IFN-γ, TNF-α and IL-1β [236, 243, 322].

IFN-γ is secreted by activated $CD4^+$ and $CD8^+$ lymphocytes and is a predominant cytokine in the inflammatory milieu. The pre-treatment of MSCs with IFN-γ is perhaps one of the most studied methods of MSC pre-activation. Krampera *et al.* demonstrated that IFN-γ MSCs significantly inhibit T lymphocyte and NK cell proliferation whereas non IFN-γ MSCs did not. Furthermore, IFN-γ blockade abrogated this observed effect [242]. Supportively, it was observed that IFN-γ MSCs significantly suppress IFN-*γ*, TNF-*α*, and IL-2 production by T lymphocytes and inhibits their proliferation [323]. Chinnadurai *et al*. [324] demonstrated that IFN-γ MSCs have a greater ability to generate Tregs *in vitro* compared to non IFN-γ MSCs. Interestingly, Fan *et al*. demonstrated in a mouse model of colitis that IL-1β MSCs had a greater ability to induce the numbers of Tregs and Th2 cells *in vivo* with decreased numbers of Th1 and Th17 cells in the spleens and lymph nodes of treated mice compared to control mice [325].

Pre-treatment of MSCs with cytokine combinations have yielded more promising results leading to the secretion and upregulation of multiple immunoregulatory molecules such as NO, IDO, PD-L1, PD-L2, PGE2, CCL5, CXCL9, CXCL10, and CXCL11 [326]. Cuerquis *et al.*[327], Li *et al.* [328], Prasanna *et al.*[329], and Jin *et al*. [330] have all demonstrated that combinations of IFN-γ and TNF-α induce the upregulation of immunomodulatory molecules leading to increased T lymphocyte suppression or Treg induction [328] by pre-treated MSCs.

These studies demonstrated that the inflammatory environment stimulates the immunoregulatory attributes of MSCs. To summarise, MSCs can secrete and upregulate chemokines and molecules which induce the accumulation of immune cells in close association with MSCs forming a microenvironment where MSCs can exert their immunoregulatory molecules which leads to strong immunosuppression [326].

Therefore, the hypothesis for this chapter was that pre-activated BALB/c MSCs acquire potent immunosuppressive properties and that pre-activated MSCs can prolong corneal allograft survival.

To test the hypothesis, MSCs were pre-treated with different combinations of the pro-inflammatory cytokines IFN-γ, TNF-α and IL-1β or singly with the anti-inflammatory cytokine TGF-β. The phenotype of the pre-treated MSCs was characterised to determine if pre-treatment negatively impacted the function of the MSCs. Pre-treated MSCs were co-cultured with activated syngeneic T lymphocytes and macrophages to determine which combination of cytokines induced the most immunosuppressive phenotype. The most potently immunosuppressive MSCs were chosen to be used in our established pre-clinical model of corneal allograft transplantation.

4.2 Hypothesis and Objectives

4.2.1 Hypothesis

The potent immunosuppressive properties of BALB/c MSCs are only acquired upon pre-activation by cytokines. Pre-activated MSCs can prolong rejection free survival in a model of corneal transplantation via the modulation of the alloantigen immune response.

4.2.2 Aims

To pre-treat MSCs with the cytokines IFN-γ, TNF-α, IL-1β and TGF-β and characterise the pre-activated MSC phenotype

To test the immunosuppressive capacity of pre-activated MSCs to modulate syngeneic innate and adaptive immune effector cells

Administer the most potent immunomodulatory pre-activated MSC in our pre-clinical model of corneal transplantation

4.3Results

4.3.1 Isolation and Characterisation of BALB/c MSCs

To generate MSCs, bone marrow was flushed from the long bones of the tibia and femur of BALB/c mice and cultured in MSC culture medium (**Figure 4.1A**). This protocol of isolation and passaging is well established and has been optimised by us in the past [18, 19]. By passage 4 (P4) we can see that all hematopoietic and myeloid cell contamination has been removed by selection for plastic adherent cells (**Figure 4.1B**). At P4 the cells were harvested and prepared for flow cytometry analysis as discussed in section 2.7.1. The MSCs were characterised by flow cytometry for markers that the International Society for Cellular Therapy (ISCT) have used to define MSCs. These included the negative markers MHC II, CD45, F4/80, CD11c, CD80 and CD86 (**Figure 4.1C**) and the positive markers CD105. CD73, CD90. CD44, SCA-I and MHC I (**Figure 4.1D**). All cells expressed the characterisation markers CD105. CD73, CD90. CD44, SCA-I and MHC I while being negative for MHC II, CD45, F4/80, CD11c, CD80 and CD86.

4.3.2 Osteogenic Differentiation of BALB/c MSCs

To differentiate MSCs to osteocytes, MSCs were cultured in specific osteogenic differentiation medium or control medium. After the culturing period, the MSCs were stained with Alizarin Red, which is used to identify calcium present in cells in vitro. MSCs treated with osteogenic medium stained positive for Alizarin Red (**Figure 4.2A(i)**) while MSCs cultured in normal MSC medium did not. MSCs cultured in osteogenic medium also had a higher concentration of calcium as tested by a StanBio Calcium Liquicolour kit (**Figure 4.2 B+C**) when compared to MSCs cultured in MSC normal culture medium.

4.3.3 Adipogenic differentiation of BALB/c MSCs

To differentiate MSCs to adipocytes, MSCs were cultured in specific adipogenic induction and maintenance medium. After the culturing period, the cells were fixed with formalin and were stained with Oil Red O which stains lipids and triglycerides red. Again, MSCs showed multipotent capacity as they differentiated into adipocytes as observed by brightfield microscopy (**Figure 4.3A(i+ii)**) and in an absorbance assay to quantify lipids (**Figure 4.3B**).

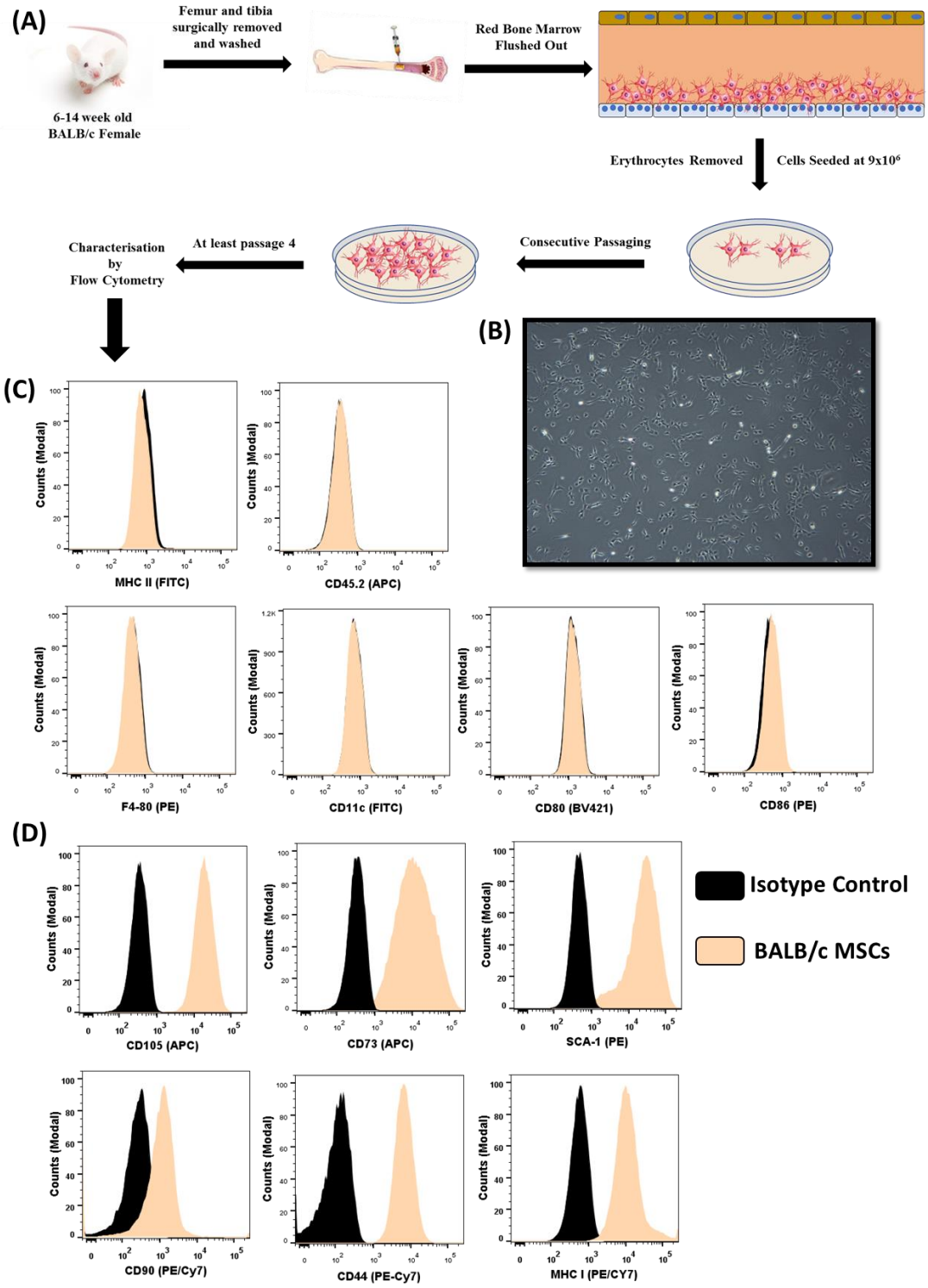

Figure 4.1 Isolation and characterisation of BALB/c MSCs. | (A) Schematic showing the process by which BALB/c MSCs are isolated from the bone marrow. (B) 4x brightfield microscopy of passage (P) 4 MSCs 24 hours after seeding. (C) Representative flow cytometry histograms for the cell surface expression of negative MSC antigens, MHCII, CD45.2, F4-80, CD11c, CD80, CD86. (D) Representative flow cytometry histograms for the cell surface expression of positive MSC antigens, CD105, CD73, SCA-1, CD90, CD44 and MHC I. (*n=4*)

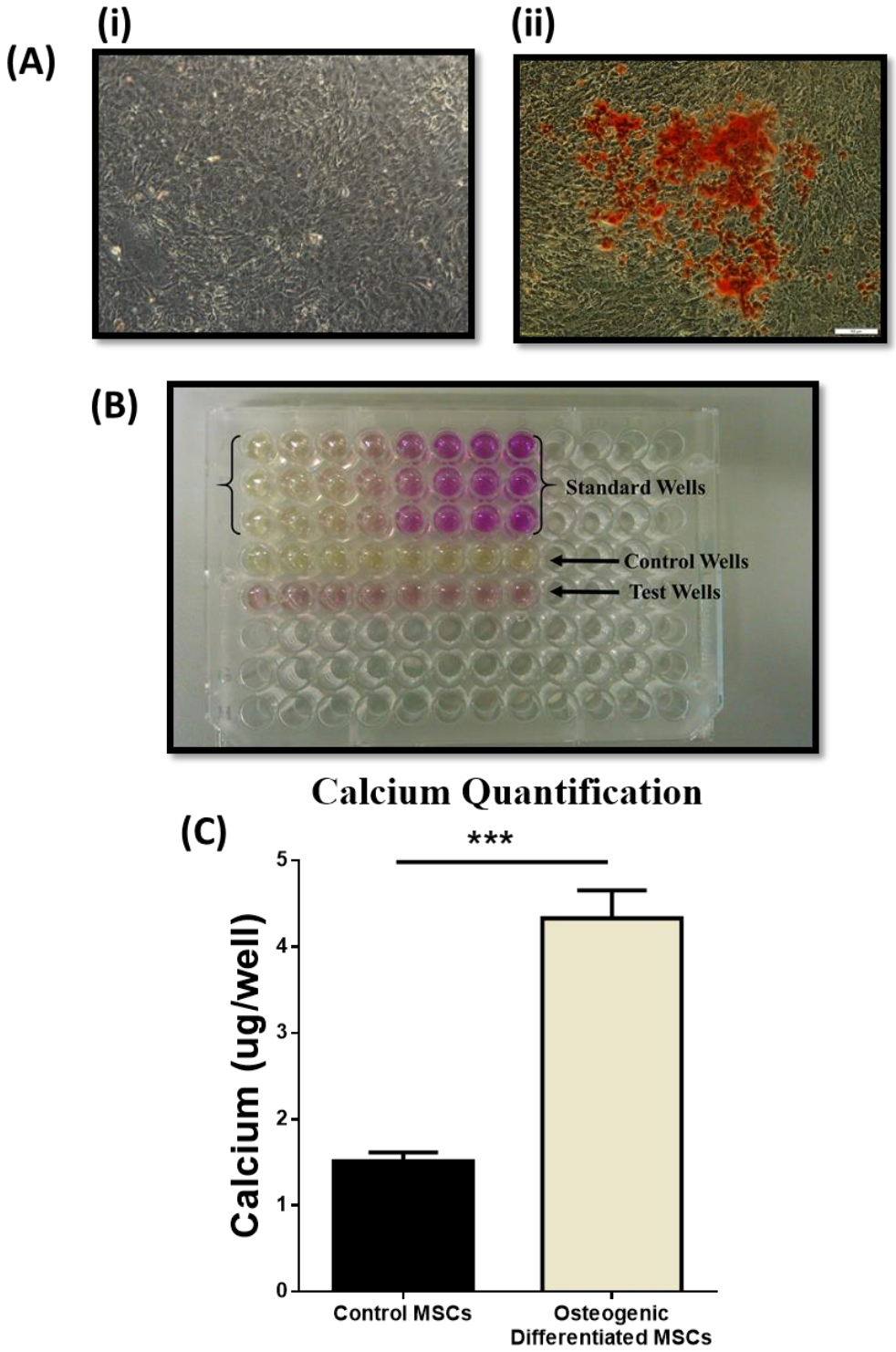

Figure 4.2 Osteogenic differentiation of BALB/c MSCs. | BALB/c MSCs were cultured in specific osteogenic differentiation medium (detailed in Materials and Methods section). (A) Brightfield microscopy of Alizarin Red staining. Osteocytes stain red (ii) while MSCs remain Alizarin Red staining free (i). (B) Picture of calcium quantification assay. (C) Colum graph quantifying calcium in MSCs vs MSCs cultured in osteogenic medium. Error bars: mean +/- SEM *p<0.05, **p<0.01 ***p<0.001 ****p<0.0001. Unpaired, two tailed student's t test. (n=3).

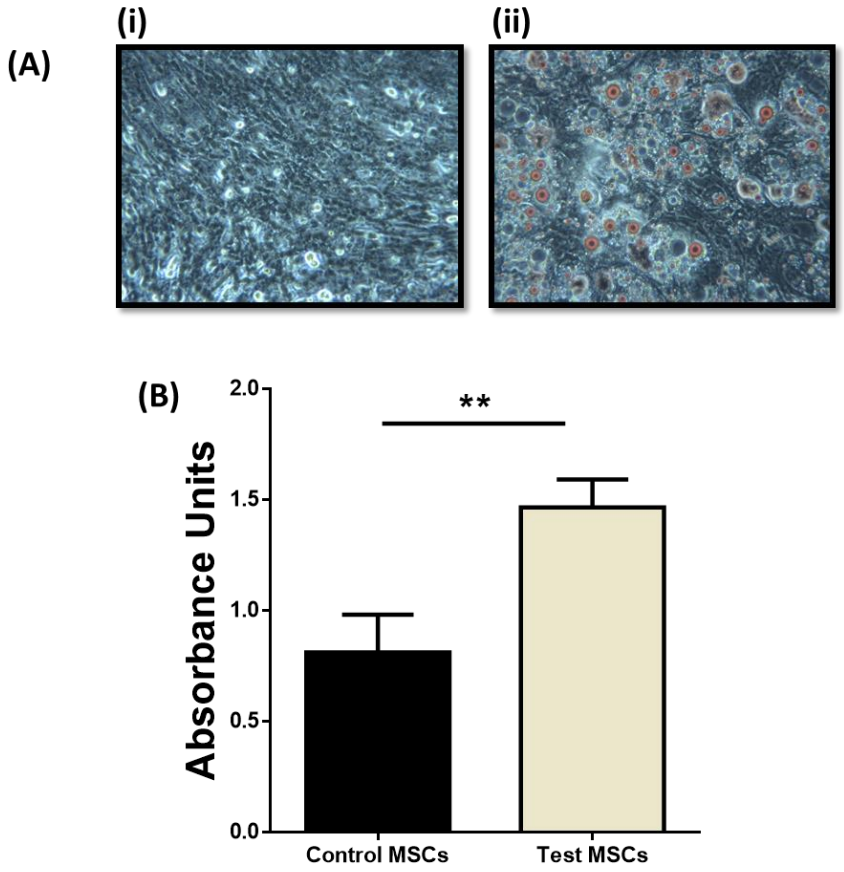

Figure 4.3 Adipogenic differentiation of BALB/c MSCs. | BALB/c MSCs were cultured in specific adipogenic induction and maintenance differentiation medium (detailed in Materials and Methods section). Oil Red O solution was used to determine adipogenic differentiation. (A) Brightfield microscopy images of Oil Red O stained control (i) and adipogenic differentiated wells (ii). (B) Quantification of Oil Red O solution absorbance read by plate reader. Error bars: mean +/- SEM *p<0.05, **p<0.01 ***p<0.001 ****p<0.0001. Unpaired, two tailed student's t test (*n=3*)

4.3.4 BALB/c MSCs Do Not Suppress Stimulated Syngeneic Lymphocyte Proliferation, nor Induce Regulatory T Lymphocytes but Do Reduce IFN-γ Secretion While Increasing PGE2 Secretion

MSCs are defined as self-renewing cells that have multilineage potential and exist *in vivo* as resident adult stem cell progenitors. In this resting state, MSCs do not possess potent immunosuppressive properties [321, 331]. This being the case, MSCs have been reported to modulate many different immune cells *in vitro* and *in vivo* [203, 332, 333]. To assess this, we assayed the ability of MSCs to modulate activated $CD4^+$ and $CD8^+$ lymphocytes and also their ability to induce regulatory T lymphocytes (Tregs).

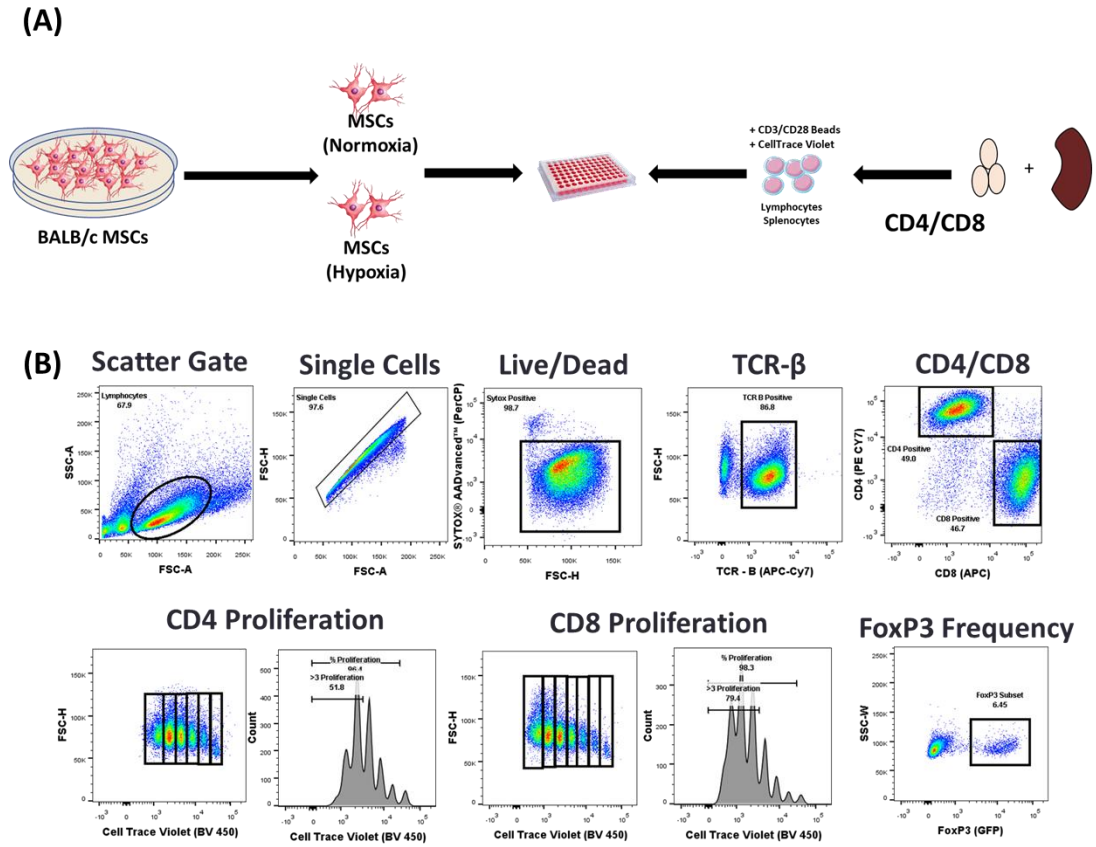

Figure 4.4 Experimental setup and representative gating strategy of mixed lymphocyte reaction for flow cytometry analysis | (A) BALB/c MSCs cultured in normoxia or hypoxia were placed in T lymphocyte co-culture for 96 hours with CD3/CD28 stimulated lymphocytes (B) Firstly, cells were selected according to size and granularity, followed by single cell selection. After live/dead discrimination based on SYTOX negative cells (live), cells were selected by TCR-β and CD4/CD8 positivity. Proliferation was measured by CTV. FoxP3 expression was determined by GFP-FoxP3 expression.

BALB/c MSCs cultured under both normoxic and hypoxic conditions were co-cultured in T lymphocyte co-culture at different ratios with CD3/CD28 stimulated lymphocytes isolated from the spleens and lymph nodes of C.Cg-Foxp3^{tm2Tch}/J BALB/c mice **(Figure 4.4A)**. After optimisation, the ratio of 1 MSC to 10 lymphocytes was found to be the ratio were MSCs exerted potent immunosuppressive effects. At ratios greater than 1:50, the immunomodulatory effects of MSCs was lost. For this reason, results will be discussed in the context of 1:10 ratio. T lymphocyte co-cultures were incubated for 96 hours. Following incubation, proliferation of TCR-β^+CD4^+ and TCR-β^+CD8^+ lymphocytes and the frequency of TCR-$\beta^+CD4^+FoxP3^+$ lymphocytes (Tregs) were analysed by flow cytometry **(Figure 4.4B)**. BALB/c MSCs did not inhibit the proliferation of activated TCR-β^+CD4^+ **(Figure 4.5(i))** and TCR-β^+CD8^+ **(Figure 4.5(ii))** lymphocytes. In fact, when the percentage of $CD4^+$

lymphocytes in each generation was analysed, it was observed that a lower percentage of lymphocytes were present in the 1st, 2nd and 3rd generations (Gen) **(Figure 4.5(ii))** of wells where MSCs where added. This would indicate the MSCs are stimulatory rather that inhibitory.

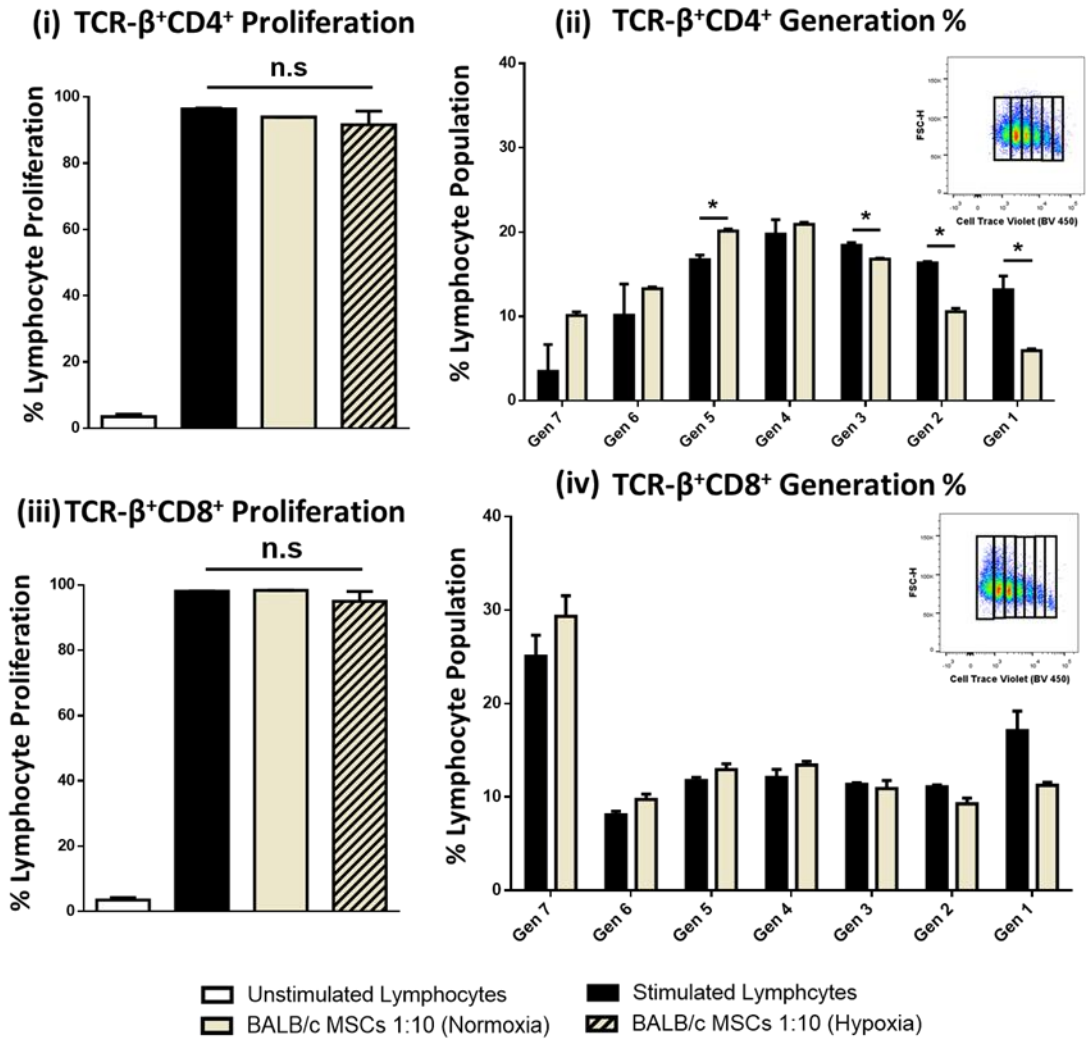

Figure 4.5 Normoxic or hypoxic cultured BALB/c MSCs do not suppress stimulated lymphocyte proliferation | BALB/c MSCs (1 MSC to 10 lymphocytes) cultured in normoxia or hypoxia were placed in T lymphocyte co-culture for 96 hours with CD3/CD28 stimulated lymphocytes. CTV was used to determine lymphocyte proliferation. (i) % proliferation of TCR-β^+CD4^+ lymphocytes. (ii) % of TCR-β^+CD4^+ lymphocyte proliferation per generation (Gen). (iii) % proliferation of TCR-β^+CD8^+ lymphocytes. (iv) % of TCR-β^+CD8^+ lymphocyte proliferation per generation. Error bars: mean +/- SEM *p<0.05, **p<0.01 ***p<0.001 ****p<0.0001. Multiple unpaired, two tailed student's t test and One-way ANOVA, Tukey's Post Hoc test (*n=3*).

Utilising the C.Cg-Foxp3^{tm2Tch}/J BALB/c mouse, TCR-$\beta^+CD4^+FoxP3^+$ (Tregs) cells were analysed after T lymphocyte co-culture. It was observed that MSCs do not increase the frequency of Tregs compared to stimulated lymphocyte controls (**Figure**

4.6). IL-2 was added to some cultures to study the effect of this potent T lymphocyte growth factor on the ability of MSCs to increase Treg frequency.

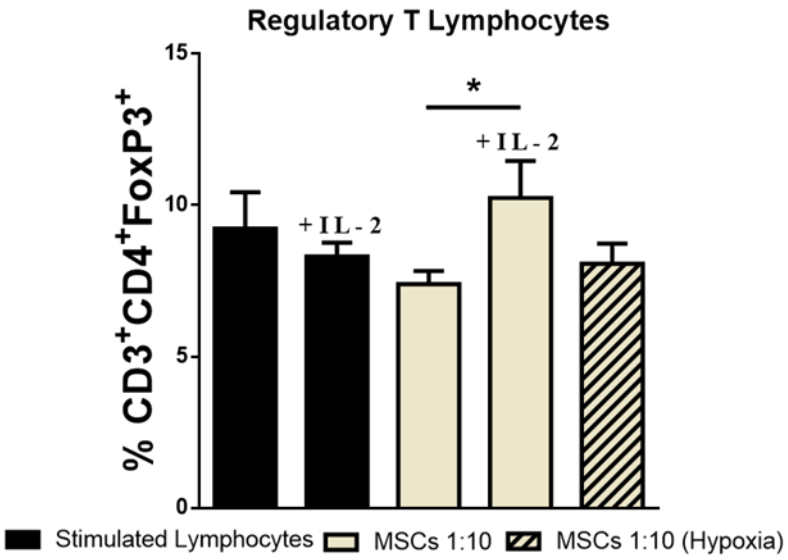

Figure 4.6 BALB/c MSCs do not induce Regulatory T lymphocyte frequency | Hypoxic or normoxic cultured BALB/c MSCs (1 MSC to 10 lymphocytes) were co-cultured in T lymphocyte co-culture in the presence or absence of IL-2 for 96 hours with CD3/CD28 stimulated lymphocytes. The frequency of Tregs was analysed by flow cytometry. Error bars: mean +/- SEM *p<0.05, **p<0.01 ***p<0.001 ****p<0.0001. One-way ANOVA, Tukey's Post Hoc test (*n=3*).

While the presence of IL-2 significantly increases Tregs in MSC wells compared to IL-2 deficient MSC wells, there was no significant increase observed when compared to stimulated controls. Normoxic or hypoxic culturing of the MSCs did not show any differences in the frequencies of Tregs (**Figure 4.6**).

Supernatants from the T lymphocyte co-culture were saved and assayed via ELISA. Quantification of Interferon gamma (IFN-γ), Prostaglandin E2 (PGE2) and Granzyme B was performed. Significantly lower levels of IFN-γ was observed in wells where MSCs were present compared to stimulated lymphocytes alone. No significant changes in the cytotoxic T-cell molecule Granzyme B were detectable. Significantly higher levels of the T-cell modulating PGE2 was observed in wells where MSCs were present compared to stimulated lymphocytes alone (**Figure 4.7**). To summarise, despite significantly reducing IFN-γ and increasing PGE2 in the T lymphocyte co-cultures, BALB/c MSCs were unable to inhibit syngeneic T lymphocyte proliferation

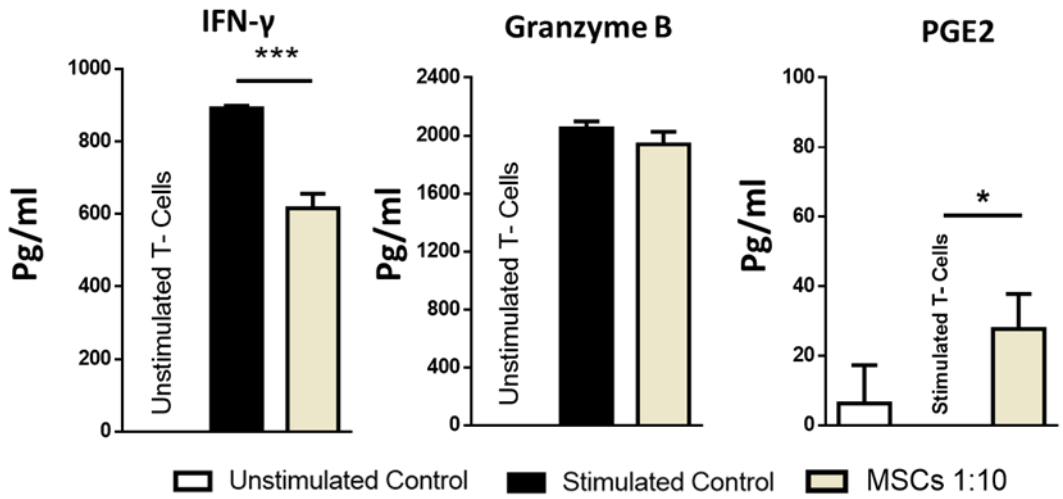

Figure 4.7 BALB/c MSCs significantly reduce IFN-γ, increase PGE2 and has no effect on Granzyme B secretion in T lymphocyte co-culture | BALB/c MSCs (1 MSC to 10 lymphocytes) were co-cultured in T lymphocyte co-culture for 96 hours with CD3/CD28 stimulated lymphocytes. Supernatants were analysed for the presence of IFN-γ, PGE2 and Granzyme B by ELISA. Error bars: mean +/- SEM *p<0.05, **p<0.01 ***p<0.001 ****p<0.0001. One-way ANOVA, Tukey's Post Hoc test. Representative graphs of three individual experiments (*n=3*).

4.3.5 BALB/c MSCs Do Not Modulate Activated Macrophage Phenotype but Do Modulate the Pro-Inflammatory Secretome

MSCs have been reported to modulate inflammatory macrophages (φ) *in vitro* [332, 334]. Macrophages have also been shown to play an important role in the transplant rejection process in rodents [83, 335, 336]. To assess this, we assayed the ability of MSCs to modulate activated syngeneic macrophages *in vitro* by directly co-culturing MSCs and macrophages for 3 days followed by flow cytometry and supernatant analysis. Macrophages were generated from the bone marrow of BALB/c mice **(Figure 4.8A)**. Macrophages were stimulated by the addition of IFN-γ (50ng/ml) for 24 hours prior to co-culture, followed by LPS (10ng/ml) stimulation for 4 hours. Following a 3-day incubation, macrophages were analysed by flow cytometry **(Figure 4.8B)**. Median fluorescence intensities of the activation markers MHC I, MHC II, CD80 and CD86 were analysed on stimulated macrophages and compared to stimulated macrophages that were co-cultured with MSCs at a ratio of 1 MSC to 5 macrophages **(Figure 4.8C)**. No significant changes were observed in the expression of MHC I, MHC II, CD80 and CD86. Co-culture supernatants were assayed for the pro-inflammatory cytokines TNF-α, IL-1β, IL-12/23 and IL-6 **(Figure 4.8D)**. In the presence of MSCs all four pro-inflammatory cytokines were significantly reduced.

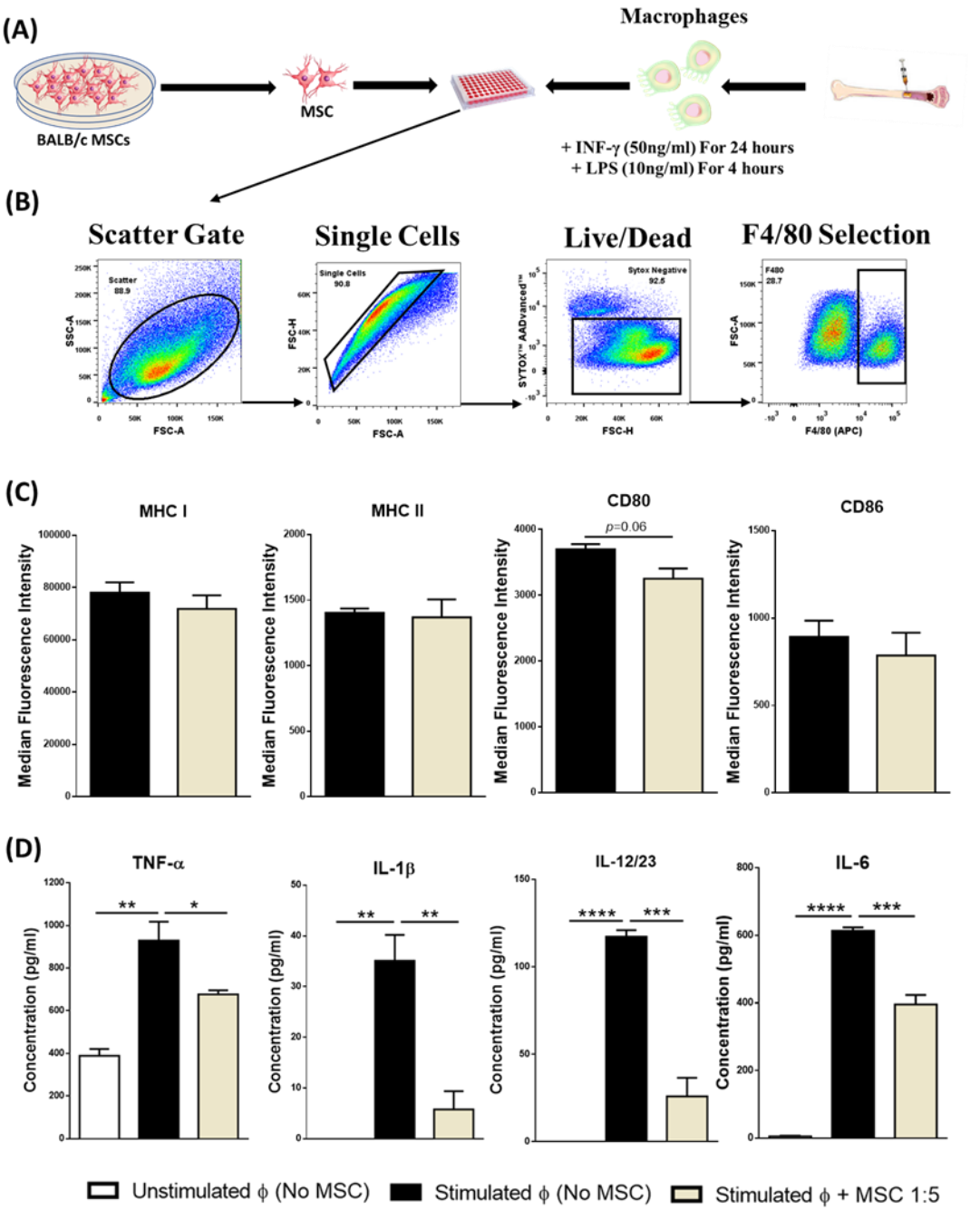

Figure 4.8 BALB/c MSCs do not modulate the activated phenotype of stimulated macrophages but do modulate the pro-inflammatory secretome | (A) BALB/c MSCs were cultured with activated bone marrow derived macrophages for 72 hours. (B) Cells were selected according to size and granularity, followed by single cell selection. After live/dead discrimination based on SYTOX negative cells (live), cells were selected for F4/80 positivity. (C) MHC I, MHC II, CD80 and CD86 expression was analysed on macrophage cell surface by flow cytometry. (D) Supernatants from MSC-macrophage co-cultures were analysed by ELISA for TNF-α, IL-1β, IL-12/23 and IL-6. Error bars: mean +/- SEM *p<0.05, **p<0.01 ***p<0.001 ****p<0.0001. One-way ANOVA, Tukey's Post Hoc test. ELISA: representative graphs of three individual experiments. All experiments (*n=3).*

4.3.6. Corneal Allograft Transplant Setup and Mode of Rejection

A fully MHC mismatched model of corneal transplantation was established and optimised. Briefly, BALB/c mice served as recipients to fully allogeneic C57BL/6 donor corneas. After eyelid sutures were removed, corneal checks were performed every 2/3 days (**Figure 4.9A**). Graft transparency (opacity) was used as the primary indicator of rejection (**Figure 4.9B**), if the graft presented with modest corneal opacity where the iris vessels were still visible it was classified as rejected (**Figure 4.9D, Day 17**). Rejection free survival (RFS) of corneal grafts was observed over 40 days. Untreated allogeneic control grafts were uniformly rejected (RFS 32.5±7.75d, *n=12*) (**Figure 4.9C**). We observed spontaneous acceptance of some allografts, this was expected as it has been reported quite frequently in the literature [32, 337].

4.3.7. Untreated MSCs Were Not Efficacious in Prolonging Rejection Free Survival

Due to the modulation of both inflammatory T lymphocyte (**Figure 4.7**) and macrophage (**Figure 4.8D**) secretome, syngeneic MSCs were administered to recipient mice at day +1 ($1x10^6$ cells intravenously) and +7 ($1x10^6$ cells intravenously) post operation day (POD). Corneal grafts were observed POD for 40 days (**Figure 4.10A**). Untreated MSCs were not only non-efficacious in prolonging survival (RFS 18.28±6.71d, *n=14*), but showed a trend decrease in RFS compared to untreated animals (**Figure 4.10A**). No significant differences in corneal opacity were noted between treated and untreated animals (**Figure 4.10B+C**). Neovascularization was also noted and compared to untreated animals (**Figure 4.10D**). No significant differences were observed.

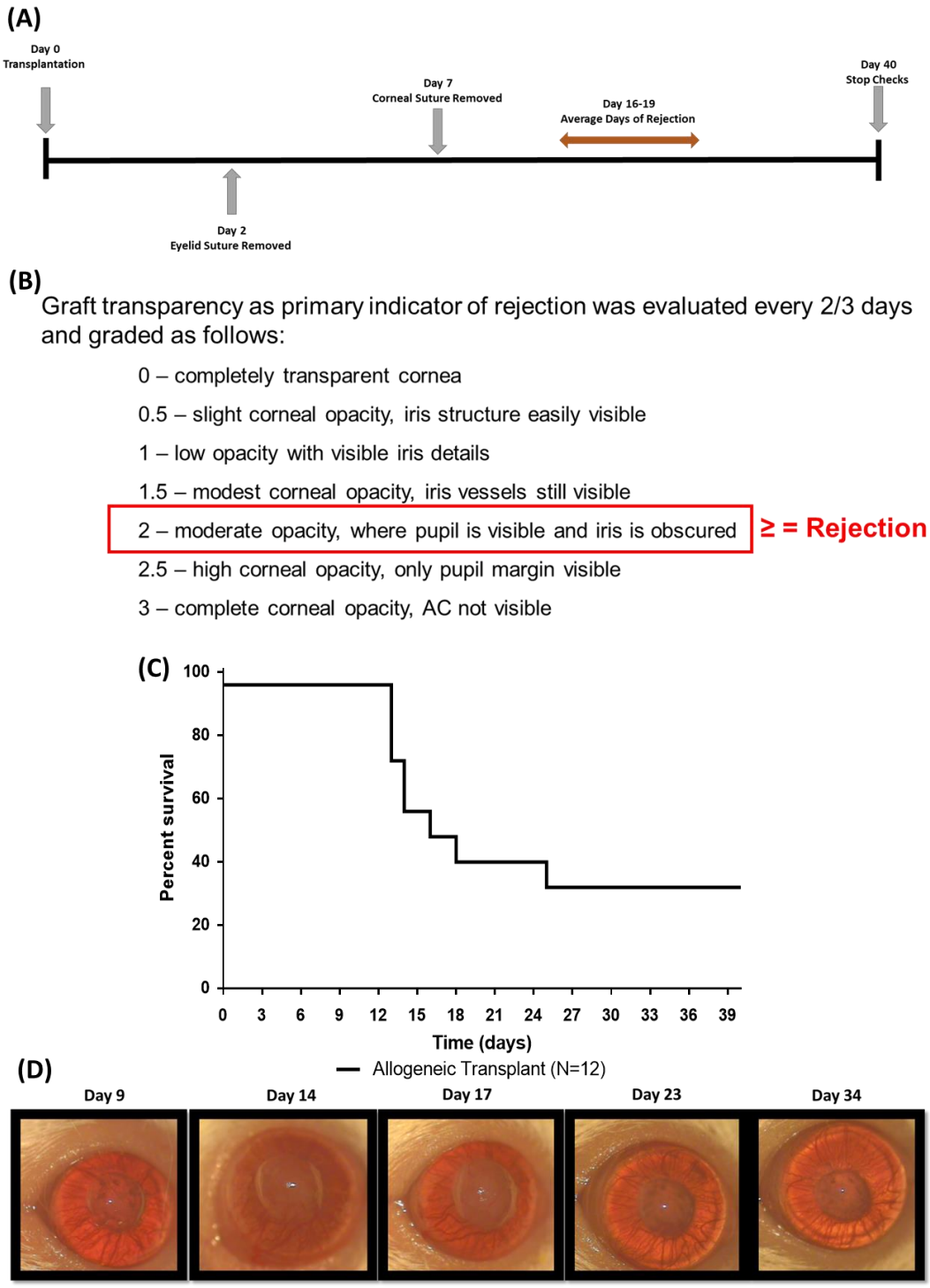

Figure 4.9 Experimental setup for allogeneic corneal transplantation, rejection criteria and mode of allograft rejection | (A) Schematic of allogeneic corneal transplantation setup. Female BALB/c mice served as recipients of female C57BL/6J corneas. Average day of rejection resided between days 16 and 19. Corneal checks started on day 4 and ceased on day 40. (B) Rejection criteria. Graft transparency was evaluated every 2/3 days. Rejection was defined as one scoring of 2. (C) Kaplan-Meier curve showing mode of allograft rejection. (*n=12*). (D) Representative corneal images of a recipient rejecter.

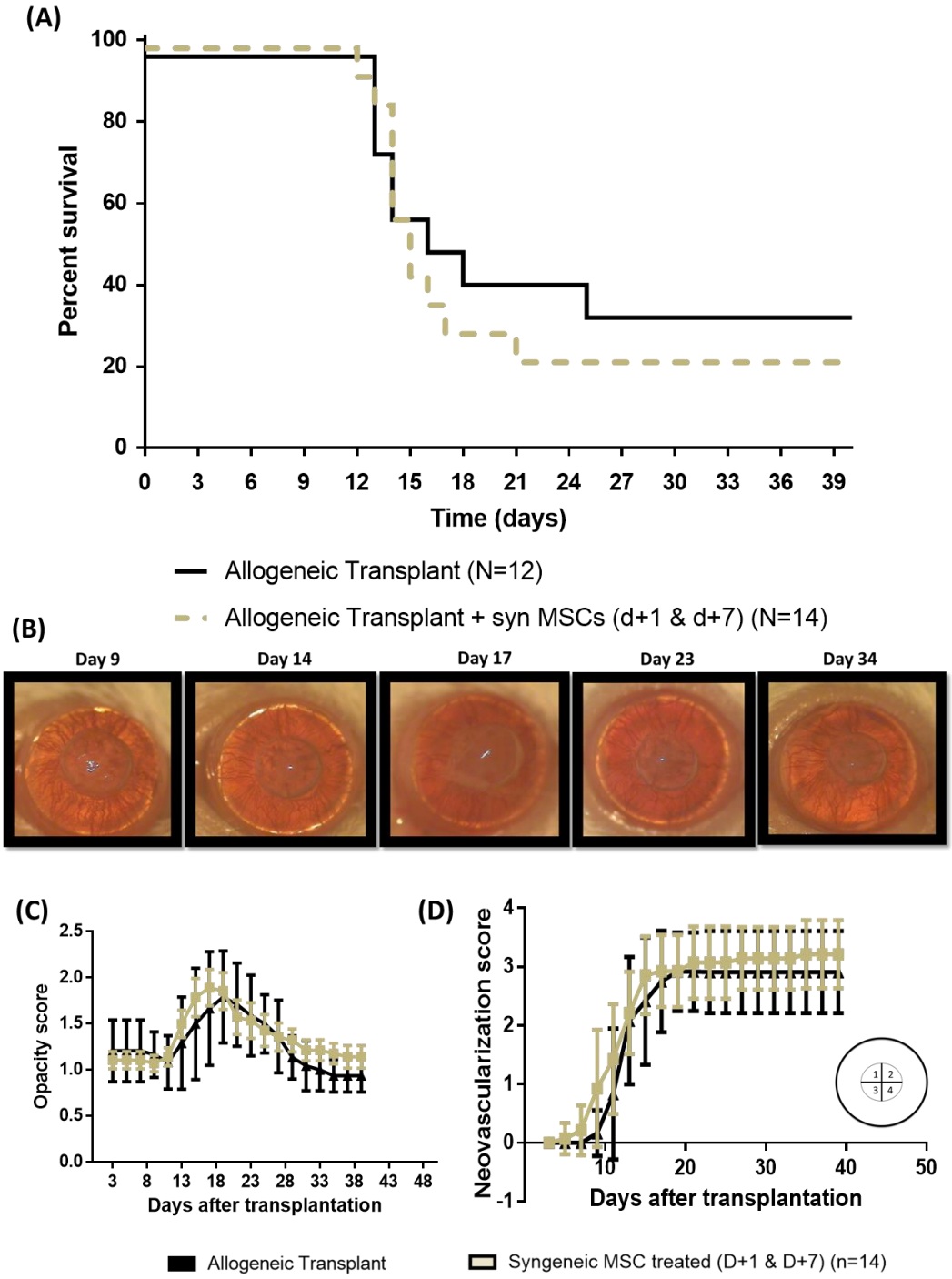

Figure 4.10 BALB/c MSCs fail to prolong rejection free survival | Female BALB/c mice served as recipients of female C57BL/6J corneas. $1x10^6$ syngeneic MSCs were injected intravenously day +1 and day +7 POD. Mice were observed every 2/3 days. (A) Kaplan-Meier curve showing RFS after administration of MSCs compared to untreated animals. (B) Representative images from a transplanted animal showing rejection at day 17. (C) Opacity scores over 40 days POD for untreated and MSC treated animals. (D) Neovascularization scores POD for untreated and MSC treated animals. Circle schematic shows how the cornea was divided into four sections to score neovascularization.

4.3.8. Cytokine Pre-activation of MSCs

It has been successfully demonstrated that pre-activation of MSCs with cytokines can improve their immunosuppressive capacity and efficacy [236, 250, 338]. To increase MSCs immunomodulatory potential, MSCs were treated with various cytokines. The proinflammatory cytokines IFN-γ, IL-1β, TNF-α and the anti-inflammatory cytokine TGF-β were used either singly or combination to pre-activate BALB/c MSCs **(Figure 4.11)**.

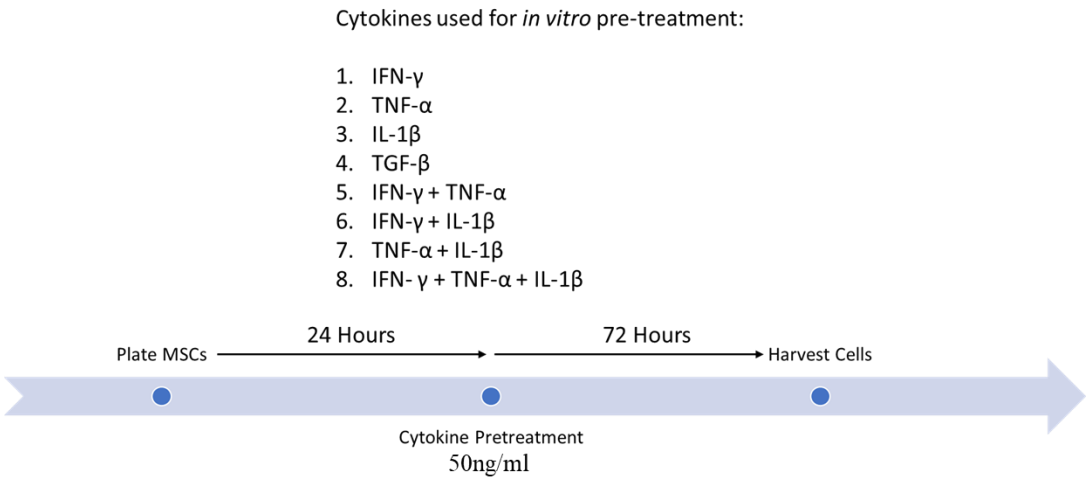

Figure 4.11 Schematic of cytokine pre-activation strategy | MSCs were seeded at 50,000 cells/ml in a T175 in 20ml of MSC medium. MSCs were given 24 hrs to adhere in either hypoxic or normoxic conditions. After this incubation time, pro-inflammatory cytokines were added alone or in combination (All cytokines were used at 50ng/ml.) TGF-β was only added alone. After addition of the cytokine, the MSCs were incubated for 72 in hypoxia or normoxia.

MSCs were pre-activated for 72 hours. Brightfield images were taken at 24 hours, 48 hours and 72 hours during the pre-activation protocol to study growth kinetics and morphological changes. Viewing the images from the 72-hour time point (**Figure 4.12)**, MSCs, IFN-γ MSCs and IL-1β MSCs did not show any morphological changes, however, TNF-α MSCs cell density was observed to be lower compared to IFN-γ MSCs and IL-1β MSCs (**Figure 4.12)**. IFN-γ + IL-1β MSCs cell density was the highest when compared to the other in combination treatments such as IFN-γ + TNF-α MSCs and TNF-α + IL-1β MSCs suggesting that TNF-α may stress the MSCs (**Figure 4.12)**. IFN-γ + TNF-α + IL-1β MSCs were observed to be heavily stressed with cell density being very low and the MSCs had taken on a highly spindle-like morphology (**Figure 4.12)**. Considering the highly inflammatory and stressful environment caused by IFN-γ + TNF-α + IL-1β treatment and because of the low

numbers of cells retrieved after harvest, this pre-activation strategy was discontinued. TGF-β MSCs were observed to have a significant change in morphology, where MSCs became more elongated and organised into "swirls", however, no visible effects on cell density was observed.

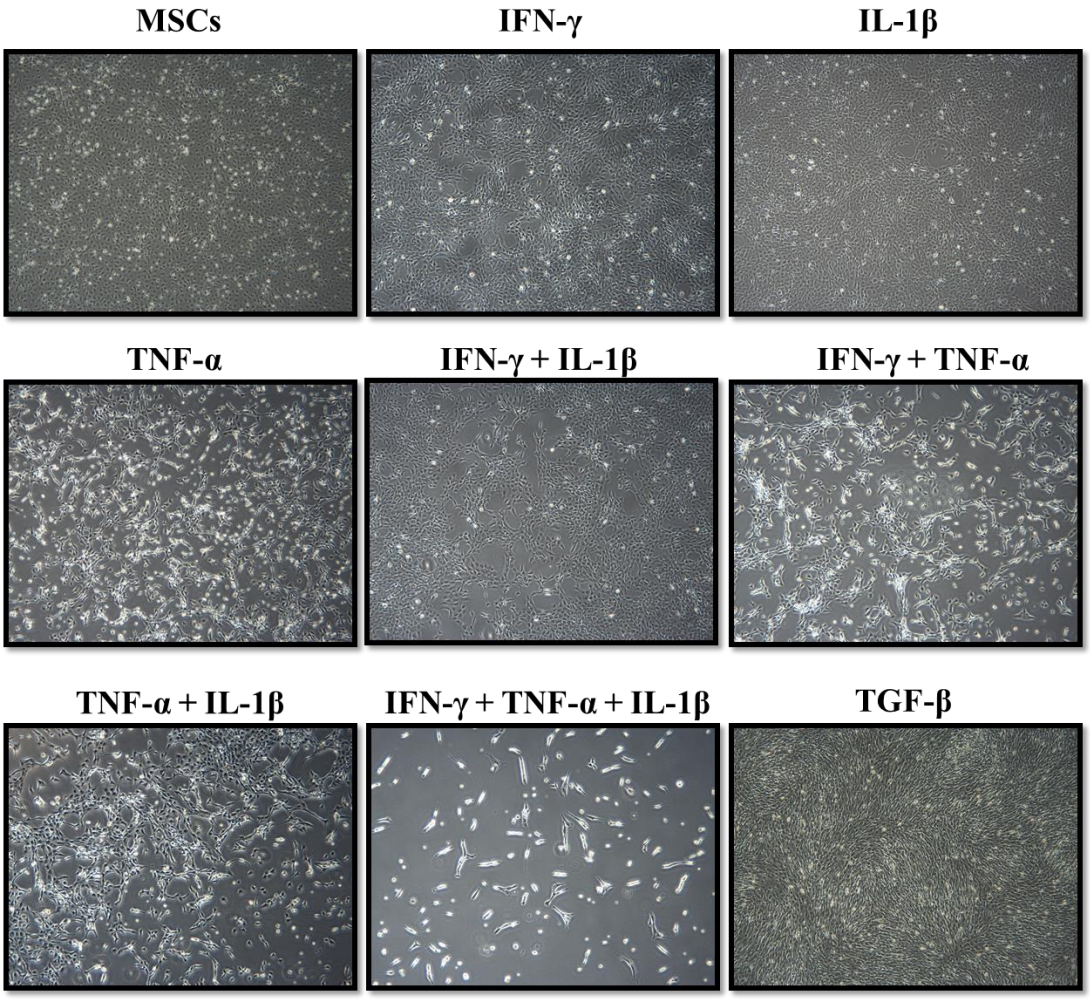

Figure 4.12 Cytokine treatment induces morphological changes in MSCs and affects growth rates. | Representative brightfield microscopy images taken at 4x magnification 72 hours after treatment.

Due to observed conformational changes, cell size, granularity, cell yield (**Figure 4.13**) and viability (data not shown) was examined. Cell size and granularity was examined via flow cytometry. FSC-A (cell size) and SSC-A (granularity) was used to assess any changes. No significant changes were observed in either cell size (**Figure 4.13A**) or cell granularity (**Figure 4.13B**) of the cells, however, there was a trend decrease observed in cell size of TNF-α + IL-1β MSCs (**Figure 4.13A**). At the end of the pre-activation process cells were counted on a haemocytometer after harvesting and the number of cells per ml of culture medium was calculated (**Figure 4.13C**). IFN-

γ + TNF-α MSCs, IFN-γ + IL-1β MSCs and TNF-α + IL-1β MSCs all had significantly lower cell yields when compared to untreated MSCs. IL-1β MSCs and TGF-β MSCs displayed trend increases in cell yield when compared to untreated MSCs **(Figure 4.12C**). Due to lower cell yield after pre-activation, viability of the cells was assessed via the use of the viability dye SYTOX™ and a combination of annexin V and propidium iodide (data not shown). No changes in viability or apoptosis was observed in any of the pre-activation treatments.

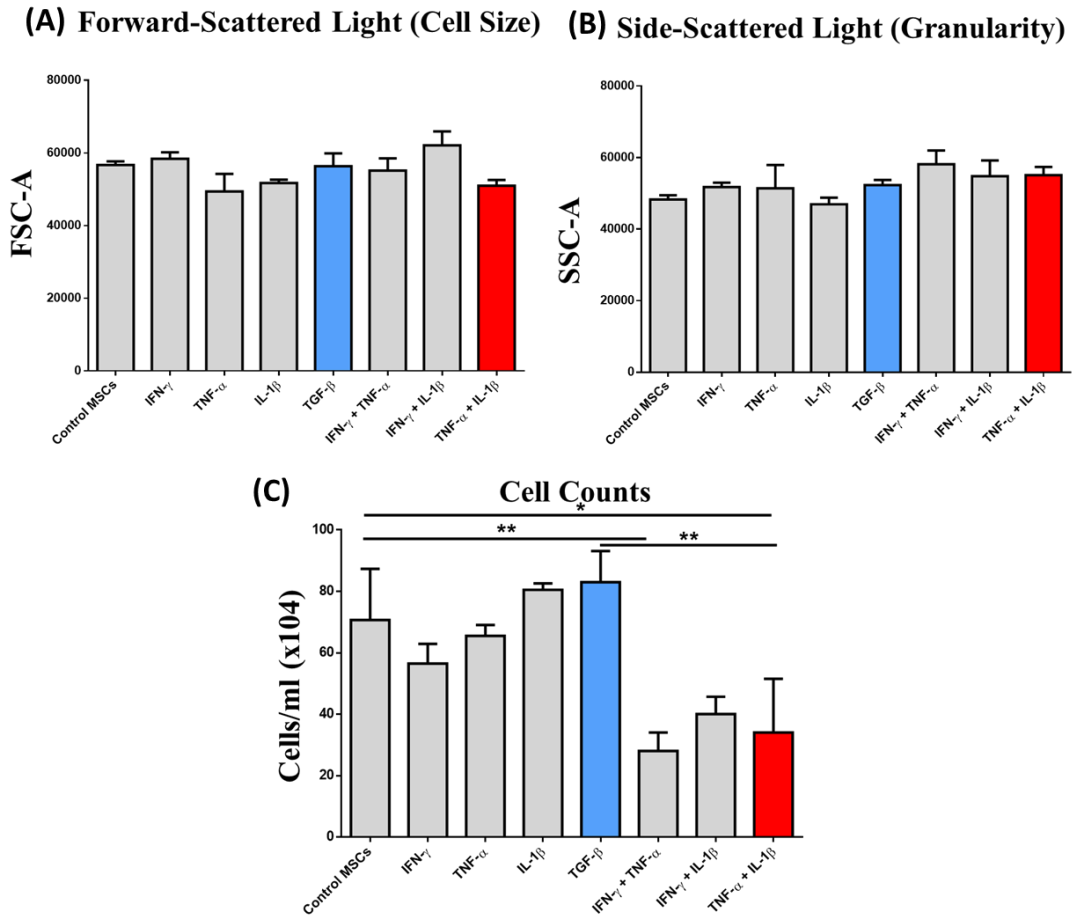

Figure 4.13 Cytokine pre-activation does not significantly affect cell size or granularity but does affect cell yield. | BALB/c MSCs were cultured with cytokines for 72 hours. Following this incubation period, cell size, granularity and yield were assessed. (A) Forward-scattered light representing cell size and (B) side-scattered light representing cell granularity was assessed by flow cytometry. (C) Haemocytometer cell counts of both pre-activated MSCs and MSCs. Error bars: mean +/- standard deviation *p<0.05, **p<0.01 ***p<0.001 ****p<0.0001. One-way ANOVA, Tukey's Post Hoc test (*n=3).*

4.3.8. In Vitro Identification of a Candidate Pre-activation Strategy for In Vivo Application

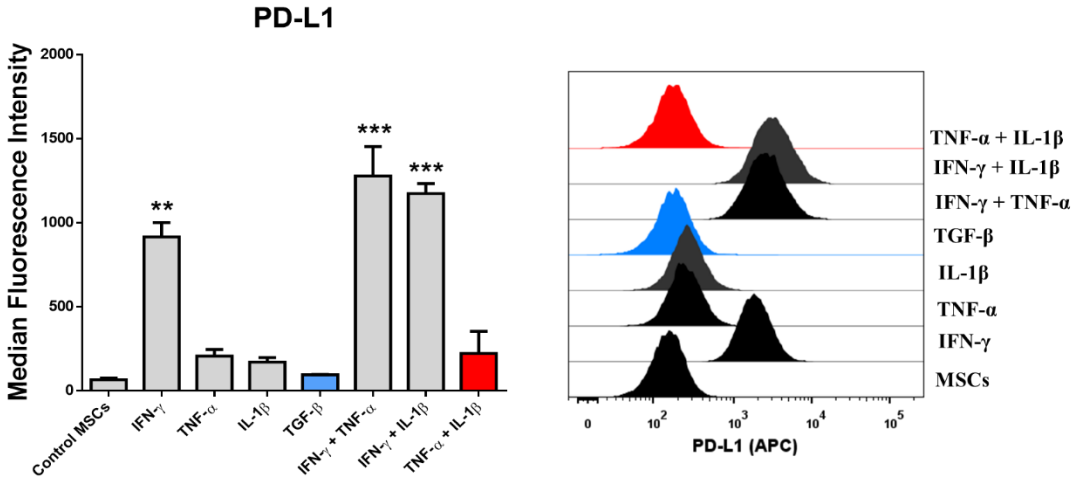

Figure 4.14 PD-L1 upregulation is dependent on IFN-γ treatment and synergises with TNF-α and IL-1β treatments. | BALB/c MSCs were cultured with cytokines for 72 hours. Following this, PD-L1 was assayed by flow cytometry. Median fluorescence intensity for the cell surface expression of PD-L1 and representative flow cytometry analysis histograms for the cell surface expression of PD-L1. Error bars: mean +/- standard deviation *p<0.05, **p<0.01 ***p<0.001 ****p<0.0001. One-way ANOVA, Tukey's Post Hoc test (*n=3).* All samples were compared to untreated MSCs.

We observed that untreated MSCs failed to prolong allograft survival (**Figure 4.10**). Identification of the most immunomodulatory efficacious pre-activation strategy was important before administering the MSCs *in vivo*. A list of criteria was devised to test the immunomodulatory potential of the cytokine pre-activated MSCs. This included, (i) the upregulation of the T lymphocyte inhibitory programmed death ligand 1 (PD-L1), (ii) secretion of immunomodulatory molecules such as IL-10, PGE2 and nitric oxide (NO) and **(iii)** inhibition of T lymphocyte proliferation. MSCs exert immunomodulatory effects via contact-dependent and independent mechanisms. PD-L1 or CD274 is a transmembrane protein that is known to play a major role in suppressing the immune system and a ligand that has been reported to be important in transplantation acceptance [339-341]. PD-L1 is known to be upregulated by IFN-γ stimulation in other cell types [342]. PD-L1 is present on the surface of MSCs and it is also secreted into the microenvironment [241]. To assess if PD-L1 was increased on MSCs after cytokine pre-activation, we cytokine treated MSCs and examined PD-L1 expression via flow cytometry (**Figure 4.14**). It was observed that cytokine pre-activation that included IFN-γ significantly upregulated PD-L1 expression on the surface of the MSCs when compared to untreated MSCs. TNF-α MSCs, IL-1β MSCs

and TNF-α + IL-1β MSCs displayed a trend increase in PD-L1 expression, however, this was not statistically significant. Interleukin-10 (IL-10), prostaglandin E2 (PGE2) and nitric oxide (NO) are molecules that have been reported to be major players in MSC immunomodulation [236, 332, 343-345]. To examine if these molecules are secreted to higher levels by cytokine pre-activation, MSCs were treated with cytokines and the supernatants were examined 72 hours after (**Figure 4.15A**). No detectable levels of IL-10 (data not shown) was present in the supernatants of any of the samples. Cytokine pre-activation increased the levels of PGE2 significantly in all samples except for IFN-γ MSCs compared to untreated MSCs (**Figure 4.15B**). TNF-α + IL-1β MSCs produced the highest levels of PGE2 and had significantly higher levels when compared to TGF-β MSCs which secreted the second highest quantity. TNF-α + IL-1β MSCs were also one of the highest producers of NO when compared to untreated MSCs (**Figure 4.15C**). IL-1β in combination with other proinflammatory cytokines seemed to be the mediator of NO secretion.

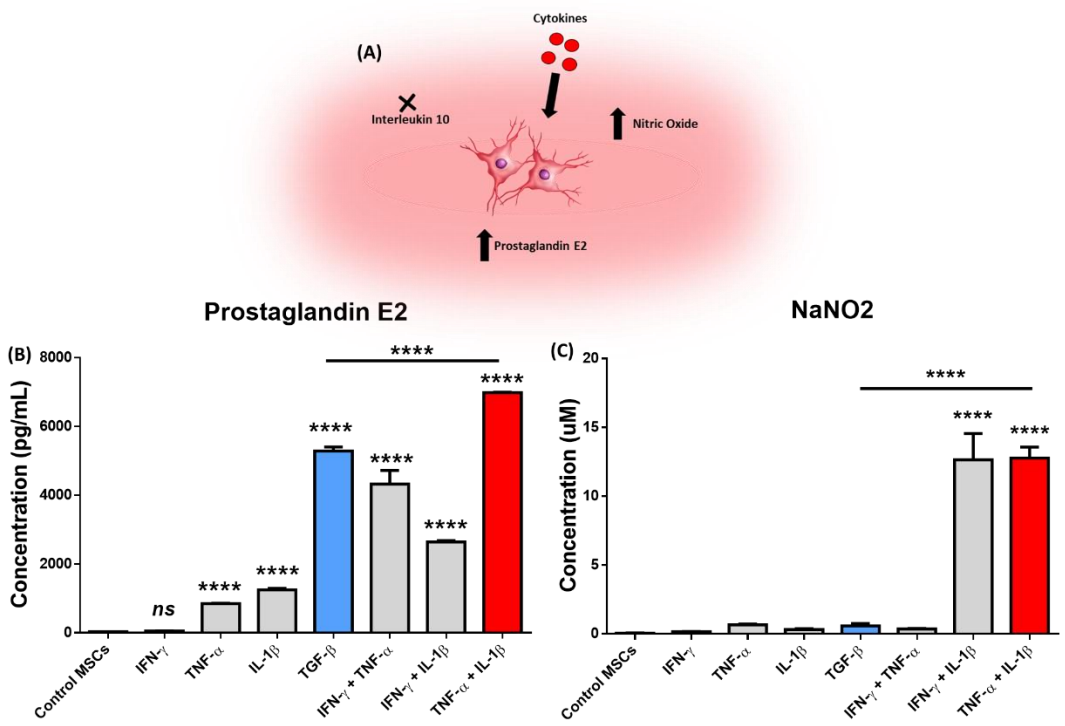

Figure 4.15 Cytokine pre-activation of MSCs increases both PGE2 and NaNO2 in monoculture. | BALB/c MSCs were cultured with cytokines for 72 hours. Following this, the supernatant was collected. ELISAs were carried out to assay PGE2 and Griess assays were carried out to assay nitric oxide production. Error bars: mean +/- standard deviation *p<0.05, **p<0.01 ***p<0.001 ****p<0.0001. One-way ANOVA, Tukey's Post Hoc test. ELISA: representative graphs of three individual experiments. All experiments (*n=3).*

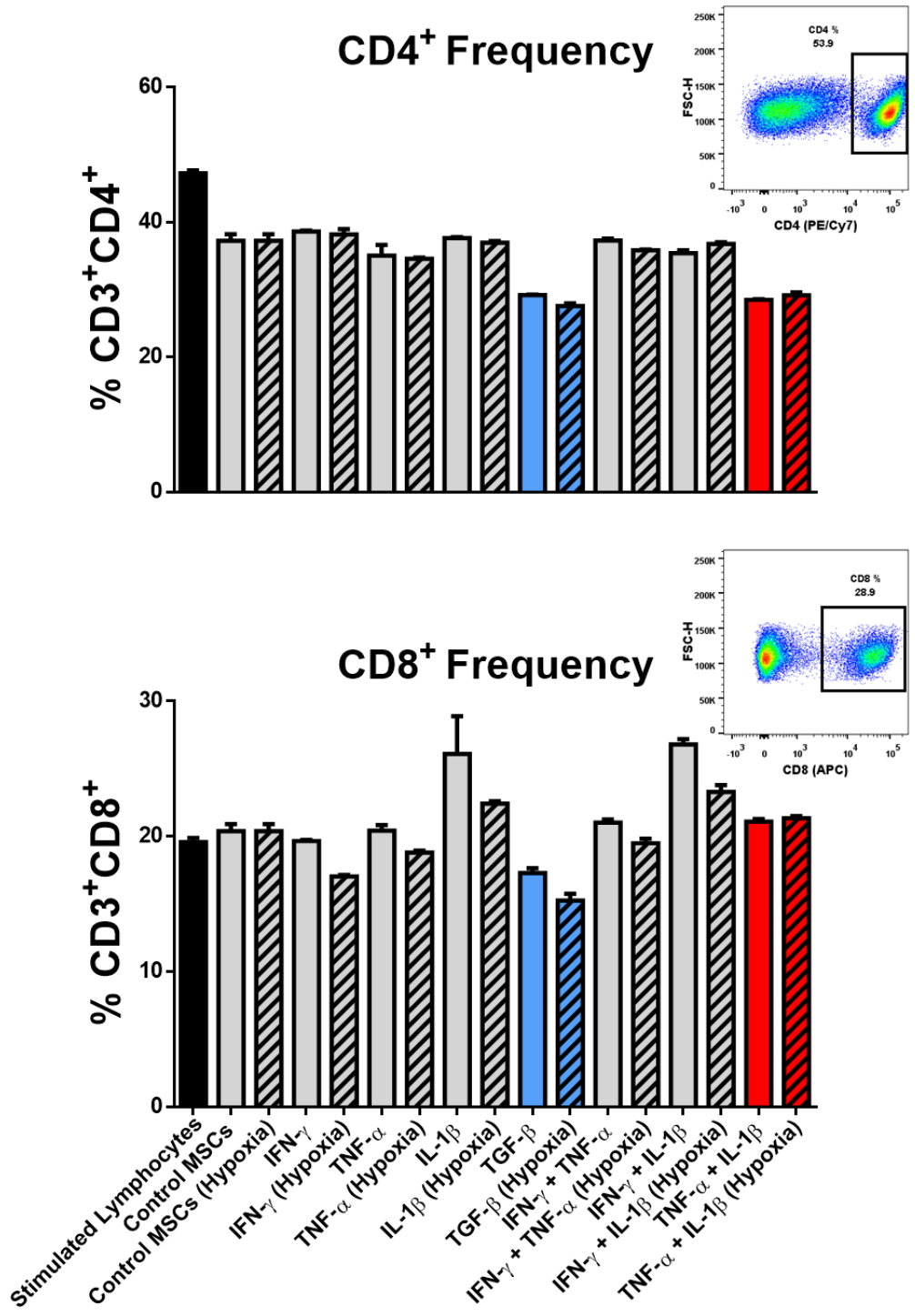

Figure 4.16 TGF-β MSCs and TNF-α + IL-1β MSCs decrease lymphocyte frequency in co-culture independent of MSC culture conditions. | Pre-activated or untreated BALB/c MSCs (1 MSC to 10 lymphocytes) cultured in normoxia or hypoxia were placed in T lymphocyte co-culture for 96 hours with CD3/CD28 stimulated lymphocytes. $CD3^+CD4^+$ and $CD3^+CD4^+$ cells were used to determine lymphocyte frequency. Error bars: mean +/- standard deviation *p<0.05, **p<0.01 ***p<0.001 ****p<0.0001. All experiments (*n=1, technical replicate of 3-4).*

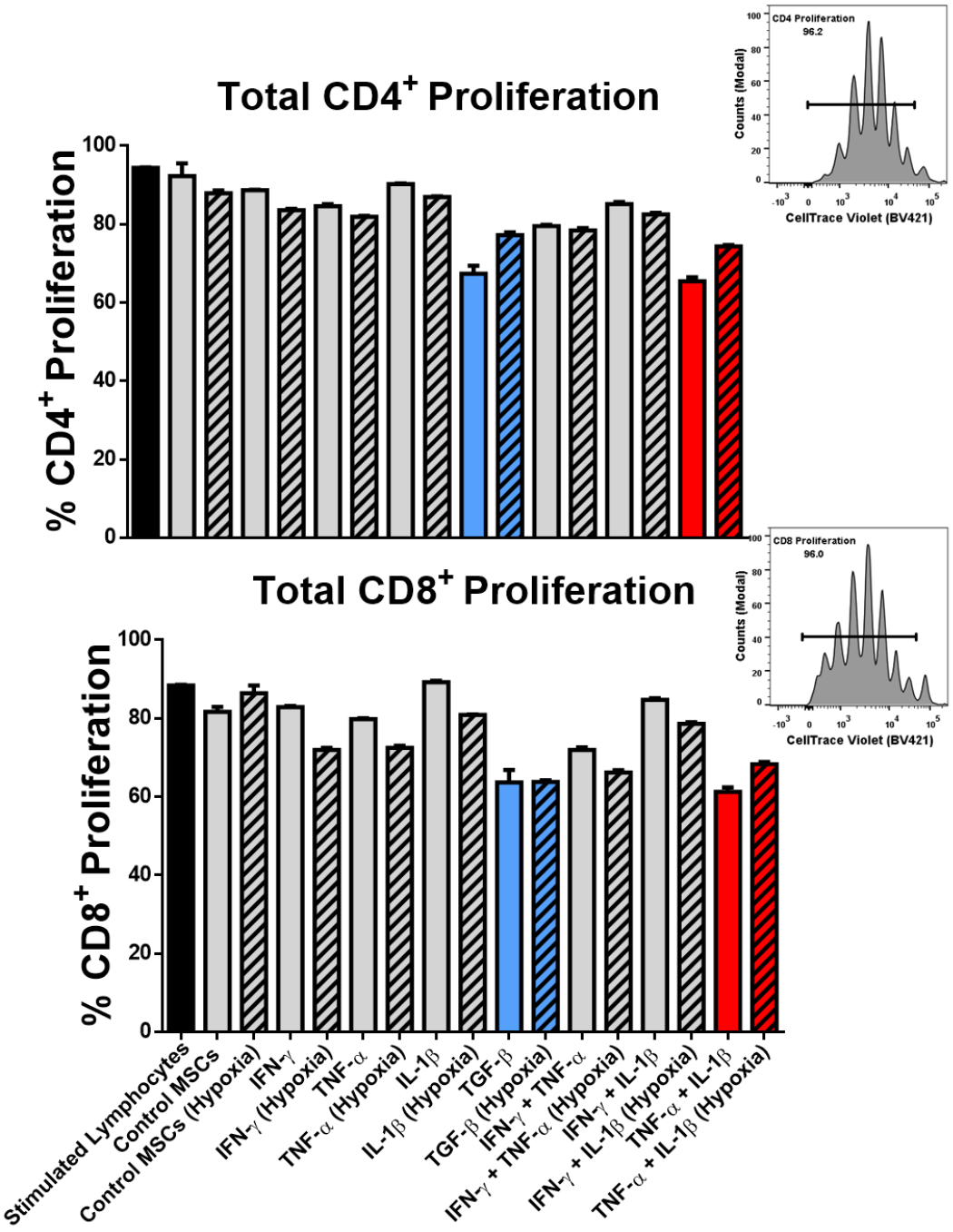

Figure 4.17 TGF-β MSCs and TNF-α + IL-1β MSCs inhibit lymphocyte proliferation in co-culture independent of MSC culture conditions. | Pre-activated or untreated BALB/c MSCs (1 MSC to 10 lymphocytes) cultured in normoxia or hypoxia were placed in T lymphocyte co-culture for 96 hours with CD3/CD28 stimulated lymphocytes. CTV was used to determine lymphocyte proliferation. Error bars: mean +/- standard deviation *p<0.05, **p<0.01 ***p<0.001 ****p<0.0001. All experiments (*n=1, technical replicate of 3-4).*

Cytokine pre-activated MSCs have been reported to inhibit T lymphocyte proliferation and function [346-348]. To assess the effect of each of the pre-activation strategies on T lymphocyte frequency and proliferation, untreated and pre-activated MSCs were

placed in co-culture with activated lymphocytes (**Figure 4.16 and Figure 4.17**). The largest decreases in lymphocyte frequency were observed in the wells where TGF-β MSCs and TNF-α + IL-1β MSCs were present (**Figure 4.16**). The stimulated control wells where no MSCs were present had frequencies of 47.2% ± 0.75% SD for $CD3^+CD4^+$ and 19.6% ± 0.5% SD for $CD3^+CD8^+$ lymphocytes. TGF-β MSCs wells had 29.2% ± 0.05% SD for $CD3^+CD4^+$ and 17.3% ± 0.06% for $CD3^+CD8^+$ while TNF-α + IL-1β MSCs had 28.5% ± 0.1% SD for $CD3^+CD4^+$ and 21.1% ± 0.22% SD $CD3^+CD8^+$ (**Figure 4.16**). These results suggest that TGF-β MSCs and TNF-α + IL-1β MSCs effect lymphocyte proliferation. To study if pre-activated MSCs modulate T lymphocyte proliferation, CTV was used to track the proliferation of lymphocytes in the wells of the co-cultures (**Figure 4.17**). Again, TGF-β MSCs and TNF-α + IL-1β MSCs were the treatments that resulted in the largest inhibition of T lymphocyte proliferation with proliferation of stimulated $CD4^+$ lymphocytes being reduced from 94.4% ± 1% SD to 67% ± 1.7% SD in TGF-β MSCs wells and 65.4% ± 1.7% SD in TNF-α + IL-1β MSCs. A similar trend was observed with $CD8^+$ lymphocytes, with stimulated $CD8^+$ lymphocytes being reduced from 88.4% ± 0.8% SD to 63% ± 1.7% SD in TGF-β MSCs wells and 61.4% ± 1.2% SD in TNF-α + IL-1β MSCs (**Figure 4.17**).

4.3.9. TNF-α + IL-1β as a Candidate Pre-activation Strategy for *In Vivo* Application

On review of the data collected on the different pre-activation strategies, TNF-α + IL-1β was picked as a candidate strategy for *in vivo* application. IFN-γ used singly and in combination resulted in the largest upregulation of PD-L1 on the MSC cell surface. This being the case, this did not correlate with T lymphocyte suppression, as seen in (**Figure 4.17).** TNF-α + IL-1β MSCs produced the highest amounts of both PGE2 and NO, not only this, TNF-α + IL-1β MSCs reduced lymphocyte frequency and proliferation in co-cultures to a higher degree compared to other treatments (**Figure 4.16 and Figure 4.17**). Hypoxic environments did not increase or decrease the potent immunomodulatory attributes of pre-activated MSCs, as a result, culturing of MSCs in hypoxic environments was discontinued from the study. In this part of the study, we investigated further the ability of TNF-α + IL-1β MSCs to modulate immune cells before administering the cells *in vivo*. Firstly, TNF-α + IL-1β MSCs were characterised by flow cytometry to study the effects of pre-activation on markers that

are used to define MSCs (**Figure 4.18**). MHC II, CD45, F4/80, CD11c, CD80 and CD86 expression did not change after TNF-α + IL-1β treatments (**Figure 4.18A**). However, the expression of CD73, CD44 and CD90 were significantly upregulated (**Figure 4.18B**) while the expression of SCA-I was significantly downregulated (**Figure 4.18B**). CD105 and MHCI expression was not significantly changed (**Figure 4.18B**).

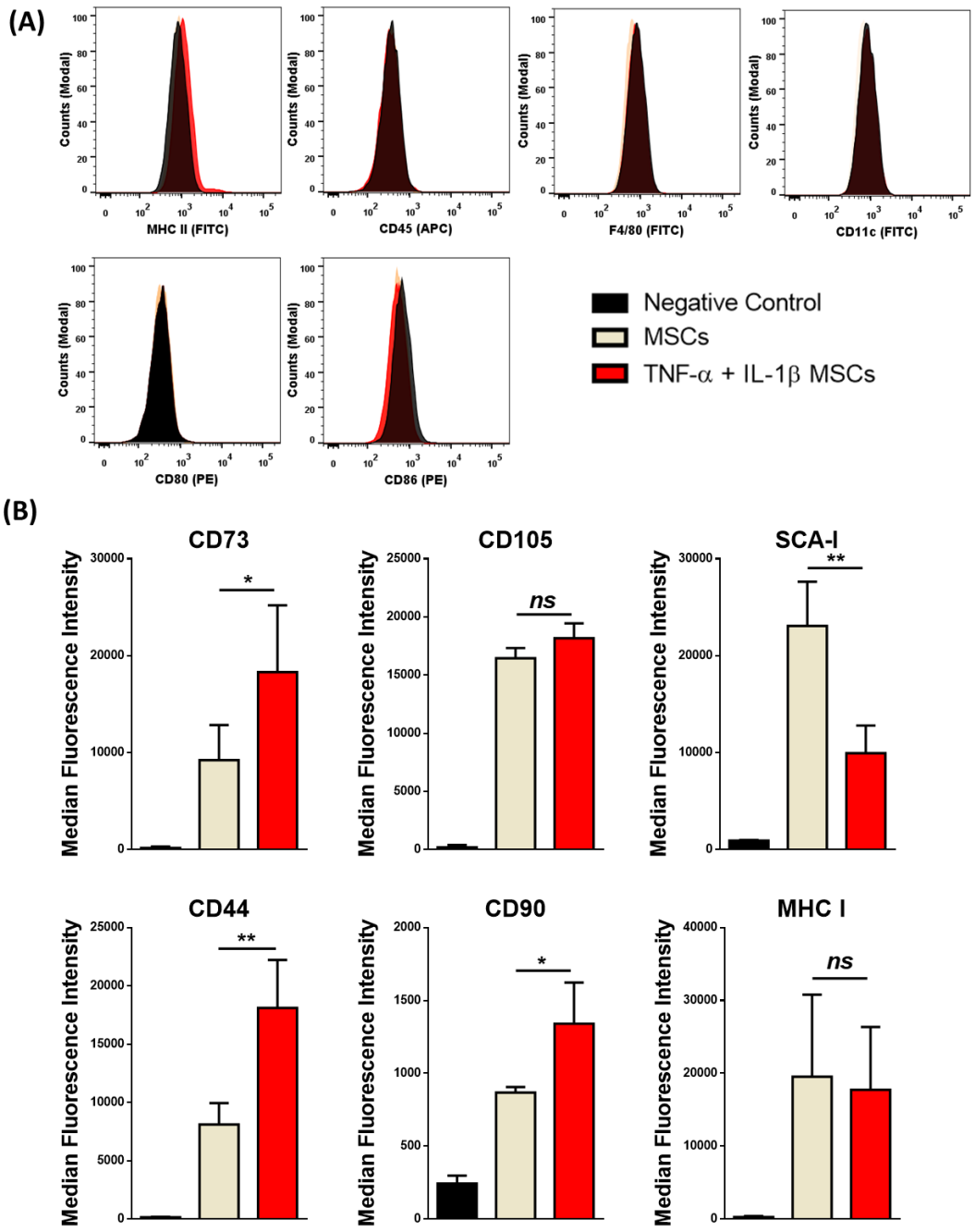

Figure 4.18 Characterisation of TNF-α + IL-1β MSCs. | (A) Representative flow cytometry histograms for the cell surface expression of negative MSC antigens, MHCII, CD45.2, F4-80, CD11c, CD80, CD86. (B) Histograms showing median fluorescence intensity for the cell

surface expression of positive MSC antigens, CD105, CD73, SCA-1, CD90, CD44 and MHC I. Error bars: mean +/- standard deviation *p<0.05, **p<0.01 ***p<0.001 ****p<0.0001. (*n=3).*

TNF-α + IL-1β MSCs had previously been observed to decrease T lymphocyte frequency and suppress activated T lymphocytes (**Figure 4.16 + Figure 4.17)**. However, these experiments were pilot studies (*n=1*) to guide us to which treatment was more efficacious at suppressing T lymphocytes. To see if this observation was statistically significant and not just an artefact, TNF-α + IL-1β MSCs were placed in T lymphocyte co-culture and their effects on T lymphocytes was studied more intensively.

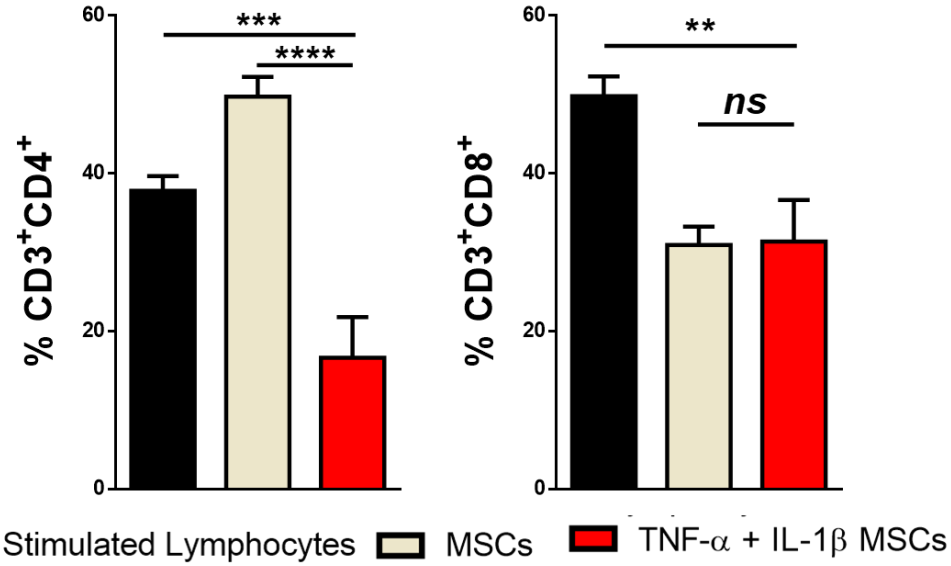

Figure 4.19 TNF-α + IL-1β MSCs significantly decrease lymphocyte frequency in T lymphocyte co-culture. | Untreated BALB/c MSCs or TNF-α + IL-1β MSCs (1 MSC to 10 lymphocytes) were cultured in normoxia and placed in T lymphocyte co-culture for 96 hours with CD3/CD28 stimulated lymphocytes. $CD3^+CD4^+$ and $CD3^+CD4^+$ cells were used to determine lymphocyte frequency. Error bars: mean +/- standard deviation *p<0.05, **p<0.01 ***p<0.001 ****p<0.0001. All experiments (*n=4).*

TNF-α + IL-1β MSCs significantly reduced both CD4+ and CD8+ lymphocyte frequency in T lymphocyte co-culture (**Figure 4.19**). Stimulated CD4+ lymphocytes frequency was reduced from 37.8% ± 1.85% SD to 16.6% ± 5.19% SD in wells that contained TNF-α + IL-1β MSC. Stimulated CD8+ lymphocytes frequency was reduced from 39.8% ± 2.52% SD to 31.3% ± 5.28% SD in wells that contained TNF-α + IL-1β MSCs

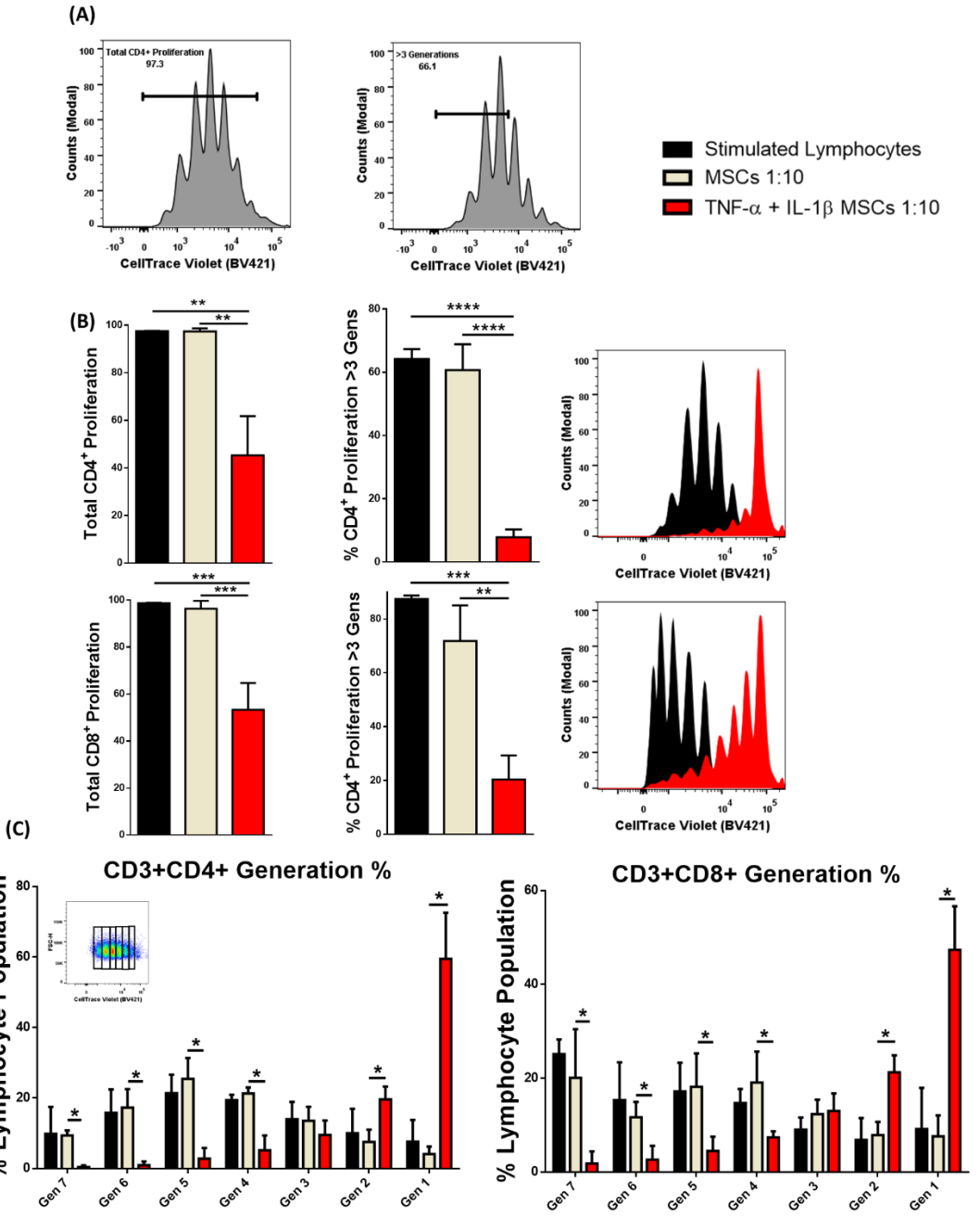

Figure 4.20 TNF-α + IL-1β MSCs inhibit lymphocyte proliferation in T lymphocyte co-culture. | Untreated BALB/c MSCs or TNF-α + IL-1β MSCs (1 MSC to 10 lymphocytes) were cultured in normoxia and placed in T lymphocyte co-culture for 96 hours with CD3/CD28 stimulated lymphocytes. CTV was used to determine lymphocyte proliferation. (A) Representative flow cytometry plots showing gating strategy for total lymphocyte proliferation and >3 generations proliferation. (B) Bar charts and histograms showing total lymphocyte proliferation, >3 generation proliferation and representative flow cytometry plot overlays. (C) % of $CD3^+CD4^+$ and $CD3^+CD8^+$ lymphocyte proliferation per generation Error bars: mean +/- standard deviation *p<0.05, **p<0.01 ***p<0.001 ****p<0.0001. Multiple unpaired, two tailed student's t test and One-way ANOVA, Tukey's Post Hoc test (*n=3-6).*

TNF-α + IL-1β MSCs cultured in normoxic conditions were placed in T lymphocyte co-culture at different ratios with CD3/CD28 stimulated lymphocytes and were

incubated for 96 hours. Following culture period, proliferation of $CD4^+$ and $CD8^+$ lymphocytes were analysed by flow cytometry using CTV to track proliferation. Both total proliferation and proliferation greater than three (>3) generations of lymphocytes were analysed (**Figure 4.20A**). The results demonstrated that TNF-α + IL-1β MSCs significantly inhibited the total proliferation of activated CD4+ and CD8+ lymphocytes (**Figure 4.20B**). Stimulated CD4+ lymphocyte total proliferation was reduced from 97.5% ± 0.55% SD to 45.3% ± 16.48% SD in wells that contained TNF-α + IL-1β MSC. Stimulated CD8+ lymphocytes total proliferation was reduced from 98.7% ± 0.3% SD to 31.3% ± 5.3% SD in wells that contained TNF-α + IL-1β MSC (**Figure 4.20B**). Subsequently, when T cell proliferation was analysed >3 generations, it was determined that TNF-α + IL-1β MSCs significantly suppressed activated CD4+ and CD8+ lymphocytes also. Stimulated CD4+ lymphocyte >3 generations proliferation was reduced from 64.2% ± 3.1% SD to 7.83% ± 2.48% SD in wells that contained TNF-α + IL-1β MSC. Stimulated CD8+ lymphocytes >3 generations were reduced from 84.4% ± 1.3% SD to 20.3% ± 8.93% SD in wells that contained TNF-α + IL-1β MSC (**Figure 4.20B**). When each generation was analysed individually, we can see that for both CD4+ and CD8+ lymphocytes, a large proportion of cells do not leave the 1st generation, 59.5% ± 13% SD and 47.3% ± 9.2% SD respectively, demonstrating how inhibitory the TNF-α + IL-1β MSCs are on lymphocyte activation and proliferation (**Figure 4.20C**). It was also observed that very few CD4+ and CD8+ lymphocytes proliferate past the 3rd generation with significantly less lymphocytes in generation 4, 5, 6, and 7 in TNF-α + IL-1β MSC wells compared to MSC wells (**Figure 4.20C**).

Supernatants from T lymphocyte co-cultures were collected, Griess assays, PGE2, granzyme B and IFN-γ ELISAs were performed (**Figure 4.21**). Significantly higher levels of nitrates were detected in the supernatants of TNF-α + IL-1β MSC wells compared to stimulated lymphocytes or MSC wells. Significantly higher levels of PGE2 was detected in TNF-α + IL-1β MSCs wells when compared to MSCs or stimulated controls (**Figure 4.21**). Furthermore, the levels of TH1 cytokine IFN-γ and cytotoxic CD8+ granzyme B was significantly lower in the TNF-α + IL-1β MSCs wells when compared to stimulated lymphocytes or MSC wells.

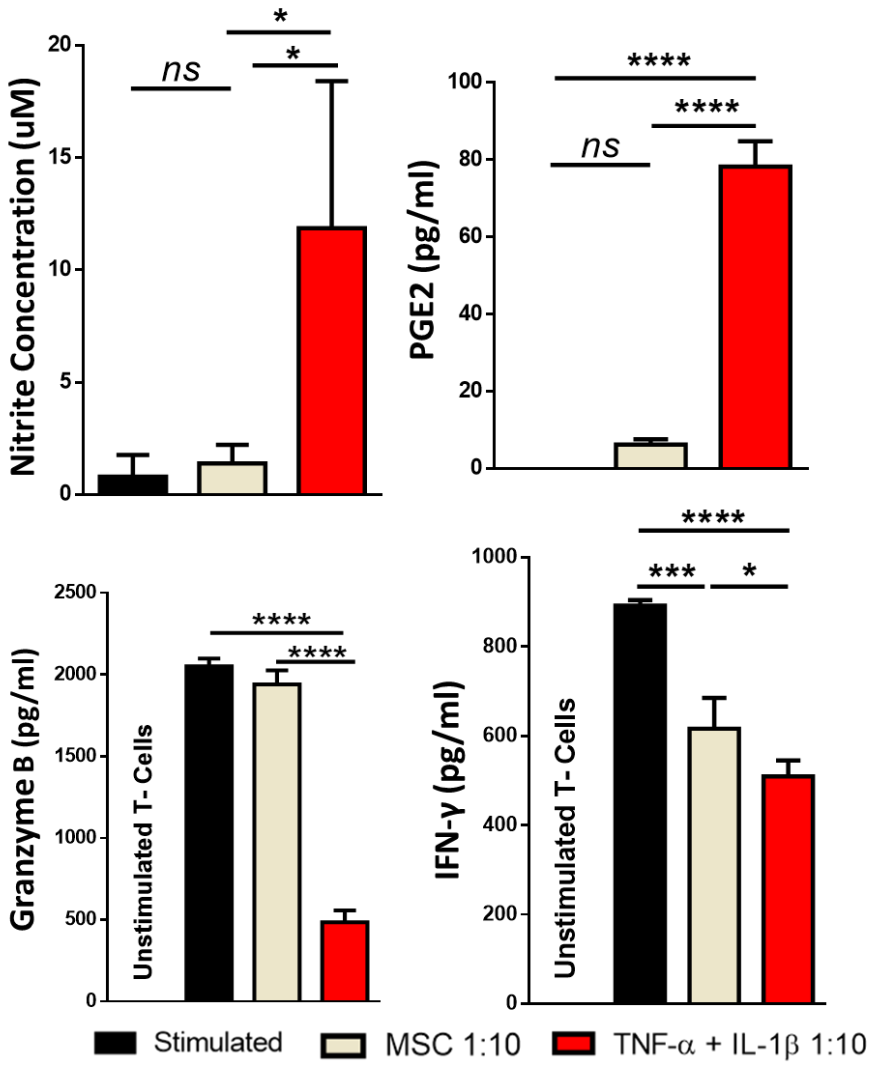

Figure 4.21 TNF-α + IL-1β MSCs increase NO and PGE2 while decreasing Granzyme B and IFN-γ in T lymphocyte co-culture. | BALB/c MSCs were cultured with cytokines for 72 hours. Following this, the supernatant was collected. ELISAs were carried out to assay PGE2, Granzyme B and IFN-γ and Griess assays were carried out to assay nitric oxide production. Error bars: mean +/- standard deviation *p<0.05, **p<0.01 ***p<0.001 ****p<0.0001. One-way ANOVA, Tukey's Post Hoc test. ELISA: representative graphs of three individual experiments. All experiments (*n=3).*

MSCs have been reported to polarize macrophages [349-351] to a tissue repair or anti-inflammatory phenotype. To investigate this phenomenon, we co-cultured MSCs or TNF-α + IL-1β MSCs with macrophages that had been pre-activated with IFN-γ (100 ng/ml) and LPS (10 ng/ml). It was observed that TNF-α + IL-1β MSCs had the ability to decrease the expression of MHC I, MHC II, CD80 and CD86 on activated macrophages (**Figure 4.22**).

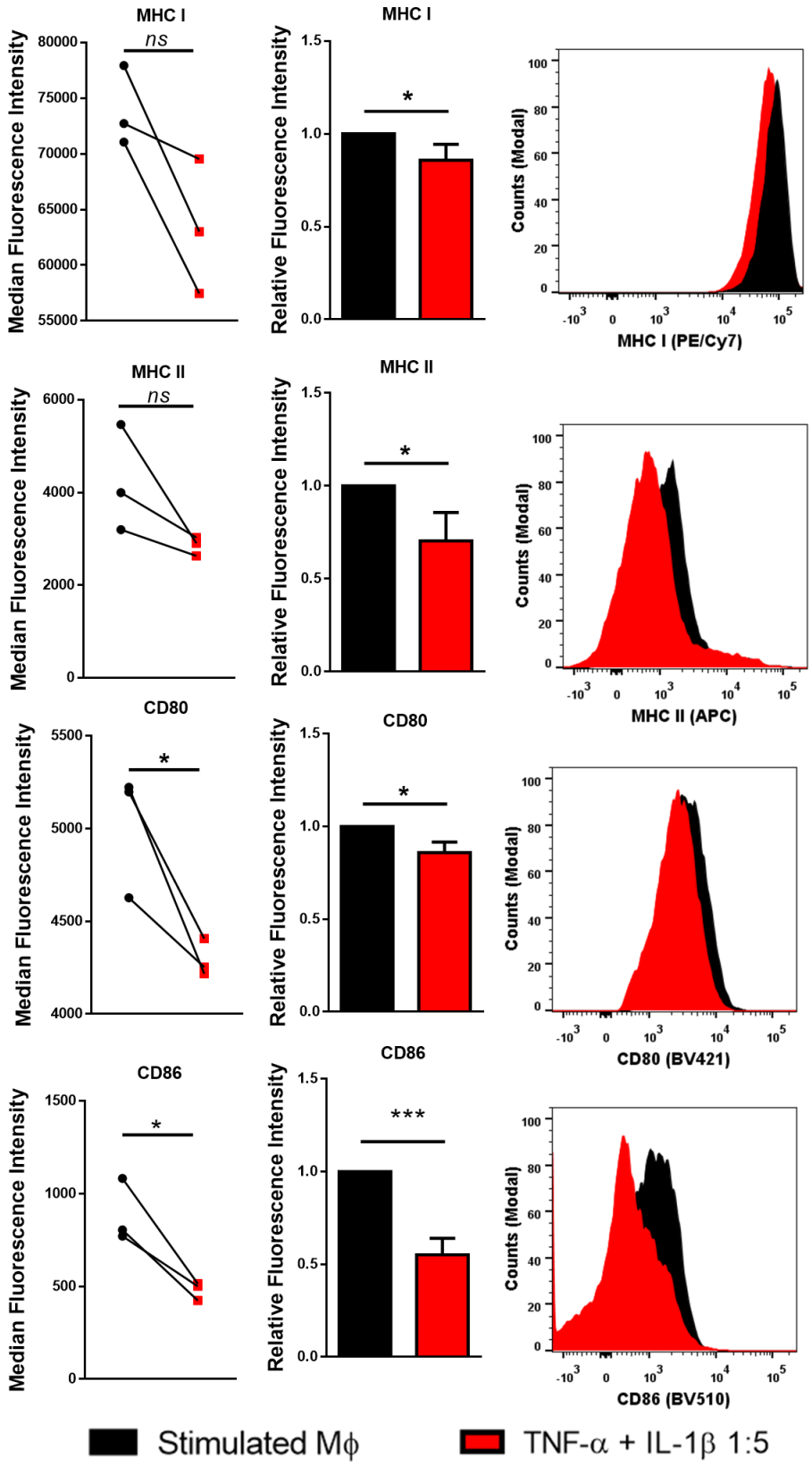

Figure 4.22 TNF-α + IL-1β MSCs suppress activated M1 macrophages. | TNF-α + IL-1β BALB/c MSCs were cultured with activated bone marrow generated macrophages for 72 hours. MHC I, MHC II, CD80 and CD86 expression was analysed on macrophage cell surface by flow cytometry. Error bars: mean +/- standard deviation *p<0.05, **p<0.01 ***p<0.001 ****p<0.0001. One-way ANOVA, Tukey's Post Hoc test (*n=3).*

4.3.10 TNF-α + IL-1β MSCs Do Not Prolong Rejection Free Survival in a Mouse Model of Corneal Transplantation

We observed that MSCs upregulated immunoregulatory markers such as CD73 and CD44 (**Figure 4.18**) after TNF-α + IL-1β treatment. We observed that TNF-α + IL-1β MSCs had an increased ability to suppress not only activated macrophages (**Figure 4.22**) but also the activation and proliferation of both $CD4^+$ and $CD8^+$ lymphocytes (**Figure 4.20**). TNF-α + IL-1β MSCs also reduced the levels of pro-inflammatory cytokines while increasing the levels of anti-inflammatory molecules in the supernatants of T lymphocyte co-cultures **(Figure 4.21**).

TNF-α + IL-1β MSCs proved immunomodulatory *in vitro*, as a result we administered $1x10^6$ TNF-α + IL-1β MSCs on day +1 and day +7 post operation day (POD) and monitored both the opacity and neovascularization over a 40-day observation period (**Figure 4.23A**). TNF-α + IL-1β MSCs were not only non-efficacious in prolonging RFS, rejection of the corneal button was accelerated (**Figure 4.23A**). All animals had rejected their transplant by day 18 (n=8). No significant differences in corneal opacity were noted between treated and untreated animals (**Figure 4.23B+C**). Neovascularization was also noted and compared to untreated animals (**Figure 4.23D**). No significant differences were observed.

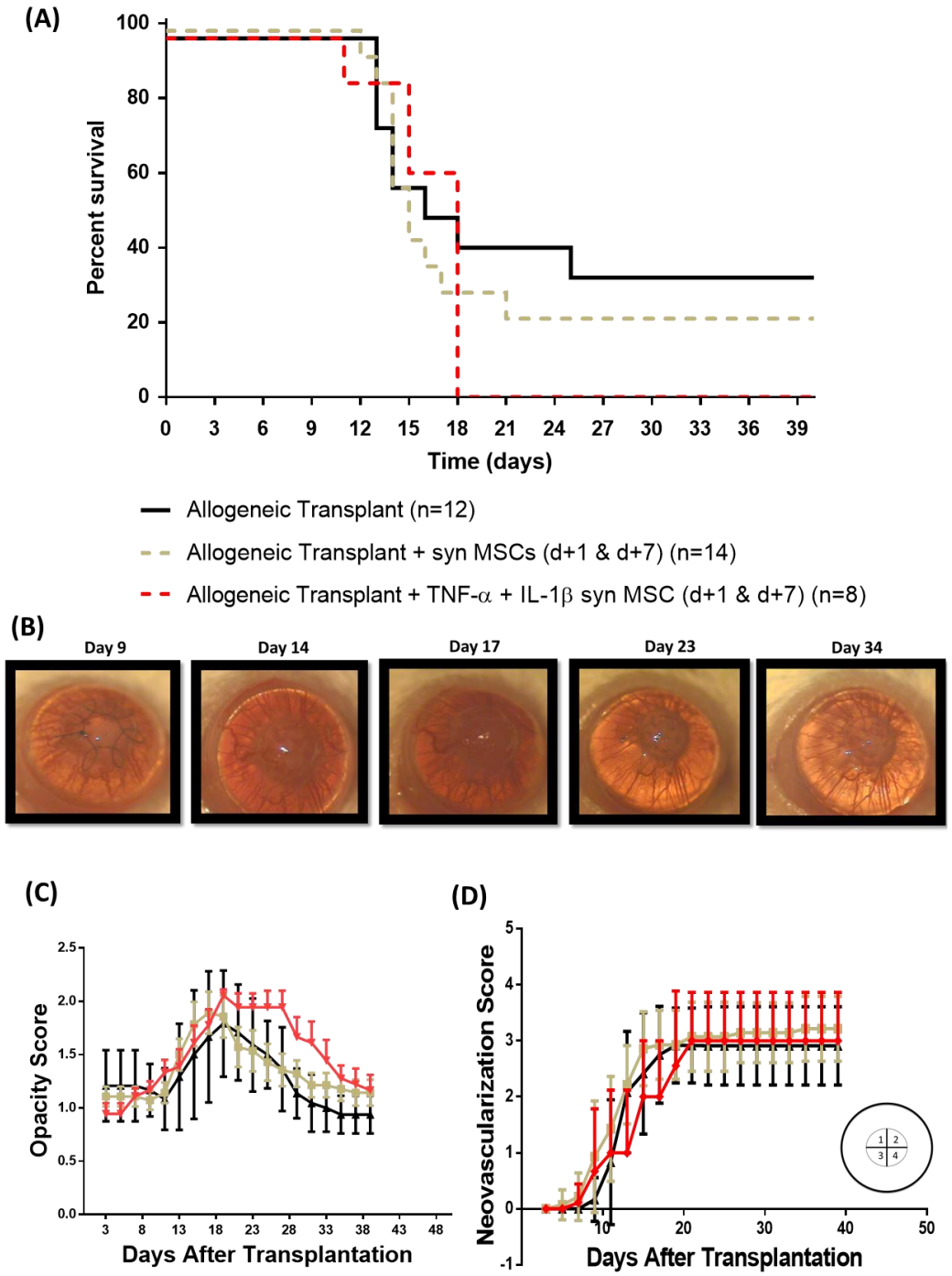

Figure 4.23 TNF-α + IL-1β BALB/c MSCs fail to prolong rejection free survival | Female BALB/c mice served as recipients of female C57BL/6J corneas. $1x10^6$ TNF-α + IL-1β MSCs were injected intravenously day +1 and day +7 POD. Mice were observed every 2/3 days. (A) Kaplan-Meier curve showing RFS after administration of MSCs compared to untreated animals. (B) Representative images from a transplanted animal showing rejection at day 17. (C) Opacity scores over 40 days POD for untreated and MSC treated animals. (D) Neovascularization scores POD for untreated and MSC treated animals.

4.4 Discussion

In this chapter we observed that while non-activated syngeneic MSCs have mild immunomodulatory attributes, they needed either a pro-inflammatory or anti-inflammatory stimulus to become potently immunosuppressive. Non-activated MSCs failed to prolong RFS in our model of corneal transplantation. While our *in vitro* screening identified TNF-α + IL-1β MSCs as the most potently immunosuppressive strategy they surprisingly failed to prolong RFS, in fact, they accelerated rejection, with all mice who received treatment rejecting their grafts faster than untreated animals. The results of Chapter 4 will briefly be discussed here and discussed in more detail in Chapter 6 in the context of the broader literature.

Due to the many different methods of isolation and expansion of MSCs, The International Society for Cellular Therapy (ISCT) proposed a set of minimal criteria for the isolation and definition of MSCs [321]. These criteria were proposed to allow the scientific community to be able to compare study outcomes more easily with less variation. The first criterion is that cells isolated from the tissue in question must be plastic adherent. MSCs can be isolated from many different tissues, such as the bone marrow [352, 353], adipose tissue [354-356] and the umbilical cord [357]. In this study we isolated MSCs from the bone marrow of 8-14-week-old female BALB/c mice (Figure 4.1A) and over successive passaging and selecting plastic adherent cells (Figure 4.1B), the population was purified. The second criterion was that the cells must be negative for myeloid and haematopoietic progenitor antigens but also positive for a list of MSC defining antigens set out by the ISCT. After sufficient passaging (P4), to ensure that all myeloid and haematopoietic contaminating populations had been removed, the MSCs were characterised by flow cytometry for markers that the ISCT have used to define MSCs. These included the negative markers MHC II, CD45, F4-80, CD11c, CD80 and CD86 (**Figure 4.1C**) and the positive markers CD105. CD73, CD90. CD44, SCA-I and MHC I (**Figure 4.1D**). The third criterion is that the cells must demonstrate a multipotent capacity. BALB/c MSCs were cultured in specific osteogenic differentiation medium to differentiate the MSCs to osteocytes. After the culturing period, the presence of osteocytes was demonstrated by Alizarin Red staining (**Figure 4.2**). To demonstrate adipogenic differentiation potential BALB/c MSCs were cultured in specific adipogenic induction and maintenance medium and adipocytes were identified using Oil Red O (Figure 4.3).

While early reports by Di Nicola *et al*. [199] and Bartholomew *et al*. [198] demonstrated that human/baboon bone marrow derived MSCs had an innate ability to suppress activated lymphocytes *in vitro*, this was not the case in our hands. The bone marrow is a hypoxic environment, MSCs grown in hypoxic conditions have been reported to be optimally primed for immunomodulation [358], not only this, they have been reported to increase their ability to suppress $CD4^+$ T lymphocyte proliferation while expanding Tregs [358]. We observed that in either normoxic or hypoxic conditions, MSCs failed to suppress CD3/CD28 stimulated T lymphocytes *in vitro* (**Figure 4.5 i-iv**). This has been described in the past by others [242] and in fact, Krampera *et al*. described that MSCs needed a pro-inflammatory stimulus in order to become potently immunomodulatory [242]. Many different groups have reported that MSCs can induce Tregs *in vitro* [245, 246, 359] and *in vivo* [254, 263, 265, 360]. The exact mechanisms of how MSCs induce Tregs is still not fully understood, however secreted molecules such as NO, PGE2, TGF-β1 and cell-cell contact are known to play vital roles [245, 246, 359]. In transplantation studies, MSC induced Treg populations have been linked to greater survival of grafts in models of corneal [263, 265], kidney [360] and heart [254, 360]. Analysing the $CD4^+FoxP3^+$ populations by flow cytometry (**Figure 4.4**) after T lymphocyte co-culture, we observed (even in the presence of IL-2) no significant increases in Treg populations compared to the stimulated lymphocyte control regardless of MSC culturing conditions (**Figure 4.6**). While MSCs did not suppress stimulated lymphocytes or induce Tregs in T lymphocyte co-cultures, they did secrete significant levels of PGE2 (**Figure 4.7**) and significantly decreased the levels of IFN-γ (**Figure 4.7**). This has been reported in the literature in both *in vitro* and *in vivo* studies, MSCs have been shown to shift the balance from a pro-inflammatory Th1 cytokine response (IFN-γ and TNF-α) to anti-inflammatory Th2 response [260, 361-363].

As previously mentioned in chapter 1, MSCs have a capacity to modulate many components of the innate immune system including toll-like receptor signalling, complement, macrophages, dendritic cells, mast cells, NK cells and neutrophils [260]. Macrophages play a role in the early phase of corneal allograft rejection [335] and it has been reported that macrophage depletion using clodronate liposomes induces tolerance to corneal grafts [83, 336], highlighting their crucial role. We observed that untreated MSCs do not modulate MHC I, MHC II, CD80 or CD86 on macrophages

that have been stimulated with IFN-γ and LPS (**Figure 4.8**). Inflammatory (M1) macrophages are characterised by the secretion of high levels of pro-inflammatory cytokines including TNF-α, IL-1β, IL-12/23 and IL-6 [364]. It was observed that untreated MSCs significantly modulated the secretome of stimulated macrophages, significantly decreasing the levels of TNF-α, IL-1β, IL-12/23 and IL-6 (**Figure 4.8**), possibly via PGE2, suggesting that MSCs were potentiating M1 inflammatory macrophages to anti-inflammatory (M2) macrophages.

During this study we successfully established a mouse model of corneal allo-transplantation (**Figure 4.9**). Graft transparency was used as the primary indicator of rejection and was evaluated every 2/3 days. Opacity was indicative of immune cell infiltrate. A scoring system was established (**Figure 4.9B**) and a single scoring of 2 was defined as rejection (**Figure 4.9D (Day 17)**) where the graft would have modest corneal opacity and the iris vessels were still visible. We observed that untreated graft recipients uniformly rejected donor corneal buttons between day 16 and day 19 after transplantation (**Figure 4.9C+D**).

Previously in our lab, in a rat model of corneal transplantation, Treacy *et al*. concluded that syngeneic MSCs administered pre-transplantation day (day -7 and day 0) failed to prolong allograft survival as they were administered to an immunologically identical non-inflamed host and hence did not receive adequate activation stimulus needed upon exposure to acquire their immunomodulatory properties enabling them to prolong graft survival [265]. However, Omoto *et al*. described that syngeneic MSCs administered POD (day 0 and day 7) were capable of prolonging graft survival by suppressing the maturation of DCs resulting in the inhibition of direct and indirect allo-sensitisation of alloreactive T cells [269]. We further hypothesised that on-going inflammation caused by the transplant may stimulate the administered MSCs, activating them, hence acquiring potent immunomodulatory potential. We chose POD +1 as the innate immune response, specifically APC mediated presentation of alloantigen, begins within hours after transplantation and MSCs had demonstrated an ability to inhibit TNF-α, IL-1β, IL-12/23 and IL-6 concentrations when cultured directly with macrophages. POD+7 was chosen as the adaptive immune response instigates later and can take up to 7 days, we observed that MSCs could modulate IFN-γ secretion while increasing the levels of the potent immunoregulatory molecule PGE2. For these reasons we administered $1x10^6$ untreated MSCs POD day +1 and

$1x10^6$ untreated MSCs POD day +7 (**Figure 4.10**). However, untreated MSCs failed to prolong RFS (**Figure 4.10A+B**) and no significant difference in opacity score (**Figure 4.10C**) or neovascularisation (**Figure 4.10D**) was observed.

It has been demonstrated that pre-activation of MSCs by pro-inflammatory cytokines, especially IFN-γ [266] can improve their immunosuppressive capacity. Duijvestein *et al*. observed that pre-activation of MSCs with IFN-γ enhances their capacity to inhibit T lymphocyte inflammatory responses *in vitro*, resulting in reduced mucosal damage in an *in vivo* model of experimental colitis [266]. This data demonstrated that IFN-γ activation of MSCs increases their immunosuppressive capabilities and importantly, their therapeutic efficacy in vivo. To investigate if the pre-activation of MSCs would increase their immunomodulatory capacity we devised a strategy for the cytokine pre-activation of MSCs **(Figure 4.11**). We used the pro-inflammatory cytokines IFN-γ, TNF-α and IL-1β singly or in combination or the anti-inflammatory cytokine TGF-β singly. Pre-activation of MSCs induced morphological changes (**Figure 4.12**), non-significant change in cell size and cell granularity (**Figure 4.13 A+B**) and a significant reduction in cell number per well (**Figure 4.13 C**). The morphological changes were most striking in the IFN-γ + TNF-α + IL-1β and TGF-β MSC treated MSC wells. IFN-γ + TNF-α + IL-1β MSC growth and proliferation was heavily effected due to treatment, as a result, this pre-activation strategy was discontinued due to concerns that we would not be able to generate sufficient number of cells if we were to take this strategy to *in vivo* application and that the overall health of the cells was not optimal. Interestingly, Klinker *et al*. have recently demonstrated that IFN-γ treated MSCs exhibited morphological changes and these changes are indicative of immunosuppressive capacity [365]. Interestingly in our study, while FSC and SSC were not significantly changed, TGF-β MSCs demonstrated to be more elongated and organised into "swirls". These cells were potently suppressive to both T lymphocytes and activated bone marrow derived macrophages (BMDMs) (which will be further discussed in chapter 5).

Apoptosis of MSCs following i.v. injection has gained attention recently with reports that MSC immunomodulatory properties are dependent upon APC phagocytosis of apoptotic MSCs [366, 367]. However, in these studies if the MSCs were apoptotic before administration their efficacy was hindered indicating that the site of apoptosis and phagocytosis by APCs is paramount [366]. Therefore, we hypothesised it is

important that our pre-activated MSCs were viable at the time of injection. Combinations of pro-inflammatory cytokines resulted in significantly lower MSC yields (**Figure 4.12C**). It was thought that this reduction in cell number was due to the cytokines inducing cell stress causing cell death or apoptosis which would not be ideal. However, when the viability of the MSCs was checked by flow cytometry all cells were viable indicating that perhaps the cytokine combinations were slowing the proliferation of the cells.

To identify which pre-treatment strategy would be best for *in vivo* administration we devised a list of criteria. The first criterion was to assess if cytokine treatment resulted in the upregulation of the co-inhibitory molecule PD-L1. We observed that the expression of PD-L1 on MSCs was IFN-γ dependent and synergises with other pro-inflammatory cytokines (**Figure 4.14**). Using single cell qRT-PCR Jin *et al*. recently demonstrated that that the combination of IFN-γ and TNF-*α* is effective for induction of the expression of high levels PD-L1 [330]. In preliminary experiments (**Figure 4.16 + 4.17**) where we tested the ability of normoxic or hypoxic cultured IFN-γ MSCs, IFN-γ + TNF-α MSCs or IFN-γ + IL-1β MSCs to suppress activated T lymphocytes we observed that while they suppressed T lymphocytes slightly, TNF-α + IL-1β MSCs and TGF-β MSCs suppressed proliferation to a higher degree. Interestingly, neither TNF-α + IL-1β MSCs nor TGF-β MSCs had significant increases PD-L1 expression (**Figure 4.14**) indicating that other factors or combinations of factors were important in the modulation of the T lymphocyte responses.

Immunoregulatory molecules such as IL-10, PGE2 and NO are reported to be, in part, responsible for the ability of MSCs to modulate immune cell populations [364]. In a model of sepsis, Nemeth *et al*. [253, 368] demonstrated that MSCs can ameliorate symptoms via a PGE2 dependent mechanism. They demonstrated that LPS and TNF-α activate TLR4 and TNFR1 on MSCs to activate nuclear factor-κB signalling (NF-κB) resulting in an increase of secreted PGE2 via upregulation of cyclooxygenase (COX)-2. They reported that PGE2 acts on the prostaglandin receptors EP2 and EP4 on macrophages to increase IL-10 secretion.

NO is a gaseous bioactive molecule and it was first described as a mediator of MSCs suppression of T cell proliferation by Sato et al. who also demonstrated it inhibited Stat5 phosphorylation in T cells [104]. It was demonstrated that the production of NO

by MSCs is dependent on pro-inflammatory cytokine stimulation [79]. Also, NO has been shown to induce Tregs from naïve CD4+CD25- T cells [105].

For these reasons, the second criterion was to investigate if cytokine treatment of MSCs resulted in increases in the secretion of IL-10, PGE2 and NO (**Figure 4.15**). Interestingly, pre-activation of MSCs with all strategies except for IFN-γ (singly) produced significant increases in PGE2 and the secretion of NO was dependent on IL-1β in combination with either IFN-γ or TNF-α (**Figure 4.15B**). It was noted that the secretion of IL-10 was not observed under any of the pre-activation conditions.

The third criterion and the principal finding in this chapter was that BALB/c MSCs only gained the ability to suppress activated T cells after pre-treatment with pro- or anti-inflammatory cytokines and this was independent of oxygen culturing conditions (**Figure 4.16+ Figure 4.17**). TNF-α + IL-1β in combination and TGF-β singly were the most potent (**Figure 4.17**). Interestingly, IL-1β was the key pro-inflammatory cytokine needed to activate MSCs immunosuppressive function and not IFN-γ which as has been reported previously in the literature [236, 242, 250, 348].

In this study, pre-treatment of MSCs with TNF-α + IL-1β resulted in the most immunosuppressive MSC phenotype. This was indicated by a trend increase of PD-L1, the highest levels of secreted NO and PGE2 and the greatest suppression of T lymphocytes in preliminary experiments. Therefore, TNF-α + IL-1β MSCs were selected for further analysis and *in vivo* administration.

Firstly, TNF-α + IL-1β MSCs were characterised by flow cytometry to study the effects of cytokine pre-treatment on cell surface identification markers. It was observed that TNF-α + IL-1β treatment did not significantly change MHC II, CD45, F4/80, CD11c, CD80 or CD86 on the surface of the MSCs. Interestingly, both MHC I and MHC II were significantly upregulated on MSCs treated with IFN-γ singly or in combinations with other cytokines (**Appendix Figure 1**) but not on TNF-α + IL-1β MSCs. If pre-activated MSCs were used in an allogeneic setting this phenomenon would have to be taken into consideration as this could increase the likelihood of an antigen specific donor response via alloreactive T lymphocytes [369]. TNF-α + IL-1β MSCs remained positive for cell surface characterisation marker CD105 while they had increased expression of CD73, CD44 and CD90 and decreased expression of SCA-I. One of the less studied immunosuppressive mechanisms of MSCs is mediated

by the adenosinergic pathway via the ectonucleotidases CD73 and CD39. Kerkela *et al*. demonstrated that adenosine (ADO) is actively produced from adenosine 5′-monophosphate (AMP) by CD73 on MSCs and ADO produced by MSCs can suppresses activated T lymphocytes *in vitro* [370]. The effect of CD73 in our study will be examined in greater detail in chapter 5 using specific CD73 inhibitors. CD44 is known to be involved in MSC migration and cell-cell interactions [371, 372] and CD90 is expressed on many different cell types and it has implication in regulating cell adhesion, migration, apoptosis and cell-cell interactions [373], this being case, the specific contributions that these two markers have in MSC immunomodulation is only speculative at this point and further investigation is needed.

As mentioned previously, the key finding in this study was that cytokine pre-treated MSCs were potently immunosuppressive. In preliminary experiments (**Figure 4.16+ Figure 4.17**) we observed that TNF-α + IL-1β MSCs decreased both the frequency and proliferation of $CD4^+$ and $CD8^+$ lymphocytes to a greater degree than other pre-treatments. To investigate if this observation was statistically significant and not just an artefact, TNF-α + IL-1β MSCs were placed in T lymphocyte co-cultures and their effects on T lymphocytes were studied more intensively. We demonstrated that TNF-α + IL-1β MSCs were potently immunomodulatory, suppressing activated T lymphocytes significantly (**Figure 4.19 + Figure 4.20**). TNF-α + IL-1β MSCs also significantly increased the concentrations of the anti-inflammatory molecules NO and PGE2 while decreasing the concentration of cytotoxic granzyme B and pro-inflammatory IFN-γ (**Figure 4.21**).

In rodents, Sato and colleagues were the first to demonstrate that NO was a crucial molecule in MSC modulation of T lymphocytes [237]. Our observed increases in NO are in line with previous studies from Ren *et al*., this study demonstrated that the secretion of NO by MSCs was dependent by pro-inflammatory cytokines IFN-γ, TNF-α and IL-1β [236]. Zinocker ***et al.*** demonstrated convincingly that MSCs lost their immunoregulatory properties when in the presence of NO inhibitor again highlighting the importance of NO in MSC immunomodulatory abilities [374]. In MSC-T lymphocyte co-cultures we noted that the majority of T lymphocytes in TNF-α + IL-1β MSC wells do not proliferate, even in the presence of the CD3/CD28 activation beads, presumably remaining in a naïve undifferentiated state evident from a large proportion of cells remaining in generation 1 (**Figure 4.20 C**). We hypothesise this is

due to high levels of NO. PGE2 is a lipid-based immunomodulatory molecule produced by cyclooxygenases (COX). It has been reported to be important in MSC-mediated suppression of both innate and adaptive immune cells [364]. Our observations that PGE2 increased after pro-inflammatory pre-treatments are in line with a number of different lab groups as they have also shown that PGE2 secretion is increased after pro-inflammatory pre-activation, mainly IFN-γ and IL-1β [375-378]. Again, our observation that TNF-α + IL-1β MSCs decrease the levels of activated Th1 cytokines has also been reported by others, Kong *et al*. reported that MSCs modulate Th1/Th2/Th17/Treg cell balance by modulating the local secretome [379].

It was demonstrated that TNF-α + IL-1β MSCs had a capacity to modulate stimulated BMDMs (**Figure 4.22**). After incubation with IFN-γ and LPS BMDMs become stimulated, upregulating MHC I, MHC II, CD80 and CD86. TNF-α + IL-1β MSCs significantly reduced MHC I, MHC II, CD80 and CD86 expression after 72-hour co-culture. As macrophages are the primary innate immune cell involved in corneal allograft rejection, an enhanced capacity to inhibit macrophage differentiation could lead to enhanced capacity to prolong corneal allograft survival [83]. As previously discussed, multiple studies have reported that MSCs undergo apoptosis and are phagocytosed in the lung following i.v. administration which confers the MSCs immunomodulatory properties to the phagocyte [366, 367, 380]. Taking this information along with recent reports stating that MSCs, via the action of TNF-stimulated gene 6 protein (TSG-6) and PGE2, induce regulatory macrophages in the lung highlights the importance of APCs as intermediaries of MSCs immunomodulatory properties [253, 267]. Therefore, the ability of TNF-α + IL-1β MSCs to modulate BMDMs may indicate a more potent capacity to modulate APCs of the lung following i.v. administration.

TNF-α + IL-1β MSCs proved to be potent modulators of both adaptive and innate immune cells. Therefore, TNF-α + IL-1β MSCs were selected for *in vivo* administration. We administered $1x10^6$ TNF-α + IL-1β MSCs POD day +1 and $1x10^6$ TNF-α + IL-1β MSCs POD day +7. TNF-α + IL-1β MSCs did not prolong RFS, surprisingly on the contrary the administration of TNF-α + IL-1β MSCs accelerated rejection, with all animals rejecting on or before POD 18 (**Figure 4.23A-B**). A trend increase in overall corneal opacity was also observed (**Figure 4.23C**) indicating a

higher number of infiltrating immune cells. This result was unexpected as TNF-α + IL-1β MSCs had shown promise *in vitro*.

It has been previously reported by multiple studies that MSCs induce Tregs both *in vitro* and *in* vivo as mentioned previously, when we analysed if TNF-α + IL-1β MSCs had the ability to increase the frequency of Tregs *in vitro* in comparison to stimulated lymphocytes, we observed that they did not (**Figure 5.3**). Tregs have been reported in multiple studies to important in the prolongation of graft survival, including corneal allograft survival [62, 263, 265, 381-383]. Jia *et al*. observed that postoperative injection of MSCs reduced Th1 pro-inflammatory cytokines and elevated IL-4 cytokine secretion from T lymphocytes derived from cornea-transplanted rats [263]. Also, they noted that Tregs were upregulated in the DLNs after MSC treatment. They attributed this increase in Tregs to the observed prolongation of corneal allograft survival. Not only this, Obermajer *et al*. attribute the prolonged survival of heart allografts to be associated with reversal of the Th17/Foxp3 ratio, they observed a potent induction of Tregs in the hearts and spleens of mice after the administration of MSCs and MMF [383]. In a separate study investigating if the administration of MSCs in a semi-allogeneic heart transplant model could prolong survival, Casiraghi *et al*. associated the MSC induced expansion of Tregs and impaired anti-donor Th1 activity with increased survival [360, 381]. Previously in our lab, Tracey *et al*. demonstrated that allogeneic MSCs administered 7 days before transplantation and on the day of transplantation resulted in a significant prolongation of corneal allograft survival, in this study both splenic and corneal Tregs were elevated in MSC treated animals [265]. These studies amongst others highlight that MSCs ability to prolong allograft survival is partially due to their ability to generate or induce Tregs. This may be a potential reason as to why TNF-α + IL-1β MSCs did not have the ability to prolong corneal allograft survival in our model.

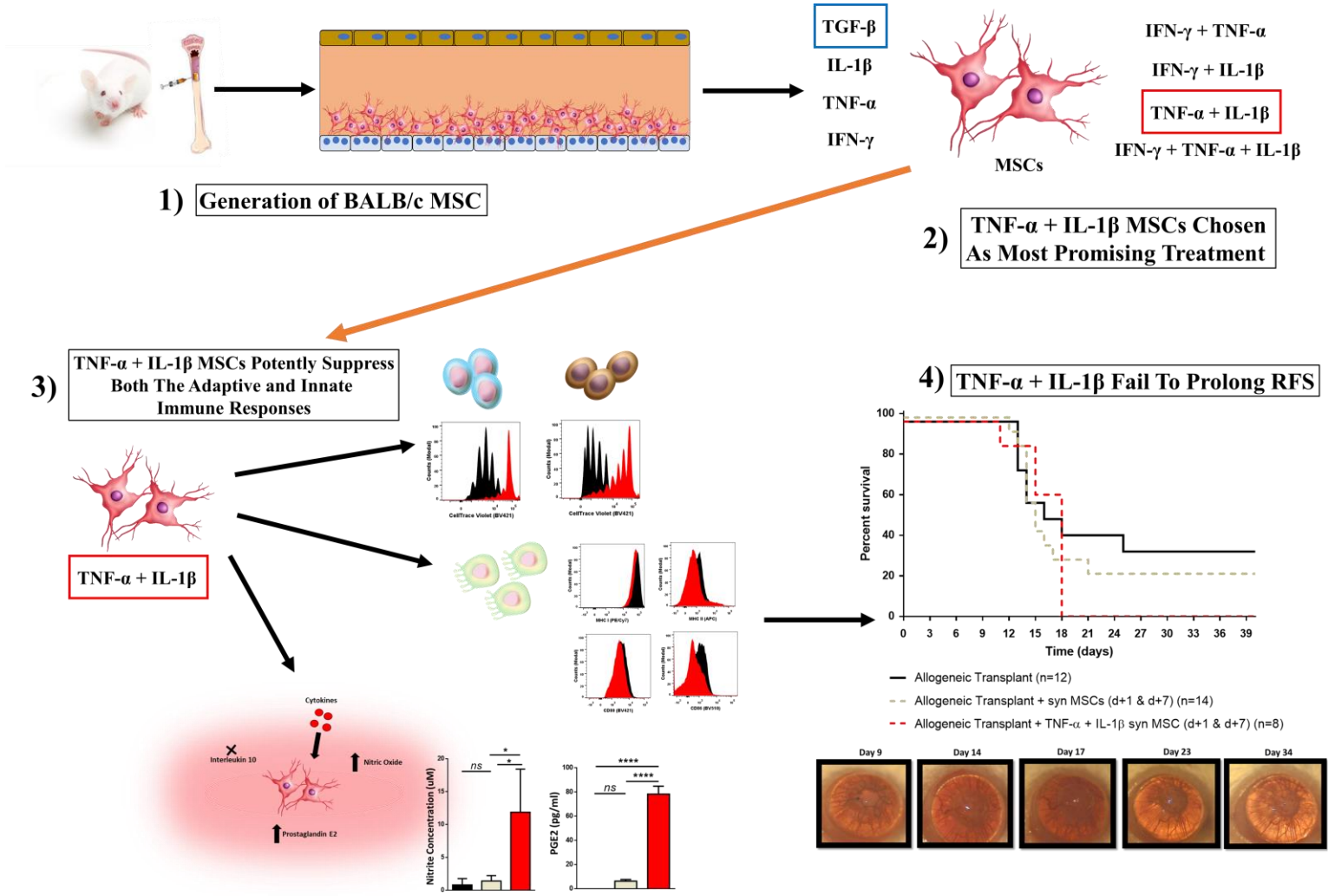

Figure 4.24. Summary of results discussed in chapter 4. |

Chapter Five:

TGF-β Pre-Activated MSCs Induce Regulatory Populations *in vivo* and Prolong Corneal Allograft Survival

5.0 Chapter Experimental Design

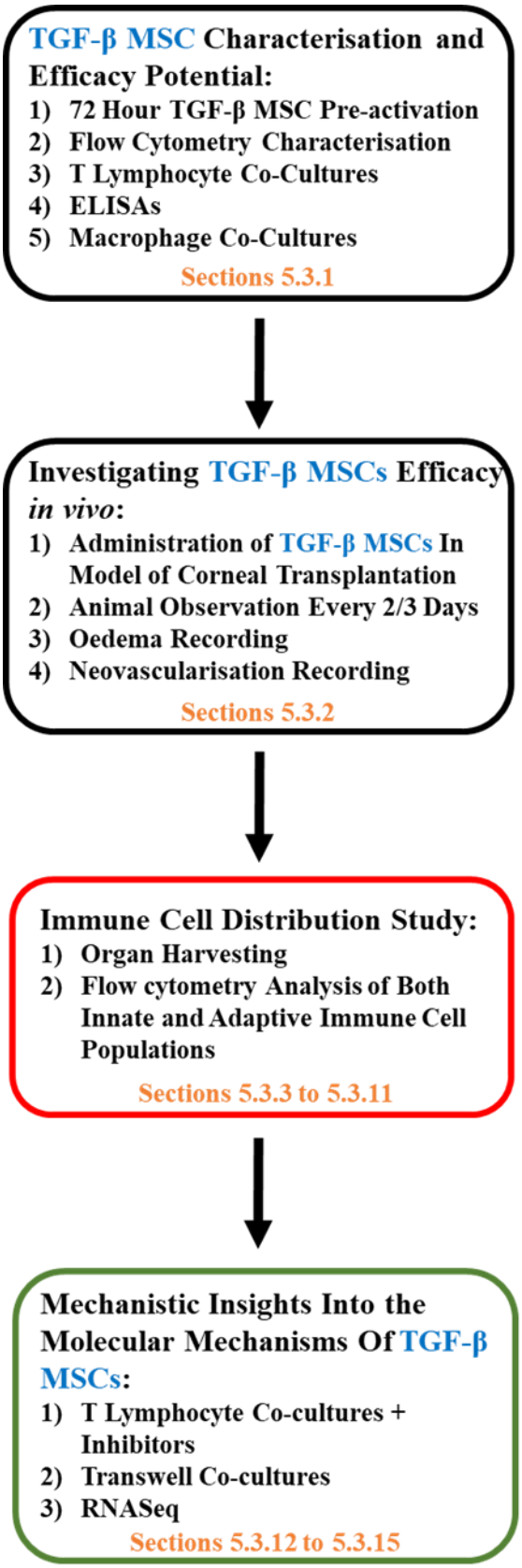

Schematic overview of chapter experimental design | A schematic presenting the sequence and progression of experiments described in this chapter.

5.1 Introduction

Pre-activation of MSCs *ex vivo* by hypoxia, cytokines, or other factors prior to their use in therapy is gaining popularity as it prepares MSCs to survive and enhance their regulatory function of the local immune responses [384]. Multiple different factors have been used to increase the efficacy of MSCs *in vitro* and *in vivo* including vitamin E [385], LPS [386], stromal-derived factor-1 [387], TNF-α [388], IFN-γ [266, 376], IL-1β [389], IL-1β + TNF-α [390, 391], TNF-α + IFN-γ [392] and migration inhibitory factor [393]. As listed, most cytokines used in the pre-activation of MSCs are pro-inflammatory in nature and are used singly or in combination. Not many studies have investigated the effects of anti-inflammatory cytokine pre-activation in the context of MSC therapeutic efficacy.

TGF-β1 (TGF-β) is a pleiotropic molecule involved in multiple biological processes including development, regulation of stem cell behaviour, carcinogenesis, tissue homeostasis, and immune responses [394, 395]. It has been reported that MSCs secrete TGF-β and it has been demonstrated that TGF-β promotes fibroblast proliferation while also playing multiple roles in MSC immunomodulation including a role in the induction of Tregs [199, 396-398]. TGF-β is also known to directly influence MSCs themselves, modulating their migration and differentiation [399, 400].

To date, several studies have investigated the effects of TGF-β treatment on MSCs. Dubon *et al*. [401] demonstrated that TGF-β activated human MSCs had increased migratory capacity into remodelling sites, synergising bone formation and reabsorption. They also noted that both the canonical and non-canonical pathways of TGF-β signalling were activated in the study suggesting a dual mechanism of action [401]. Van Zoelen *et al*. [402] performed experiments that demonstrated that TGF-β treatment of MSCs potentiated them towards osteoblast differentiation and inhibited adipogenic differentiation and that this was dependent on small mothers against decapentaplegic (SMAD) signalling. Interestingly, in a rat model of LPS-induced acute lung injury Li *et al*. demonstrated that low concentrations of TGF-β (0.1 ng/ml) enhanced fibronectin production by MSCs leading to increased MSC survival *in vivo*, increasing the effective therapy time in the damaged lungs [403].

These studies demonstrate that TGF-β is important in the differentiation, survival and migration of MSCs, however, to our knowledge no studies have documented the changes in immunoregulatory potency after pre-activation with TGF-β.

Therefore, the hypothesis for this chapter was that TGF-β MSC treated BALB/c MSCs acquire unique potent immunosuppressive properties that set them aside from pro-inflammatory pre-activated MSCs and that TGF-β pre-activated MSCs can prolong corneal allograft survival by modulating immune cells *in vivo* via the action of PGE2.

To test the hypothesis, MSCs were pre-treated with the anti-inflammatory cytokine TGF-β. The phenotype of the TGF-β MSCs was characterised. TGF-β MSCs were co-cultured with activated syngeneic T lymphocytes and macrophages to determine if they were immunomodulatory. TGF-β MSCs were then administered into an allogeneic model of corneal transplantation. It was observed that TGF-β MSCs had the ability to significantly prolong RFS in our model. To gain some clarity as to how TGF-β MSCs were prolonging RFS, a full immune cell distribution study was performed in the DLNs, spleens and lungs of treated and non-treated animals. Cells of both the adaptive and innate immune system were analysed.

Finally, as we had observed high levels of PGE2 secretion and CD73 expression *in vitro*, we selectively inhibited prostaglandin receptors (EP) on T lymphocytes or CD73 on MSCs to study if either of these molecules were important for the observed inducement of Tregs or suppression of T lymphocytes.

5.2 Hypothesis and Objectives

5.2.1 Hypothesis

The potent immunosuppressive properties of TGF-β MSCs are only acquired upon pre-activation by cytokines. Pre-activated TGF-β MSCs can prolong rejection free survival in a model of corneal transplantation via the modulation of the alloantigen immune response. This prolongation of RFS is in part due to the action of immunomodulatory molecules such as CD73 and PGE2

5.2.2 Aims

I. To pre-treat MSCs with TGF-β and characterise the pre-activated phenotype.
II. To test the immunosuppressive capacity of TGF-β MSCs to modulate syngeneic innate and adaptive effector cells.
III. Administer TGF-β MSCs in our pre-clinical model of corneal transplantation.
IV. To investigate the mechanisms of immune modulation which mediate MSCs ability to prolong allograft survival
V. Investigate if CD73 and/or PGE2 play an important role in TGF-β MSC immunomodulation.

5.3 Results

5.3.1. TGF-β as a Candidate Pre-activation Strategy for In Vivo Application

We observed in the last chapter that TNF-α + IL-1β MSCs failed to prolong RFS in a fully allogeneic MHC I/II mismatched model of corneal transplantation despite very promising *in vitro* indications. In this chapter, it is demonstrated that TGF-β licensing of MSCs display unique characteristics that indicated its potential as another candidate for *in vivo* administration. MSCs were treated with TGF-β at 50ng/ml for 72 hours, following this TGF-β MSCs were characterised by flow cytometry for the expression of negative markers MHC II, CD45, F4-80, CD11c, CD80 and CD86 (**Figure 5.1A**) and the expression of positive markers CD105. CD73, CD90. CD44, SCA-I and MHC I (**Figure 5.1B**). No significant changes in MHC II, CD45.2, F4/80, CD11c CD86 or CD80 were observed. We observed highly significant increases in the ecto-nuclease CD73 with significant decreases in SCA-I and MHC I. No significant changes in CD44, CD90 and CD105 expression were observed.

Next TGF-β MSCs were placed in T lymphocyte co-cultures with anti CD3/CD28 stimulated lymphocytes and were incubated for 96 hours. Following culturing period, proliferation of CD4+ and CD8+ lymphocytes were analysed by flow cytometry using CTV to track proliferation. Both total proliferation and proliferation greater than three (>3) generations of lymphocytes were analysed. The results demonstrated that TGF-β MSCs significantly inhibited the total proliferation of activated CD4+ and CD8+ lymphocytes (**Figure 5.2A**). Stimulated CD4+ lymphocyte total proliferation was reduced from 97.5% ± 0.55% SD to 68% ± 9.6% SD in wells that contained TGF-β MSC. Stimulated CD8+ lymphocytes total proliferation was reduced from 98.7% ± 0.3% SD to 76% ± 5.5% SD in wells that contained TGF-β MSC (**Figure 5.2A**). Subsequently, when T cell proliferation was analysed >3 generations, it was determined that TGF-β MSCs significantly suppressed activated CD4+ and CD8+ lymphocytes also. Stimulated CD4+ lymphocyte >3 generations proliferation was reduced from 64.2% ± 3.1% SD to 15.85% ± 6.3% SD in wells that contained TGF-β MSC. Stimulated CD8+ lymphocytes >3 generations were reduced from 84.4% ± 1.3% SD to 16.3% ± 7.7% SD in wells that contained TGF-β MSC (**Figure 5.2A**). When each generation was analysed individually, it was observed for CD4+ lymphocytes that a large proportion of cells do not leave the first three generations.

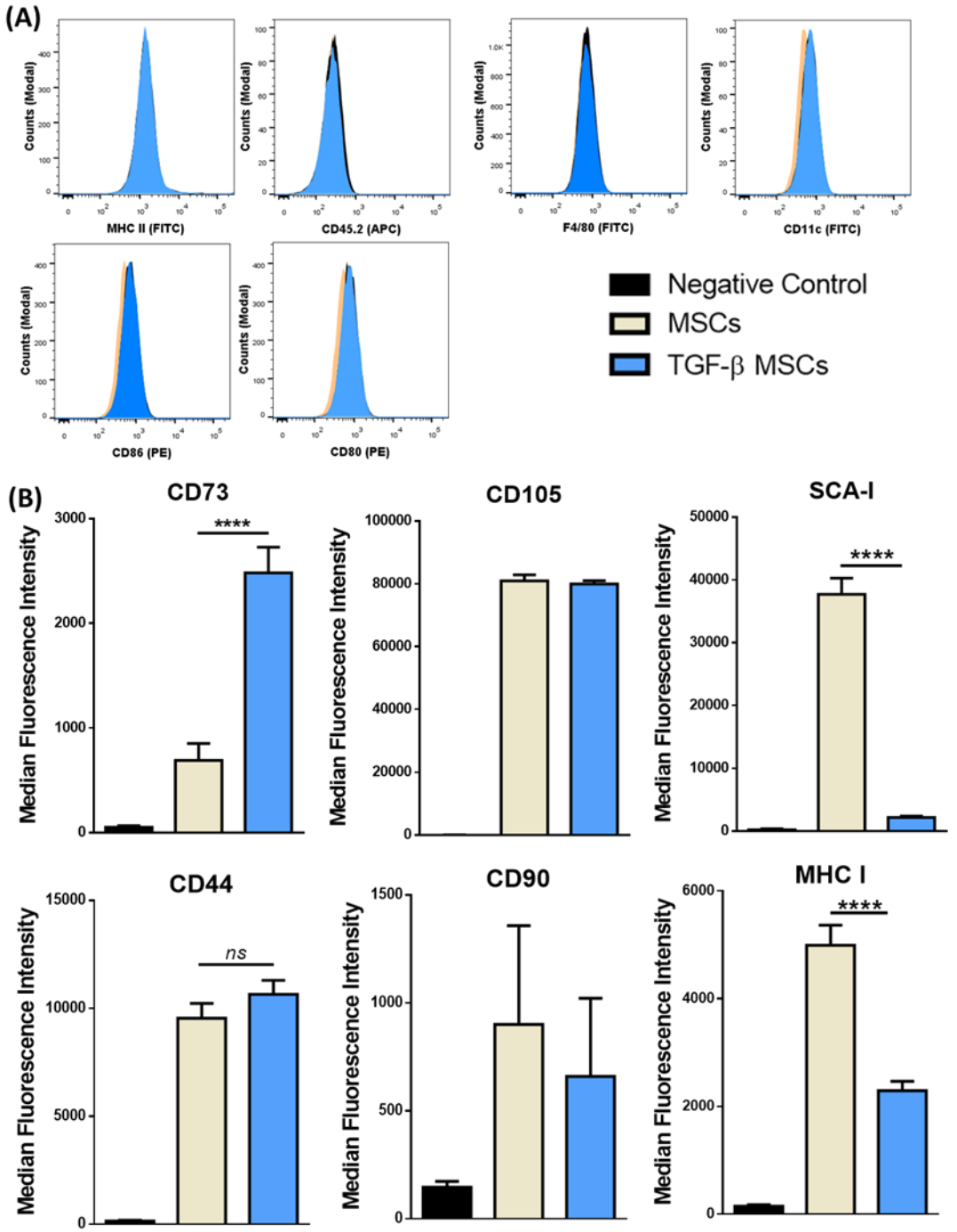

Figure 5.1 TGF-β MSCs display a unique phenotype when compared to MSCs. | (A) Representative flow cytometry histograms for the cell surface expression of negative MSC antigens, MHCII, CD45.2, F4-80, CD11c, CD80, CD86. (B) Histograms showing median fluorescence intensity for the cell surface expression of positive MSC antigens, CD105, CD73, SCA-1, CD90, CD44 and MHC I. Error bars: mean +/- standard deviation *p<0.05, **p<0.01 ***p<0.001 ****p<0.0001. (*n=3).*

In the 1st generation, CD4+ lymphocyte proliferation in the TGF-β wells was 22.42% ± 5.58 SD compared to 5.8% ± 0.18 SD in the MSC wells. In the 2nd generation, CD4+ lymphocyte proliferation was 17.98% ± 2.17 SD compared to 9.4% ± 1.7 SD

and in the 3rd generation CD4+ lymphocyte proliferation was 24.2% ± 4.8 SD compared to 15.78% ± 1.5 SD.

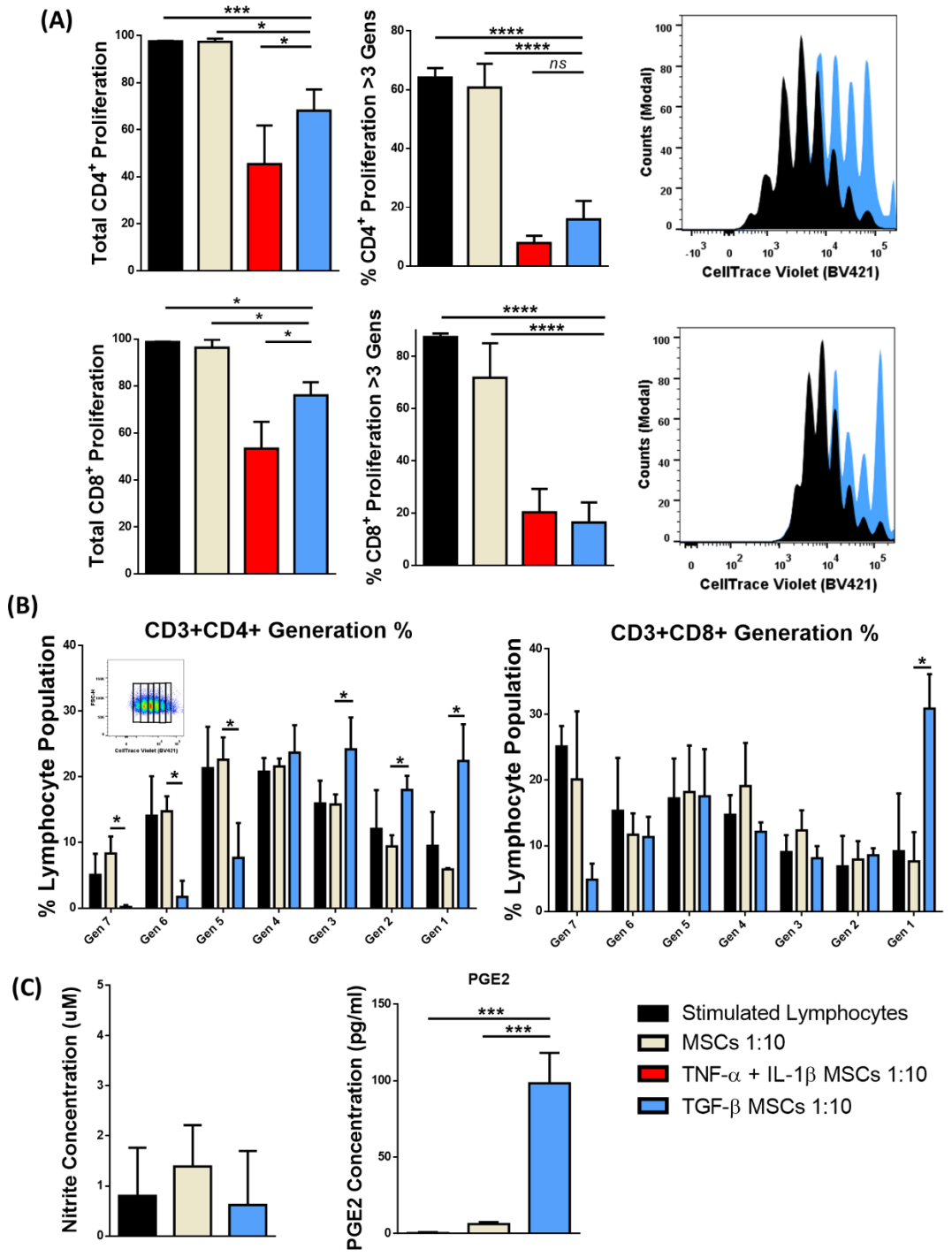

Figure 5.2 TGF-β MSCs inhibit lymphocyte proliferation in T lymphocyte co-cultures. | Untreated BALB/c MSCs or TGF-β MSCs (1 MSC to 10 lymphocytes) were cultured in normoxia and placed in T lymphocyte co-cultures for 96 hours with anti CD3/CD28 stimulated lymphocytes. CTV was used to determine lymphocyte proliferation. (A) Bar charts and histograms showing total lymphocyte proliferation, >3 generation proliferation and representative flow cytometry plot overlays. (B) % of $CD3^+CD4^+$ and $CD3^+CD8^+$ lymphocyte proliferation per generation (C) Following co-culture, supernatant from the cultures was

collected. ELISAs were carried out to assay PGE2 and Griess assays were carried out to assay nitric oxide production. Error bars: mean +/- standard deviation *p<0.05, **p<0.01 ***p<0.001 ****p<0.0001. Multiple unpaired, two tailed student's t test and One-way ANOVA, Tukey's Post Hoc test (*n=3-6).*

The effect was observed to a higher degree for CD8+ lymphocytes with 31% ± 5.2 of cells remaining in the 1st generation compared to 7.6% ± 4.4 SD in MSC wells. Again, it was also observed that very few CD4+ and CD8+ lymphocytes proliferate past the 3rd generation with significantly less lymphocytes in generation 4, 5, 6, and 7 in TGF-β MSC wells compared to untreated MSC wells (**Figure 5.2B)**. Supernatants from T lymphocyte co-cultures were collected and Griess assays and PGE2 ELISAs were preformed (**Figure 5.2C).** Low levels of nitrates were detected in the supernatants with no significant changes observed when compared to MSCs or stimulated controls. Significantly higher levels of PGE2 was detected in TGF-β wells when compared to MSCs or stimulated controls **(Figure 5.2C).**

Utilising the FoxP3-GFP transgenic BALB/c mouse, the frequency of Tregs were analysed by flow cytometry. It was observed that TGF-β significantly increased the frequency of Tregs in T lymphocyte co-cultures when compared to stimulated controls, MSCs and TNF-α + IL-1β MSCs (**Figure 5.3B**). As it was observed that a significantly lower number of lymphocytes were present in TGF-β MSC wells when compared to stimulated control wells and MSC wells (**Figure 5.3C**) we were interested to see if this increase in frequency was due to an increase in the absolute number of Tregs or if it was due to an increase in the ratio between conventional T cells and Tregs. To investigate this, absolute numbers of Tregs was calculated. It was observed that TGF-β MSCs significantly increased the absolute numbers of Tregs per $1x10^5$ live lymphocytes (**Figure 5.3D**).

Inflammatory macrophages play a vital role in corneal graft rejection [83, 336]. To investigate if TGF-β MSCs could modulate activated M1 macrophages they were placed into co-cultures with LPS + IFN-γ stimulated macrophages for 72 hours. TGF-β MSCs significantly decreased the expression of antigen presentation molecules MHCI and MHCII and the co-stimulatory molecule CD80 (**Figure 5.4**). Expression levels of CD86 were not significantly altered.

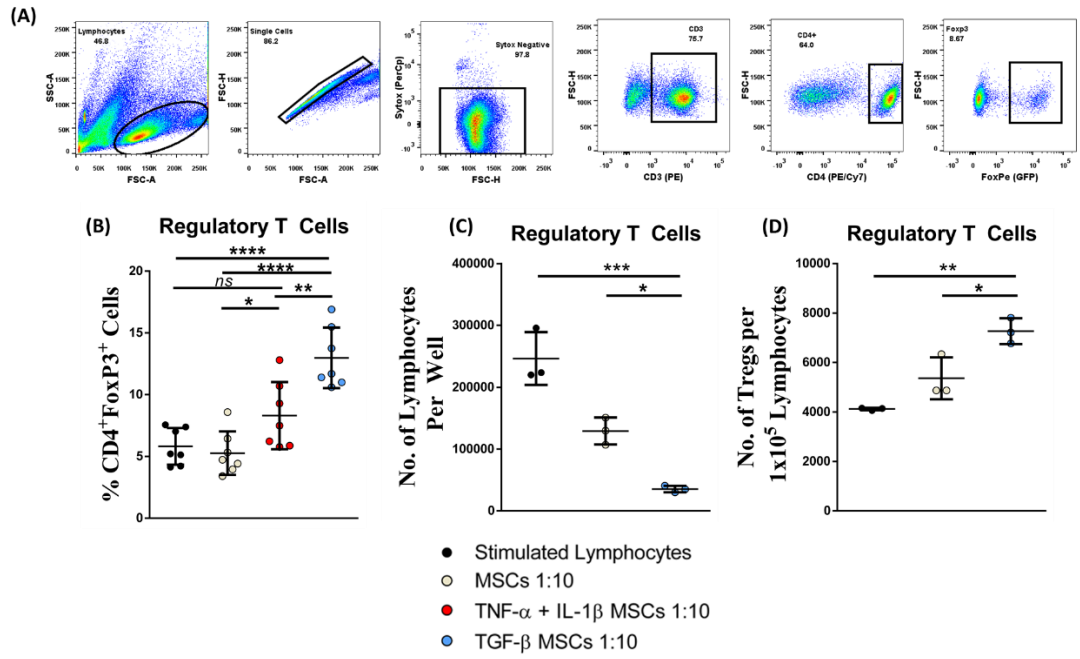

Figure 5.3 TGF-β MSCs significantly increase both the frequency and number of Tregs in T lymphocyte co-cultures | Untreated BALB/c MSCs or TGF-β MSCs (1 MSC to 10 lymphocytes) were cultured in normoxia and placed in T lymphocyte co-cultures for 96 hours with CD3/CD28 stimulated lymphocytes. $CD3^+CD4^+FoxP3^+$ Treg frequency and number was calculated using flow cytometry. (A) Flow cytometry gating strategy. Cells were selected according to size and granularity, followed by single cell selection. Live/dead discrimination based on Sytox negative cells (live) was then carried out. Tregs were selected by CD3 (PE), CD4 (PE/CY7) and FoxP3 (GFP) positivity. (B) Frequency of Tregs. (C) Total number of live lymphocytes per well directly after T lymphocyte co-culture. (D) Absolute counts of Tregs per 100,000 live lymphocytes. Error bars: mean +/- standard deviation *p<0.05, **p<0.01 ***p<0.001 ****p<0.0001. One-way ANOVA, Tukey's Post Hoc test (*n=3-7).*

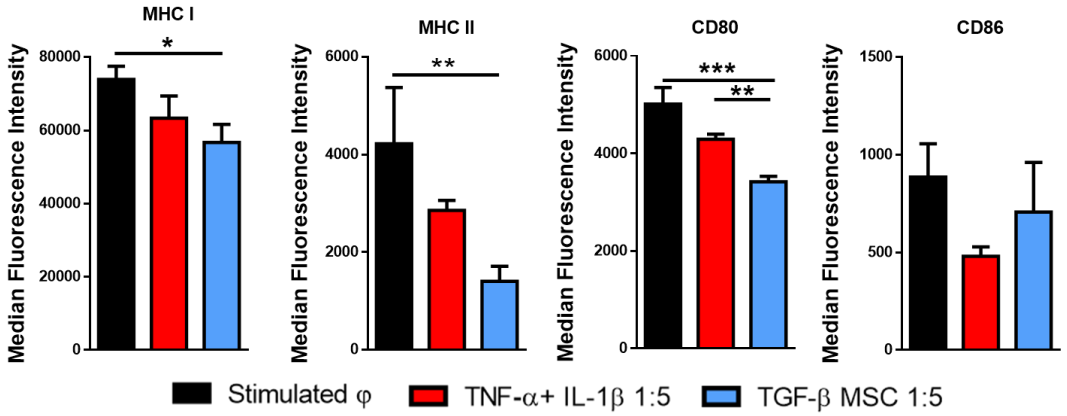

Figure 5.4 TGF-β MSCs suppress activated M1 macrophages. | TGF-β BALB/c MSCs were cultured with activated bone marrow generated macrophages for 72 hours. MHC I, MHC II, CD80 and CD86 expression was analysed on macrophage cell surface by flow cytometry. Error bars: mean +/- standard deviation *p<0.05, **p<0.01 ***p<0.001 ****p<0.0001. One-way ANOVA, Tukey's Post Hoc test (*n=3).*

5.3.2. Administration of TGF-β MSCs Prolong Rejection Free Survival in a Model of Corneal Allograft Rejection

Neither the administration of MSCs nor TNF-α + IL-1β MSCs prolonged RFS. TGF-β MSCs demonstrated the unique attribute of increasing the absolute numbers of Tregs in T lymphocyte co-cultures. Considering that Tregs are a regulatory population of $CD4^+$ lymphocytes that have been shown to prolong RFS in models of bone marrow [113], skin [113], heart [113], liver [114], kidney [115] and cornea transplantation [112] we administered TGF-β MSCs *in vivo*. MSCs ranging from P 6-8 were treated with 50ng/ml of TGF-β for 72 hours. After this incubation period the MSCs were washed in PBS and trypsinised. Afterwards, the MSCs were washed twice in PBS and counted. The TGF-β MSCs were resuspended at a concentration of $1x10^6$ cells per 100ul of PBS. TGF-β MSCs were administered to treated animals via the tail vein at day +1 POD and day +7 POD. The animals were monitored every 2/3 days for a 40-day period. TGF-β MSCs significantly prolonged RFS with 70% of the transplanted animals surviving until day 40 (**Figure 5.5A**). Accepted grafts remained transparent throughout the observation period (**Figure 5.5B)**. The overall opacity of grafts in TGF-β MSC treated animals was very low and did not increase until late into the observation period (**Figure 5.5C**) and neovascularization followed a similar trend (**Figure 5.5D**). When analysing opacity and neovascularization at the average day of rejection (day 19 POD) it was observed that TGF-β MSC treated animals had significantly lower opacity when compared to untreated, MSC treated and TNF-α + IL-1β MSC treated animals (**Figure 5.6**). TGF-β MSC treated animals demonstrated significantly lower neovascularization at day 19 POD when compared to untreated and MSC treated animals and trend decreases when compared to TNF-α + IL-1β MSC treated animals (**Figure 5.6**). This is suggestive of less angiogenesis and infiltration of immune cells into the graft.

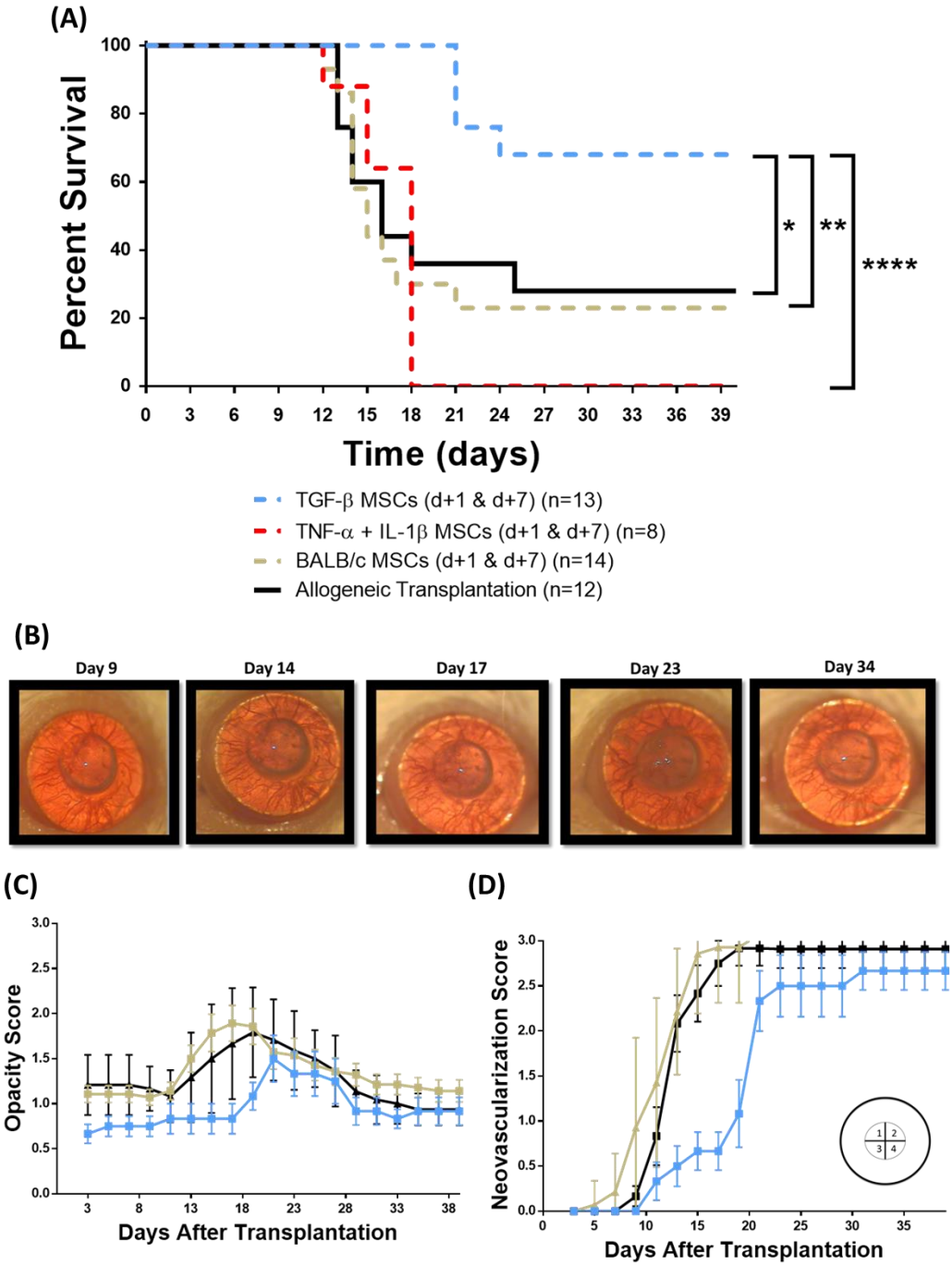

Figure 5.5 TGF-β MSCs significantly prolong RFS in a mouse model of corneal transplant | Female BALB/c mice served as recipients of female C57BL/6J corneas. $1x10^6$ TGF-β MSCs were injected intravenously day +1 and day +7 POD. Mice were observed every 2/3 days. (A) Kaplan-Meier curve showing RFS after administration of MSCs compared to untreated animals. (B) Representative images from a transplanted animal receiving TGF-β MSCs showing RFS over a period of 40 days. (C) Opacity scores over 40 days POD for untreated, MSC treated and TGF-β MSC treated animals. (D) Neovascularization scores POD for untreated MSC and TGF-β MSC treated animals. Error bars: mean +/- standard deviation *p<0.05, **p<0.01 ***p<0.001 ****p<0.0001. Gehan-Breslow-Wilcoxon test.

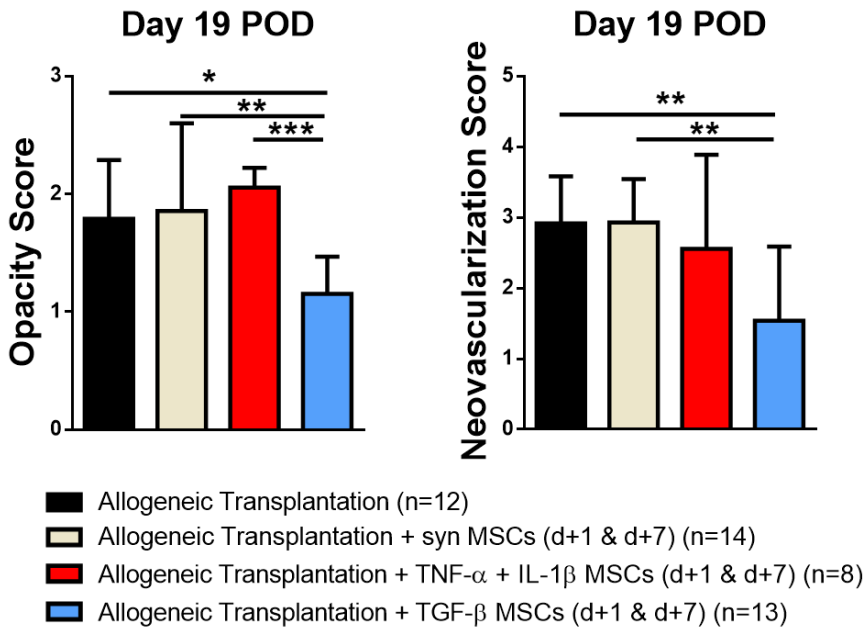

Figure 5.6 Opacity and neovascularization scores at day 19 in TGF-β MSC treated animals are significantly lower | Opacity scores and neovascularization scores were compared on Day 19, which was the average day of rejection. Error bars: mean +/- standard deviation *p<0.05, **p<0.01 ***p<0.001 ****p<0.0001. One-way ANOVA, Tukey's Post Hoc test.

To summarise, we had previously shown that MSCs and TNF-α +IL-1β MSC treatments did not successfully prolong RFS. In contrast, TGF-β MSCs showed increased potential as a cellular therapy as not only did they suppress activated lymphocytes and macrophages, but they also increased the absolute number of Tregs in T lymphocyte co-cultures. After administration *in vivo,* it was observed that TGF-β MSCs significantly prolonged RFS. The process of corneal transplant rejection is a complex event. The draining lymph node (DLN) is a vital location in the rejection process where alloantigen is presented to naive T lymphocytes. This will initiate the effector T lymphocyte response [82]. In studies where the DLN was removed from cornea transplanted animals, 100% RFS was observed [93], highlighting it's importance. For these reasons, immune cell populations of the DLN from transplant recipients receiving no treatment or TGF-β MSC treatment were analysed. It has been reported by us and others that systemically administered MSCs increase regulatory immune populations in the spleen of rodents which have received corneal transplants and these populations have been associated with prolonged RFS [263, 265] . As a result, it was investigated whether TGF-β MSCs modulated immune cell populations

in the spleen of treated animals. It is known that when MSCs are administered to rodents via tail vein injection that the majority of cells get trapped in the lungs and recently it was shown that the lungs are the primary site of immune modulation by MSCs [253, 267, 404, 405]. For these reasons we wanted to investigate if TGF-β MSCs influence immune cell populations in these tissues. The DLN, spleen and lungs were harvested from untreated and treated animals (as described in **section 2.10.5**) and the profiles of B cells, CD4 lymphocytes, CD8 lymphocytes, Tregs, macrophages, dendritic cells, neutrophils and NK cells were analysed (**Figure 5.7**).

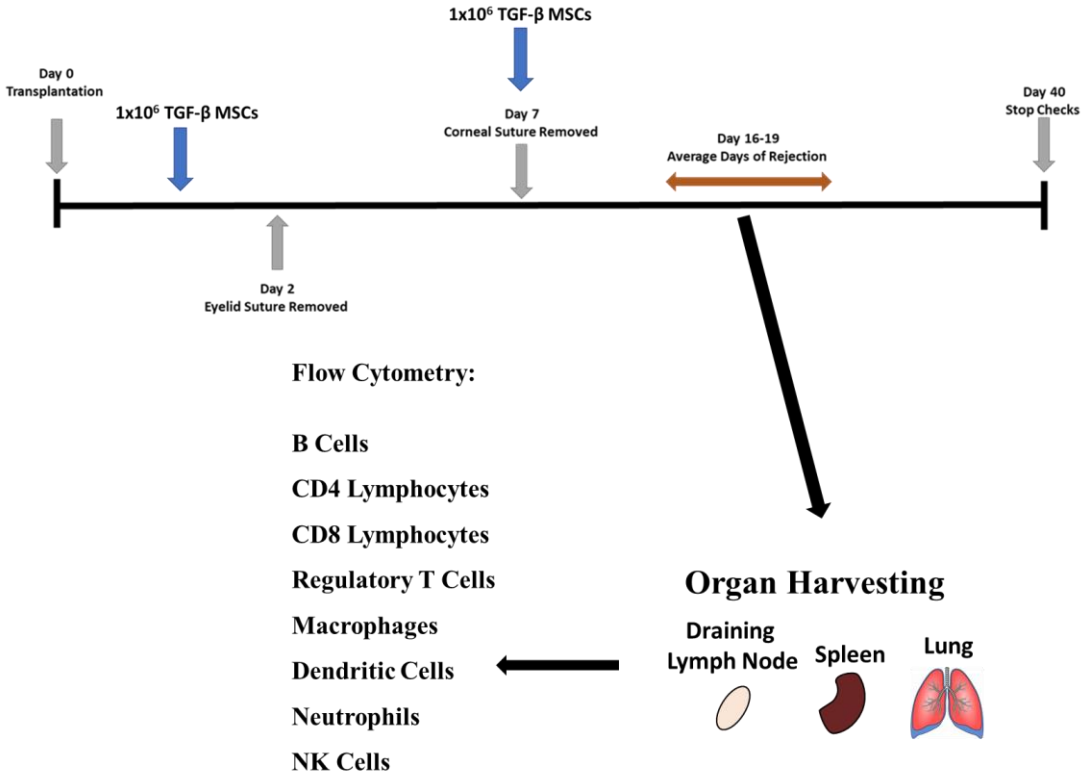

Figure 5.7 Workflow schematic following animal observation period | On the day of rejection, allogeneic control animals were euthanised and the draining lymph node (DLN), spleen and lungs were harvested and prepared for flow cytometry analysis. For TGF-β MSC treated animals, mice were euthanised on the average days of rejection 16-19 and DLN, spleen and lungs were harvested and prepared for flow cytometry analysis.

5.3.3. TGF-β MSCs Significantly Reduce Overall B Cell Frequencies while Increasing $CD5^+$ Regulatory B Cell Frequencies in the Draining Lymph Node and Spleens of Transplanted Animals.

Adaptive immune responses to transplanted tissue is the major impediment to a successful transplantation. In solid tissue transplantation B cells are responsible for the production of alloantibodies leading to both acute and chronic allograft rejection [406, 407]. B cells have also been shown to present graft-derived antigens to alloreactive T lymphocytes via the indirect pathway of allorecognition [407-409]. Also, as mentioned previously, B cells have a vital role to play in tolerance induced in ACAID. For these reasons, using multi-coloured flow cytometry we analysed both the frequency of $CD45^+CD19^+CD24^+$ positive B cells in the DLNs, spleens and lungs of untreated and TGF-β MSC treated animals and the frequency of $CD5^+$ regulatory B cells (Bregs) in these organs because of the link between corneal allograft acceptance and the role of Bregs in ACAID [56].

The DLNs, spleen and lungs of both untreated and TGF-β MSC treated animals were harvested on the average day of rejection. The organs were prepared as previously described in **section 2.10.5**. B Cells were analysed by gating on $CD45^+CD19^+CD24^+$ positive cells (**Figure 5.8A**). It was observed that TGF-β MSC treated animals had an overall decrease in the frequency of $CD45^+CD19^+CD24^+$ positive B cells in both the DLNs (**Figure 5.8B**) and spleen (**Figure 5.8C**) while frequencies in the lung remained unchanged (**Figure 5.8D**). The expression of CD5 was analysed on these B cells (**Figure 5.9A**) and it was observed that there were increases of this Breg population in both the DLNs and the spleens of TGF-β MSC treated animals while there was no significant change in the lungs (**Figure 5.9B**).

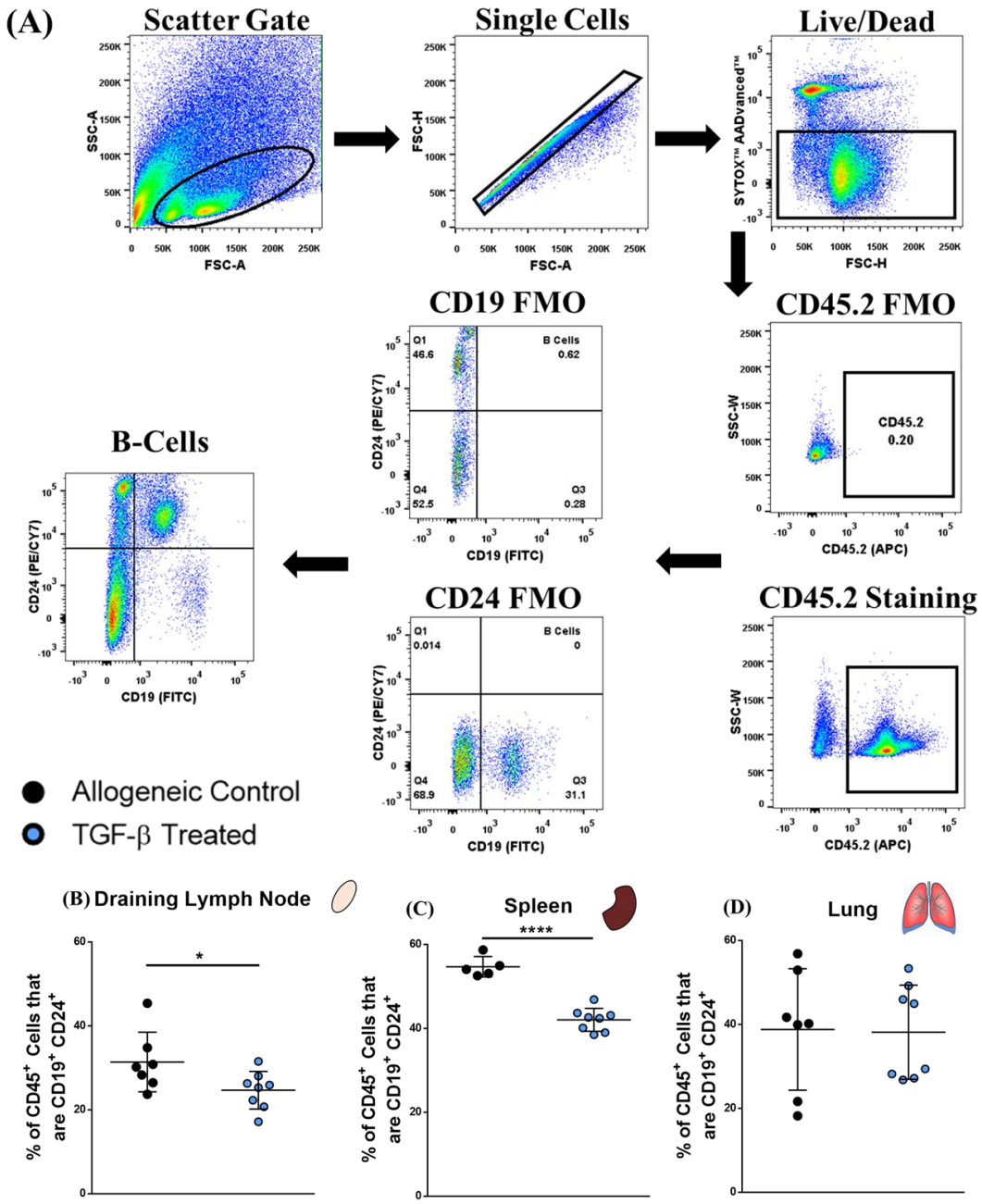

Figure 5.8 Significantly lower percentages of B cells were observed in the DLN and spleens of TGF-β MSC treated animals | (A) Representative B cell gating strategy. Cells were selected according to size and granularity, followed by single cell selection, live cells were selected based on SYTOX negative cells. B cells were selected by CD45 (APC) positivity, followed by CD19 (FITC) + CD24 (PE/CY7) double positivity staining. Frequency of B cells in (B) the DLNs (C) the spleens and (D) the lungs of untreated Vs TGF-β MSC treated animals. Error bars: mean +/- standard deviation *p<0.05, **p<0.01 ***p<0.001 ****p<0.0001. D'Agostino & Pearson omnibus normality test and Shapiro-Wilk normality test used to determine distribution of data. ROUT testing was used to identify outliers. Parametric unpaired two tailed students T tests used for data was normally distributed. Non-parametric unpaired two tailed students T tests used for data that was not normally distributed

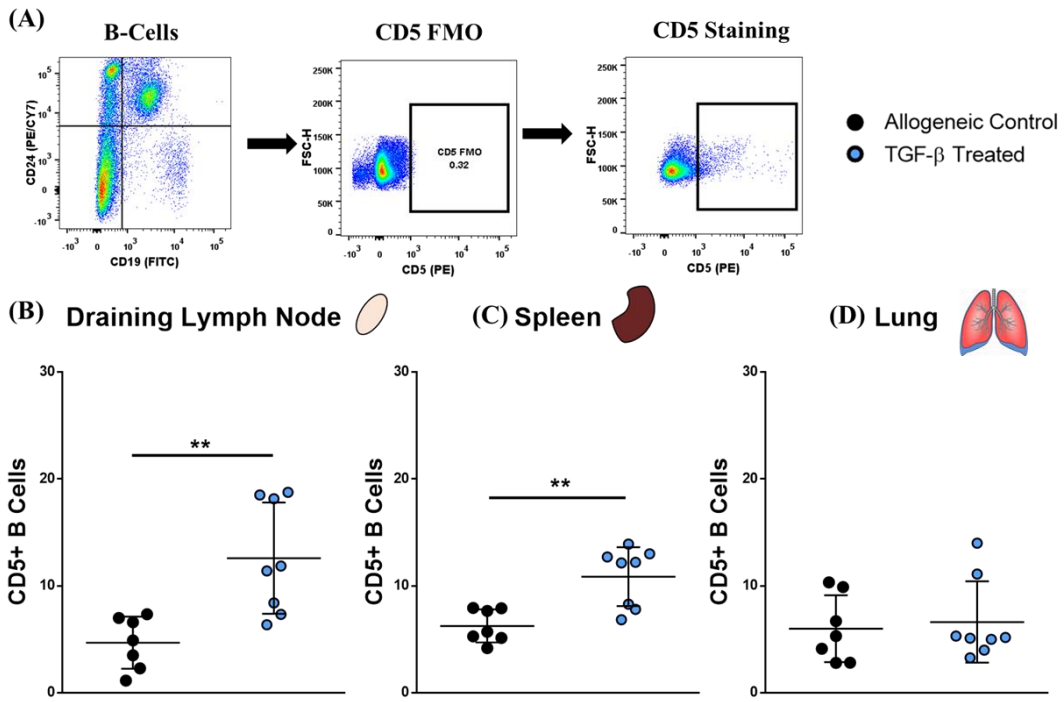

Figure 5.9 Significantly higher frequencies of CD5$^+$ B cells (Bregs) were observed in the DLN and spleens of TGF-β MSC treated animals | (A) Representative Breg cell gating strategy. Cells were selected according to size and granularity, followed by single cell selection, live cells were selected based on SYTOX negative cells. B cells were selected by CD45 (APC) positivity, followed by CD19 (FITC) + CD24 (PE/CY7) double positivity staining. CD5 (PE) was used a as marker for the detection of Bregs. Frequency of Bregs in (B) the DLNs (C) the spleens and (D) the lungs of untreated Vs TGF-β MSC treated animals. Error bars: mean +/- standard deviation *p<0.05, **p<0.01 ***p<0.001 ****p<0.0001. D'Agostino & Pearson omnibus normality test and Shapiro-Wilk normality test used to determine distribution of data. ROUT testing was used to identify outliers. Parametric unpaired two tailed students T tests used for data was normally distributed. Non-parametric unpaired two tailed students T tests used for data that was not normally distributed.

5.3.4. TGF-β MSCs Significantly Increase the Expression of CD25 on CD3$^+$CD4$^+$ Lymphocytes in the Spleens and Lungs of Transplanted Animals

CD25 (IL-2R) is known to regulate both immune tolerance and CD4$^+$/CD8$^+$ lymphocyte immunity [410]. CD25 signalling regulates differentiation of effector cells and aspects of memory recall responses [411]. CD25 signalling also regulates the development, homeostasis and function of Tregs. Thus, CD25 expression was of interest to us in this study. Using a multi-coloured flow cytometry panel (**Figure 5.10**), we analysed the expression of CD25 on the overall CD3$^+$CD4$^+$ (**Figure 5.11 A-C**) and CD3$^+$CD8$^+$ (**Figure 5.11 D-F**) lymphocyte populations in the DLNs, spleens and lungs of untreated and TGF-β MSC treated animals. It was observed that CD25 (BV421) expression was increased on CD3$^+$CD4$^+$ populations in the spleen (**Figure 5.11 B)** and lungs (**Figure 5.11 C)** of TGF-β MSC treated animals while no significant differences

were observed in the DLNs (**Figure 5.11 A)**. CD25 expression on $CD3^+CD8^+$ remained unchanged across all populations (**Figure 5.11 D-F)**.

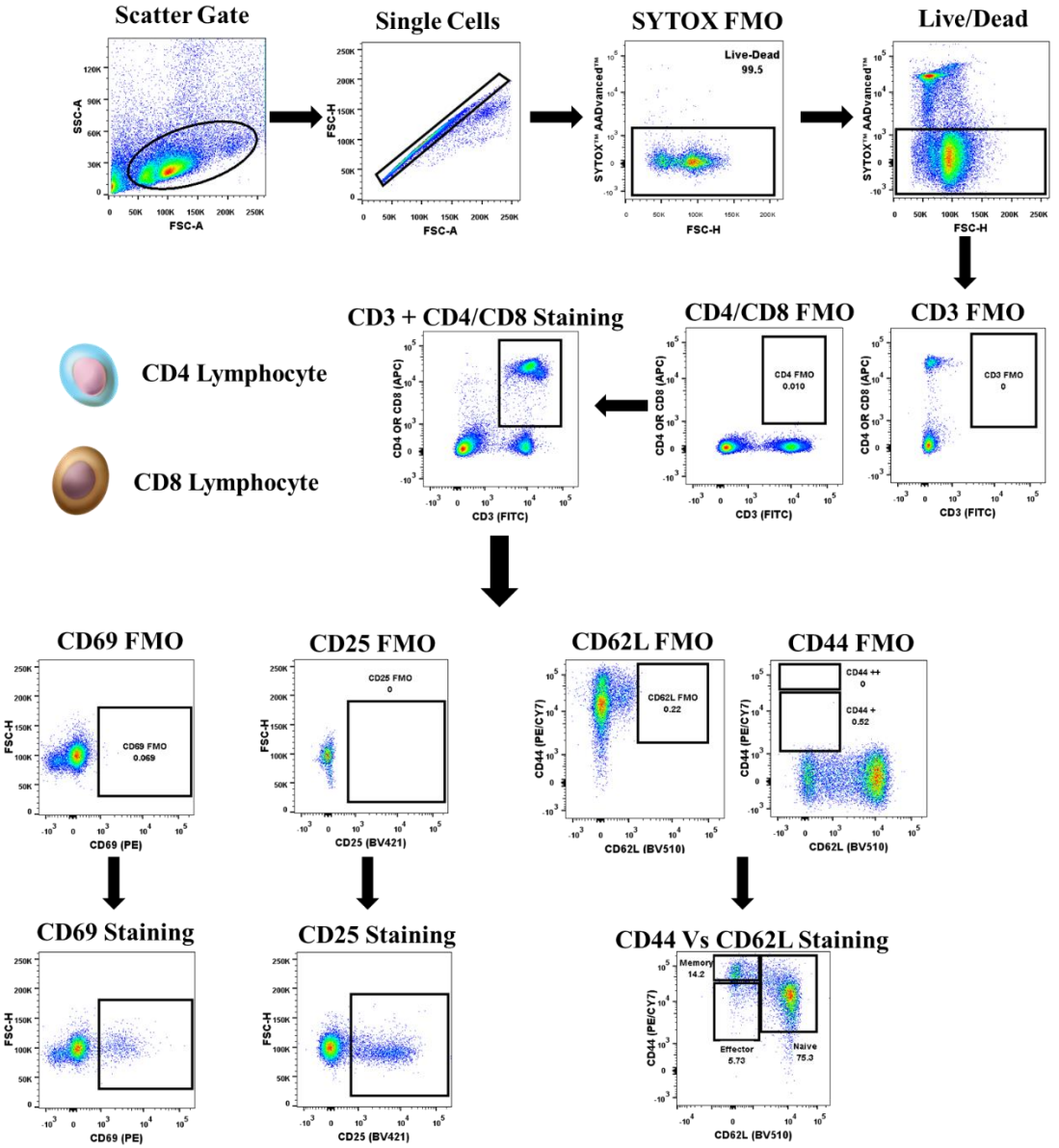

Figure 5.10 Gating strategies used for the comprehensive analysis of $CD4^+$ and $CD8^+$ lymphocyte activation markers on the average day of rejection | Cells were selected according to size and granularity, followed by single cell selection, live cells were selected based on SYTOX negative cells. $CD3^+CD4^+$ and $CD3^+CD8^+$ were selected on double positivity. CD69 and CD25 were used as marker of lymphocyte activation. CD44 Vs CD62L were used to divide populations up into naïve, memory and effector populations.

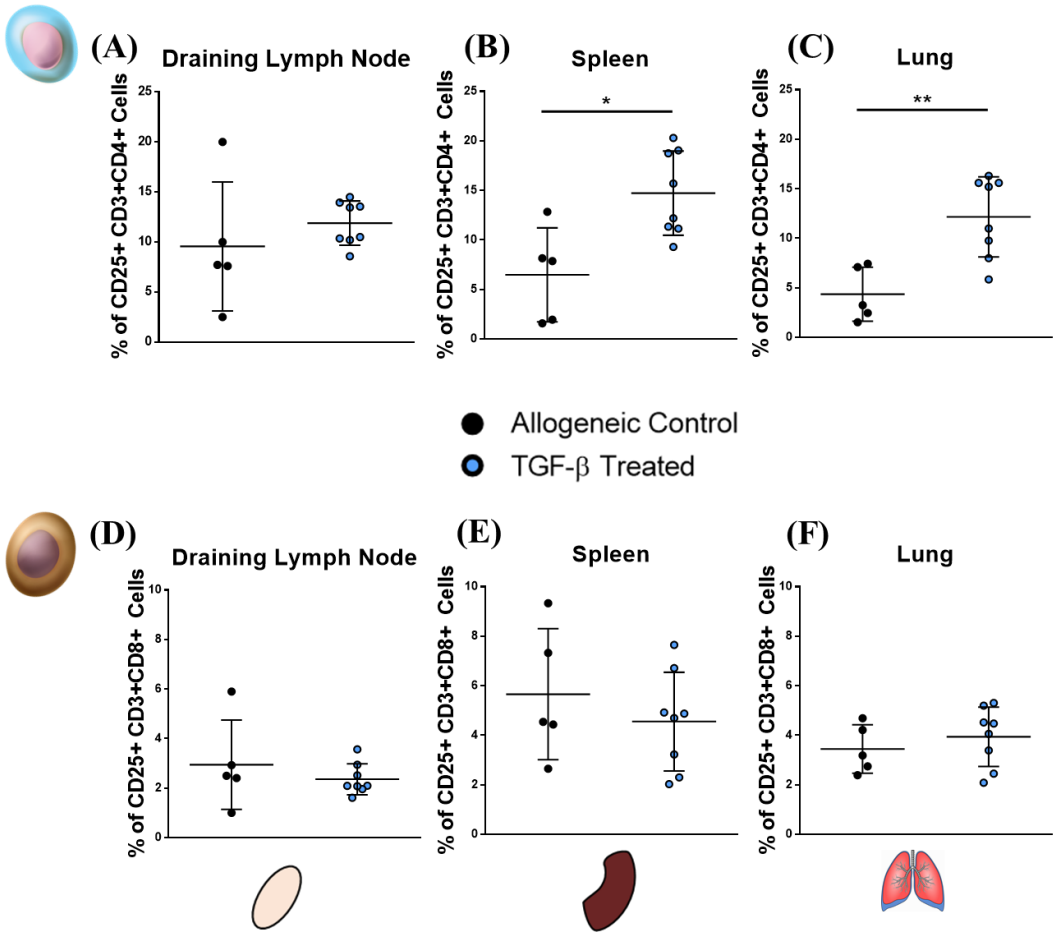

Figure 5.11 Significantly increased CD25 expression was observed on $CD3^+CD4^+$ lymphocytes in the spleens and lungs of TGF-β MSC treated animals | Cells were selected according to size and granularity, followed by single cell selection, live cells were selected based on SYTOX negative cells. T lymphocytes were selected by CD3 (FITC) and CD4/CD8 double positivity (APC) positivity, followed by CD25 (BV421) staining. Percentage expression of CD25 on $CD3^+CD4^+$ in the DLNs (A) the spleen (B) and lungs (C). Percentage expression of CD25 on $CD3^+CD8^+$ in the DLNs (D) the spleen (E) and lungs (F). Error bars: mean +/- standard deviation *p<0.05, **p<0.01 ***p<0.001 ****p<0.0001. D'Agostino & Pearson omnibus normality test and Shapiro-Wilk normality test used to determine distribution of data. ROUT testing was used to identify outliers. Parametric unpaired two tailed students T tests used for data that was normally distributed. Non-parametric unpaired two tailed students T tests used for data that was not normally distributed.

5.3.4. TGF-β MSCs Significantly Modulate the Expression of CD69 on Lymphocytes

CD69 is type II C-lectin receptor that is an early marker of lymphocyte activation. It rapidly appears (30 minutes) on the surface plasma membrane after stimulation [412]. For this reason, it is widely used as an activation marker. The precise role of CD69 has yet to be defined but it has been implicated in cytokine release (IFN-γ, IL-17 and IL-22), homing and migration of activated lymphocytes and the regulation of Tregs

[413-415]. Again, using a multi-coloured flow cytometry panel (**Figure 5.12**), we analysed the expression of CD69 (PE) on the overall $CD3^+CD4^+$ (**Figure 5.12 A-C**) and $CD3^+CD8^+$ (**Figure 5.12 D-F**) lymphocyte populations in the DLNs, spleens and lungs of untreated and TGF-β MSC treated animals.

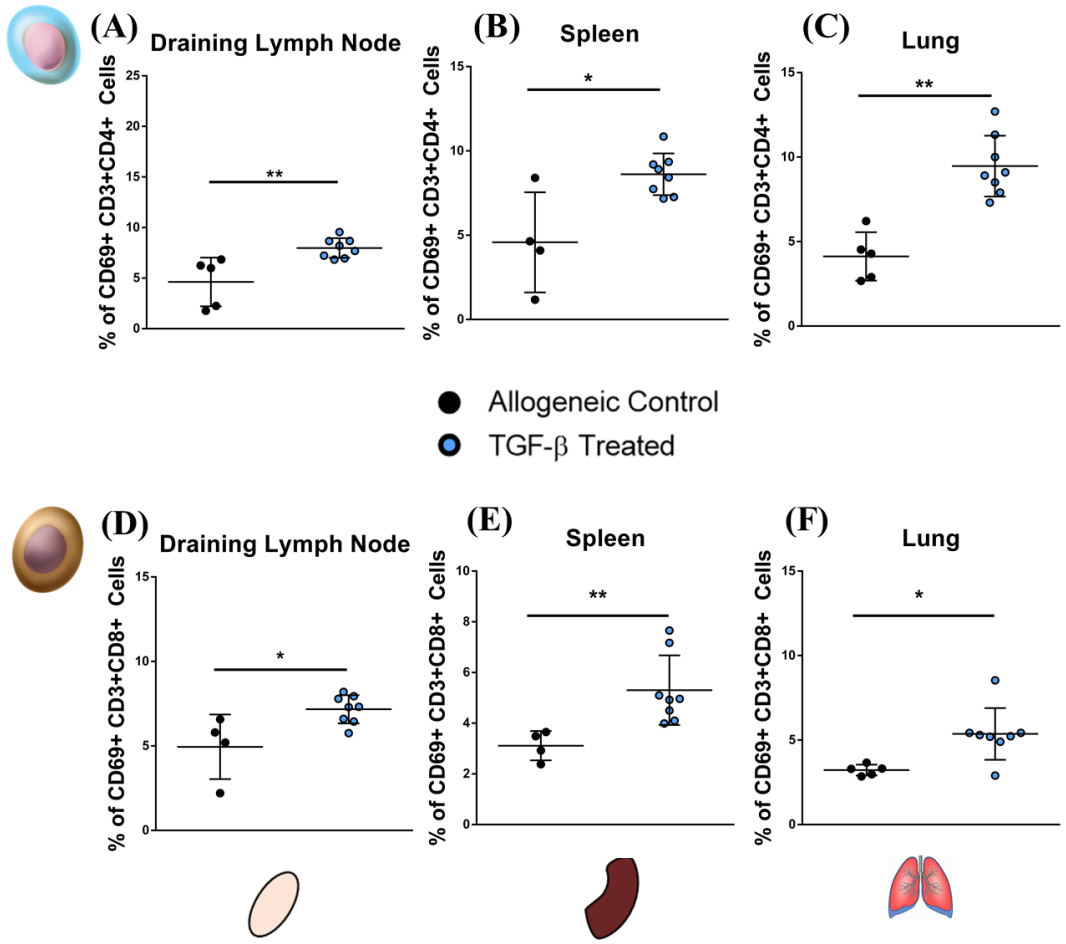

Figure 5.12 Significantly increased CD69 expression was observed on $CD3^+CD4^+$ and $CD3^+CD8^+$ lymphocytes in the organs of TGF-β MSC treated animals | Cells were selected according to size and granularity, followed by single cell selection, live cells were selected based on SYTOX negative cells. T lymphocytes were selected by CD3 (FITC) and CD4/CD8 double positivity (APC) positivity, followed by CD69 (PE) staining. Percentage expression of CD69 on $CD3^+CD4^+$ in the DLNs (A) the spleen (B) and lungs (C). Percentage expression of CD69 on $CD3^+CD8^+$ in the DLNs (D) the spleen (E) and lungs (F). Error bars: mean +/- standard deviation *p<0.05, **p<0.01 ***p<0.001 ****p<0.0001. D'Agostino & Pearson omnibus normality test and Shapiro-Wilk normality test used to determine distribution of data. ROUT testing was used to identify outliers. Parametric unpaired two tailed students T tests used for data that was normally distributed. Non-parametric unpaired two tailed students T tests used for data that was not normally distributed.

TGF-β MSC treated animals demonstrated significantly higher percentages of CD69 expression on both $CD4^+$ and $CD8^+$ lymphocytes in all organs analysed (**Figure 5.12**). CD69 expression on $CD3^+CD4^+$ lymphocytes increased from 4.62% ± 2.4% SD to

7.97% ± 0.96% SD in the DLNs (**Figure 5.12A**), from 4.57% ± 2.96% SD to 8.61% ± 1.23% SD in the spleen (**Figure 5.12B**) and from 4.12% ± 1.43% SD to 9.46% ± 1.8% in the lungs (**Figure 5.12C**). The expression of CD69 on $CD3^+CD8^+$ lymphocytes (**Figure 5.12D-F**) followed a similar trend to $CD3^+CD4^+$ lymphocytes. CD69 expression increased from 4.94% ± 1.9% SD to 7.17% ± 0.83% SD in the DLNs (**Figure 5.10D**), from 3.11% ± 0.57% SD to 5.3% ± 1.37% SD in the spleen (**Figure 5.12E**) and from 3.22% ± 0.3% SD to 5.36% ± 1.53% in the lungs (**Figure 5.12F**).

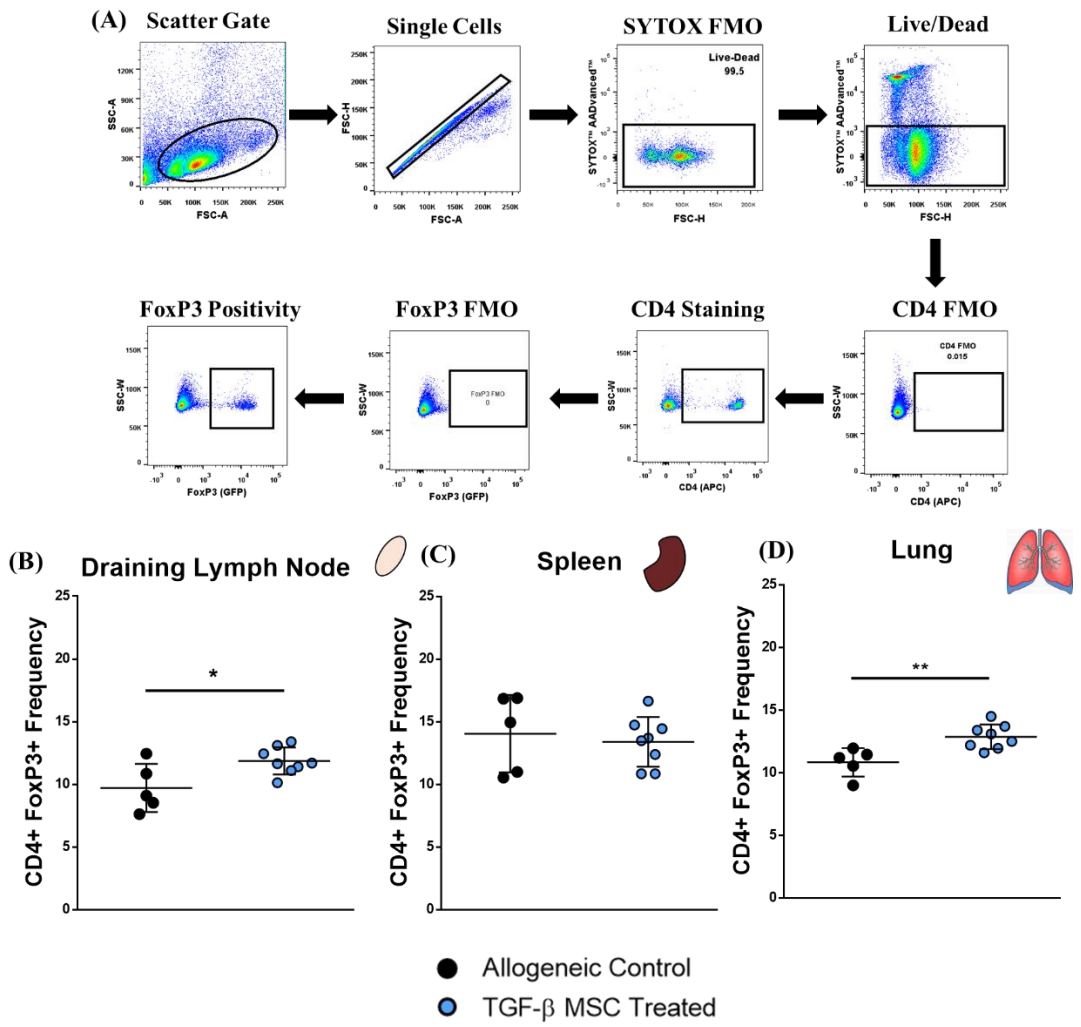

Figure 5.13 The frequency of $CD4^+FoxP3^+$ lymphocytes is significantly increased in the DLNs and lungs of TGF-β MSC treated animals | (A) Cells were selected according to size and granularity, followed by single cell selection, live cells were selected based on SYTOX negative cells. CD4 T lymphocytes were selected by CD4 (PE/CY7) and Tregs were selected via FoxP3 (GFP). Frequency of Tregs in the DLNs (B) the spleen (C) and lungs (D). Error bars: mean +/- standard deviation *p<0.05, **p<0.01 ***p<0.001 ****p<0.0001. D'Agostino & Pearson omnibus normality test and Shapiro-Wilk normality test used to determine distribution of data. ROUT testing was used to identify outliers. Parametric unpaired two tailed students T tests used for data that was normally distributed. Non-parametric unpaired two tailed students T tests used for data that was not normally distributed.

5.3.5. TGF-β MSCs Increase the Frequency of Regulatory Lymphocyte Populations in the Organs of Treated Animals

Due to the observed increase in both frequency and number of Tregs *in vitro* (**Figure 5.3**) we investigated if TGF-β MSC treated animals had an increased frequency of Tregs in their organs. The DLNs, spleen and lungs of both untreated and TGF-β MSC treated animals were harvested on the average day of rejection and prepared for flow cytometry. Again, taking advantage of the FoxP3-GFP transgenic mice we were accurately able to observe Treg frequency in these animals via flow cytometry (**Figure 5.13A**). While Treg frequency in the spleens (**Figure 5.13C**) of TGF-β MSC treated animals was not significantly changed we did observe a significant increase in the both the DLNs (**Figure 5.13B**) and lungs of treated animals where frequencies increased from 9.7% ± 1.9% SD to 11.9% ± 1% SD and 10.83% ± 1.14% SD to 12.9 ± .98% SD respectively (**Figure 5.13D**).

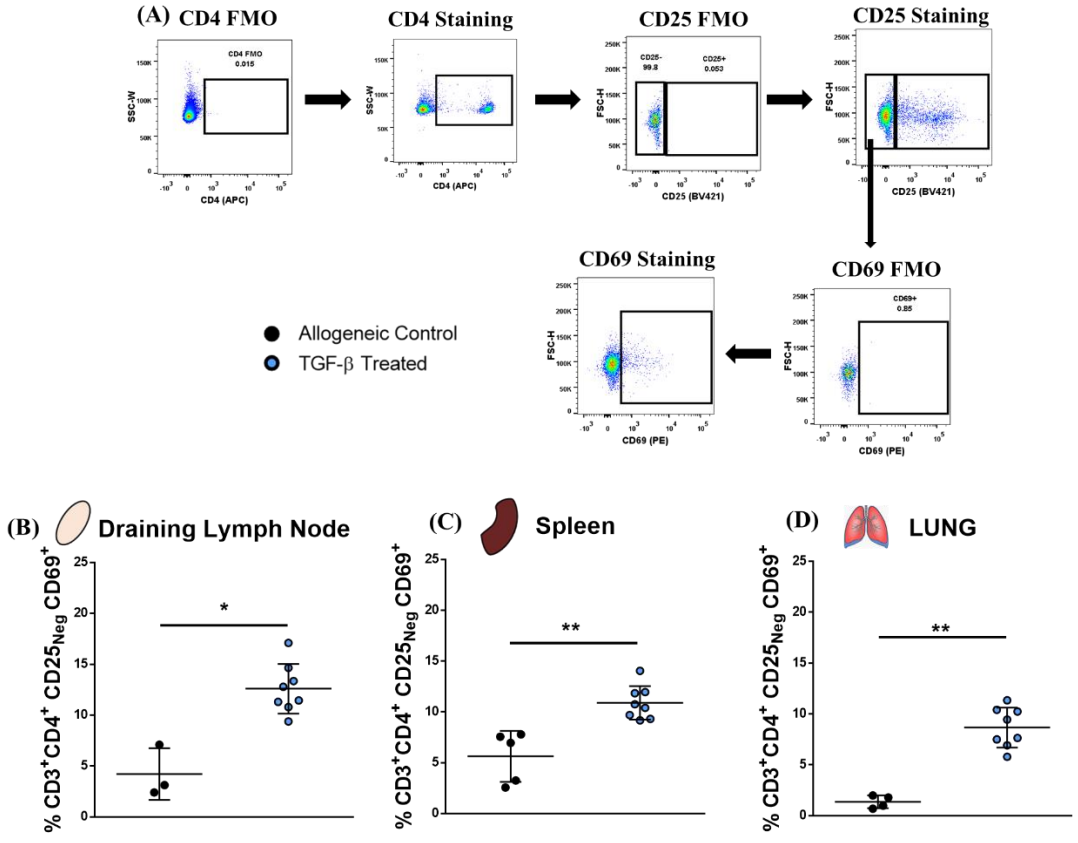

Figure 5.14 Significantly increased CD69 expression was observed on $CD3^{+}CD4^{+}CD25^{Neg}$ lymphocytes in the organs of TGF-β MSC treated animals | (A) Cells were selected according to size and granularity, followed by single cell selection, live cells were selected based on SYTOX negative cells. $CD3^{+}CD4^{+}$ T lymphocytes were selected by CD3 (FITC) followed by CD4 (PE/CY7). CD25 (BV421) negative cells were selected followed by CD69 (PE). Frequency of $CD3^{+}CD4^{+}CD25^{Neg}$ in the DLNs (B) the spleen (C) and

lungs (D). Error bars: mean +/- standard deviation *p<0.05, **p<0.01 ***p<0.001 ****p<0.0001. D'Agostino & Pearson omnibus normality test and Shapiro-Wilk normality test used to determine distribution of data. ROUT testing was used to identify outliers. Parametric unpaired two tailed students T tests used for data that was normally distributed. Non-parametric unpaired two tailed students T tests used for data that was not normally distributed.

5.3.6. TGF-β MSCs Increase the Frequency of $CD3^+CD4^+CD25^{Neg}CD69^+$ Lymphocytes in the Organs of Treated Animals

One of the principal therapeutic responses hoped for upon delivery of an efficacious cellular therapy is the induction or increase in T lymphocyte populations that negatively regulate the immune responses. There have been at least four reported subsets of CD4 lymphocytes that are regulatory, these being, $CD3^+CD4^+FoxP3^+$, Tr1, Tr3 Tregs and $CD3^+CD4^+CD25^{Neg}CD69^+$ lymphocytes [416-419]. Regulatory $CD3^+CD4^+CD25^{Neg}CD69^+$ lymphocytes like $CD3^+CD4^+FoxP3^+$ Tregs have been reported to suppress the tumour mediated immune responses and suppress activated $CD4^+$ lymphocytes in a cell contact dependent manner [417]. Considering the significant increases observed in CD69 expression on the lymphocytes of treated animals (**Figure 5.14**) we analysed the frequency of $CD3^+CD4^+CD25^{Neg}CD69^+$ in the DLNs, spleens and lungs. $CD3^+CD4^+$ T lymphocytes were selected by CD3 followed by CD4 staining. CD25 expression was determined and negative cells were selected followed by CD69 staining (**Figure 5.14A**). We observed significant increases of $CD3^+CD4^+CD25^{Neg}CD69^+$ lymphocytes in all organs. Frequencies increased from 4.21% ± 2.52% SD to 12.6% ± 2.43% SD in the DLNs (**Figure 5.14B**), from 5.62% ± 2.5% to 10.89% ± 1.65% SD in the spleen (**Figure 5.14C**) and from 1.35% ± 0.62% SD to 8.66 ± 1.96% SD in the lungs (**Figure 5.14D**).

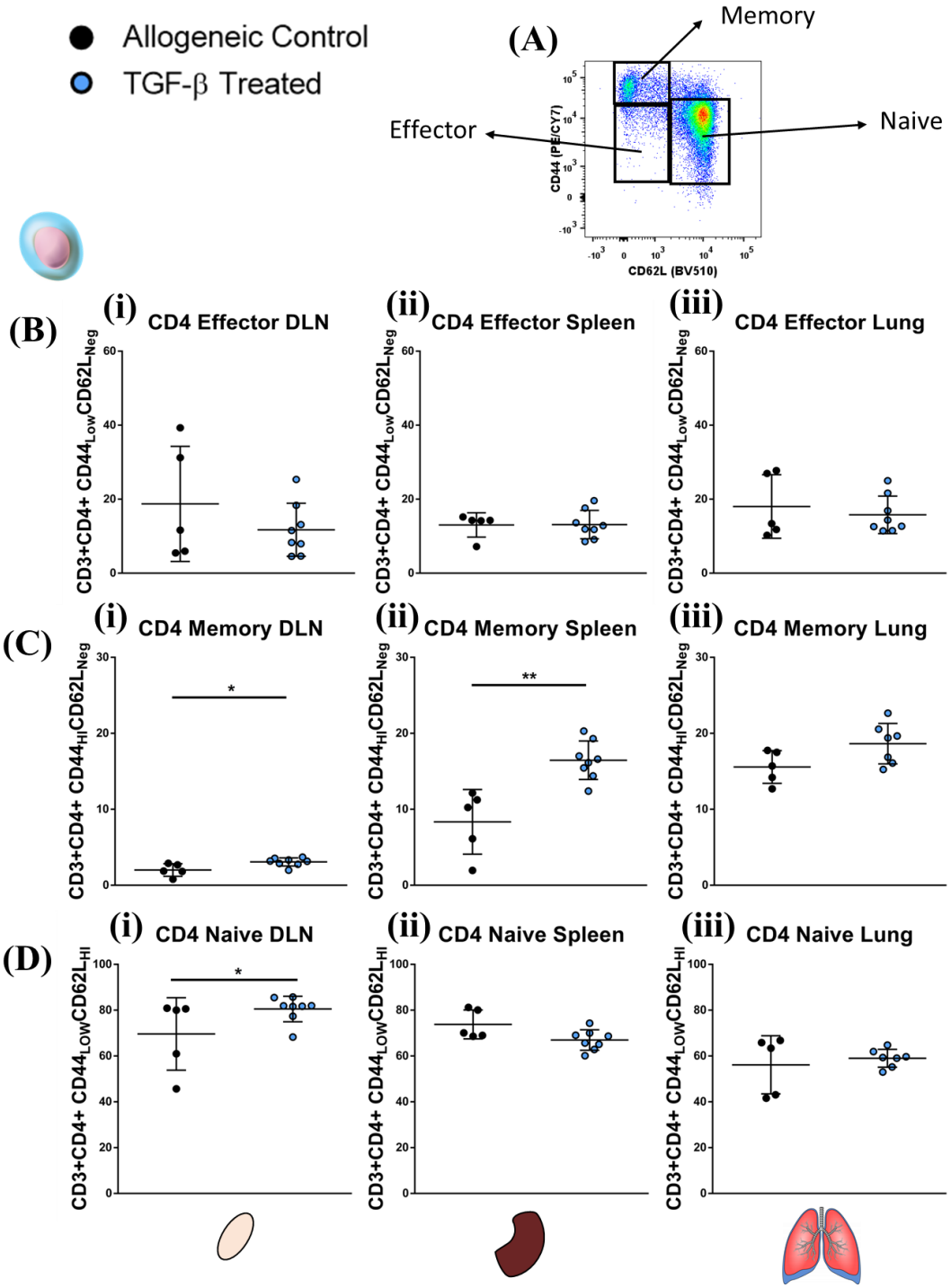

Figure 5.15 $CD3^+CD4^+$ subsets are modulated in the organs of TGF-β MSC treated animals | Cells were selected according to size and granularity, followed by single cell selection, live cells were selected based on SYTOX negative cells. T lymphocytes were selected by CD3 (FITC) and CD4/CD8 double positivity (APC) positivity, followed by CD44 (PE/CY7) and CD62L (BV510) (A). Percentage frequency of effector (B), memory (C) and naïve (D) subsets on $CD3^+CD4^+$ populations in the DLNs (i) the spleen (ii) and lungs (iii). Percentage Error bars: mean +/- standard deviation *p<0.05, **p<0.01 ***p<0.001 ****p<0.0001. D'Agostino & Pearson omnibus normality test and Shapiro-Wilk normality test used to determine distribution of data. ROUT testing was used to identify outliers. Parametric unpaired two tailed students T tests used for data that was normally distributed.

Non-parametric unpaired two tailed students T tests used for data that was not normally distributed.

5.3.7. Effector Memory and Naïve Subsets are Significantly Altered in the Organs of TGF-β MSC Treated Animals

$CD4^+$ and $CD8^+$ T lymphocytes can be rudimentarily broken up into effector, effector memory and naïve subsets based on their expression of CD44 and CD62L (**Figure 5.15A**). It has been reported that effector cells employ a multitude of different mechanisms that aid in the destruction of corneal tissue, including the release of IFN-γ, TNF-α and FasL-mediated apoptosis of corneal endothelial cells [79, 82, 420-422]. There is a subset of lymphocytes that can rapidly respond to antigens that have been previously encountered, these are known as effector memory lymphocytes and are characterised by their lack of CD62L. Memory T lymphocytes are a fundamental aspect of the allograft rejection process and as a result they are a major barrier to the induction of transplant tolerance due to their low activation threshold and their strong effector attributes [423, 424]. To investigate if these subsets of lymphocytes are modulated by TGF-β MSC infusion we analysed the DLNs, spleens and lungs of untreated and TGF-β MSC treated animals by flow cytometry (**Figure 5.15**). While trend decreases of $CD4^+$ effector cells were observed in the DLNs and lungs, the populations remained significantly unchanged in all organs (**Figure 5.15B i-iii**). However, significant increases in effector memory cells were observed in the DLNs (**Figure 5.15C i**) and spleens (**Figure 5.15C ii**) of treated animals with trend increases in the lungs (**Figure 5.15C iii**). A significant increase in naïve $CD4^+$ lymphocytes was observed in the DLNs of TGF-β MSC treated animals (**Figure 5.15D i**) with no significant changes observed in the spleens (**Figure 5.15D ii**) or lungs (**Figure 5.15D iii**). Looking at the $CD8^+$ T lymphocyte subset counterpart, we observed no significant changes in effector $CD8^+$ lymphocytes in any organs (**Figure 5.16A**), however a trend decrease was observed in the DLNs (**Figure 5.16A i**) and lungs (**Figure 5.16A iii**) of treated animals. Similar to $CD4^+$ lymphocytes, effector memory $CD8^+$ lymphocytes were significantly increased in the spleens (**Figure 5.16B ii)** of TGF-β MSC treated animals with no significant changes in the DLNs (**Figure 5.16B i)** or lungs (**Figure 5.16B iii)**. The percentage of naïve populations remained unchanged in the DLNs (**Figure 5.16C i**) and spleens (**Figure 5.16C ii**) and were significantly increased in the lungs (**Figure 5.16C iii**) of treated animals.

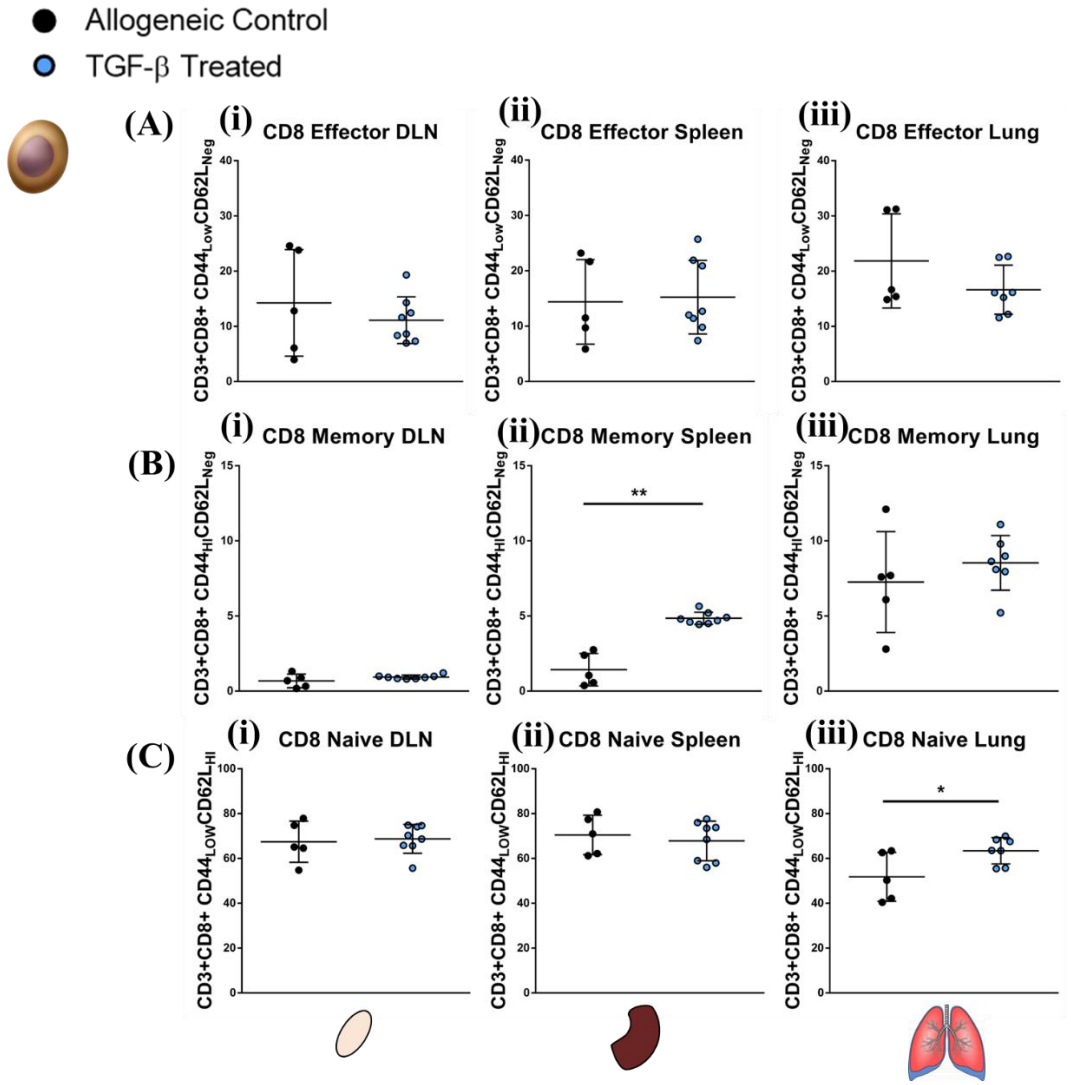

Figure 5.16 $CD3^+CD8^+$ subsets are modulated in the organs of TGF-β MSC treated animals | Cells were selected according to size and granularity, followed by single cell selection, live cells were selected based on SYTOX negative cells. T lymphocytes were selected by CD3 (FITC) and CD4/CD8 double positivity (APC) positivity, followed by CD44 (PE/CY7) and CD62L (BV510). Percentage frequency of effector (A), memory (B) and naïve (C) subsets on $CD3^+CD4^+$ populations in the DLNs (i) the spleen (ii) and lungs (iii). Percentage Error bars: mean +/- standard deviation *p<0.05, **p<0.01 ***p<0.001 ****p<0.0001. D'Agostino & Pearson omnibus normality test and Shapiro-Wilk normality test used to determine distribution of data. ROUT testing was used to identify outliers. Parametric unpaired two tailed students T tests used for data that was normally distributed. Non-parametric unpaired two tailed students T tests used for data that was not normally distributed.

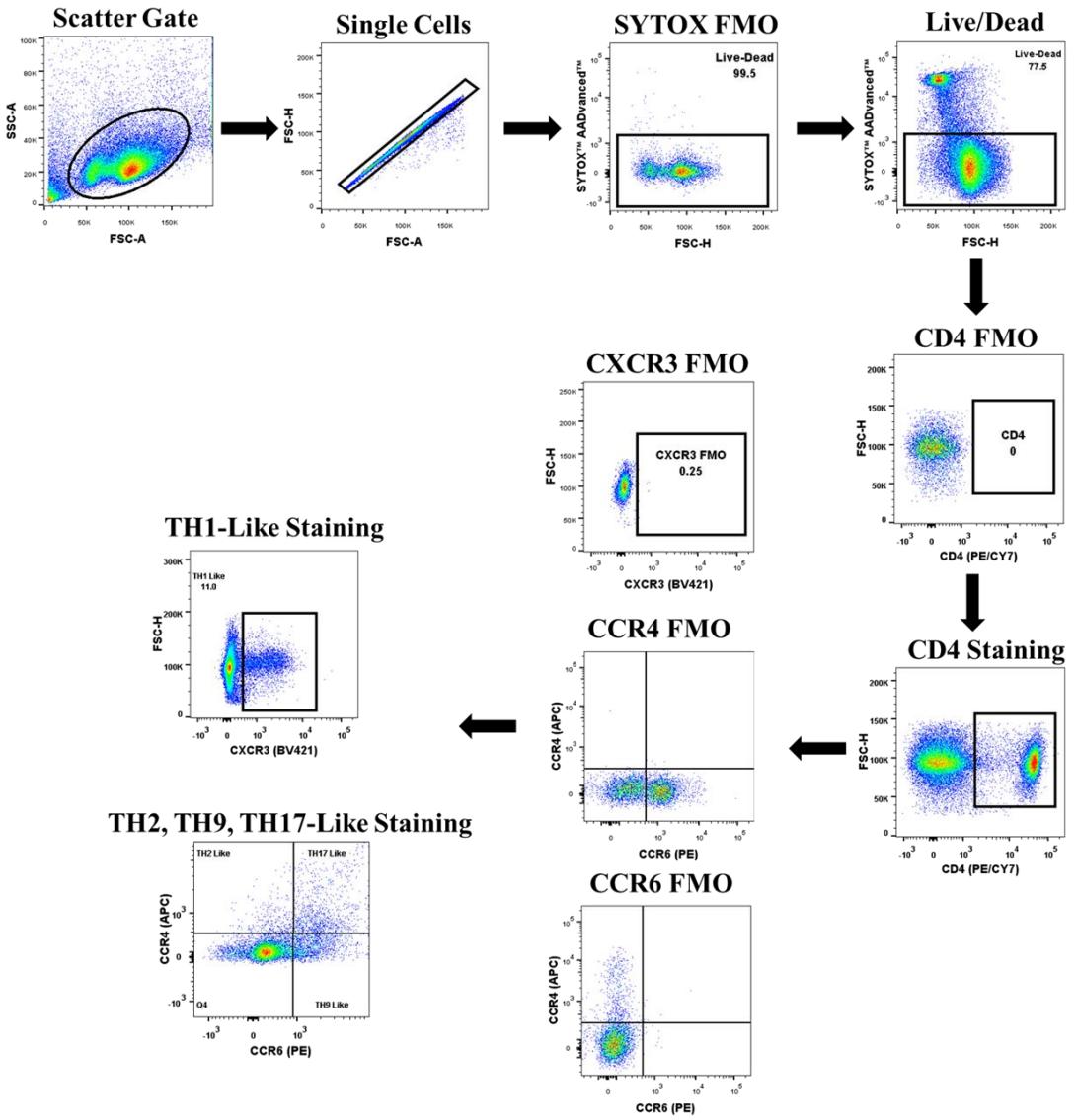

Figure 5.17 Gating strategies used for the analysis of CD4$^+$ TH subset frequencies on the average day of rejection | Cells were selected according to size and granularity, followed by single cell selection, live cells were selected based on SYTOX negative cells. CD4$^+$ lymphocytes were selected by using CD4 (PE/CY7) followed by either CXCR3 (BV421) for TH1-like populations or CCR4 (APC) and CCR6 (PE) for TH2-like, TH17-like and TH9 like lymphocytes.

5.3.8. TGF-β MSC Treated Animals Have Significantly Altered T Helper (Th) Subset Populations in the Spleens and Lungs.

The discovery of T lymphocyte subsets and our knowledge of their biology have increased remarkably in recent years. It is now known that Th1, Th2, Th9, Th17, Th22, follicular T helper (Tfh) and Treg subpopulations all interact with each other, either directly or indirectly, and that they can regulate each other [425]. The importance of these interactions has been highlighted in transplantation [425, 426].

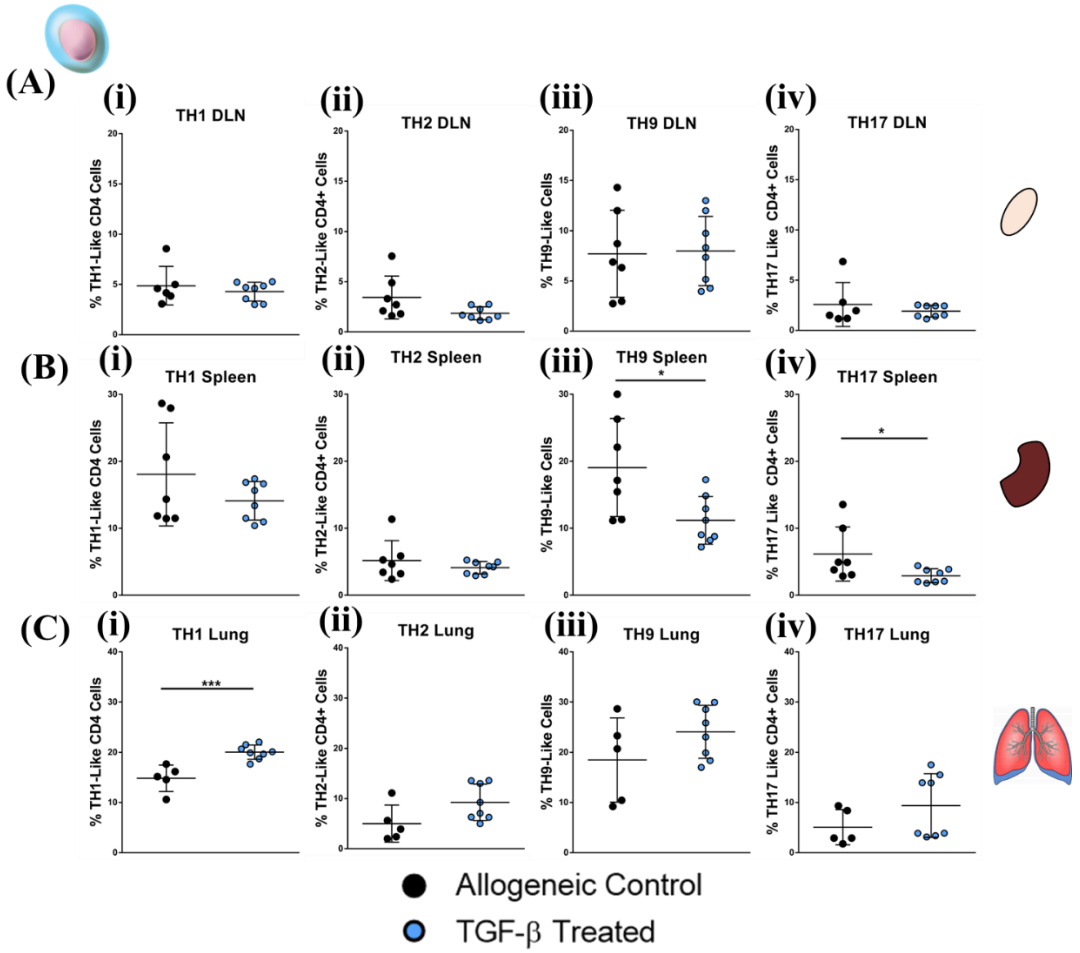

Figure 5.18 Frequencies of TH Subsets are modulated in the spleens and lungs of TGF-β MSC treated animals | Cells were selected as per figure 5.17. Percentage frequency of TH1-like (i), TH2-like (ii), TH9-like (iii) and TH17-like (iv) lymphocytes in the DLNs (A), spleens (B) and lungs (C) of animals on the average day of rejection. Percentage Error bars: mean +/- standard deviation *p<0.05, **p<0.01 ***p<0.001 ****p<0.0001. D'Agostino & Pearson omnibus normality test and Shapiro-Wilk normality test used to determine distribution of data. ROUT testing was used to identify outliers. Parametric unpaired two tailed students T tests used for data that was normally distributed. Non-parametric unpaired two tailed students T tests used for data that was not normally distributed.

During the corneal allograft rejection process, APCs present allo-antigen to naïve T lymphocytes. This primes naïve T lymphocytes to effector Th1 cells, which have been shown to be the main mediators of the corneal rejection process [26, 427-429] and as such were of interest to this study. Using CXCR3 as marker of Th1-like cells, we analysed frequencies of this population in the organs of treated animals and compared them to untreated animals that had rejected their grafts (**Figure 5.18**). While a trend decrease of Th1-like cells were observed in the spleens of treated animals, there were

no significant differences noted in the DLNs (**Figure 5.18 A(i)**) or spleens (**Figure 5.18 B(i)**) of said animals. Interestingly, we observed that Th1-like cells were increased significantly in the lungs of treated animals compared to untreated animals (**Figure 5.18 C(i)**). Yamada et al observed that if the allo-immune response was shifted to a Th2 phenotype it enhanced the survival of corneal allografts in a high-risk model of murine corneal transplantation [105]. Due to this study it was thought that a Th2 phenotype would be desirable, however, more recent studies [106, 107] have found that if graft recipients previously suffered with allergic conjunctivitis, a disease that leads to an elevated Th2 phenotype, they rejected their grafts at accelerated rates. While it is thought that Th1 lymphocytes are the primary effector cells responsible for destruction of the graft, Th2 cells have a role to play in the process. We analysed the frequency of Th2-like cells by looking at $CCR6_{neg}CCR4$ positive $CD4^+$ lymphocytes in the organs of transplanted animals with and without TGF-β MSC treatment. No significant changes were observed in DLNs, spleens or lungs of MSC TGF-β animals compared to untreated animals (**Figure 5.18 A-C(ii)**). Th9 lymphocytes are a subset of T lymphocytes that secrete the pleiotropic cytokine Interleukin 9 (IL-9). While a recently observed population, they have been found to play a role in allergic inflammation, autoimmune diseases, and tumour immunity [430]. Little or no information exists as to if they play a role in the corneal rejection process. We investigated if TH9-like populations were modulated in treated animals compared to non-treated animals. We analysed the frequency of $CCR4_{neg}CCR6$ positive $CD4^+$ lymphocytes (**Figure 5.17**) in the organs of untreated and treated animals. A significant decrease in Th9-like cells were observed in the spleens of treated animals compared to non-treated animals (**Figure 5.18 B(iii)**). Finally, due to the reported involvement of Th17 cells in chronic ocular inflammatory diseases [431] and how their involvement in lung allograft rejection [432] we analysed the frequency of these cells in the organs of untreated and treated animals. $CD4^+$ $CCR4^+CCR6^+$ was used to analyse Th17-like populations (**Figure 5.17**). We observed no significant changes in Th17-like populations in the DLNs (**Figure 5.18 A(iv)**) or lungs (**Figure 5.18 C(iv)**) of treated animals compared to untreated animals with a significant decrease in the spleens of treated animals (**Figure 5.18 B(iv)**).

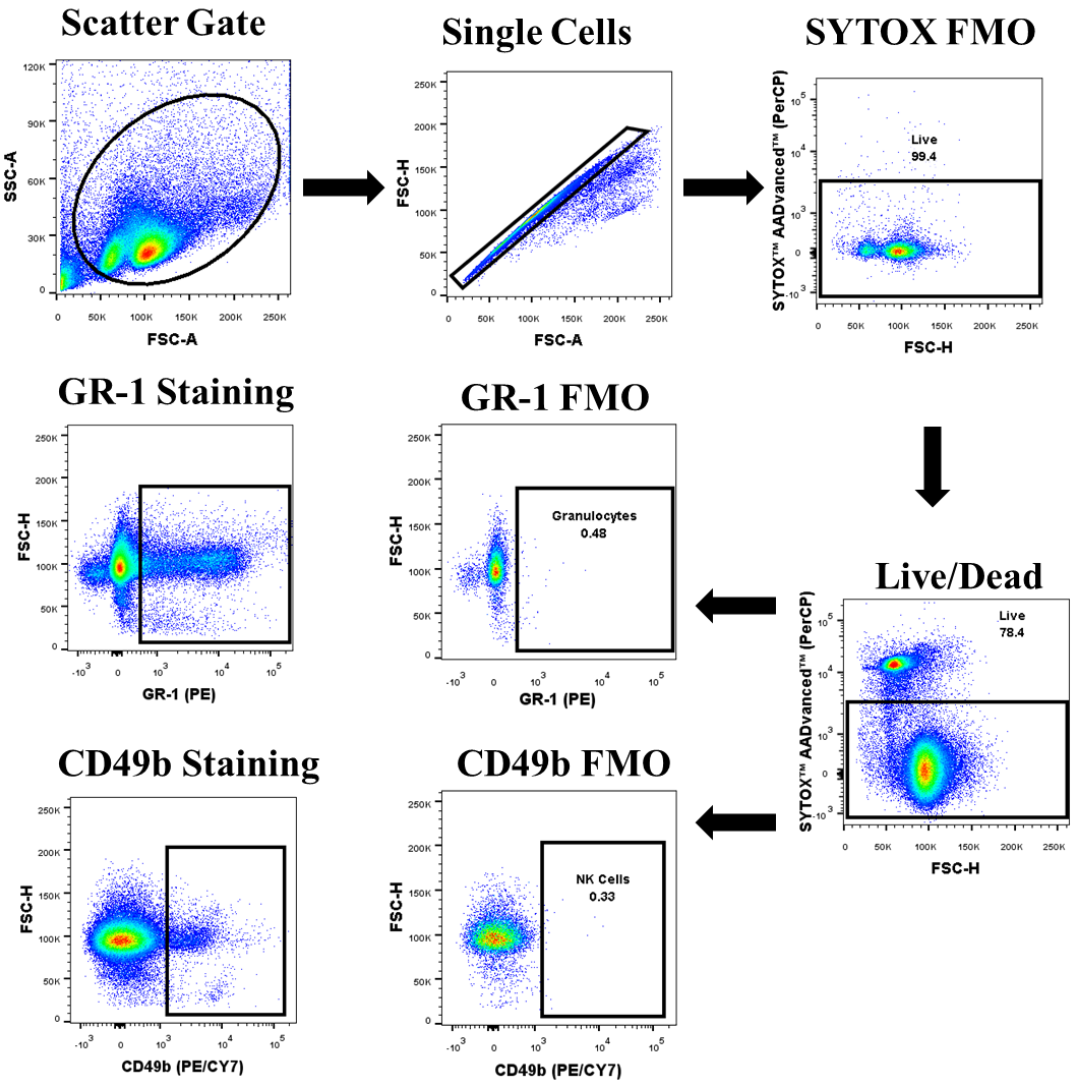

Figure 5.19 Gating strategies used for the analysis of granulocytes and NK Cells frequencies on the average day of rejection | Cells were selected according to size and granularity, followed by single cell selection, live cells were selected based on SYTOX negative cells. Neutrophils were selected by using GR-1 (PE) and NK cells were selected by using CD49b (PE/CY7).

5.3.9. Natural Killer (NK) Cells and Neutrophils Are Not Significantly Changed in The Organs of TGF-β MSC Treated Animals Compared to Untreated Animals.

While $CD4^+$ effector lymphocytes are the main mediators of corneal allograft rejection, there has been reports that both NK cells [433, 434] and neutrophils [216] have their roles to play in the complex process. We analysed the frequency of GR-1

(neutrophils, granulocytes) positive cells and CD49b (NK cells) positive cells in the organs of untreated and treated animals on the average day of rejection (**Figure 5.19**). While trend increases, and decrease were observed in both CD49b (**Figure 5.20 A(i-iii)**) positive populations and GR-1 positive populations (**Figure 5.20 B(i-iii)**), no significant changes were observed in the DLNs, spleens or lungs.

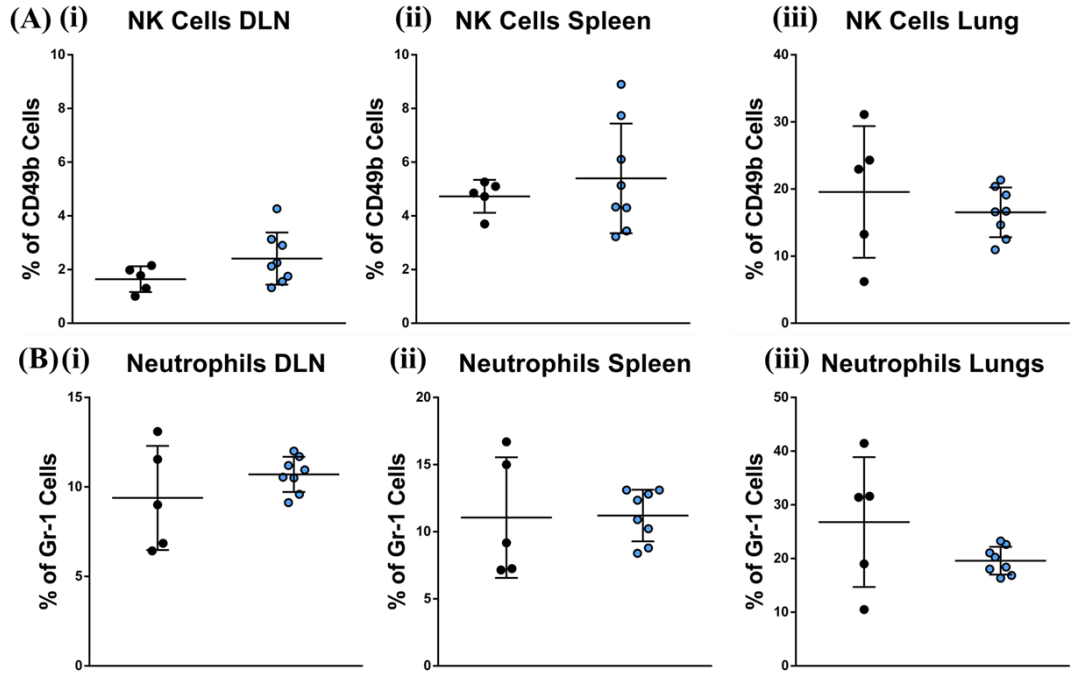

Figure 5.20 No significant changes in NK cells or Neutrophils were observed in the organs of treated animals compared to untreated animals | Cells were selected as per figure 5.19. Percentage frequency of CD49b cells (A) and GR-1 (B) in the DLNs (i), spleens (ii) and lungs (iii) of animals on the average day of rejection. Percentage Error bars: mean +/- standard deviation *p<0.05, **p<0.01 ***p<0.001 ****p<0.0001. D'Agostino & Pearson omnibus normality test and Shapiro-Wilk normality test used to determine distribution of data. ROUT testing was used to identify outliers. Parametric unpaired two tailed students T tests used for data that was normally distributed. Non-parametric unpaired two tailed students T tests used for data that was not normally distributed.

5.3.10. Macrophage and Dendritic Cell Frequencies Are Significantly Reduced in The Organs of TGF-β MSC Treated Animals with Significantly Lower CD80 and CD86 Expression Observed

There are three essential prerequisites in the initiation of graft rejection, these are the presence of the non-self-antigens, the presence of antigen presenting cells (APCs) and host lymphocytes [435]. The indirect pathway of antigen presentation is proposed to be the most important in corneal allograft rejection, this occurs when recipient APCs process and present antigens to lymphocytes. This is speculated to happen at many

different sites, the DLN being considered as a very important one in corneal rejection [85, 93, 435].

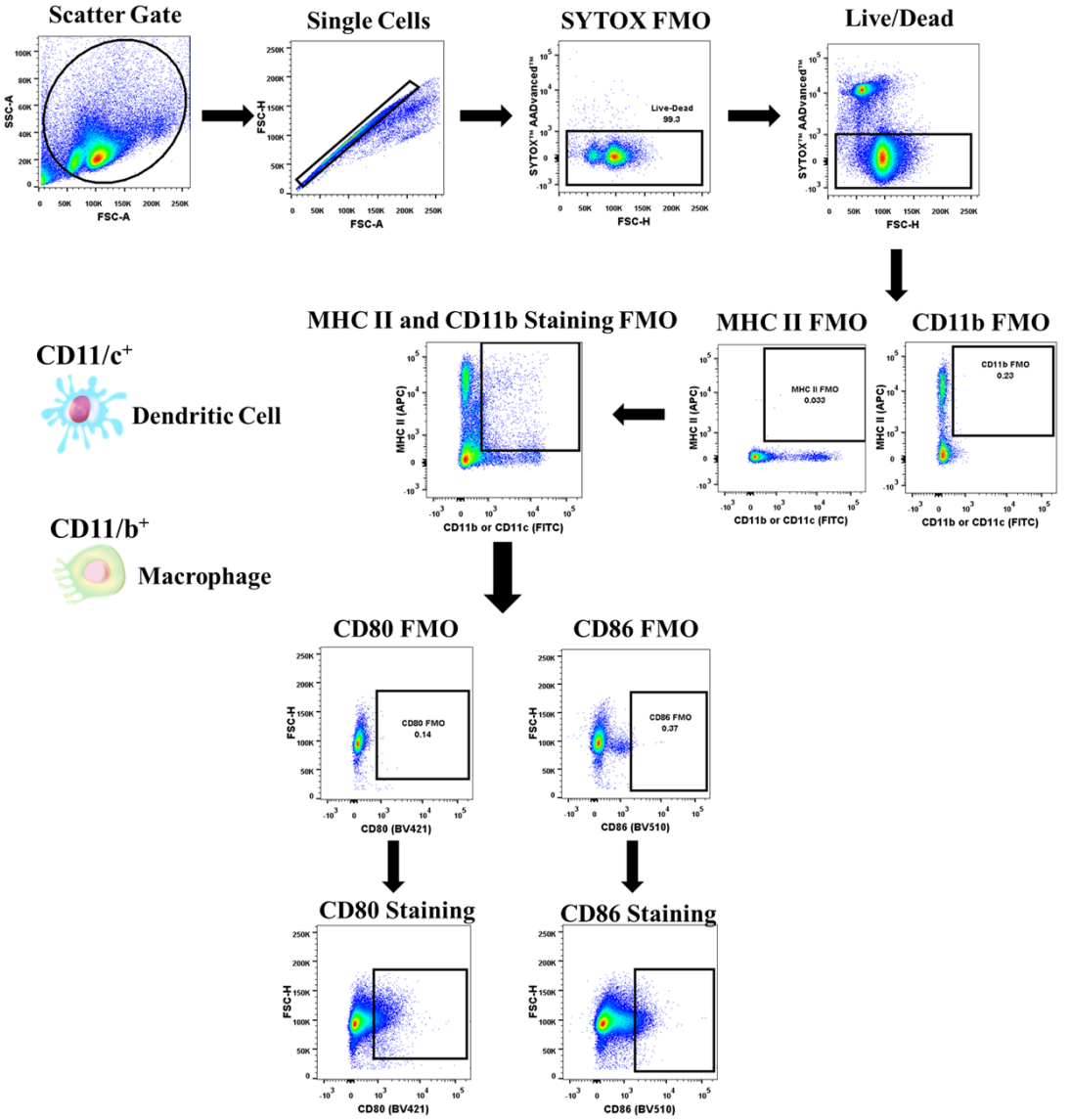

Figure 5.21 Gating strategies used for the analysis of macrophages and dendritic cells on the average day of rejection | Cells were selected according to size and granularity, followed by single cell selection, live cells were selected based on SYTOX negative cells. Macrophages were selected by using CD11b (FITC) and MHC II (APC) double positivity. Dendritic cells were selected by using CD11c (FITC) and MHC II (APC) double positivity. CD80 (BV421) and CD86 (BV510) were used to analyse the expression of co-stimulatory molecules.

For this reason, we analysed the frequency of both macrophages and DCs in the DLN, spleens and lungs of both untreated and TGF-β MSC treated animals. We also analysed the expression of the co-stimulatory molecules CD80 and CD86.

$CD11b^{+}MHCII^{+}$ double positivity was used to analyse macrophages (**Figure 5.21**) and $CD11c^{+}MHCII^{+}$ double positivity was used to analyse dendritic cells (**Figure 5.21**). We observed a significant reduction in the frequency of macrophages in the DLN with decreases from 7.14% ± 4% SD to 3.14% ±0.62% SD (**Figure 5.22 A(i)**). Significant reductions were also observed in the spleens of treated animals, decreasing from 5.67% ± 2.1% SD to 2.47% ±0.4 SD (**Figure 5.22 B(i)**) Similar to the DLNs and spleens of TGF-β MSC treated animals, the frequency of macrophages in the lungs were significantly reduced from 19.16% ± 2.8% SD to 11.10% ± 6.3% SD (**Figure 5.22 C(i)**). The percentage expression of CD80 (**Figure 5.22 A(ii)**) and CD86 (**Figure 5.22 A(iii)**) on the macrophage populations in the DLN were significantly reduced in TGF-β MSC treated animals compared to untreated animals, being reduced from 27% ± 4.6% SD to 12.8% ± 3.5% SD and 29.19% ± 11.1% SD to 12.92% ± 4.7% SD respectively. CD86 expression on macrophage populations in both the spleens (**Figure 5.22 B(iii)**) and lungs (**Figure 5.22 C(iii)**) of TGF-β were also significantly decreased, reducing from 30% ± 5.19% SD to 6.8% ± 5.19% SD and 18.2% ± 7.6% SD to 3.14 ± 0.96% SD respectively.

Very similarly, a significant decrease in the $CD11c^{+}MHCII^{+}$ populations were also observed in the organs of TGF-β MSC treated animals. DCs were significantly decreased in the DLNs (**Figure 5.23 A(i)**), spleens (**Figure 5.23 B(i)**), and lungs (**Figure 5.23 C(i)**) of TGF-β MSC treated animals when compared to allogeneic controls. When analysing the expression of co-stimulatory molecules on DC populations in the three organs it was observed that CD80 (**Figure 5.23 A-C (ii)**) and CD86 (**Figure 5.23 A-C (iii)**) was significantly decreased in TGF-β MSC treated animals also. These results taken together indicate that antigen presenting cell populations are being significantly modulated in the animals where TGF-β MSCs have been administered. The licensed MSCs seem to not only affect the frequency but also the activation status of these cells in all three organs, showing the potent immunomodulatory capacity of TGF-β MSCs.

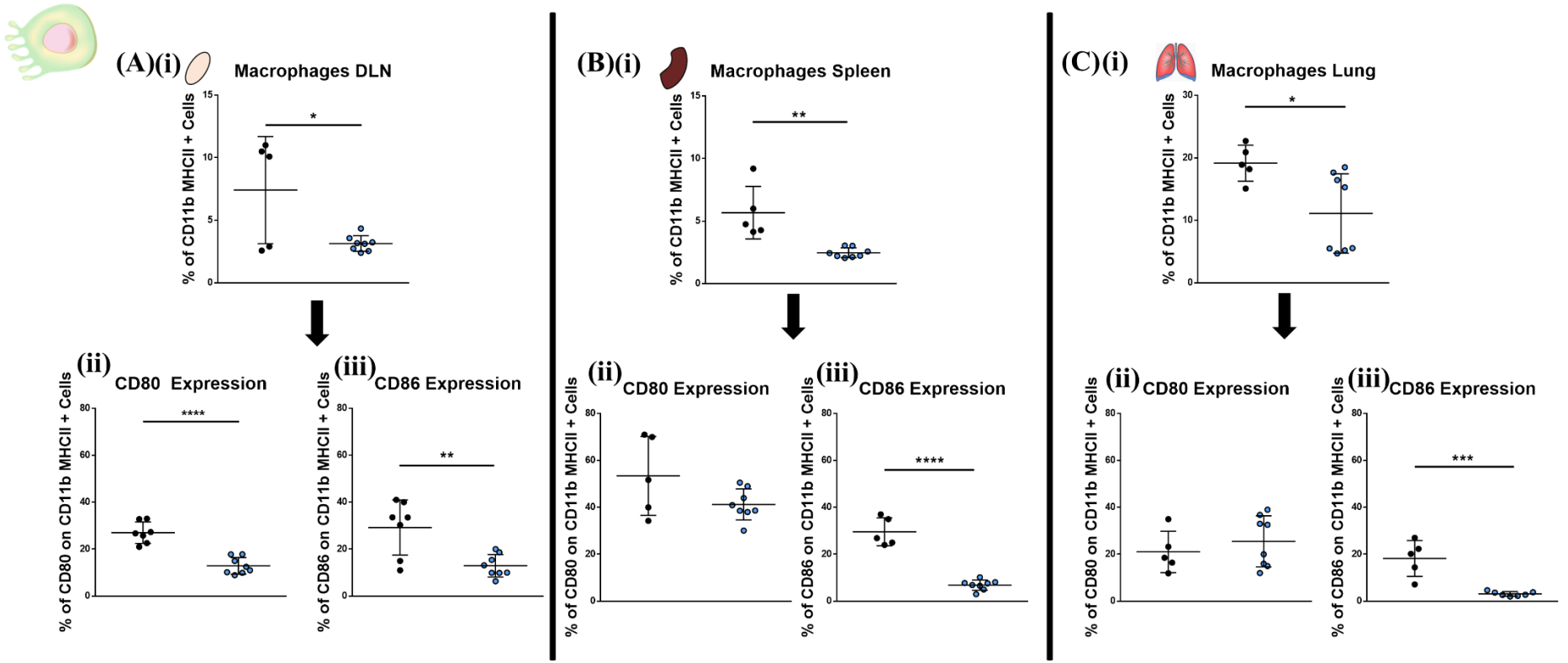

Figure 5.22 Both the frequency of macrophage populations and expression of co-stimulation molecules are significantly reduced in organs of TGF-β MSC treated animals | Cells were selected as per **Figure 5.21**. Percentage frequency of $CD11b^{+}MHCII^{+}$ in the DLNs (**A(i)**), spleens (**B(i)**) and lungs (**C(i)**) of animals on the average day of rejection. CD80 (**A-C (ii)**) and CD86 (**A-C (iii)**) expression on $CD11b^{+}MHCII^{+}$ on average day of rejection. Percentage Error bars: mean +/- standard deviation *p<0.05, **p<0.01 ***p<0.001 ****p<0.0001. D'Agostino & Pearson omnibus normality test and Shapiro-Wilk normality test used to determine distribution of data. ROUT testing was used to identify outliers. Parametric unpaired two tailed students T tests used for data that was normally distributed. Non-parametric unpaired two tailed students T tests used for data that was not normally distributed.

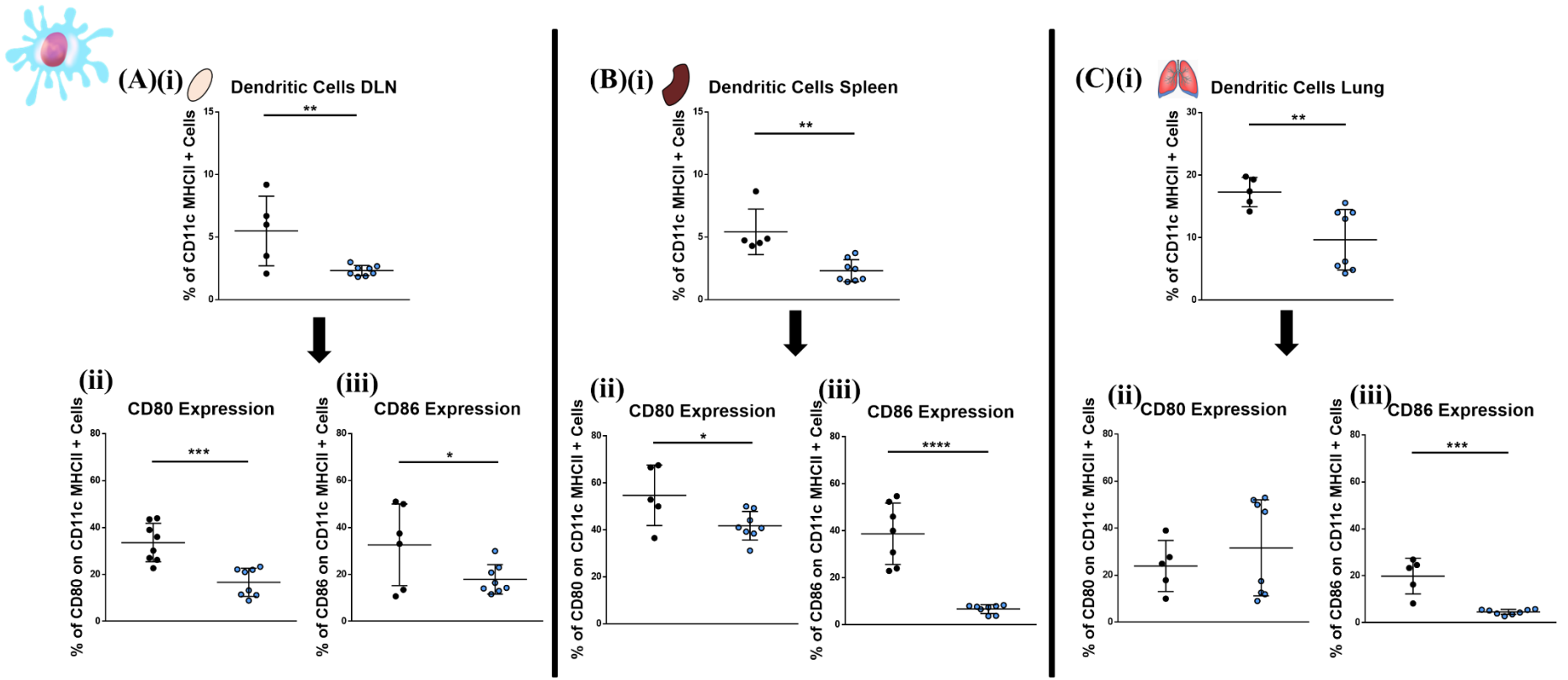

Figure 5.23 Significantly reduced dendritic populations with significantly decreased expression of co-stimulation molecules are observed in organs of TGF-β MSC treated animals | Cells were selected as per **Figure 5.21**. Percentage frequency of $CD11c^{+}MHCII^{+}$ in the DLNs (**A(i)**), spleens (**B(i)**) and lungs (**C(i)**) of animals on the average day of rejection. CD80 (**A-C (ii)**) and CD86 (**A-C (iii)**) expression on $CD11c^{+}MHCII^{+}$ on average day of rejection. Percentage Error bars: mean +/- standard deviation *p<0.05, **p<0.01 ***p<0.001 ****p<0.0001. D'Agostino & Pearson omnibus normality test and Shapiro-Wilk normality test used to determine distribution of data. ROUT testing was used to identify outliers. Parametric unpaired two tailed students T tests used for data that was normally distributed. Non-parametric unpaired two tailed students T tests used for data that was not normally distributed

5.3.11. Summary of Immune Cell Distribution Study

Organ	Increased	Decreased
DLNs 	**$CD5^+$ B cells** **$CD4^+CD69^+$ T cells** **$CD8^+CD69^+$ T cells** **$CD3^+CD4^+CD25_{Neg}CD69^+$** **Naïve CD4s** **Memory CD4s** **$CD4^+FoxP3^+$ T cells**	**B cells** **Macrophages** **Macrophage CD80** **Macrophage CD86** **Dendritic Cells** **Dendritic Cell CD80** **Dendritic Cell CD86**
Spleen 	**$CD5^+$ B cells** **$CD4^+CD25^+$ T cells** **$CD4^+CD69^+$ T cells** **$CD8^+CD69^+$ T cells** **$CD3^+CD4^+CD25_{Neg}CD69^+$** **Memory CD8s**	**B cells** **TH9-Like** **TH17-Like** **Macrophages** **Macrophage CD86** **Dendritic Cells** **Dendritic Cell CD80** **Dendritic Cell CD86**
Lungs 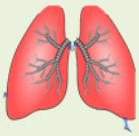	**$CD4^+CD25^+$ T cells** **$CD4^+CD69^+$ T cells** **$CD4^+FoxP3^+$ T cells** **$CD4^+CD69^+$ T cells** **$CD3^+CD4^+CD25_{Neg}CD69^+$** **Naïve CD8s** **TH1-Like**	**Macrophages** **Macrophage CD86** **Dendritic Cells** **Dendritic Cell CD86**

Table 5.1. A summary of signifcant results observed in immune cell distribution study.

5.3.12. *In Vitro* Investigation into the Molecular Mechanisms of TGF-β MSCs

Thus far we have shown that TGF-β MSCs prolong corneal allograft survival significantly, we have also shown that i.v. infusion of $1x10^6$ TGF-β MSCs on day +1 and on +7 POD induces profound changes in the immune cell repertoire and surface expression markers present in the DLNs, spleens and lungs compared to animals that have received no cells. In this section we identify potential factors that we hypothesize are influencing the immune cells which result in prolongation of graft survival.

TGF-β1 plays a very important role under normal physiological conditions but also during disease processes. TGF-β1 can regulate cell growth, differentiation, migration, apoptosis, and extracellular matrix production [436-438]. Typically, TGF-β1 signalling is initiated with oligomerization of serine/threonine receptor kinases and phosphorylation of the signalling molecules Smad2 and Smad3 in the cytoplasm [439], this being the case, there are multiple non-Smad dependent signalling pathways [438]. These non-Smad pathways include multiple arms of the MAP kinase pathways, Rho-like GTPase signalling pathways, and phosphatidylinositol-3-kinase/AKT pathways [438]. To investigate if TGF-β licensing was activating the MSCs via the canonical Smad2/3 signalling pathway or if it was Smad2/3 independent, we used the Smad2 inhibitor SB431542. MSCs were treated with SB431542 (10μM final concentration) 4 hours before treatment with TGF-β (50ng/ml). As previously described, MSCs were incubated for 72 hours in the presence of TGF-β before use in experiments. Light microscopy at 4x magnification was used to examine cell morphology 48 hours after the addition of either TGF-β or Smad2 inhibitor + TGF-β (**Figure 5.24 A**). Observing the images, the expected "swirled" morphology can be seen in the TGF-β MSC flask but is absent in the Smad2 inhibitor TGF-β MSC flask indicating that Smad2/3 signalling was responsible for said morphological changes. To investigate if the TGF-β MSC mediated T-lymphocyte suppression was a result of Smad2/3 signalling, Smad2 inhibited TGF-β MSCs were placed in T lymphocyte co-cultures at a 1 MSC to 10 lymphocyte ratio with CD3/CD28 stimulated lymphocytes and incubated for 96 hours (**Figure 5.24 B**). Following the culturing period, proliferation of $CD4^+$ and $CD8^+$ lymphocytes were analysed by flow cytometry using CTV to track proliferation. Both total proliferation and proliferation >3 generations of lymphocytes were analysed (**Figure 5.24 C**).

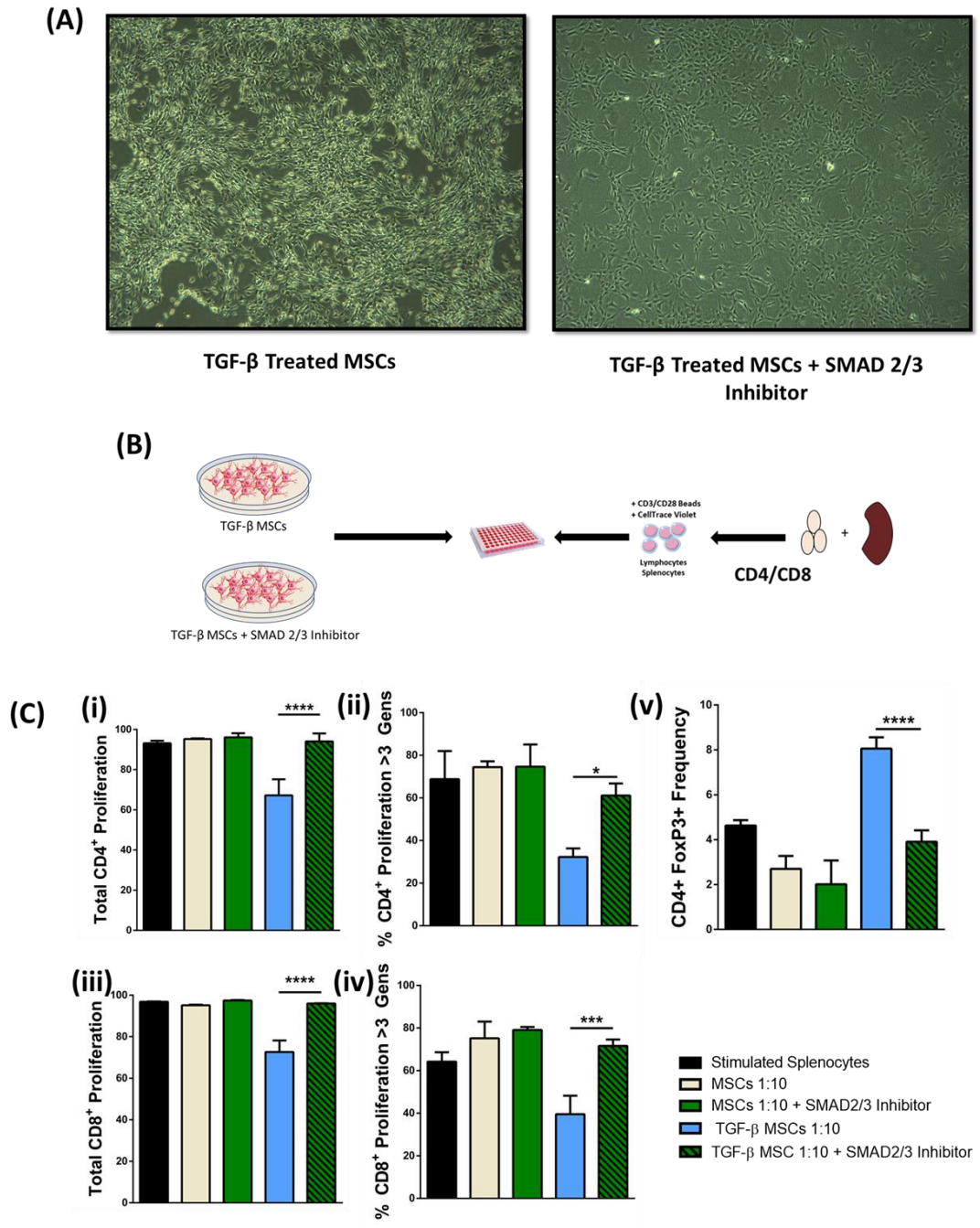

Figure 5.24 The efficacious attributes of TGF-β licensed MSCs can be contributed to the Smad2/3 canonical signalling pathway | Untreated BALB/c MSCs, TGF-β MSCs, Smad inhibitor + MSCs or TGF-β MSCs + Smad2 inhibitor (1 MSC to 10 lymphocytes) were cultured in normoxia and placed in T lymphocyte co-cultures for 96 hours with CD3/CD28 stimulated lymphocytes. CTV was used to determine lymphocyte proliferation (**A**) Light microscopy of TGF-β MSCs and Smad2 inhibited MSCs at 48 hours after TGF-β addition. (**B**) Schematic of how the T lymphocyte co-culture was set up. (**C**) Bar charts and histograms showing total lymphocyte proliferation, >3 generation proliferation. (**C** (v)) % of $CD4^{+}FoxP3^{+}$ cells. Error bars: mean +/- standard deviation *p<0.05, **p<0.01 ***p<0.001 ****p<0.0001. Multiple unpaired, two tailed student's t test and One-way ANOVA, Tukey's Post Hoc test (*n=3).*

It was observed that following Smad2 inhibition, T lymphocyte proliferation was significantly restored to the levels of untreated MSCs. This was demonstrated for both total proliferation (**Figure 5.24 C (i + iii**)) and >3 generations (**Figure 5.24 C (ii + iv**)) of both CD4+ lymphocytes and CD8+ lymphocytes. Analysing the CD4+FoxP3+ frequencies in the lymphocyte co-cultures it was observed that following Smad2 inhibition the frequencies of Tregs was also restored to the percentages of untreated MSCs (**Figure 5.24 C (v)).** From this experiment we concluded that TGF-β was signalling via the canonical Smad2/3 pathway and the therapeutic attributes that TGF-β MSCs possess can be contributed to molecules downstream of Smad2/3 signalling.

It has been reported that MSCs have both contact dependent and contact independent mechanisms of immunomodulation [203, 322, 440, 441]. To investigate if TGF-β MSC immunomodulation was contact dependent or contact independent we repeated our T lymphocyte co-cultures in a slightly modified setting. Instead of placing the MSCs and lymphocytes together in wells we used transwells (TW) to house the MSCs above the lymphocytes during the experiment (**Figure 5.25 A**). The pores in the TW were 0.8μm in diameter allowing for secreted factors to interact with the T lymphocytes while preventing MSC-lymphocyte contact. While not statistically significant, TW TGF-β MSC total $CD4^+$ proliferation was partially restored (**Figure 5.25 B (i)**). When examining TW TGF-β MSCs >3 generations proliferation, $CD4^+$ proliferation was a significantly restored in comparison to contact dependent TGF-β MSCs (**Figure 5.25 B (i)**). When examining the $CD8^+$ proliferation in the TW TGF-β MSC wells it was demonstrated that for both total (**Figure 5.25 B (iii)**) and >3 generations (**Figure 5.25 B (iv)**), proliferation was partially restored, but this restoration was non-significant. In the TW TGF-β MSC wells no increase in $CD4^+FoxP3^+$ frequencies were observed, and frequencies were comparable to stimulated controls and TW MSC (**Figure 5.25 B (v)**). Together these results indicate that TGF-β MSC T lymphocyte immunomodulation is predominately dependent on cell-cell contact, indicated by the failure to inhibit T lymphocyte proliferation significantly when in transwells. TW TGF-β MSCs also failed to increase frequencies of $CD4^+FoxP3^+$ lymphocytes in cultures again indicating the significance of cell contact.

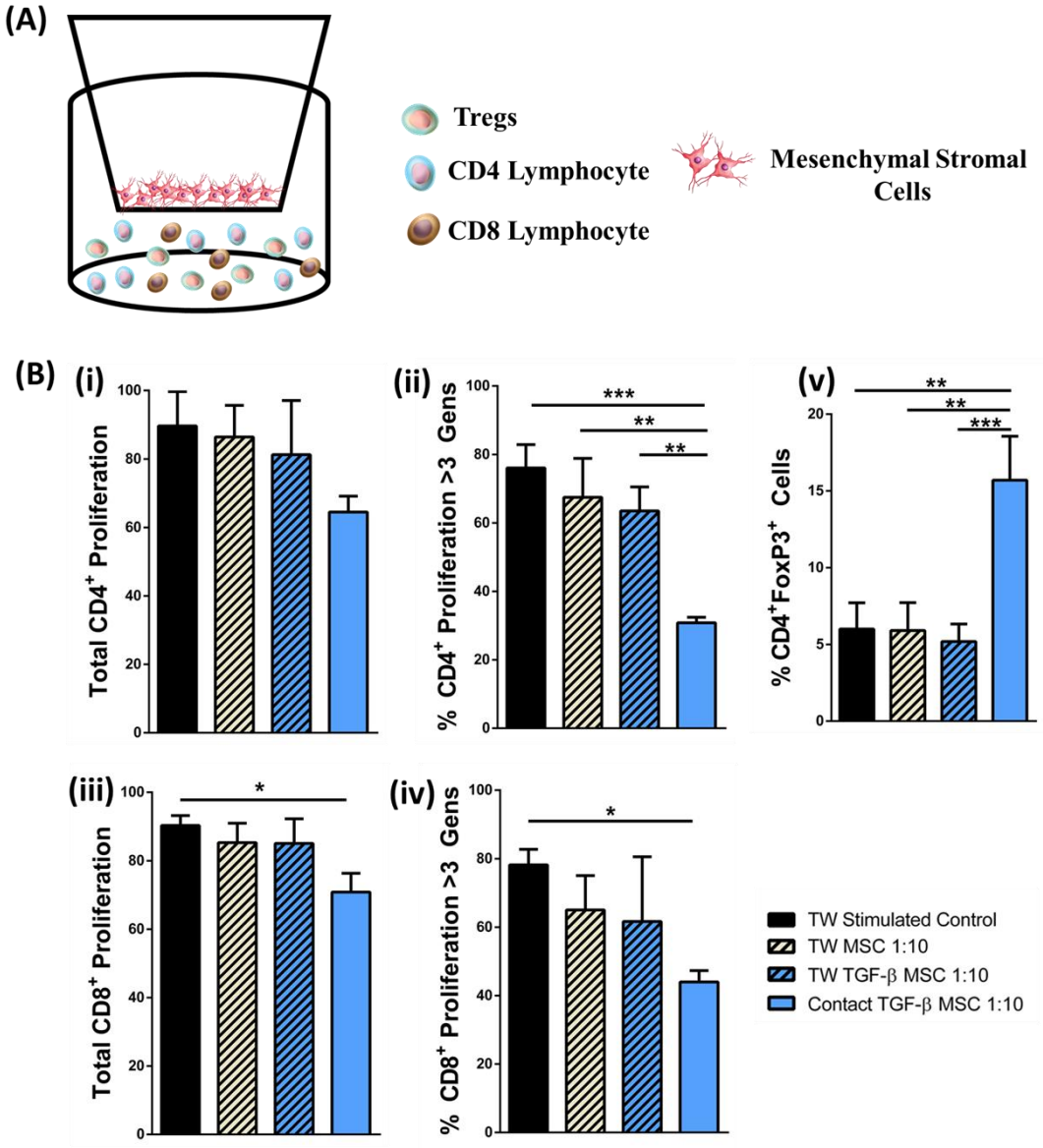

Figure 5.25 TGF-β MSCs require cell contact to elicit T lymphocyte immunosuppressive attributes | Untreated BALB/c MSCs or TGF-β MSCs (1 MSC to 10 lymphocytes) were cultured in normoxia and then placed in transwell (TW) modified T lymphocyte co-cultures for 96 hours with CD3/CD28 stimulated lymphocytes. **(A)** Schematic showing experimental procedure, MSCs were placed in a 0.8µm transwell and stimulated lymphocytes were placed in the bottom of a 24 well flat bottom plate. **(B) (i)** Total $CD4^+$ proliferation, **(ii)** >3 CD4+ proliferation, **(iii)** Total $CD8^+$ proliferation, **(iv)** >3 CD8+ proliferation and **(v)** $CD4^+FoxP3^+$ lymphocyte frequency. Error bars: mean +/- standard deviation *p<0.05, **p<0.01 ***p<0.001 ****p<0.0001. Multiple unpaired, two tailed student's t test and One-way ANOVA, Tukey's Post Hoc test (*n=3).*

5.3.13. CD73 as a regulatory factor in TGF-β MSC immunoregulation.

Adenosine (ADO) production and signalling has been described as one of the many mechanisms by which MSCs modulate immune cells. One of the main molecules in ADO signalling is the ectonucleotidase CD73, which converts adenosine monophosphate (AMP) to ADO [442]. To evaluate if the increase in expression of CD73 on MSCs after TGF-β treatment (**Figure 5.1 B)** contributes to their T lymphocyte immunomodulation, we used the CD73 inhibitor α,β-Methyleneadenosine 5′-diphosphate (AMP-CP).

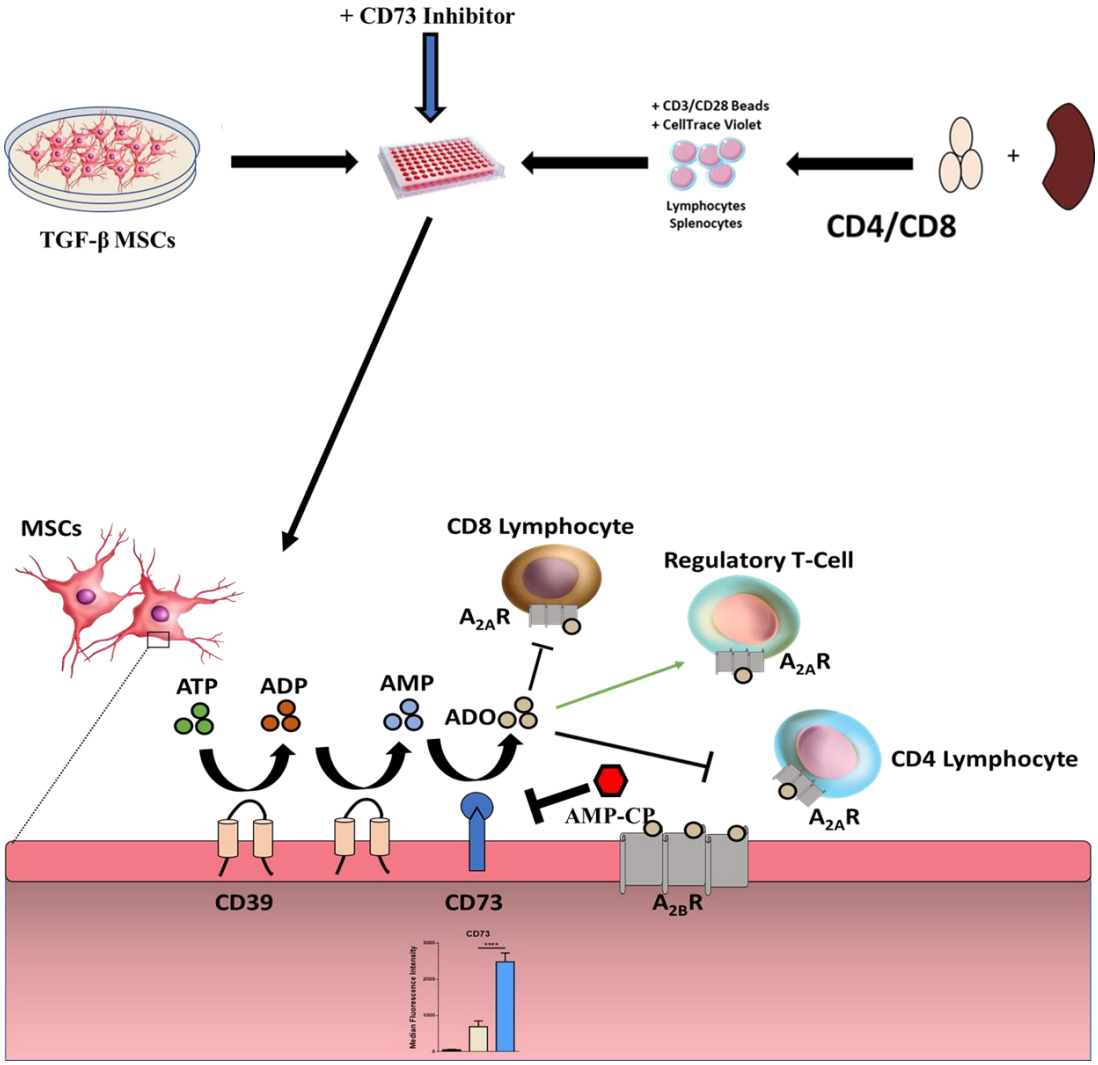

Figure 5.26 Experimental setup to investigate the importance of CD73 in TGF-β MSC immunomodulation | Untreated MSCs, AMP-CP MSCs, TGF-β MSCs and AMP-CP TGF-β MSCs (1 MSC to 10 lymphocytes) were cultured in normoxia and placed in T lymphocyte co-cultures for 96 hours with CD3/CD28 stimulated lymphocytes. CTV was used to determine lymphocyte proliferation. AMP-CP/CD73 inhibitor: Blocks ecto-5'-nucleotidase-mediated adenosine production by preventing the conversion of AMP to adenosine. ATP: adenosine triphosphate, ADP: adenosine diphosphate, AMP: adenosine monophosphate, ADO: adenosine.

AMP-CP blocks ecto-5'-nucleotidase-mediated adenosine production by preventing the conversion of AMP to adenosine (**Figure 5.26)**. MSCs were pre-activated for 72 hours in the presence of TGF-β before use in experiments (**Figure 5.26)**. TGF-β MSCs were placed in T lymphocyte co-cultures in the presence of AMP-CP (100 µM final concentration) for 96 hours, following incubation, proliferation of lymphocytes and the frequency of $CD4^+FoxP3^+$ lymphocytes were examined by flow cytometry. It was observed that proliferation >3 generations of the $CD4^+$ lymphocytes was partially restored in the wells that contained AMP-CP, although this restoration was not significant (**Figure 5.27 A**). While not restored to the same percentage proliferation as untreated MSCs, proliferation >3 generations of the $CD8^+$ lymphocytes were significantly restored in the AMP-CP wells (**Figure 5.27 B**). $CD4^+FoxP3^+$ frequencies were analysed in the AMP-CP wells and it was observed that the CD73 inhibitor had no observable effects on the percentages of the $CD4^+FoxP3^+$ populations

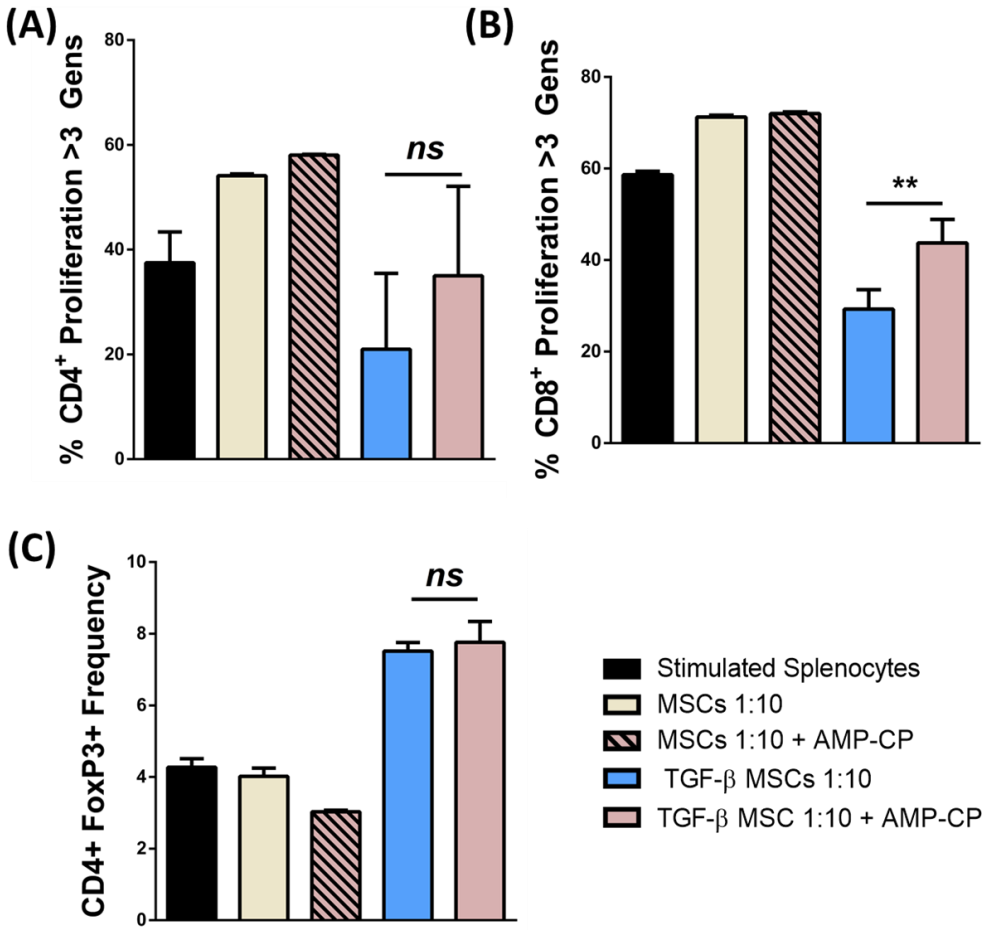

Figure 5.27 Inhibition of CD73 in lymphocyte co-cultures resulted in significantly increased $CD8^+$ proliferation | MSCs, MSCs + AMP-CP, TGF-β MSCs and TGF-β MSCs + AMP-CP (1 MSC to 10 lymphocytes) were cultured in T lymphocyte co-cultures for 96 hours with CD3/CD28 stimulated lymphocytes. **(A)** >3 CD4+ proliferation, **(B)** >3 CD8+

proliferation and **(C)** $CD4^{+}FoxP3^{+}$ lymphocyte frequency. Error bars: mean +/- standard deviation *p<0.05, **p<0.01 ***p<0.001 ****p<0.0001. Multiple unpaired, two tailed student's t test and One-way ANOVA, Tukey's Post Hoc test (*n=3).*

5.3.14. RNASeq Analysis Potentially Identifies PGE2 as an Important Molecule in TGF-β MSC Immunomodulation.

Considering the multitude of pathways activated by TGF-β and to better understand what potential molecules could be responsible for the prolongation of allograft survival we decided to investigate the mRNA expression profile of TGF-β MSCs. Both MSCs and TGF-β MSCs were analysed by RNA sequencing (RNASeq) technology. mRNA was isolated from MSCs and TGF-β MSCs in triplicate, quantified using a nanodrop and samples were sent to the company ArrayStar®. RNASeq experimental workflow (**Figure 5.28**) and RNASeq data analysis (**Figure 5.29**), including bioinformatics, was carried out by ArrayStar®.

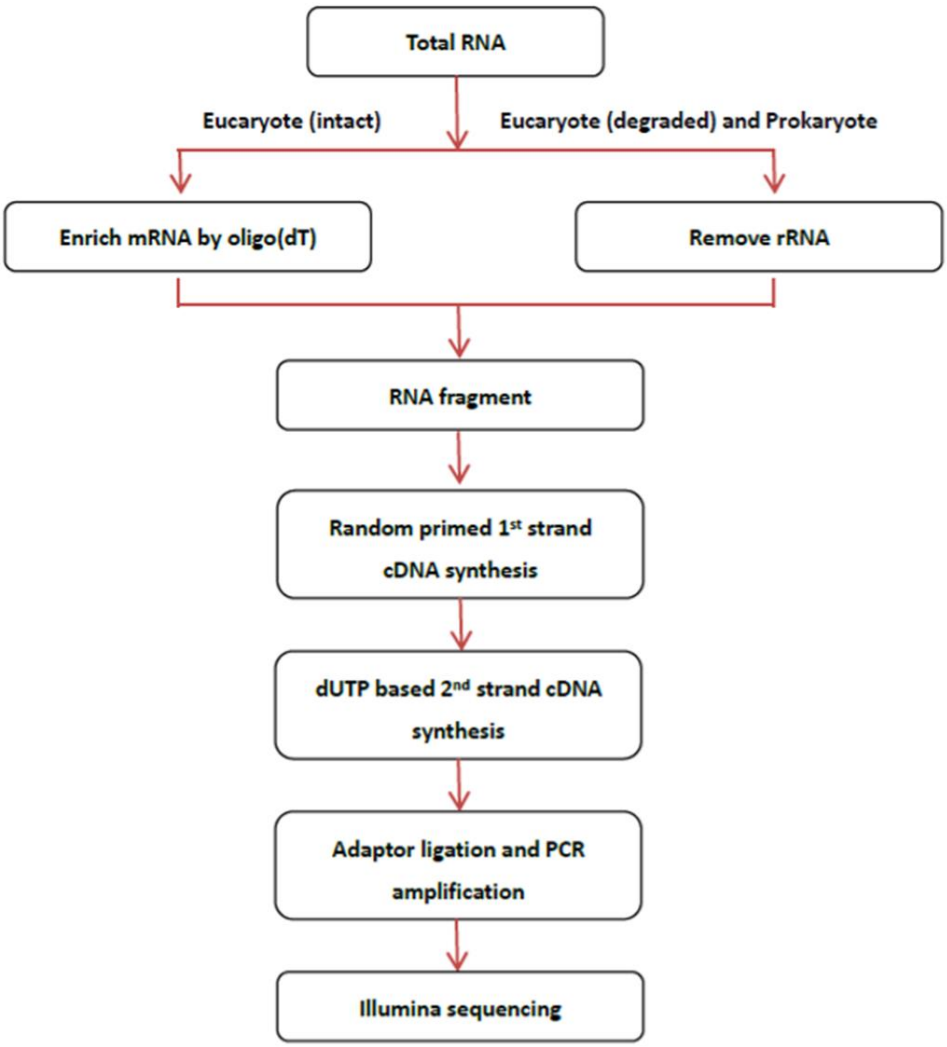

Figure 5.28 Experimental workflow for RNASeq analysis as carried out by ArrayStar® | Total RNA samples are quantified using Nanodrop and qualified by agarose gel

electrophoresis. Illumina kits were used for the RNASeq library preparation, which include procedures of RNA fragmentation, random hexamer primed first strand cDNA synthesis, dUTP based second strand cDNA synthesis, end-repairing, A-tailing, adaptor ligation and library PCR amplification. Finally, the prepared RNASeq libraries were qualified using Agilent 2100 Bioanalyzer and quantified by qPCR absolute quantification method. The sequencing was performed using Illumina Hiseq 4000. Information and diagram adapted from ArrayStar® sequencing report.

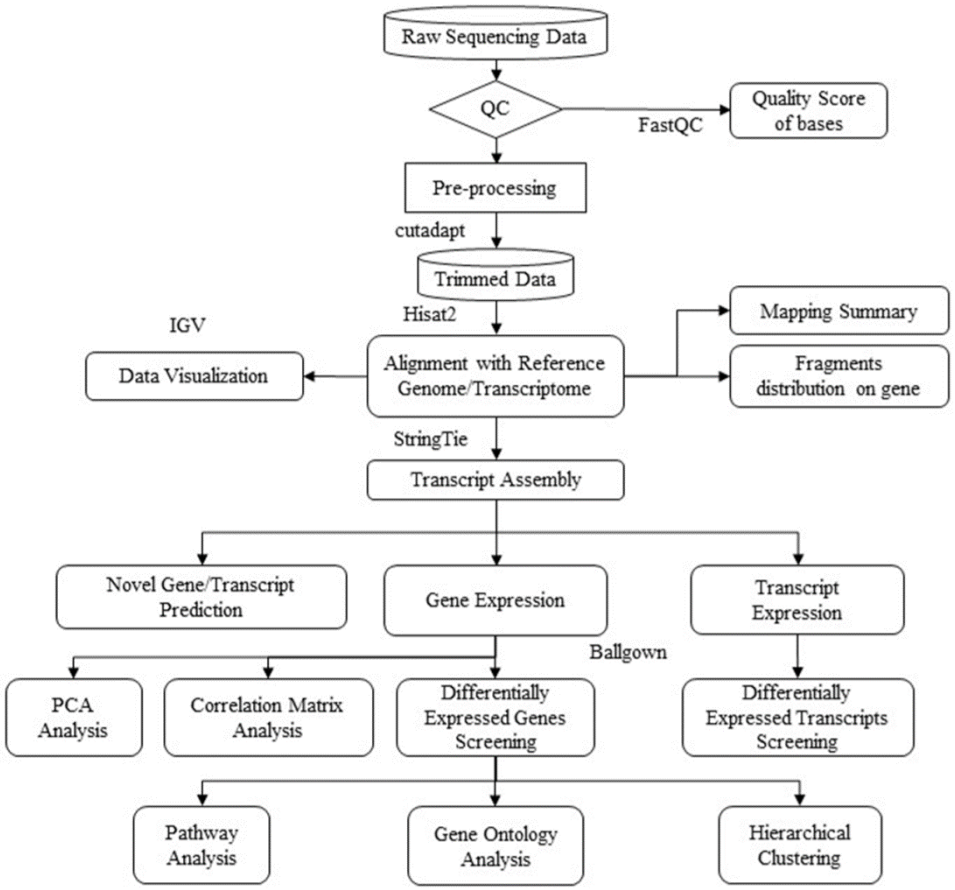

Figure 5.29 Data analysis workflow for RNASeq analysis as carried out by ArrayStar® | Raw sequencing data generated from Illumina HiSeq 4000 are used for following analysis. Trimmed reads (trimmed 5', 3'-adaptor bases) are aligned to reference genome. Based on alignment statistical analysis it was determined whether results can be used for subsequent data analysis. Expression profiling differentially expressed genes and differentially expressed transcripts were calculated. Novel genes and transcripts were also predicted. Principal Component Analysis (PCA), Correlation Analysis, Hierarchical Clustering, Gene Ontology (GO), Pathway Analysis, scatter plots and volcano plots were performed for the differentially expressed genes in R or Python environment for statistical computing and graphics. Information and diagram adapted from ArrayStar® sequencing report.

We have only recently received the RNASeq data, as such, results will be presented here in a rudimentary format. 9 genes from a list of the 20 most differentially expressed genes comparing MSCs to TGF-β MSCs were selected based on their gene products

having implications in immune regulation, tissue repair, cell proliferation, cytoprotection or migration (**Figure 5.30**). Prostaglandin-Endoperoxide Synthase 2 (*Ptgs2*), also known as cyclooxygenase (COX2), was the most differentially expressed gene when comparing the MSC Vs TGF-β MSC group, being 73-fold increased. The gene product being a key enzyme in prostaglandin biosynthesis [443], which reinforces our observed significant increase of PGE2 in T lymphocyte co-culture experiments (**Figure 5.2 C**).

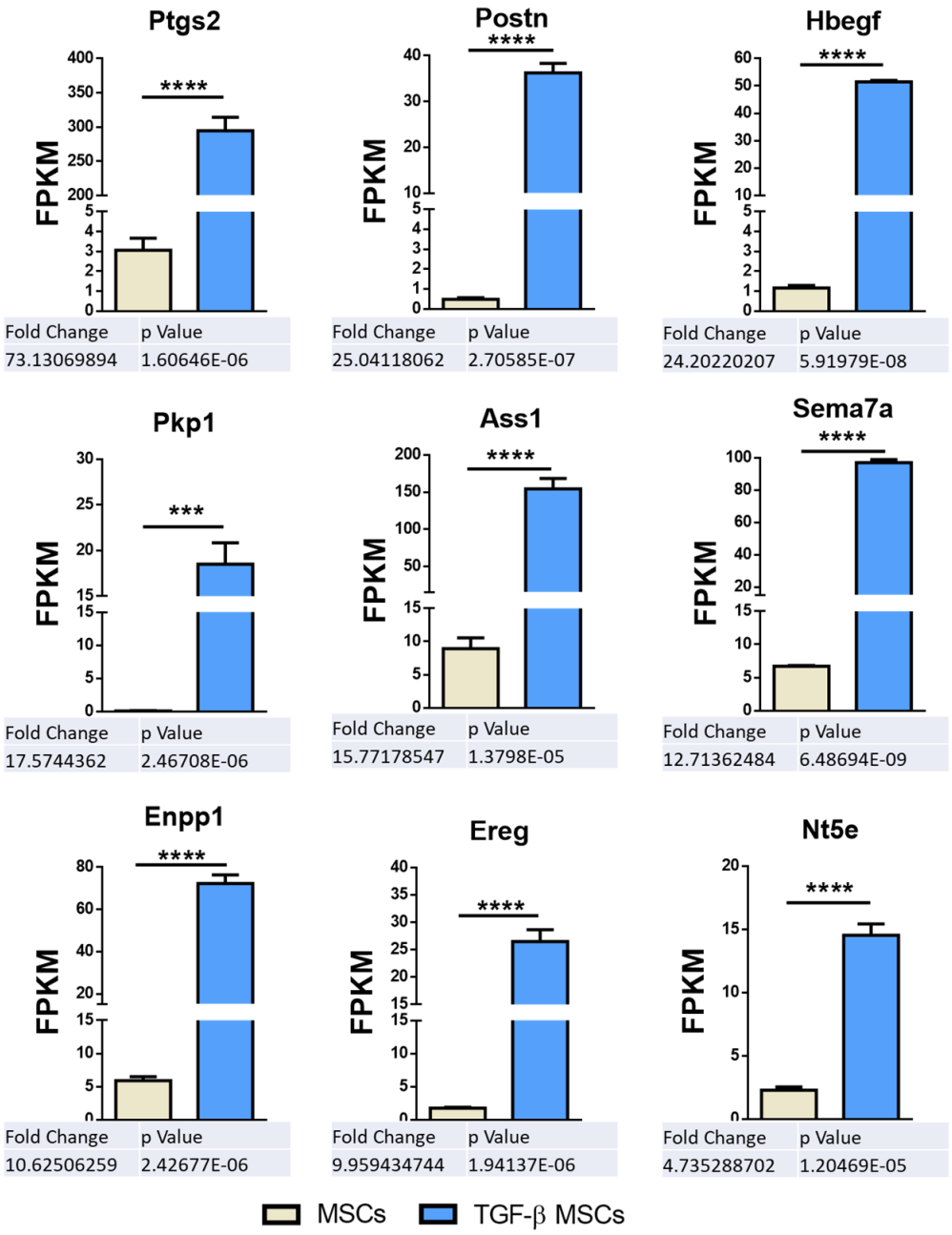

Figure 5.30 | Fragments Per Kilobase of transcript per Million mapped reads. The expression level (FPKM value) of known genes and transcripts were calculated using ballgown

Periostin (*Postn*) is a secreted extracellular matrix protein. It is important in tissue regeneration [444], tissue repair [445] and in the migration of fibroblasts [445]. *Postn* was increased 25-fold in TGF-β MSCs compared to MSCs. Heparin Binding EGF Like Growth Factor (*Hbegf*) is a protein coding gene whose gene product is a mitogen for fibroblasts [446] and stimulates proliferation and migration [447] of MSCs. It also has cytoprotective attributes protecting MSCs from apoptosis [447].There was 24-fold increase in *Hbegf* expression in the TGF-β MSCs compared to MSCs. Plakophilin 1 (*Pkp1*) links cadherins to intermediate filaments in the cytoskeleton forming strong intercellular adhesion mediated by desmosomes [448]. This suggests an essential role for *Pkp1* in tight junction formation, growth control and wound healing [448]. *Pkp1* was 17.5-fold upregulated in the TGF-β MSCs compared to MSCs. Argininosuccinate Synthase 1 (*Ass1*) encodes the enzyme that catalyses the second last step of the arginine biosynthetic pathway. In myeloid cells, arginine is metabolised either by nitric oxide synthases or by arginases and the fate of arginine metabolism is an integral regulator of innate and adaptive immune response [449, 450], where nitric oxide metabolism is linked to a pro-inflammatory outcome and arginine is linked to an anti-inflammatory outcome. *Ass1* was 15-fold upregulated in TGF-β MSCs compared to MSCs. Semaphorin 7A (*Sema7a*) or *Cd108* encodes membrane bound protein. It is typically expressed on lymphocytes and cells of myeloid origin. It contributes to innate immune responses by stimulation of macrophage chemotaxis and aids cytokine production, it is also known to regulate both T lymphocyte function and dendritic cell migration [451, 452]. *Sema7a* was 12-fold upregulated in TGF-β MSCs compared to MSCs. Ectonucleotide Pyrophosphatase/Phosphodiesterase 1 (*ENPP1*) encodes an ecto-nucleotide which converts extracellular ATP to AMP [453] and as discussed previously (**Figure 5.26**) this is a process in ADO production and has been described as one of the many mechanisms by which MSCs modulate immune cells. A 10-fold increase in *Enpp1* was observed in the TGF-β MSCs compared to MSCs. Epiregulin (*Ereg*) encodes a hormone peptide that is a member of the epidermal growth factor family and epiregulin is known to contribute to inflammation, tissue repair and wound healing under normal physiological conditions [454]. *Ereg* was observed to be 10-fold upregulated in TGF-β MSCs compared to MSCs. Lastly, it was observed that *Nt5e* was 4.7-fold upregulated in TGF- β MSCs compared to MSCs. The gene product of *Nt5e* is CD73, this molecule converts extracellular nucleotides like AMP into membrane permeable nucleosides like ADO [455].

5.3.15. Prostaglandin EP_4 Receptor (EP4) Blockade Impedes Increases in Treg Frequencies Observed in T Lymphocyte Co-Cultures.

PGE2 has been reported to be both pro-inflammatory and anti-inflammatory [456]. In the context of MSC immunomodulation it has been consistently reported to be one of the main mediators of their immunosuppressive attributes [457]. PGE2 inhibits T lymphocyte homing to DCs by preventing the secretion of cytokines and chemokines from DCs, it suppresses effector functions of neutrophils, macrophages, cytotoxic $CD8^+$ lymphocytes and natural killer cells and has been reported to increase the frequencies of both Tregs and myeloid-derived suppressor cells in tissues where it is present [458]. For these reasons but also because of our observed increase of PGE2 in T lymphocyte co-cultures and that the largest fold increase in gene expression was *Ptgs2*, we blocked EP4, one of the 4 receptors that binds PGE2.

To study if the observed suppression of T lymphocyte proliferation or if the increases of $CD4^+FoxP3^+$ frequencies was due to PGE2 signalling via the EP4 receptor the chemical compound L-161,982, which is a highly selective EP4 antagonist and was used at a final concentration of 1 mM in TGF-β MSC-T lymphocyte co-cultures. The cultures were incubated for 96 hours at 37ºC. While the restoration was not significant, it was observed that EP4 blockade partially restored $CD4^+$ lymphocyte >3 gens proliferation (**Figure 5.31 A)**. EP4 blockade significantly restored $CD8^+$ >3 gens proliferation to the percentages of the stimulated lymphocyte control (**Figure 5.31 B).** Interestingly, it was demonstrated that the blockade of EP4 inhibited the increase of $CD4^+FoxP3^+$ in the TGF-β MSC + EP4 inhibitor wells when compared to TGF-β MSC wells (**Figure 5.31 C)**.

In summary, we have observed that TGF-β signals via the canonical TGF-β1 signalling pathway when incubated with MSCs (**Figure 5.24**), indicating their therapeutic attributes is a result of molecules downstream of this pathway. We observed that the T lymphocyte modulatory attributes of TGF-β MSCs is cell-cell contact dependent, as when they are separated in co-culture by transwells their inhibitory effect is lost. Also, they lose their ability to increase $CD4^+FoxP3^+$ frequencies (**Figure 5.25**). Using the CD73 inhibitor AMP-CP we demonstrated a restoration of $CD8^+$ proliferation with a partial restoration of proliferation of $CD4^+$ populations (**Figure 5.27)**. While CD73 inhibition did not affect $CD4^+FoxP3^+$ frequencies (**Figure 5.27)**, the blocking of the EP4 on T lymphocytes did, significantly

reducing the $CD4^+FoxP3^+$ frequencies (**Figure 5.31)**. This would indicate, as one would expect, a multifarious mechanism of action of TGF-β MSCs.

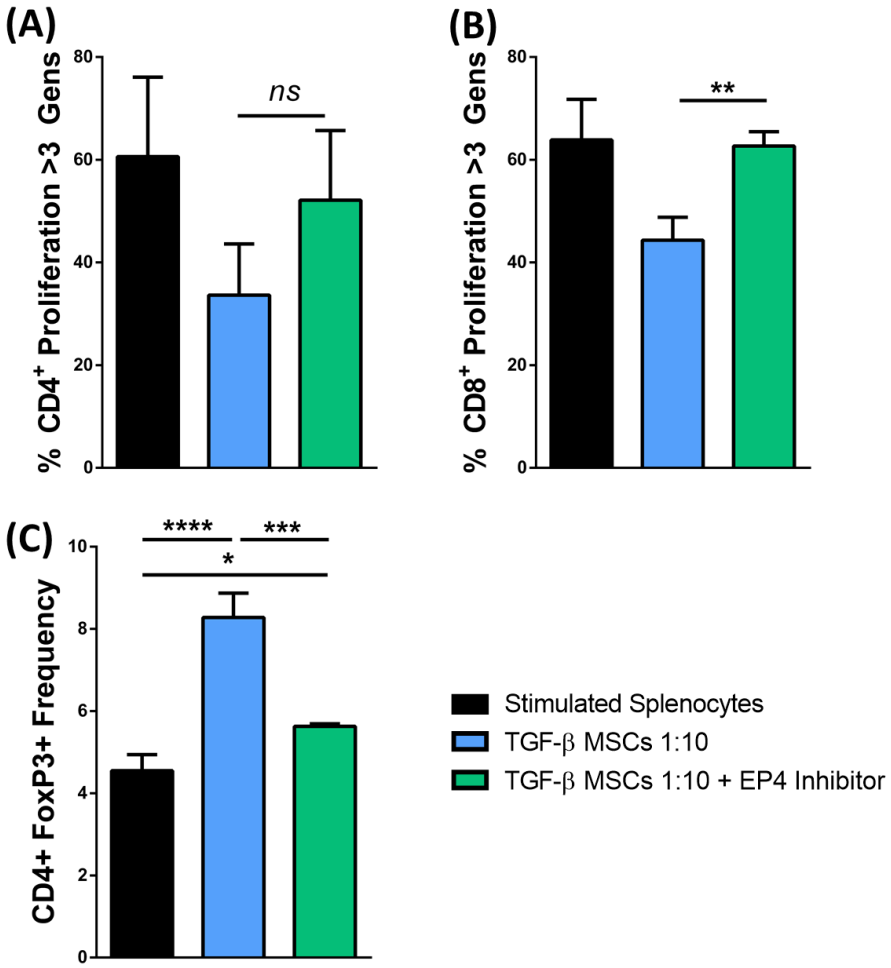

Figure 5.31 EP4 antagonist significantly restores $CD8^+$ proliferation and prevents increases in $CD4^+FoxP3^+$ frequencies in TGF-β MSC T lymphocyte co-cultures. | TGF-β MSCs and TGF-β MSCs + EP4 Inhibitor (1 MSC to 10 lymphocytes) were cultured in normoxia in T lymphocyte co-cultures for 96 hours with CD3/CD28 stimulated lymphocytes. **(A)** >3 CD4+ proliferation, **(B)** >3 CD8+ proliferation and **(C)** $CD4^+FoxP3^+$ lymphocyte frequency. Error bars: mean +/- standard deviation *p<0.05, **p<0.01 ***p<0.001 ****p<0.0001. Multiple unpaired, two tailed student's t test and One-way ANOVA, Tukey's Post Hoc test (n=3).

5.4 Discussion

In this chapter we observed that the pre-treatment of MSCs with TGF-β significantly modulated their phenotype and increased their ability to suppress both cells of the adaptive and innate immune system *in vitro*. We had observed and described in the previous chapter that MSCs and TNF-α + IL-1β MSCs could not prolong RFS, however, TGF-β MSCs significantly promoted RFS after administration of $1x10^6$ cells on POD +1 and POD + 7. To investigate the mechanisms of immune modulation which mediate MSCs ability to prolong allograft survival, we performed immune cell distribution studies in the DLNs, spleen and lungs, investigating increases or decreases of B cells, T lymphocytes, Tregs, macrophages, DCs, neutrophils and NK cells along with their activation status. We observed that the administration of TGF-β MSCs modulated multiple immune cell populations as summarised in Table 5.1. Of note, we observed significant increases in Breg populations in the DLNs and spleens of TGF-β MSCs treated animals, significant increases in Tregs in the DLNs and lungs of TGF-β MSCs treated animals, we observed significant increases in an alternative Treg ($CD3^+CD4^+CD25_{Neg}CD69^+$) population in all organs examined and significant decreases in not only the frequencies of both DCs and macrophages but also their activation status (decreases in CD80 and CD86).

Lastly, when investigating a potential mechanism by which TGF-β MSCs suppress activated T lymphocytes and induce Treg populations *in vitro*, we demonstrated that TGF-β signals via the canonical TGF-β1 signalling pathway and their ability to suppress activated lymphocytes and to induce Tregs is cell-cell contact dependent. Not only this, while CD73 was mildly responsible for the suppression of $CD4^+$ and $CD8^+$ lymphocytes, the inhibition of its activity had no bearing on the ability of TGF-β MSCs to induce Treg populations *in vitro*. We had previously observed that TGF-β MSCs secrete significantly higher concentrations of PGE2 and after observing that the gene for COX2 (Ptgs2) was 73-fold increased in the RNASeq reports, we decided to inhibit EP4, a prostaglandin receptor on T lymphocytes. We observed that inhibition of EP4 restored both $CD4^+$ and $CD8^+$ T lymphocyte proliferation but also inhibited the induction of Tregs. These results indicated that both CD73 and PGE2 play a role in TGF-β MSCs immunomodulation.

Firstly, TGF-β MSCs were characterised by flow cytometry to study the effects of TGF-β pre-treatment on cell surface identification markers (**Figure 5.1)**. It was observed that TGF-β treatment did not significantly change MHC II, CD45, F4/80, CD11c, CD80 or CD86 on the surface of the MSCs. Interestingly, TGF-β MSCs remained positive for CD105, CD44, and CD90 while they had increased expression of CD73 and decreased expression of SCA-I and MHC I. As discussed previously CD73 is an ectonucleotidase which has been implicated MSC immunoregulation, TGF-β MSCs had significantly elevated CD73 expression. This result will be discussed in greater detail in the context of CD73 inhibitors in the ensuing discussion. SCA-I is a maker of mouse MSCs, it has been used in the past to isolate MSCs that have increased growth potential and robust tri-lineage differentiation compared with MSCs that are isolated by plastic adherence alone [459]. Interestingly, we see large significant decreases in SCA-I after TGF-β treatment. Although Houlihan *et al*. [459] reported that SCA-I sorted MSCs have increased differentiation and proliferative capacity, Li and colleagues [460] demonstrated that SCA-I negative MSCs have significant immunomodulatory capacity. In the context of allogeneic cell treatments, an ideal cellular therapy would have no MHC II and little or no MHC I, in this regard, our observed decreases in MHC I are interesting, as this would decrease the potential likelihood of an antigen specific donor response via alloreactive T lymphocytes [369].

As discussed previously, the pre-activation of MSCs before *in vivo* administration has become a common strategy to improve therapeutic efficacy [236, 243, 253, 266, 330, 364, 368]. We had observed in preliminary experiments (**Figure 4.16+ Figure 4.17**), discussed in chapter 4, that both TNF-α + IL-1β MSCs and TGF-β MSCs decreased the frequency and proliferation of $CD4^+$ and $CD8^+$ lymphocytes to a greater degree than other pre-treatments. To investigate if this observation was statistically significant and not just an artefact, TGF-β MSCs were placed in T lymphocyte co-cultures and their effects on T lymphocytes were studied more intensively (**Figure 5.2**). It was demonstrated that TGF-β MSCs significantly suppressed the activation of T lymphocytes *in vitro*. When the percentage of proliferation >3 generations were analysed for $CD4^+$ and $CD8^+$ lymphocytes it was observed that TGF-β MSCs suppressed both cell populations to the same extent as TNF-α + IL-1β MSCs (**Figure 5.2A**). Interestingly, one significant

difference was that while TGF-β MSCs secreted high levels of PGE2 (**Figure 5.2C**), they failed to secrete significant levels of NO while TNF-α + IL-1β MSCs had been observed to secrete high levels of both immunoregulatory molecules (**Figure 4.21**). Comparable to TNF-α + IL-1β MSCs, TGF-β MSCs had an enhanced ability to suppress activated macrophages (**Figure 5.4**) while non-treated MSCs did not (**Figure 4.8**). Analysing the differences between TNF-α + IL-1β MSCs and TGF-β MSCs revealed a trend decrease in MHC II and a significant decrease in CD80 indicating that TGF-β MSCs are slightly more efficient at suppressing activated macrophages. Not only this, where TNF-α + IL-1β MSCs had failed to induce Treg populations *in vitro* (**Figure 5.3B**), TGF-β MSCs significantly increased both the frequencies and numbers of Tregs (**Figure 5.3B + D**). Tregs have been reported in several studies to important in the prolongation of graft survival, including corneal allograft survival [62, 263, 265, 381-383] and the inducement of Tregs has been attributed to the immunomodulatory molecule PGE2, in which we had observed significant increases in our *in vitro* co-culture systems [364, 377].

Previously, we had administered untreated MSCs (**Figure 4.10**) and TNF-α + IL-1β MSCs (**Figure 4.24**) in our model of corneal transplantation and both treatments failed to prolong RFS. We observed that TGF-β MSCs had an ability to induce Tregs *in vitro,* that they suppressed the proliferation of activated T lymphocytes, that they suppressed stimulated macrophages to a higher degree than other treatments and that TGF-β treatment did not inhibit the ability of MSCs to proliferate, while TNF-α + IL-1β did (**Figure 4.13**). For these reasons, we administered $1x10^6$ TGF-β MSCs POD day +1 and $1x10^6$ TGF-β MSCs POD day +7. We observed a significant increase in RFS in TGF-β MSC treated animals (70%) compared to allogeneic controls (22%), MSC treated animals (18%) and TNF-α + IL-1β MSC treated animals (0%) (**Figure 5.5A**). Not only this, we also noted that the opacity scores and neovascularization scores on the average day of rejection were significantly lower in the TGF-β MSC treated group when compared to all other treatment groups, indicating that significantly less immune cells infiltrated the graft (**Figure 5.6**).

To investigate the potential mechanisms by which TGF-β MSCs prolong RFS we designed an immune cell distribution study (**Figure 5.7)**. On the day of rejection, allogeneic control animals were euthanised and the DLN, spleen and lungs were harvested

and prepared for flow cytometry analysis. For TGF-β MSC treated animals, mice were euthanised on the average days of rejection (d16-d19) and the DLN, spleen and lungs were prepared. Flow cytometry panels were designed to analyse both innate and adaptive immune cell populations including B cells, CD4 lymphocytes, CD8 lymphocytes, Tregs, macrophages, dendritic cells, neutrophils and NK cells.

Once administered via tail vein injection, it is known that MSCs collect as a bolus of cells in the lungs. Recent studies have suggested that because of their size and the number of MSCs injected, the majority of MSCs do not migrate out of the lung, also it has been reported that the *in vivo* viability of MSCs is limited. As a result it seems possible that MSCs modulate intermediary immune effector populations which then migrate to other organs and sites of inflammation and exert immunosuppressive effects which were acquired from the MSCs [404, 405]. Interestingly, we observed significant increases in Th1-like cells after the intravenous administration of TGF-β MSCs (**Figure 5.18C (i)**), this increase in inflammatory $CD4^+$ positive cells may be due to the mechanical stress applied on the capillaries because of the large bolus of cells that was administered. Th1-like cells could also be recruited via the secretion of chemokines by the TGF-β MSCs or even due to the release of soluble mediators by resident lung immune cells.

We observed increases in $CD3^+CD4^+CD25^+$ populations in the lungs of TGF-β MSC treated animals and increases in $CD3^+CD4^+CD69^+$ populations also. Both CD25 and CD69 are T lymphocyte activation markers [461, 462]. CD25 also has been historically used as an identification marker for Tregs [462] and a recently identified population of Tregs have been reported to be CD25 negative but $CD69^+$ [417]. For these reasons we investigated if the increases in CD25 or CD69 expression that were observed in the organs of TGF-β MSC treated animals were a result of increases in these populations. It was demonstrated that both conventional Treg populations in the lungs were increased (**Figure 5.13D**) and $CD3^+CD4^+CD25^{Neg}CD69^+$ cells were increased in all organs (**Figure 5.14**). This result will be discussed in further detail in chapter 6.

It was recently demonstrated by Ko *et al*. that intravenously administered human MSCs confer long-term therapeutic benefits even though they only engraft transiently, and that a population of $CD11b^+$ regulatory macrophages were enriched in the lung after

administration, these macrophages remain in circulation for up to 7 days and are capable of suppressing the T cell response and prolonging graft survival [267]. In line with this study but also due to the possibility of MSCs directly modulating APC populations as demonstrated *in vitro* but also because of the possibility of MSCs dying shortly after administration and being phagocytosed by APCs, which in turn may cause the APCs to become immunoregulatory, both $CD11b^+$ (macrophages) and $CD11c^+$ (DCs) APC populations were analysed. We observed significant decreases in the frequencies of both macrophages and DCs in the lungs of TGF-β MSC treated animals. Not only this, we observed significant reductions in the co-stimulatory molecule CD86 (**Figure 5.22C+ 5.23C**) which is indicative of an iDC or tDC phenotype [463].

As recent evidence suggests [267] and as we have seen in our study, MSCs can modulate immune effector populations in lungs, these cells can then migrate to peripheral organs such as the spleen and DLNs. The spleen filters the blood removing damaged or dead blood cells from circulation, it can also sequester immune effector cells such as lymphocytes and APCs. It has been reported by us and others that systemically administered MSCs increase regulatory immune populations in the spleen of rodents which have received corneal transplants and these populations have been associated with prolonged RFS [263, 265]. As a result, it was investigated whether TGF-β MSCs modulated immune cell populations in the spleens of treated animals. A vital step in the corneal allograft rejection process is the presentation of alloantigen from donor or recipient APCs to allo-reactive T lymphocytes, this occurs either in the cornea, in the area surrounding the eye and conjunctiva or in the DLN [435]. The importance of the DLN in corneal allograft rejection has been demonstrated by Yamagami *et al*. [93, 94] whereby they removed the DLNs in both a model of low risk and high risk corneal transplantation. Removal of the DLNs prevents graft rejection in both models demonstrating the importance of the initial antigen presentation phase and the subsequent expansion of alloreactive effector T lymphocytes. For this reason, it was investigated whether TGF-β MSCs modulated immune cell populations in the DLNs of treated animals.

While T effector cells are the main mediators of rejection, B cells are known to be responsible for the production of alloantibodies leading to both acute and chronic allograft

rejection [406, 407]. They are also known to present graft derived antigens to alloreactive T lymphocytes via the indirect pathway of allorecognition [407-409]. We observed decreases in overall B cell frequencies (**Figure 5.8**) but increases in Breg frequencies (**Figure 5.9**) in the DLNs and spleens of TGF-β MSC treated animals. Interestingly, $CD19^{+}CD24^{high}CD5^{high}$ B cells have recently been reported to be able to induce Tregs *in vitro* [464], not only this but $CD19^{+}$ $CD5^{+}B220^{low}$ Bregs were able to reduce symptoms of uveitis in mice after administration [465]. Our results may also possibly indicate that MSCs may induce an environment whereby ACAID is facilitated. This will be discussed further in chapter 6.

Comparable to the observations in the lungs of TGF-β MSC treated animals, frequencies of $CD3^{+}CD4^{+}FoxP3^{+}$ Tregs were significantly increased in the DLNs (**Figure 5.13A**) of TGF-β MSC treated animals on the average days of rejection. This observation is in line with a study previously published by Jia *et al*., in this study they demonstrated that postoperative injection of MSCs reduced Th1 pro-inflammatory cytokines and elevated IL-4 cytokine secretion from T lymphocytes derived from cornea-transplanted rats. They also noted that Tregs were upregulated in the DLNs after MSC treatment. They attributed this increase in Tregs to the observed prolongation of corneal allograft survival [263]. This increase in Tregs may contribute to the suppression of the alloreactive T lymphocyte response directly, or indirectly by acting on APCs in the DLN. We observed significant decreases in both DC and macrophage frequencies in the DLNs, with significant decreases in both CD80 and CD86 (**Figure 5.22A + 5.23A)**.

We observed increases in a $CD8^{+}$ memory phenotype in the spleen of TGF-β MSC treated animals (**Figure 5.16B (ii)**), a recently reported $CD8^{+}CD44^{+}CD62L^{+}CD25^{Neg}$ memory phenotype is capable of suppressing T lymphocyte responses [466]. However more investigation would be needed in order to clarify if the $CD8^{+}$ memory population we observe is similar to this regulatory $CD8^{+}CD44^{+}CD62L^{+}CD25^{Neg}$ memory phenotype.

Decreases in both Th9-like and Th17-like populations were observed in the spleen in TGF-β MSC treated animals (**Figure 5.18B(i+iv)**). Th9 T lymphocytes are a recently observed and defined population of $CD4^{+}$ lymphocytes. They were demonstrated to play a role in in allergic inflammation, autoimmune diseases, and tumour immunity [430].

Little or no information exists as to if they play a role in the graft rejection process. Interestingly, in a model of allogeneic skin transplantation, Lu *et al*. demonstrated the importance of an IL-9 secreting $CD4^+CD25^+FoxP3^+$ population in tolerance to the graft [467]. They adoptively transferred the *in vitro* expanded IL-9 secreting population into allogeneic skin transplanted animals and observed acceptance of the graft, however, after administering an IL-9 blocking antibody, this tolerance was lost. The caveat to this study was that the transferred IL-9 secreting population was selected based on the $CD4^+CD25^+$ expression, the concern being that FoxP3 negative cells were transferred also. Other studies [430, 468, 469] investigating IL-9 production from *in vitro* expanded Treg cultures were not able to demonstrate the section of IL-9, raising the question if the IL-9 transferred cells in the Lu *et al*. study were Th-9 cells Further studies would need to be completed in order to define the source of the IL-9 in these models and indeed if Th9 T lymphocytes contribute to corneal graft rejection.

The role of Th17 cells in the corneal allograft rejection process is conflicting, with some studies demonstrating that IL-17 is needed for corneal allograft survival [110] while others demonstrate the contrary [108]. In both the renal and cardiac graft rejection process, Th17 cells have been identified as mediators of rejection. Cunnusamy *et al.* investigated if Th17 cells were important in mediating mouse corneal graft rejection using anti-IL17 antibodies [110]. They demonstrated that neutralisation of IL-17 increased the incidence of rejection with 90% of animals rejecting their transplants and found that the inhibition of Th17 cells lead to an emergence of Th2 cells which independently and inevitability destroyed the graft. However, both Chen *et al.* and Yin *et al*. demonstrated that Th17 cells played a role in both the early and late stages of corneal rejection respectively [108, 470]. We observed that Th17-like populations were decreased in the spleen of TGF-β MSC treated animals. Duffy *et al*. demonstrated that MSCs can potently inhibit Th17 differentiation from both memory and naïve T lymphocyte precursors and inhibit the differentiation of Th17 cells isolated from sites of inflammation. They also demonstrated that this was PGE2 dependent and could be inhibited by blocking of the EP4 receptor on the T lymphocytes [471]. This is interesting in the context of our study as we observed high levels of PGE2 secreted from TGF-β MSCs and in addition, we also observed increases in Tregs and inhibition of proliferation in conventional T lymphocyte

populations was PGE2 dependent via the EP4 receptor, this will be discussed further in chapter 6.

TGF-β is a pleiotropic molecule which plays many important roles during normal physiological conditions but also during disease progression, it can regulate cell growth, differentiation, apoptosis, extracellular matrix synthesis and migration of cells [472]. Considering that TGF-β signals via multiple SMAD dependent and independent pathways [473] we inhibited SMAD2 pharmacologically (SB431542, an ALK5/Smad2 inhibitor) to investigate if our therapeutic effects were a result of SMAD dependent signalling. While in different cell types, it has been demonstrated that TGF-β can signal via SMAD2/3 [474] or mitogen-activated protein kinase (MAPK) [475] to induce COX-2 resulting in the production of PGE2. It was observed that SB431542 inhibited TGF-β MSCs lost their ability to suppress activated T lymphocytes and failed to induce Tregs *in vitro* indicating that TGF-β signalled via the canonical SMAD2/3 pathway and the subsequent production of PGE2 may be a potential mechanism of action of TGF-β MSCs.

The beneficial effects of MSCs have been reported to be both cell-cell contact dependent and independent. Many studies have shown that MSCs can actively inhibit immune cells via growth factors, enzymes and by the secretion of cytokines. In a rat model of fulminant hepatic failure, it was shown that concentrated MSC conditioned medium was capable of reversing the adverse effects of this disease [476]. Contrastingly, Tse *et al*. [238] demonstrated that cell contact was important in MSCs ability to suppress T lymphocyte responses and the authors suggested that cell-cell contact was more important than soluble mediators secreted by the cells. Krampera *et al*. has also demonstrated that inhibition of T lymphocyte responses is cell-cell dependent [242, 322, 477]. Furthermore, both English *et al*. [246] and Zanjani *et al*. [478] have reported that both cell-cell contact, and mediated factors are important for MSC mediated immunosuppression. To investigate if TGF-β MSC immunomodulation was contact dependent or contact independent we used TW co-culture systems (**Figure 5.25**). We observed that cell-cell contact was important for TGF-β MSC mediated suppression of T lymphocytes (**Figure 5.25B (i-iv)**) and TGF-β MSC mediated increases in Treg frequencies (**Figure 5.25B (v)**).

Considering the highly significant increases observed in CD73 surface expression after TGF-β pre-treatment (**Figure 5.1**) and because of the 4.7-fold increase observed in preliminary RNASeq analysis (**Figure 5.30**) we decided to investigate if CD73 activity was important in TGF-β MSC mediated modulation of T lymphocytes. Inhibition of the enzymatic activity of CD73 via AMP-CP (**Figure 5.26**) resulted in a loss of ability to suppress activated T lymphocytes by TGF-β MSCs, however it did not affect the ability of TGF-β MSCs to induce Tregs (**Figure 5.27**). Interestingly, Chen *et al*. recently described that the CD73/adenosine pathway was important in MSCs mediated alleviation of autoimmune uveitis [479]. Inhibition of CD73 activity using AMP-CP resulted in loss of the therapeutic effects exhibited by MSCs in their model. Interestingly, not only did we observe an increase in CD73 expression on TGF-β MSCs we also observed increased CD73 and PD-L1 expression on the induced Tregs generated in our TGF-β MSC – T lymphocyte cultures (**Appendix Figure 2**). While inhibition of CD73 activity in our co-cultures may not have reduced the frequencies of Tregs, it may inhibit their immunosuppressive function.

Additionally, we observed high concentrations of PGE2 secreted from TGF-β MSCs alone (**Figure 4.15**) and in TGF-β MSC - T lymphocyte co-cultures (**Figure 5.2C**). This coincided with our observed 73-fold increase of ptgs2 in our RNASeq analysis (**Figure 5.30**). Accordingly, we investigated if the engagement of the EP4 receptor was important in TGF-β MSC-PGE2 mediated suppression of activated T lymphocytes and inducement of Tregs. We observed a restoration of T lymphocyte proliferation for both $CD4^+$ and $CD8^+$ lymphocytes, not only this, we also observed that the previously observed induction of Tregs was inhibited by EP4 blockade. This result will be discussed in more detail in chapter 6.

To summarise, our study demonstrated that TGF-β pre-activation of MSCs potently suppresses T lymphocyte proliferation and induces Tregs *in vitro*. TGF-β signals via the canonical SMAD 2/3 pathway which leads to the production of PGE2. PGE2 acts via the EP4 receptor and its immunomodulation of both conventional T lymphocytes and Tregs is cell-cell contact dependent. TGF-β MSCs potently modulated immune cells *in vivo*, increasing the frequencies of both Tregs and Bregs in the organs of treated animals. TGF-

β MSCs reduced the frequencies of APCs in all organs analysed, also decreasing their co-stimulation markers (**Table 5.1**). The results discussed in chapter five have been summarised below (**Figure 5.32**)

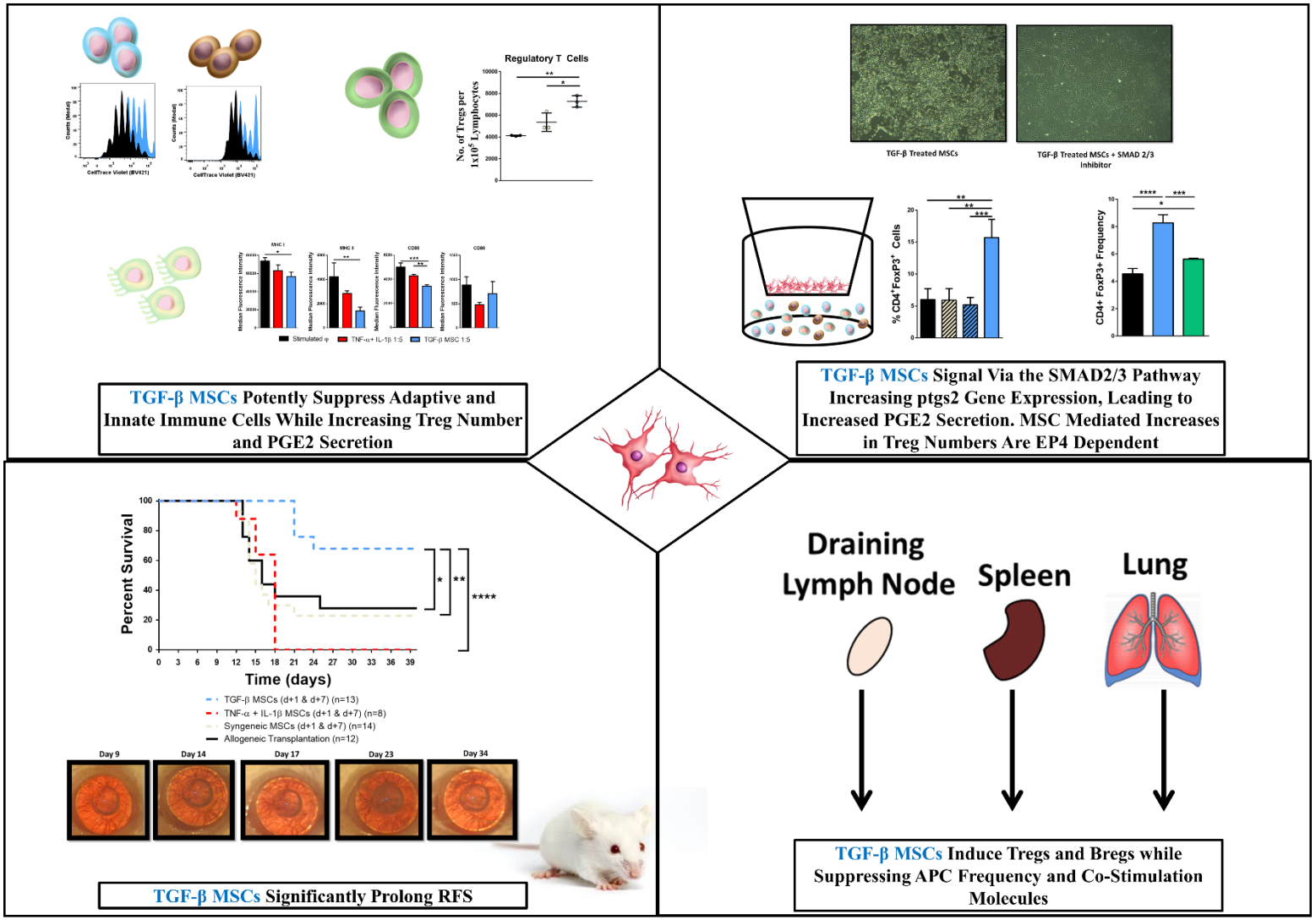

Figure 5.32. Schematic summarising results discussed in chapter 5

Chapter Six:

General Discussion

6.1 Discussion

Corneal blindness occurs due to physical damage to the corneal surface or due to a range of inflammatory, dystrophic, infectious and degenerative corneal diseases. Corneal transplantation is the most frequently performed transplant worldwide with 42,000 transplants being performed in the USA alone in 2010. Putting that into perspective of solid organ transplantation, collectively only 12600 kidney, liver, lung, pancreas, heart, and intestine transplantations were performed in the same year [2]. Closer to home in the UK, 3565 corneal transplantations were performed in 2010 with 2671 kidney, and 689 liver transplantations performed in the same timeframe [2]. In low-risk settings it has been reported that up to 80% of corneal transplantations remain rejection free without the use of prophylaxis due to the immune privilege status of the cornea [480]. During acute corneal endothelial rejection, the rapid loss of endothelial cells leads to corneal transplant failure due to the loss of corneal endothelial pump function. These cells do not self-renew, and as a result the damage is irreversible. This can occur in high-risk patients who had a previously inflamed corneal bed before transplantation or when the corneal stroma was vascularised. In these high-risk situations the recipient is at an increased risk of corneal rejection with 50% of grafts rejecting after 5 years in this setting [2, 481]. If topical steroids prove to be inadequate in circumventing rejection, systemic immunosuppressive therapy has then to be used. Systemic immunosuppressants such as cyclosporine [482], tacrolimus [122] and sirolimus [483] are administered, however, there is controversy in the use of systemic immunosuppressants in the treatment of corneal rejection as corneal blindness is a non-fatal disease and systemic immunosuppression comes with a heavy burden of negative side effects [2].

The ideal outcome would be to induce a state of immune unresponsiveness without the use of immunosuppressive drugs. We envision that cellular therapies may fill this role. The work described thus far highlights how different strategies can be implemented to improve cellular based therapies, in the absence of immunosuppressive drugs, for the treatment of corneal allograft rejection in mice. The potential mechanisms of action by which DCs and MSCs prolong corneal allograft survival in rodents was also discussed. In this chapter we reflect on what we believe to be the most significant results with an

emphasis on how these findings could be pursued further and on how we could potentially improve experimental design.

6.2 Dexamethasone Generated tDCs Have Distinct Glycosylation Patterns

DCs have been investigated for potential use as a cellular therapy in transplantation due to their ability to maintain peripheral tolerance. Pre-clinical experiments suggested the potential therapeutic use of both donor and recipient derived tolerogenic dendritic cells to prevent organ graft rejection [288]. In a rat model of corneal transplantation, we have recently shown that pre-treatment of donor iDCs with Dexa *ex-vivo* prevents the maturation of iDCs (tDCs) and administration of these cells *in vivo* prolongs RFS of transplant recipients [169]. In this study it was observed that tDCs had increased levels of cell surface α2-6-linked Sia, however it was unclear if this increase in α2-6-linked Sia had any functional consequences.

In chapter three, using both lectin microarray and lectin coupled flow cytometry we demonstrated that generation of tDCs using Dexa treatment leads to significant alterations in cell surface glycosylation. To our knowledge, this is the first time that this has been investigated. Significant differences amongst many different branching structures were observed with SNA-I increasing with the highest significance. For this reason, we pursued α2-6-linked Sia for the remainder of this study, but many other interesting observations were noted with changes in SNA-II, BPA, PNA, DSA, LEL, RCA-I, CPA, ECA, LTA, UEA-I, EEA, GS-I-B4, MPA, VRA and AAL binding. Interestingly, AAL, LTA and UEA-I are all lectins which bind fucosylated glycans, Conde *et al*. recently demonstrated that DC-SIGN-expressing macrophages can inhibit $CD8^+$ T lymphocyte immunity and promote the induction of Tregs which resulted in transplantation tolerance in their model. They demonstrated that DC-SIGN engagement by fucosylated ligands was required for production of IL-10 and they associated this with prolonged allograft survival, as when DC-SIGN signalling was interrupted, tolerance was lost. This study highlights how glycosylation could be targeted and exploited to enhance transplantation tolerance or indeed enhance anti-tumour immunity.

As mentioned, we focused on analysing α2-6-linked Sia in our study as it was the most significantly upregulated glycan after Dexa tDC generation ($p=2x10^{-10}$). Interestingly, the

importance of glycosylation in Treg function has recently been investigated in our lab, Cabral *et al*. described that Treg cell surface glycosylation profiles are distinct depending on anatomical location and this glycosylation profile is vital for their ability to regulate activated T cell responses [484]. Cabral *et al* also investigated if α2-6-linked Sia was functionally important on Tregs and they noted that α2-6-linked Sia was significantly higher on Treg populations when compared to conventional T cell populations. When cleaved using sialidase, Tregs also lost their ability to suppress activated Tregs (unpublished data). This was in line with previous observations from Jenner *et al* who described that Tregs have higher levels of α2-6-linked Sia when compared to activated conventional T cells [308]. Jenner *et al*. also compared human iDCs with iDCs matured with a cytokine cocktail (IL-6, IL-1β, TNF-α and prostaglandin E2) and they observed decreases in α2-6-linked Sia with no changes in α2-3-linked Sia on the more immunogenic DC, this may suggest a possible link between α2-6-linked Sia content and tolerogenicity as we observed significant increases in α2-6-linked Sia on our tDCs with no significant changes in α2-3-linked Sia. These studies, including our own, also demonstrate how highly regulated Sia metabolism is as only increases in α2-6-linked Sia were observed and not a blanket change in Sia molecules.

6.3 α2-6-linked Sia Deficient iDCs and tDCs elicit Immunogenic Responses

After cleaving Sias on the cell surface using neuraminidase we observed increases in MHC I, MHC II and CD86 and increases in pro-inflammatory Th1 mRNA transcripts such as IL-6, IL-1β, iNOS (iDCs only), TNF-α and IL-12p40 (iDCs only) with significant decreases in anti-inflammatory or tolerogenic IL-10. The lab group directed by Paula Videira have investigated the effects of Sia loss on the maturation and function of human monocyte derived dendritic cells. They have reported in the past [144, 180, 182, 192, 310, 311] that Sia loss increases immunogenicity markers, increases pro-inflammatory cytokine gene expression, negatively effects migration and increases phagocytosis. Our study demonstrated that neuraminidase treated iDCs not only lose the ability to suppress allogeneic T lymphocytes, but they become immunogenic themselves. This may indicate that the removal of Sia uncaps underlying structures which are then recognized as a signal for T-cell proliferation or that the Sias may act as ligands for inhibitory Siglecs on the surface of effector cells and once removed, this inhibitory effect is lost. Interestingly, very

recently Li *et al*. [485] demonstrated in a model of triple negative breast cancer that PD-L1 is N-glycosylated and that removal of glycosylation specifically from PD-L1 blocks co-inhibition with its receptor PD-1. They carried out qRT-PCR arrays and analysed the Cancer Genome Atlas dataset on triple-negative breast cancer samples and interestingly the gene ST6GAL1, which codes the sialyltransferase responsible for capping lipids and proteins with α2-6-linked Sia, was one of the most highly expressed N-glycosyltransferases. While the study was extensive and very impressive, they never identified particularly how PD-L1 was glycosylated. It would be very interesting to investigate if α2-6-linked Sia is a requirement of PD-L1 function.

In our study we observed that Sia removal of tDCs did not significantly induce T lymphocyte proliferation. Interestingly, this indicates that, despite the increase of immunogenicity markers and the transcript increase in several pro-inflammatory mRNAs, Dexa treatment of iDCs was sufficient to keep the cells, at least partially, in a non-immunogenic state. Neuraminidase treatment would only cleave cell surface sialic acid, it will not affect glycoconjugates which are secreted from the cells, also it does not prevent the recycling of Sia from the microenvironment. A potential solution is to use a sialyltransferase inhibitor such as 3Fax-Peracetyl Neu5Ac (SI). This SI is cell permeable and acts on the enzymes responsible for capping proteins and lipids with Sia. SI was not readily and cheaply available at the beginning of our study, it is widely available now. Enzymatic treatments such as neuraminidase are harsh on cells, one concern of ours was that potentially the enzymatic digestions were indirectly activating the DCs. Use of a SI would also circumvent this. In work that was not discussed in this thesis, we have used 3Fax-Peracetyl Neu5Ac to treat immunosuppressive TNF-α + IL-1β MSCs (**Appendix Figure 3**). We showed that SI was non-toxic to MSCs, that it did not change morphology, that it did not affect proliferation and did not lead to changes in cell surface phenotype markers (**Appendix Figure 3)**. In line with what we have discussed here, we observed that when we treated MSCs with TNF-α + IL-1β to make them more immunoregulatory we noticed an increase in α2-6-linked Sia. When we used SI to inhibit α2-6-linked Sia we observed that TNF-α + IL-1β MSCs lost their ability to suppress activated T lymphocytes (**Appendix Figure 4**). It would be interesting to repeat the iDC and tDC study using this SI and see if the results indicating the importance of α2-6-linked Sia on iDC cell surface

would be replicated, also to administer the SI treated iDCs and tDCs in our model of corneal transplantation and study if these SI treated cell preparations can still prolong allograft survival.

Together, these results highlight the importance of Sia's in DC biology, especially in the context of iDC allogeneic cellular therapy. In the context of disease, cell glyco-engineering could have positive implications in the treatment of autoimmunity, DC-based vaccines, the tumour microenvironment and transplant biology.

6.4 TGF-β Pre-activated MSCs Have an Altered Phenotype, Can Suppress Activated Immune Cells and Induce Treg Populations *in vitro*

MSCs were originally discovered in murine hematopoietic stem cell studies by Caplan and colleagues in 1991 [486], it was only 4 years after their discovery before they were used as pharmaceutical agents in human bone marrow transplantation for cancer patients by Lazarus and colleagues [487]. MSCs are now the most clinically studied cell therapy candidate for which there is no marketing approval in the USA [488, 489]. As a result of this, there is a substantial interest in research which broadens our understanding of MSC biology and the mechanisms by which they mediate their beneficial effects. A substantial number of studies have been carried out investigating different pre-activation strategies, as pre-activated MSCs have been shown to have increased cell survival, increased differentiation capacity, enhanced paracrine capacity and an increased ability to home to sites of inflammation and injury [377, 384, 477, 490]. In our study we focused on cytokine pre-activation, but other groups have successfully shown that pre-conditioning MSCs by hypoxic environments, pharmacological agents, chemical agents, trophic factors and physical conditions can all improve their efficacy [384].

In the fourth and fifth chapter of this thesis we pre-activated MSCs to enhance their therapeutic efficacy and administered them in our pre-clinical model of corneal transplantation. Before administration we analysed TGF-β MSC phenotype, we also assayed TGF-β MSCs to test if they had immunoregulatory attributes. We observed that TGF-β MSCs expressed the classical MSC cell surface markers such as CD73, CD105, CD44 and CD90 and lacked the expression of MHC II, CD45, F4/80, CD11c, CD86 and

CD80. We observed a significant decrease in MHC I, which is interesting in the context of allogeneic cell therapy and is unique to the TGF-β pre-activation strategy. In our transplant model, the therapeutic cell is derived from the recipient of the graft and thus immunogenicity is not a concern but other pre-activation studies in allogeneic models have demonstrated that pro-inflammatory pre-activation can increase the levels of MHC I and MHC II leading to a negative outcome. Work performed previously in our lab observed an *in vivo* donor-specific antibody response to IFN-γ allogeneic MSCs [491]. Studies by Rafei *et al*. reported that IFN-γ pre-activation of MSCs ablated the therapeutic benefits of allogeneic MSCs in an EAE model and resulted in increased $CD4^+$ T lymphocyte infiltration [492]. Additionally, Cho *et al.*[493]. demonstrated that IFN-γ pre-activated allogeneic MSCs resulted in an increased alloantibody response with increased IgG-mediated humoral responses compared to untreated allogeneic MSCs. A potential obstacle using autologous (syngeneic) MSCs as a therapy is that you would have to aspirate the bone marrow (or other tissue), isolate the MSCs, expand them in culture and then have them pass the required quality control/assurance before release for administration. However, in solid organ transplantation such as heart, lung or kidneys, organ failure is life threatening and the process of isolating MSCs, expanding them and clearing them for release is a long and tedious process. This is where allogeneic MSCs would be convenient as they could be cryopreserved and ready to be administered. Recently, we administered C57BL/6 MSCs locally (subconjunctival injection) 7 days before transplantation and we observed that 70% of transplanted mice experienced RFS over a 40-day period with single injection with doses as low as $5x10^4$ cells (**Appendix Figure 5**). Pre-activation of C57BL/6 MSCs could improve this result dramatically. However, considering our observed increases of MHC I and MHC II on BALB/c MSCs after IFN-γ treatment (**Appendix Figure 1**) and the reported increases in MHC I and MHC II with other pro-inflammatory pre-activation strategies [369, 494-496] maybe TGF-β pre-activation would be the more suitable strategy.

In this study we used the pro-inflammatory cytokines IFN-γ, TNF-α and IL-1β singly and in combination and the anti-inflammatory cytokine TGF-β singly to pre-activate our MSCs. A review of the literature shows that pro-inflammatory cytokines have been almost exclusively used to pre-activate MSCs before *in vivo* administration [236, 242, 266, 348,

497, 498]. Considering that T lymphocytes have been reported to be the main mediators of corneal graft rejection but also because T lymphocyte suppression assays are the main technique employed to measure MSC potency [499] we assayed the ability of pre-activated MSCs to suppress activated T lymphocytes. We observed that both TNF-α + IL-1β MSCs and TGF-β MSCs potently suppressed activated lymphocytes. Reviewing the literature it has been reported that IFN-γ appears to be the key cytokine required to pre-activate MSCs with TNF-α or IL-1β augmenting their potency [236, 266, 348, 365, 499]. Recently it was reported by Jin *et al*. [330] that a duel combination of IFN-γ and TNF-α induced a potently suppressive MSC with significant increases in IDO secretion and PD-L1 expression. This work reinforced studies by Cuerquis *et al*. [327] and Li *et al*. [328] who also reported on combinations of IFN-γ and TNF-α pre-activated MSCs being potently suppressive to T lymphocytes. However, in our study, IFN-γ MSCs were not selected as a candidate, as while they significantly upregulated PD-L1, this did not correlate with T lymphocyte suppression.

Tregs have been reported in several studies to important in the prolongation of graft survival, including corneal allograft survival [62, 263, 265, 381-383] and the induction of Tregs has been attributed to the immunomodulatory molecule PGE2 [364, 377], in which we had observed significant increases in our *in vitro* co-culture systems. Multiple studies investigating the ability of pre-activated MSCs to induce or generate Tregs have been performed. IFN-γ treated umbilical cord derived MSCs have demonstrated an ability to induce Tregs *in vitro* [324], additionally, IL-1β treated umbilical cord-derived MSCs demonstrated an ability to induce Tregs *in vivo* [500] in a model of colitis. Similarly, IFN-γ and TNF-α pre-activated MSCs could induce the differentiation of $CD4^{+}IL\text{-}10^{+}$ and $CD8^{+}IL\text{-}10^{+}$ Treg subpopulations [328]. In our study, TGF-β MSCs significantly increased both the frequencies and numbers of Tregs while TNF-α + IL-1β MSCs did not, this may be the potential reason as to why TNF-α + IL-1β MSCs enviably failed to prolong RFS despite such promise as a candidate *in vitro*. Interestingly, not only did we observe an increase Tregs in the TGF-β MSCs wells, we also observed increased CD73 and PD-L1 expression on the induced Tregs generated in our TGF-β MSC – T lymphocyte cultures (**Appendix Figure 2**), indicating that TGF-β MSCs are not only increasing the number of Tregs in co-culture but these Tregs are potentially more immunomodulatory.

It is a possibility that MSCs response to cytokine pre-activation is strain and species specific. It was demonstrated by Hashemi *et al*. that adipose derived MSCs from BALB/c or C57BL/6 mice have different and distinct immunosuppressive properties [54]. C57BL/6 MSCs respond to LPS stimulation by increasing the secretion of NO while the BALB/c counterpart did not. Therefore, the reported *in vivo* therapeutic benefits from pro-inflammatory MSCs in the literature which range across syngeneic, allogeneic and xenogeneic therapies and the failure of pro-inflammatory pre-activation that we reported here in this study may be due to a strain- and species-specific difference. This is important when considering MSCs as a therapeutic product for sale and hints at a possible personalised medicine approach where the background and immunological make-up of the donor and the disease in question may have to be considered when selecting an appropriate MSC therapy.

6.5 TGF-β MSCs Do Not Secrete TGF-β After Pre-activation and Mediate Their Immunosuppressive Effects Via PGE2

MSC mediated immunomodulation can occur via cell-cell contact, secretion of soluble factors or combinations of both. The soluble mediators that have been reported to be vital in MSC mediated immunomodulation are IDO, TGF-β, IL-10 PGE2 and NO [252]. Further investigation into TGF-β mediated immunosuppression of T lymphocytes and Treg induction revealed mechanistic insights. Along with PGE2, TGF-β itself has been reported to be responsible for MSC mediated immunosuppression and Treg production *in vitro* and *in vivo [199, 364, 379, 397, 398]*. To investigate if the exogenous TGF-β treatment resulted in MSC derived TGF-β secretion and in turn Treg inducement, we pre-activated MSCs with TGF-β, incubated the MSCs for 72 hours and then washed off the TGF-β containing media. We replaced the TGF-β containing media with fresh media and then assayed the supernatants after 24 and 48 hours via ELISA (**Appendix Figure 6**). It was noted that TGF-β MSCs did not secrete MSC-derived TGF-β after pre-activation. Recently, glycoprotein A repetitions predominant (GARP) was shown to bind latency-associated peptide (LAP)/TGF-β1 to the cell surface of activated Tregs [501]. It has been recently demonstrated that both human and mouse MSCs express GARP which presents LAP/TGF-β1 on their cell surface [396]. GARP can sequester and activate latent TGF-β produced by the cell or in the local microenvironment, this process has been reported to

be important for Treg mediated suppression of T lymphocytes [502]. Carrillo-Galvez *et al*. demonstrated that GARP expression on MSCs contributed to their ability to inhibit T-cell responses in vitro [396]. In line with the previous experiment we investigated if TGF-β pre-activation increased the GARP/LAP complex on the surface of MSCs via flow cytometry (**Appendix Figure 6**). We noticed no significant changes, concluding that TGF-β MSC mediated immunosuppression and Treg induction was MSC-derived TGF-β independent.

Mechanisms of MSC-mediated immunosuppression vary among different species [243]. Traditionally, IDO has been described one of the main mediators of immunosuppression by human MSCs, whereas NO is one of the main mediators of immunosuppression by mouse MSCs under the same culture conditions [243]. Ren *et al*. demonstrated that mouse MSCs are potently immunosuppressive both *in vitro* and *in vivo* and that suppression was mediated by NO after pre-conditioning with pro-inflammatory cytokines [236]. As our study confirmed, Ren *et al*. reported that MSCs secrete high levels of NO and chemokines in response to pro-inflammatory pre-activation and they convincingly proved that MSCs directly suppress proliferation and cytokine production by lymphocytes in a NO dependent manner using knockout studies [236]. NO is a temperamental and rapidly diffusing gaseous molecule [503] and studies have demonstrated that NO can modulate many enzymes, ion channels, and receptors [236]. NO is known to affect T cell receptor signalling, cytokine receptor expression and to modulate T lymphocyte phenotype and importantly it is a highly unstable immunoregulatory molecule and its effects are mediated locally [236]. Although TNF-α + IL-1β MSCs secreted high levels of NO and were potently immunosuppressive, when administered in our model they failed to prolong corneal allograft survival whereas TGF-β MSCs secreted no detectable NO and significantly prolonged corneal allograft survival indicating the NO is not important in TGF-β MSC mediated prolongation in RFS. Interestingly, we observed an increase in Argininosuccinate Synthase 1 (*Ass1*) in TGF-β MSCs which encodes the enzyme that catalyses the penultimate step of the arginine biosynthetic pathway. In myeloid cells, it has been reported that arginine is metabolised either by nitric oxide synthases or by arginases and the fate of arginine metabolism is an integral regulator of innate and adaptive immune response [449, 450], where nitric oxide metabolism is linked to a pro-

inflammatory outcome and arginine is linked to an anti-inflammatory outcome. *Ass1* was 15-fold upregulated in TGF-β MSCs compared to MSCs with *Nos2* being undetectable, potentially explaining why NO was not produced by TGF-β MSCs as the arginine was potentially being competitively catalysed by arginases.

We observed that TGF-β MSCs secreted relatively high levels of PGE2, our preliminary RNASeq data showed a 73-fold increase in COX-2 gene expression. COX2 when induced, leads to the production of prostaglandins. PGE2 is a potent immunosuppressant that inhibits the ability of T lymphocytes to proliferate [249, 250, 252]. Furthermore, PGE2 has been reported to increase IL-10 production by macrophages [253, 368] and to inhibit the differentiation of monocytes into functional DCs [504]. Not only this, PGE2 has been shown to increase the secretion of factor H, an inhibitor to complement activation. Additionality, PGE2 induces Tregs from $CD4^{+}CD25^{-}$ T lymphocytes by modulating the expression of the transcription factor FoxP3 and therefore contributes to Treg function [251]. Interestingly, PGE2 has been reported to function in a cell-cell contact dependent manner [246] as we have also observed in this study. MSC pre-activation increases the levels of secreted PGE2, studies using IFN-γ [376], IL-1β [325], LPS + IL-1β [375], and IFN-γ + TNF-*α* [252, 329] have all confirmed increases in PGE2 after pre-activation. In a study carried out by Gray and colleagues [375] where they screened several cytokine\s (IFN-*β*, IFN-*γ*, IL-1*β*, IL-6, LPS, and poly(I:C)) ability to enhance MSC mediated immunosuppression via PGE2, they demonstrated that a combination of IL-1β and TLR4 stimulation by LPS produced most PGE2.

PGE2 can selectively suppress many different effector cells such as macrophages, neutrophils, Th1 cells, NK cells and cytotoxic T lymphocytes while promoting Th2 and Treg responses [458]. While suppressing activated immune cells, PGE2 also actively inhibits the recruitment of new inflammatory cells encouraging the sequestering of Tregs and myeloid-derived suppressor cells (MDSCs) [458]. PGE2 exerts its biological effects via the E-type prostanoid (EP) receptors of which there are four, EP1-EP4 [505]. The heterogenicity of PGE2 signalling is highlighted by the fact that it has 4 different receptors. To add another layer of complexity, 8 splice variants of EP3 exist in humans and at least 3 forms in mouse [458]. The advanced biology of the EP receptors has been

extensively reviewed [458, 505] and will not be discussed here in detail. PGE2's interactions with its receptors are thought to be dependent on location, tissue type, cell type and binding affinity [506]. EP3 and EP4 are high affinity receptors while EP1 and EP2 require significantly higher concentrations of PGE2 in order to initiate signalling [458]. PGE2 signalling via the EP4 receptor has been shown to inhibit cytotoxic T lymphocyte function [507] and induce Tregs [508]. Interestingly, we also pharmacologically inhibited EP1 signalling in our co-culture systems and no changes in TGF-β MSC mediated suppression of T lymphocyte proliferation or induction of Tregs was noted (**Appendix 7**), from this we concluded that TGF-β MSC mediated modulation of immune cells was EP4 dependent.

To summarise thus far, our study demonstrated that TGF-β pre-activation of MSCs potently suppresses T lymphocyte proliferation and induces Tregs *in vitro*. TGF-β signals via the canonical SMAD 2/3 pathway which leads to the production of PGE2. PGE2 signals via the EP4 receptor and its immunomodulation of both conventional T lymphocytes and Tregs is cell-cell contact dependent. To our knowledge, this study is the first to investigate TGF-β as a credible pre-activation strategy to generate an enhanced therapeutic MSC for *in vivo* administration.

6.6 TGF-β MSCs Induce Tregs In the Lungs of Treated Animals and Potentially Polarize Lung APCs To A Regulatory Phenotype

Intravenously (i.v.) administered MSCs become trapped in the lungs of treated animals and it is now becoming clear that immune cells of the lung play an important role in mediating MSC immunomodulatory effects. Multiple studies have demonstrated that once trapped in the lungs MSCs are cleared or migrate approximately 24 hours after administration [269, 509-512], the caveat in these studies is that they cannot distinguish between live/intact MSCs and dead/phagocytosed MSCs. A recent study utilising radiolabelled MSCs to track them *in vivo* (mouse) demonstrated that viable MSCs can be isolated from the lungs up to 24 hours after administration, however, after this time they can be identified in other tissues, when these MSCs were isolated, no live cells were recovered. Considering that MSCs have been reported to migrate to sites of injury, this group induced an ischemic-reperfusion injury in the liver, it was noted that this did not

trigger the migration of viable MSC to the liver [405]. This potentially suggests that APCs are phagocytosing dead or dying MSCs and the radio-label being detected in other organs after 24 hours are MSC particles inside APCs. While this study alone cannot rule out the potential of MSCs migrating to other organs and exerting their immunomodulatory effects it does seem likely that the immune cells of the lung play an important role in MSC mediated effects.

Anti-inflammatory APCs, such as tDCs and M2 macrophages along with Tregs are modulated by MSCs and act as intermediaries in MSC mediated immunosuppression [245, 246, 253, 267, 513]. It has been demonstrated that MSCs can reprogram lung macrophages to a regulatory phenotype via MSC derived PGE2 and TSG6 [253, 267]. Interestingly, we observed a significant decrease in CD80 and CD86 on macrophages in the lungs of TGF-β MSC treated animals, suggesting a M2 phenotype. TGF-β MSCs secrete high levels of PGE2 but also reviewing the RNASeq data we observed a 2.2-fold (p= 0.006) increase in *Tnfaip6* whose gene product is TSG-6 (**Appendix Figure 8**), potentially indicating a mechanism for the observed decrease in APC frequencies and a decrease in their activation status. Recently, Braza *et al*. [380] administered PKH26 labelled MSCs and demonstrated that the vast majority of PKH26 labelled cells after 1-10 days expressed macrophage markers, reinforcing the idea that MSCs are phagocytosed shorty after administration *in vivo*. The key finding and most interesting observation in this study was that they demonstrated that $PKH26^+$ but not $PKH26^-$ macrophages displayed an M2 phenotype [380]. Additionally, Galleu and colleagues demonstrated in a mouse model of graft-versus-host disease (GvHD) that MSC mediated immune modulation was dependent on apoptosis and subsequent phagocytosis by lung APCs which then secrete IDO to suppress the immune system [366]. A key finding in this study was that i.v. administration of MSCs, that were already apoptotic, did not induce immunoregulatory APC populations. This potentially indicates that the site of apoptosis or possibly how the MSCs become apoptotic is important. The authors suggested that the MSCs could possibly modulate the local environment prior to apoptosis and this could be a key event in their immunosuppression [366].

As mentioned previously, Tregs have been reported to be induced by MSCs after i.v. injection [514-516]. Akiyama *et al*. demonstrated that i.v. administration of MSCs into mice resulted in apoptotic T lymphocytes in the peripheral blood of the treated animals between 6-72 hours after administration. They reported that the apoptotic T lymphocytes reprogramed macrophages in the spleen to produce TGF-β and that subsequently resulted in the up-regulation of Tregs [517]. Findings by Ko *et al*. [516] supported this study and findings in our study as after administration (i.v.) of human MSCs in mice they reported increases of Tregs in the peripheral blood, the DLNs and in the lungs of treated animals in a model of ocular autoimmunity [516].

In review, it is likely that MSCs become trapped in the lungs of injected animals for at least 24 hours post administration. Here they secrete factors into the local microenvironment modulating lung immune cells and potentially increasing Tregs as we observed in our model. The MSCs will then enter apoptosis where their debris is phagocytosed by APCs thereby modulating the APC phenotype to a regulatory phenotype, it is then possible that these APCs migrate out of the lung to the peripheral immune organs whereby they can act as an intermediary in system MSC mediated immunosuppression.

6.7 TGF-β MSCs Induce Bregs, Tregs and Modulate APCs in the DLNs and Spleens of Treated Animals

As discussed above, there is a lot of evidence in the literature to suggest that i.v. administered MSCs become trapped in the lungs and from here distribute their beneficial effects via intermediary immune populations. However, this does not rule out the possibility that small numbers of MSCs could migrate to the peripheral immune organs and exert their suppressive effects directly. Regardless as to if MSCs mediate their effects indirectly or directly, it is clear that MSCs modulate the splenic compartment after i.v. administration [267, 366, 518]. It has been reported by us and others that systemically administered MSCs increase regulatory immune populations in the spleens of rodents which have received corneal transplants and these populations have been associated with prolonged RFS [263, 265].

The adaptive immune response to transplanted tissue is the major barrier to a successful transplantation, for this reason we analysed the frequencies of B cells, $CD4^+$ lymphocyte

populations, $CD8^+$ lymphocyte populations and Tregs in the organs of untreated and treated animals to investigate if TGF-β MSCs were modulating the adaptive immune cells. While T effector cells are the main mediators of rejection, B cells are known to be responsible for the production of alloantibodies leading to both acute and chronic allograft rejection [406, 407]. Not only this, they are known to present graft derived antigens to alloreactive T lymphocytes via the indirect pathway of allorecognition [407-409]. We analysed the frequency of B cells in the organs of both TGF-β MSC treated animals and allogeneic controls and observed that there were significantly lower B cell percentages in the DLN and the spleen of treated animals with no significant changes in the lungs. Interestingly, when we analysed the percentage of Bregs ($CD19^+CD24^+CD5^+$ cells) in this decreased B cell population we observed a significant increase in the frequency these cells in both the DLNs and spleens.

As previously discussed in the introduction, ACAID is a phenomenon whereby alloantigen in the eye is processed by macrophages which migrate to the spleen and induce alloantigen specific Tregs [519]. There is evidence that ACAID is induced after corneal transplantation, generating regulatory alloantigen specific responses in the spleen [20, 93, 520, 521]. ACAID induction has also been reported to be dependent on the presence of regulatory splenic B cells [56], it is speculated that alloantigen released by the macrophages is processed by regulatory splenic B cells and presented to the T lymphocytes to induce tolerance. The importance of splenic cells in ACAID has been demonstrated by Niederkorn *et al*. whereby the removal of the spleen in transplanted animals increased the incidence of graft rejection [520]. With our observed significant increases of Bregs in the DLNs and spleens of TGF-β MSC treated animals coupled with our observed significant increases in Tregs in the DLNs, this may indicate that TGF-β MSCs are creating an environment where this phenomenon has an increased ability to occur. This could be examined further by a splenectomy prior to corneal allograft transplantation, if the administration of TGF-β MSCs failed to produce Tregs in the DLNs of transplanted animals it would indicate the importance of the spleen and the observed induced Bregs populations.

As mentioned previously, a vital step in the corneal allograft rejection process is the presentation of alloantigen from donor or recipient APCs to allo-reactive T lymphocytes. This occurs either in the cornea, in the area surrounding the eye and conjunctiva or in the DLN [435]. The importance of the DLN in corneal allograft rejection has been demonstrated by Yamagami *et al*. [93, 94] where they removed the DLNs in both a model of low risk and high risk corneal transplantation. Removal of the DLNs inhibit graft rejection via inhibition of the allo-specific DTH responses [93], demonstrating the importance of the initial antigen presentation phase and the subsequent expansion of alloreactive effector T lymphocytes in the DLNs. In our study, in TGF-β MSC treated animals at the average day of rejection we observed a significant enrichment of Treg frequencies and decreases in overall APC frequencies with decreases in co-stimulation markers. DTH is crucial in the mechanism of corneal allograft rejection with DLN being vital to its initiation [82, 93]. TGF-β MSCs potentially interrupt this process by increasing the frequencies of Tregs, thereby suppressing effector T lymphocyte function. TGF-β MSCs significantly decrease activation markers on APC populations in all organs indicating that they may also interrupt the allo-antigen presentation process preventing the expansion of all-reactive T lymphocytes.

6.8 Limitations and Future Direction

An interesting question that we were unable to answer in this study is whether TGF-β MSCs can migrate from the lung to other tissues to exert their immunomodulatory effects. We observed changes to immune populations in the spleen and DLNs of TGF-β MSC treated animals, it would be interesting to investigate if the MSCs modulate these immune populations directly. As discussed above, due to the size of culture expanded MSCs they become trapped in the lung as a bolus of cells upon i.v. administration. As a result, it is thought that MSCs may mediate their immunomodulatory effects via an intermediary immune population. Several studies focusing on the fate of i.v. administered MSCs in rodent models have suggested that MSCs are cleared from the lung within 24 hours of injection and these studies have also suggested that the apoptosis of MSCs is a requirement of their immunomodulatory attributes [366, 367, 380, 405]. The caveat in these studies is that they were unable to assess if the particles detected were MSCs or

MSC fragments inside phagocytes. One possible solution for this would be to label the MSCs with a fluorescent dye and inject them via the tail vein., then harvest the organs in question and prepare a single cell suspension. The cells could then be analysed using an imaging flow cytometer. Imaging flow cytometers render high resolution images of every cell in the image stream. This technology could identify each labelled MSC co stained with specific phagocyte markers and the images would demonstrate whether the MSCs remain whole or are phagocytosed. Alternatively, more recent *in vivo* imagining systems such as 3D cryo-imaging could be utilized. This technology is capable of sectioning a whole cryo-preserved animal taking thousands of individual high-resolution images. These images can then be rendered to create a 3D model of the animal which has single cell resolution. These technologies could elucidate if MSCs are actively migrating to organs and directly mediating their effects or are they being phagocytosed and mediating their immunomodulatory effects indirectly via intermediary cell populations. Recently, studies using 3D cryo-imaging have backed up reports suggesting that MSCs are preferentially found in the lung or liver after i.v. infusion and that the majority of MSCs are cleared within 24 hours [522, 523].

We observed that TGF-β MSCs had an ability to increase the numbers and frequency of Tregs in MSCs-T lymphocyte co-cultures. Also, that the Tregs in these wells had increased immunomodulatory potential via elevated PD-L1 and CD73 cell surface expression. Furthermore, we observed that TGF-β MSCs increased the number of Tregs in the lungs and DLNs of treated animals. However, it is still unknown if these Tregs are important in TGF-β MSC-mediated prolongation of survival. It would be interesting to investigate using Treg knockout mice if these induced populations of Tregs are important in mediating survival of the transplanted corneal graft. Alternatively, lungs or DLNs from TGF-β MSC treated animals could be harvested and the Treg populations could be sorted using a cell sorting flow cytometer based on their GFP positivity. The collected Tregs could then be injected in the absence of TGF-β MSCs and we could study if the Tregs themselves could prolong corneal allograft survival.

In line with this, our study demonstrated that TGF-β MSCs induced multiple regulatory immune populations which were associated with graft survival. However, it does not

answer the question if TGF-β MSCs are inducing immune tolerance to the graft or are they inducing survival of the graft due to a non-specific immune hypo-responsiveness? To answer this question, future studies should monitor corneal allograft transplant recipients for 100+ days until the immunomodulatory effects of the TGF-β MSC have subsided. Corneal allograft transplanted animals should then receive an allogeneic skin transplantation from the same donor as the corneal tissue. The rejection kinetics of this skin transplant would indicate if TGF-β MSCs induce a memory regulatory immune response and transplantation tolerance

A limitation to our study was that we were unable to collect information regarding how the immune populations of the cornea differ from a rejected allograft compared to an accepted allograft after the administration of TGF-β MSCs. We observed significantly less corneal opacity and neovascularization on the average day of rejection in TGF-β MSC treated animals. It would be interesting to analyse how the immune cell compartment changes in corneas of animals that received TGF-β MSCs. However, the cornea is a delicate tissue, our attempts to characterise the immune cell compartment of the cornea failed for two main reasons. Firstly, the cornea contains very few cells, even a rejected opaque cornea in our hands had ≤ 100,000 cells. This made immune profiling very difficult via flow cytometry. Secondly, the enzymatic digestion process is harsh on the cornea, this resulted in high levels of cell death leading to large variation of results between animal groups. A potential solution to this would be to pool several corneas from the same treatment groups together to obtain the appropriate number of live cells for analysis. Another solution would be to develop and optimise immunohistochemistry protocols to profile the immune cell compartment of the cornea. Another option would be to analyse the corneal tissues using mass cytometry were antibodies are labelled with heavy metal ions instead of fluorochromes which allows the use of more antibody combinations without the risk of significant spill over between channels.

6.9 Concluding Remarks

These studies detail how syngeneic MSCs can be pre-activated with TGF-β to enhance their therapeutic efficacy before administration in vivo, it also details the importance of glycosylation, specifically sialic acid, on the tolerogenic properties of DCs. The results of

the experiments in chapter 3 point towards the potential of DC surface sialylation as a therapeutic target to improve and diversify DC-based therapies and treatments. In the context of disease, cell glycoengineering could have positive implications in DC-based vaccines, the tumour microenvironment and transplant biology. The results of chapter 4 and 5 identify new therapeutic strategies to enhance MSC based therapy to promote the success of allogeneic tissue transplantation

Appendices

Appendix A:

Supplementary Figures

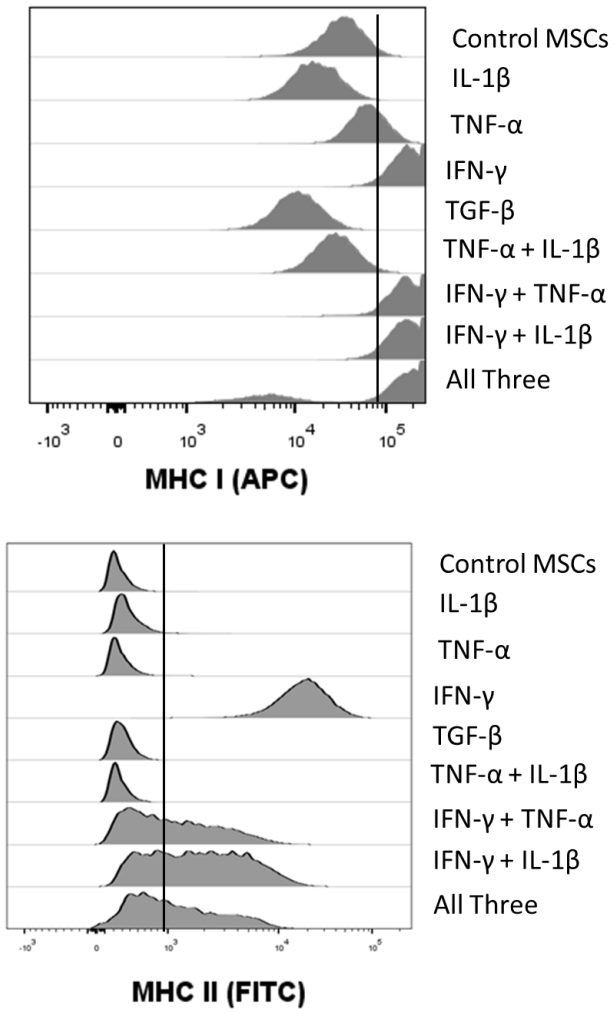

Appendix Figure 1. IFN-γ increases the levels of MHC I and MHC II on BALB/c MSCs. MSCs were treated with either pro or anti-inflammatory cytokines and the expression of MHC I (APC) or MHC II (FITC) was analysed by flow cytometry. Preliminary experiment. n=*2*.

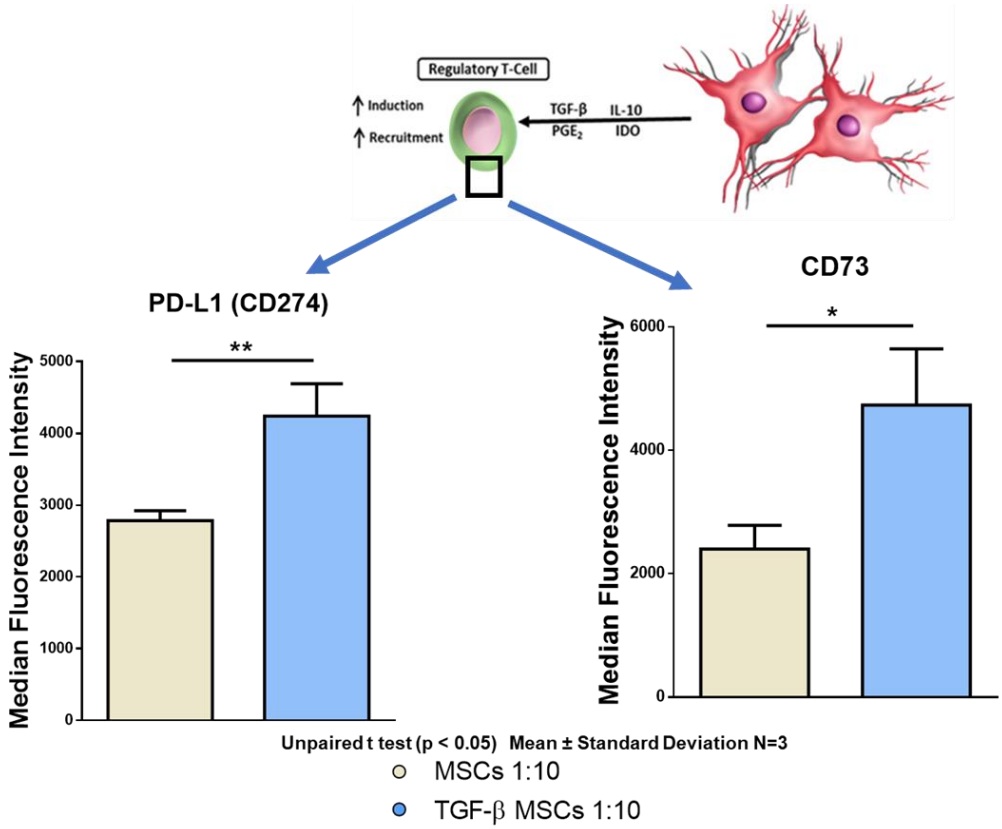

Appendix Figure 2. TGF-β MSC generated Tregs have increased expression of PD-L1 and CD73. Tregs from TGF-β MSCs – T lymphocyte co-cultures were analysed after 96-hour co-culture. The expression of either PD-L1 (PE) or CD73 (APC) was analysed by flow cytometry. (*n=3)*. Unpaired t test.

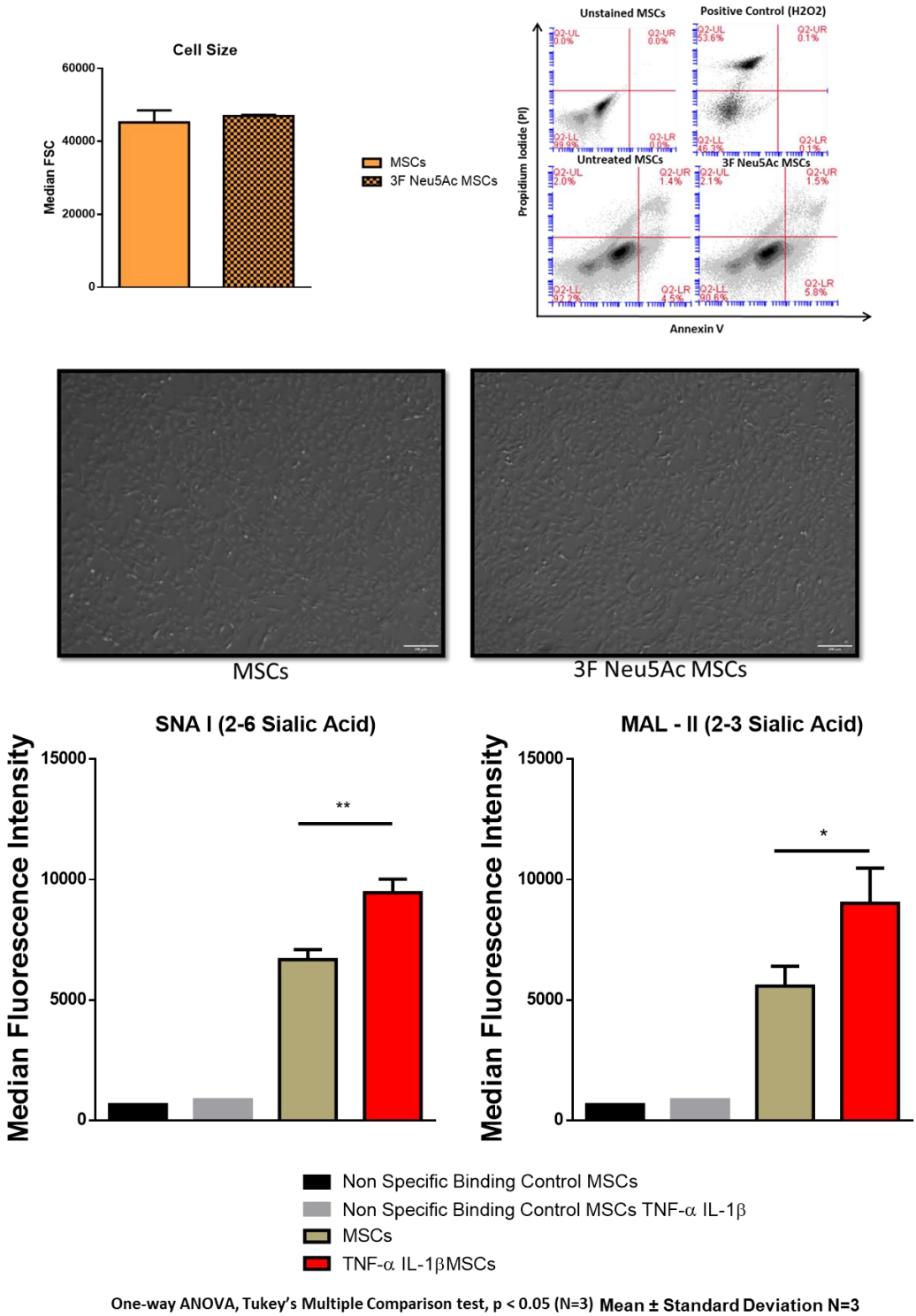

Appendix Figure 3. SI treatment of MSCs does not affect cell size or viability. Pro-inflammatory pre-activated MSCs have increased levels of sialic acid compared to untreated MSCs. MSCs were treated with 3Fax-Peracetyl Neu5Ac, a potent sialyltransferase inhibitor for two consecutive passages. Cell size and viability were analysed by flow cytometry. The expression of sialic acid was assayed on the surface of pro-inflammatory pre-activated MSCs via lectin-coupled flow cytometry. Error bars: mean +/- standard deviation *p<0.05, **p<0.01 ***p<0.001 ****p<0.0001. One-way ANOVA, Tukey's Post Hoc test (n=3).

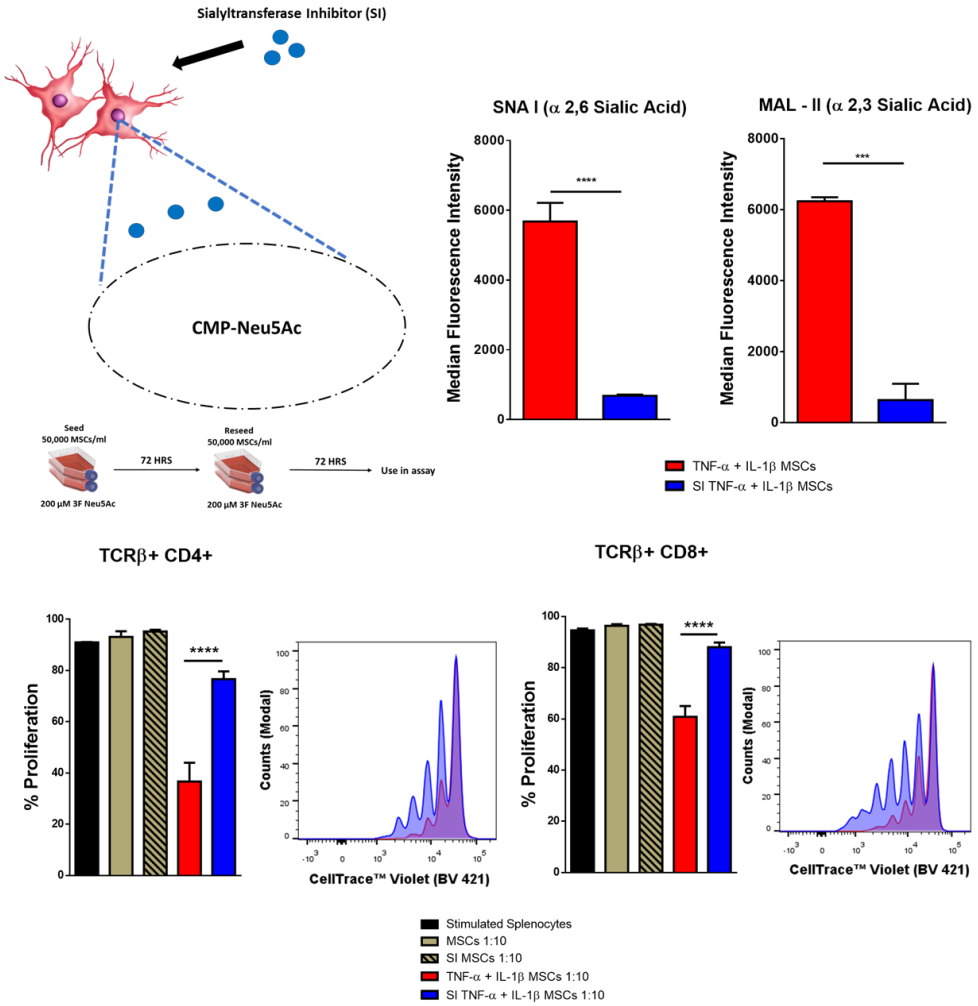

Appendix Figure 4. SI successfully removes Sia from pro-inflammatory pre-activated MSCs which results in loss of T lymphocyte suppression attributes. MSCs were treated with 3Fax-Peracetyl Neu5Ac, a potent sialyltransferase inhibitor for two consecutive passages. The loss of Sia was assayed via flow cytometry using MAL II to detect α2,3 linked sialic acid and SNA I to detect α2,6 linked sialic acid. TNF-α+IL-1β MSCs were treated with or with SI and co-cultured for 96 hours with CD3-CD28 stimulated T lymphocytes to study the effect of Sia loss on MSCs. Error bars: mean +/- standard deviation *p<0.05, **p<0.01 ***p<0.001 ****p<0.0001. One-way ANOVA, Tukey's Post Hoc test (n=3).

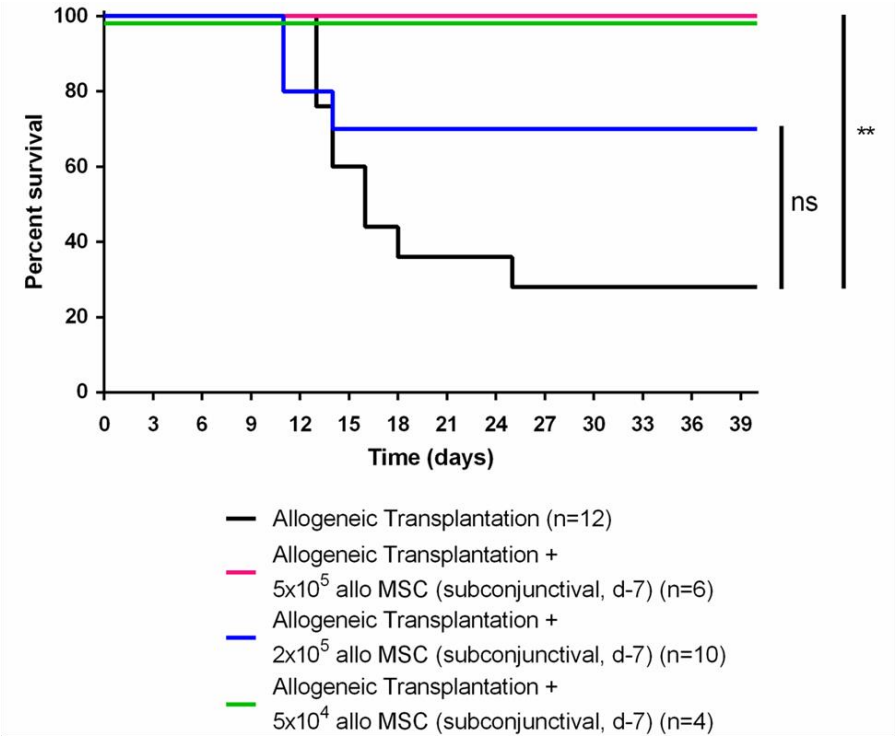

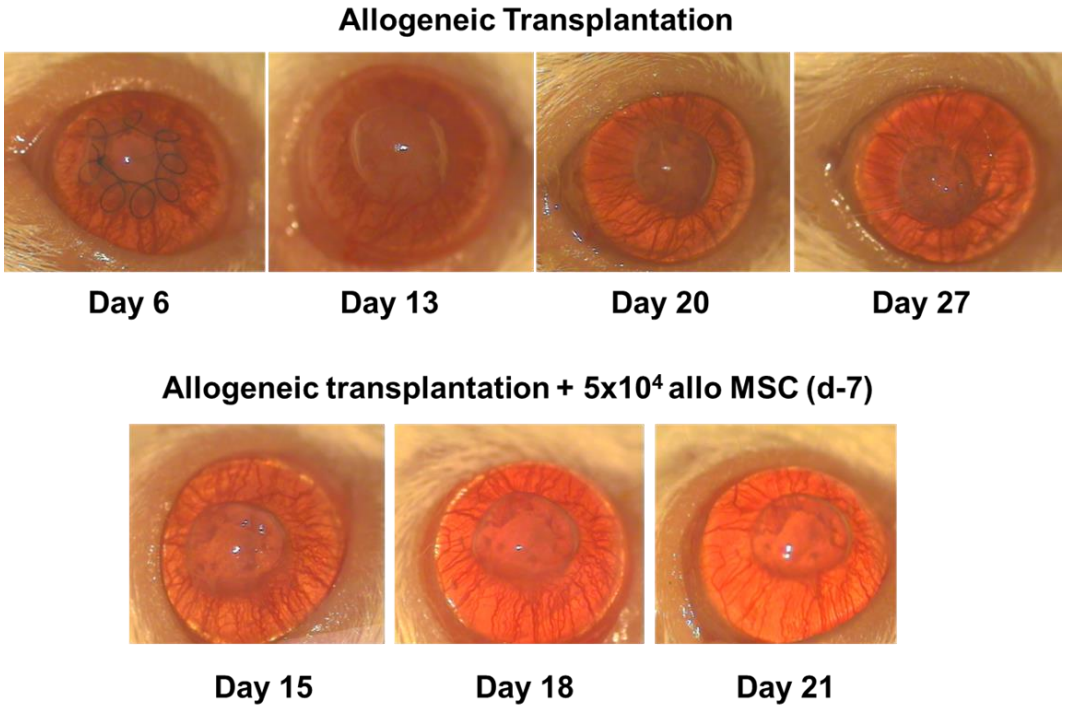

Appendix Figure 5. Subconjunctivally administered MSCs prolong corneal allograft survival. C57BL/6 MSCs were injected subconjunctivally seven days prior to allogeneic transplantation (day -7). BALB/c mice received either no injection or a single bolus injection of 5 x 10^5 (high-dose), 2 x 10^5 (medium-dose) or 5 x 10^4 (low-dose) allogeneic C57BL/6 MSCs in the subconjunctival space followed by allogeneic corneal transplantation 7 days later. Allogeneic transplant survival was monitored over a period of 40 days by microscopy. Graft opacity as the main indicator of cellular infiltration and endothelial dysfunction was also recorded.

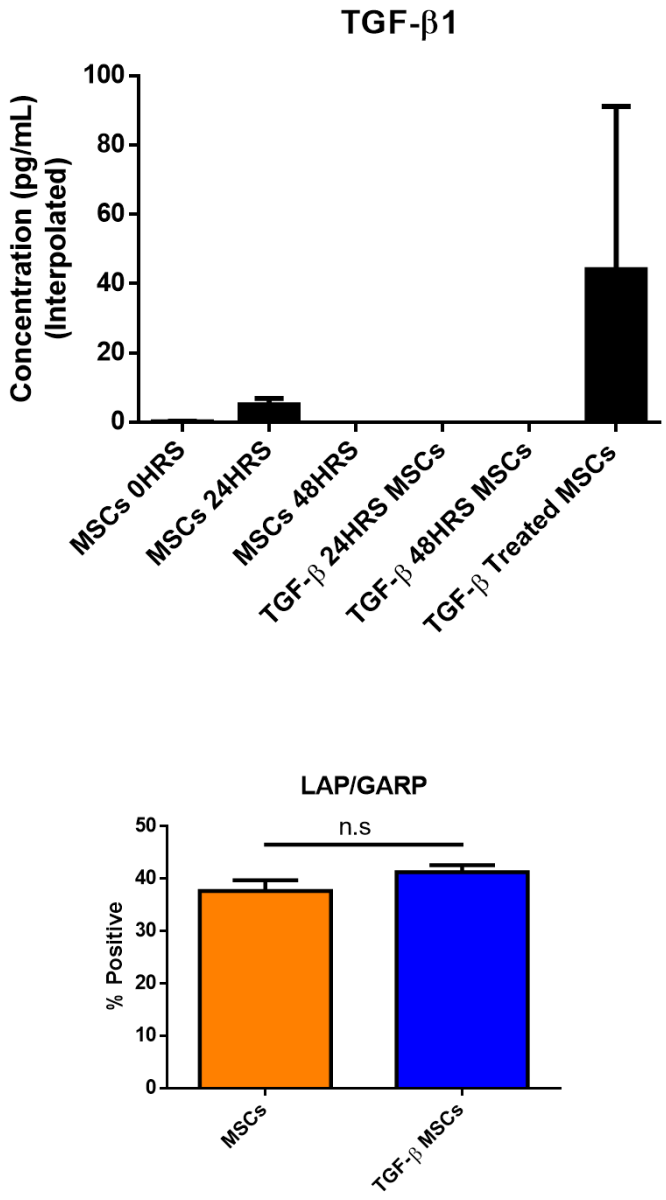

Appendix Figure 6. TGF-β MSCs do not secrete TGF-β nor sequester it on their cell surface after pre-activation. MSCs were conditioned with TGF-β for 72 hours. The conditioned media was then taken off the MSCs and the MSCs were washed three times with PBS. Fresh media was then placed on the cells and collected 24 hours and 48 hours later. The collected media was assayed on a TGF-β ELISA using media containing TGF-β as a control (TGF-β MSC treated MSCs). MSCs have been reported to hold latent TGF-β on their surface via the LAP/GARP complex. Untreated MSCs and TGF-β MSC treated MSCs were assayed via flow cytometry. Error bars: mean +/- standard deviation *p<0.05, **p<0.01 ***p<0.001 ****p<0.0001. Student's t test and One-way ANOVA, Tukey's Post Hoc test (n=3).

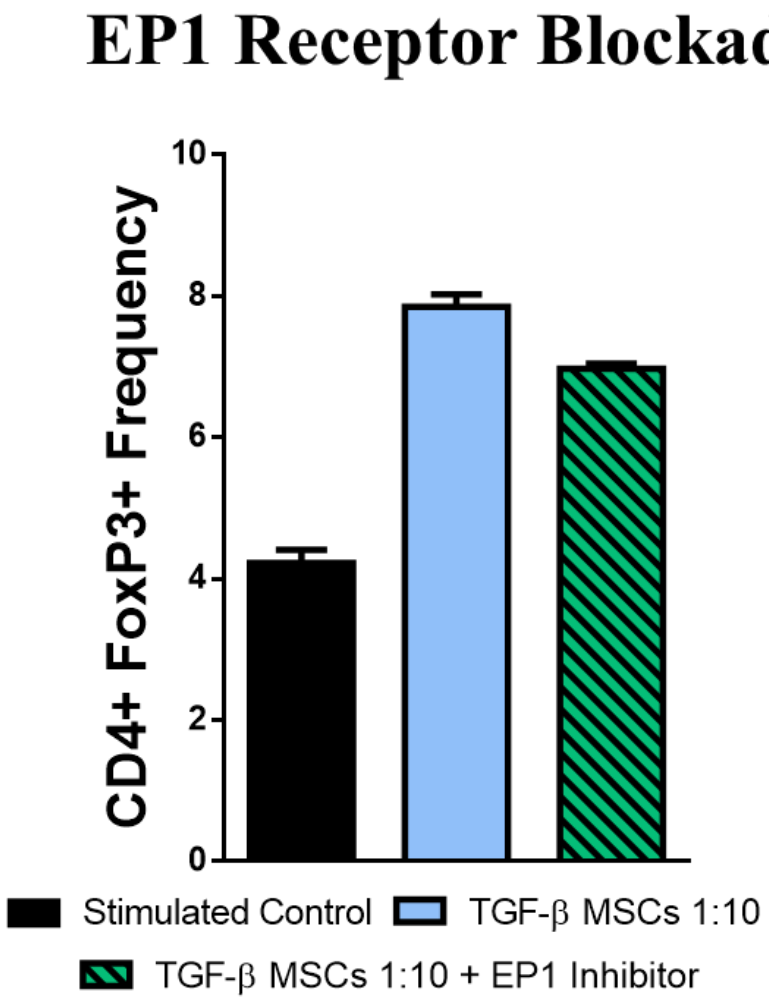

Appendix Figure 7 EP1 antagonist does not significantly affect TGF-β MSCs ability to generate Tregs in MSC T lymphocyte co-cultures. | TGF-β MSCs and TGF-β MSCs + EP1 Inhibitor (1 MSC to 10 lymphocytes) were cultured in normoxia in T lymphocyte co-cultures for 96 hours with CD3/CD28 stimulated lymphocytes. $CD4^{+}FoxP3^{+}$ lymphocyte frequency. Error bars: mean +/- standard deviation *p<0.05, **p<0.01 ***p<0.001 ****p<0.0001. One-way ANOVA, Tukey's Post Hoc test (n=3).

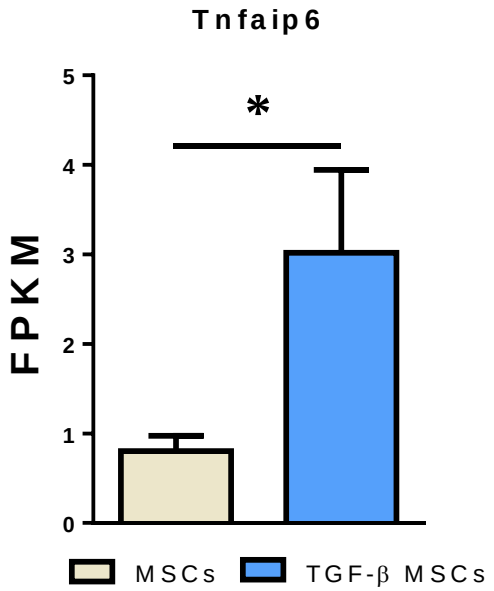

Appendix Figure 8. Fragments Per Kilobase of transcript per Million mapped reads. The expression level (FPKM value) of known genes and transcripts were calculated using ballgown. (Tnfaip6 = TSG-6). Error bars: mean +/- standard deviation *p<0.05, **p<0.01 ***p<0.001 ****p<0.0001. Student's t test (*n=3*).

Appendix B:

Reagents, Plastics, Buffers and Media Formulations

Cell Culture Medium and Additives		
Item	**Supplier**	**Cat. No.**
alpha-MEM	Gibco-Biosciences	32561029
Ascorbic acid 2-Phosphate	Sigma	A8960
Bone Morphogenetic Protein		
Bovine Serum Albumin	Sigma	A2153
Dexamethasone	Sigma	D4902
DMEM (high glucose)	Gibco-Biosciences	31966-021
Dumethyl Sulfoxide (DMSO)	Sigma	2650
Equine Serum	Fisher	10407223
Fetal Bovine Serum (FBS)	Sigma	F7524
ITS+ Supplement	Sigma	I3143
L-Proline	Sigma	P5607
Penicillin/Streptomycin	Sigma	P4333
Sodium Pyruvate	Gibco	15240062
TGF-β1	Bio-techne	7666-MB-005
TNF-α	Peprotech	400-14
Trypsin 0.25% EDTA	Biosciences	25200056
Hematoxylin	Sigma	H36
L-Glutamine	Biosciences	25030024
Mouse activatror CD3/CD28 Dynabeads	Life Technogies	11456D
Plastics		
Item	**Supplier**	**Cat. No.**
15ml tubes	Sarstedt	62.554.502
25ml blow out pipette	Sarstedt	86.1685.001
5ml blow out pipette	Sarstedt	86.1253.001
5ml Facscan	Sarstedt	55.1578
6 well plates, flat bottom	Sarstedt	83.392
T175 Culture Flask	Fisher	10246131
24 well plates, flat bottom	Sarstedt	83.3922
96-well plates, round bottom	Sarstedt	83.3926
50ml tubes	Sarstedt	62.547.254
ELISAs and Bioplex		
Item	**Supplier**	**Cat. No.**
human/mouse TGF-beta ELISA	eBioscience	88-8350-22
IFN-g ELISA	eBioscience	88-7314
Granzyme B ELISA	eBioscience	88-8022
PGE_2 ELISA	Abcam	ab133021
Bioplex Plate and Reagents	Fannin Heaalthcare	M60-009RDPD
Western Blotting		

Item	Supplier	Cat. No.
30% acrylamide mix	Sigma	A3699 5x100ml
Amersham Protran 0.2um NC	Biosciences	15249794
ammonium persulfate	Sigma	A3678 - 100g
Anti-mouse HRP	Cell Signalling	7076s
Anti-rabbit HRP	Cell Signalling	7074s
a-SMA antibody	MSC	PA5-19465
CL-Xposure Film	Sigma	34088
ECL Western Blotting Substrate	Sigma	32106
Glycerol	Sigma	G2025 500ml
Hydrochloric Acid		H1758-100ml
Lamin B1 antibody	MSC	PA5-19468
Methanol	Sigma	34860 - 2.5L
N,*N*′,*N*′-Tetramethylethylenediamine	Sigma	T9281 - 50ml
Sodium dodecyl sulfate	Sigma	L3771-100G
X2 PageRuler prestained protein ladder	Fisher	11832124

T cell medium

RPMI-1640	
Fetal bovine serum (FBS)	10%
Penicillin-streptomycin	1%
L-Glutamine	1%
Non-essential amino acids	1%
β-Mercaptoethanol	0.10%

Freezing medium

FBS	
DMSO	10%

Murine MSC medium

MEM-α	
Fetal bovine serum (FBS)	10%
Equine serum	10%
Penicillin-streptomycin	1%

FACS Buffer

PBS	
FBS	2%
Sodium Azide	0.05%

Appendix C:

Publications, Presentations and Achievements

Publications

Lynch, Kevin; Murphy, Nick; Lohan, Paul; Treacy, Oliver; Ritter, Thomas. Mesenchymal stem cell therapy to promote corneal allograft survival: current status and pathway to clinical translation. Curr Opin Organ Transplant. 2016 Dec

Kevin Lynch, Oliver Treacy, Jared Q. Gerlach, Heidi Annuk, Paul Lohan, Joana Cabral, Lokesh Josh, Aideen E. Ryan and Thomas Ritter. Regulating Immunogenicity and Tolerogenicity of Bone Marrow Derived Dendritic Cells through Modulation of Cell Surface Glycosylation by Dexamethasone Treatment Front Immunol. 2017 Oct 30;8:1427. doi: 10.3389/fimmu.2017.01427. eCollection 2017

Kevin Lynch, O'Malley Grace, Aideen Ryan, Thomas Ritter and Michael O'Dwyer. Mesenchymal Stromal Cell Sialylation Enhances Immune Suppression in Multiple Myeloma. Blood 2017 130:124;

Lynch, Kevin; Treacy, Oliver; Murphy, Nick; Lohan, Paul; MD Griffin, Ryan, Aideen Ritter, Thomas. Pre-activated Mesenchymal Stem Cells Induce Regulatory Immune Populations and Prolong Corneal Allograft Survival. **In preparation**

P Lohan, O Treacy, **K Lynch,** F Barry, M Murphy, MD Griffin, T Ritter, AE Ryan. Culture expanded primary chondrocytes have potent immunomodulatory properties and do not induce an allogeneic immune response.

O'Malley G, **Lynch K**, Oliver Tracey, Serika Naicker, Niamh A Leonard, Lohan P, Ritter T, Egan LJ, Ryan AE Stromal cell immunomodulatory potential in the tumour microenvironment is regulated by inflammatory signalling and stromal PD-L1 expression Cancer Research Immunology, June 2017

Oral Presentations

Mesenchymal Stromal Cell Sialylation Enhances Immune Suppression in Multiple Myeloma. American Society for Haematology, Georgia. 2017

Pre-activated Mesenchymal Stromal Cells Induce Regulatory Immune Populations In vivo And Prolong Corneal Allograft Survival. CMNHS, NUIG 2018.

Grants/Awards

Grants

EFIS travel grant to attend the European Congress of Immunology, 2015 (€600)

Early Career Travel Award from Janssen Pharmaceuticals (€2500)

Prizes

Best Poster Prize, College of Medicine, Nursing and Health Science research day, June 2017

Best Oral Price, College of Medicine, Nursing and Health Science Research Day, May 2018

[4]

Bibliography

1. DelMonte, D.W. and T. Kim, *Anatomy and physiology of the cornea.* Journal of Cataract & Refractive Surgery. **37**(3): p. 588-598.
2. Tan, D.T., et al., *Corneal transplantation.* Lancet, 2012. **379**(9827): p. 1749-61.
3. Fu, H., D.F.P. Larkin, and A.J.T. George, *Immune modulation in corneal transplantation.* Transplantation Reviews. **22**(2): p. 105-115.
4. Niederkorn, J.Y., *Cornea: Window to Ocular Immunology.* Curr Immunol Rev, 2011. **7**(3): p. 328-335.
5. Tan, Y., et al., *Role of T Cell Recruitment and Chemokine-Regulated Intra-Graft T Cell Motility Patterns in Corneal Allograft Rejection.* American Journal of Transplantation, 2013. **13**(6): p. 1461-1473.
6. Bron, A.J., *The architecture of the corneal stroma.* Br J Ophthalmol, 2001. **85**(4): p. 379-81.
7. Geroski, D.H., et al., *Pump function of the human corneal endothelium. Effects of age and cornea guttata.* Ophthalmology, 1985. **92**(6): p. 759-63.
8. Claerhout, I., H. Beele, and P. Kestelyn, *Graft failure: I. Endothelial cell loss.* Int Ophthalmol, 2008. **28**(3): p. 165-73.
9. Stiemke, M.M., H.F. Edelhauser, and D.H. Geroski, *The developing corneal endothelium: correlation of morphology, hydration and Na/K ATPase pump site density.* Curr Eye Res, 1991. **10**(2): p. 145-56.
10. Hori, J., J.L. Vega, and S. Masli, *Review of ocular immune privilege in the year 2010: modifying the immune privilege of the eye.* Ocul Immunol Inflamm, 2010. **18**(5): p. 325-33.
11. Masli S., V.J.L., *Ocular Immune Privilege Sites. In: Cuturi M., Anegon I. (eds) Suppression and Regulation of Immune Responses*. Vol. vol 677. 2010, Methods in Molecular Biology (Methods and Protocols): Humana Press, Totowa, NJ.
12. Niederkorn, J.Y. and J. Stein-Streilein, *History and physiology of immune privilege.* Ocul Immunol Inflamm, 2010. **18**(1): p. 19-23.
13. Stein-Streilein, J., *Immune regulation and the eye.* Trends Immunol, 2008. **29**(11): p. 548-54.
14. Taylor, A.W., *Ocular immune privilege.* Eye (Lond), 2009. **23**(10): p. 1885-9.
15. Taylor, A.W., *Ocular Immune Privilege and Transplantation.* Front Immunol, 2016. **7**: p. 37.
16. Taylor, A.W. and T.F. Ng, *Negative regulators that mediate ocular immune privilege.* J Leukoc Biol, 2018.
17. Medawar, P.B., *Immunity to Homologous Grafted Skin. III. The Fate of Skin Homographs Transplanted to the Brain, to Subcutaneous Tissue, and to the Anterior Chamber of the Eye.* British Journal of Experimental Pathology, 1948. **29**(1): p. 58-69.
18. Streilein, J.W., *Ocular immune privilege: therapeutic opportunities from an experiment of nature.* Nat Rev Immunol, 2003. **3**(11): p. 879-89.
19. Streilein, J.W., *New thoughts on the immunology of corneal transplantation.* Eye (Lond), 2003. **17**(8): p. 943-8.
20. Niederkorn, J.Y., *Corneal Transplantation and Immune Privilege.* International reviews of immunology, 2013. **32**(1): p. 10.3109/08830185.2012.737877.
21. Tan, Y., et al., *Immunological disruption of antiangiogenic signals by recruited allospecific T cells leads to corneal allograft rejection.* J Immunol, 2012. **188**(12): p. 5962-9.
22. Feizi, S., A.A. Azari, and S. Safapour, *Therapeutic approaches for corneal neovascularization.* Eye Vis (Lond), 2017. **4**: p. 28.

23. Albuquerque, R.J.C., et al., *Alternatively spliced vascular endothelial growth factor receptor-2 is an essential endogenous inhibitor of lymphatic vessel growth.* Nature Medicine, 2009. **15**: p. 1023.
24. Ambati, B.K., et al., *Corneal avascularity is due to soluble VEGF receptor-1.* Nature, 2006. **443**: p. 993.
25. Zhivov, A., et al., *In vivo confocal microscopic evaluation of Langerhans cell density and distribution in the normal human corneal epithelium.* Graefes Arch Clin Exp Ophthalmol, 2005. **243**(10): p. 1056-61.
26. Hamrah, P., et al., *The Corneal Stroma Is Endowed with a Significant Number of Resident Dendritic Cells.* Investigative Ophthalmology & Visual Science, 2003. **44**(2): p. 581-589.
27. Hamrah, P. and M.R. Dana, *Corneal antigen-presenting cells.* Chem Immunol Allergy, 2007. **92**: p. 58-70.
28. Cunha-Vaz, J., R. Bernardes, and C. Lobo, *Blood-retinal barrier.* Eur J Ophthalmol, 2011. **21 Suppl 6**: p. S3-9.
29. Coca-Prados, M., *The Blood-Aqueous Barrier in Health and Disease.* Journal of Glaucoma, 2014. **23**: p. S36-S38.
30. Sugita, S. and J.W. Streilein, *Iris Pigment Epithelium Expressing CD86 (B7-2) Directly Suppresses T Cell Activation In Vitro via Binding to Cytotoxic T Lymphocyte–associated Antigen 4.* The Journal of Experimental Medicine, 2003. **198**(1): p. 161-171.
31. Griffith, T.S., et al., *Fas Ligand-Induced Apoptosis as a Mechanism of Immune Privilege.* Science, 1995. **270**(5239): p. 1189-1192.
32. Niederkorn, J.Y., *The immune privilege of corneal grafts.* J Leukoc Biol, 2003. **74**(2): p. 167-71.
33. Stuart, P.M., et al., *CD95 ligand (FasL)-induced apoptosis is necessary for corneal allograft survival.* Journal of Clinical Investigation, 1997. **99**(3): p. 396-402.
34. Yamagami, S., et al., *Role of Fas-Fas ligand interactions in the immunorejection of allogeneic mouse corneal transplants.* Transplantation, 1997. **64**(8): p. 1107-11.
35. Hori, J., et al., *B7-H1-induced apoptosis as a mechanism of immune privilege of corneal allografts.* J Immunol, 2006. **177**(9): p. 5928-35.
36. Lee, H.O., et al., *TRAIL: a mechanism of tumor surveillance in an immune privileged site.* J Immunol, 2002. **169**(9): p. 4739-44.
37. Shen, L., et al., *The function of donor versus recipient programmed death-ligand 1 in corneal allograft survival.* J Immunol, 2007. **179**(6): p. 3672-9.
38. Goel, M., et al., *Aqueous Humor Dynamics: A Review.* The Open Ophthalmology Journal, 2010. **4**: p. 52-59.
39. Bora, N.S., et al., *Differential expression of the complement regulatory proteins in the human eye.* Invest Ophthalmol Vis Sci, 1993. **34**(13): p. 3579-84.
40. Flynn, T.H., et al., *Aqueous humor alloreactive cell phenotypes, cytokines and chemokines in corneal allograft rejection.* Am J Transplant, 2008. **8**(7): p. 1537-43.
41. Lau, C.H. and A.W. Taylor, *The Immune Privileged Retina Mediates an Alternative Activation of J774A.1 Cells.* Ocular immunology and inflammation, 2009. **17**(6): p. 380-389.
42. Lee, D.J. and A.W. Taylor, *Both MC5r and A2Ar are required for protective regulatory immunity in the spleen of post-experimental autoimmune uveitis in mice.* Journal of immunology (Baltimore, Md. : 1950), 2013. **191**(8): p. 4103-4111.
43. Taylor, A.W., et al., *Aqueous Humor Induces Transforming Growth Factor-β (TGF-β)-Producing Regulatory T-Cells.* Ocular Immunology and Inflammation, 2007. **15**(3): p. 215-224.

44. Kaplan, H.J. and J.W. Streilein, *Immune Response to Immunization Via the Anterior Chamber of the Eye.* I. F₁ Lymphocyte-Induced Immune Deviation, 1977. **118**(3): p. 809-814.
45. Kaplan, H.J., J.W. Streilein, and T.R. Stevens, *Transplantation Immunology of the Anterior Chamber of the Eye.* II. Immune Response to Allogeneic Cells, 1975. **115**(3): p. 805-810.
46. Jiang, L.Q. and J.W. Streilein, *Immunologic privilege evoked by histoincompatible intracameral retinal transplants.* Reg Immunol, 1990. **3**(3): p. 121-30.
47. Sonoda, K.-H., et al., *The analysis of systemic tolerance elicited by antigen inoculation into the vitreous cavity: vitreous cavity-associated immune deviation.* Immunology, 2005. **116**(3): p. 390-399.
48. Wenkel, H., et al., *Immune Privilege Is Extended, then Withdrawn, from Allogeneic Tumor Cell Grafts Placed in the Subretinal Space.* Investigative Ophthalmology & Visual Science, 1999. **40**(13): p. 3202-3208.
49. *Induction of anterior chamber-associated immune deviation requires an intact, functional spleen.* The Journal of Experimental Medicine, 1981. **153**(5): p. 1058-1067.
50. Lin, H.-H., et al., *The macrophage F4/80 receptor is required for the induction of antigen-specific efferent regulatory T cells in peripheral tolerance.* The Journal of Experimental Medicine, 2005. **201**(10): p. 1615-1625.
51. Hara, Y., et al., *Evidence that peritoneal exudate cells cultured with eye-derived fluids are the proximate antigen-presenting cells in immune deviation of the ocular type.* The Journal of Immunology, 1993. **151**(10): p. 5162-5171.
52. Hsu, S.M., et al., *Ex-vivo tolerogenic F4/80+ antigen-presenting cells (APC) induce efferent CD8+ regulatory T cell-dependent suppression of experimental autoimmune uveitis.* Clinical & Experimental Immunology, 2013. **176**(1): p. 37-48.
53. Wilbanks Garth, A., M. Mammolenti, and J.W. Streilein, *Studies on the induction of anterior chamber-associated immune deviation (ACAID) III. Induction of ACAID depends upon intraocular transforming growth factor-β.* European Journal of Immunology, 1992. **22**(1): p. 165-173.
54. Wilbanks Garth, A. and J. Wayne Streilein, *Fluids from immune privileged sites endow macrophages with the capacity to induce antigen-specific immune deviation via a mechanism involving transforming growth factor-β.* European Journal of Immunology, 1992. **22**(4): p. 1031-1036.
55. Faunce, D.E. and J. Stein-Streilein, *NKT Cell-Derived RANTES Recruits APCs and CD8⁺ T Cells to the Spleen During the Generation of Regulatory T Cells in Tolerance.* The Journal of Immunology, 2002. **169**(1): p. 31-38.
56. D'Orazio, T.J. and J.Y. Niederkorn, *Splenic B cells are required for tolerogenic antigen presentation in the induction of anterior chamber-associated immune deviation (ACAID).* Immunology, 1998. **95**(1): p. 47-55.
57. Sonoda, K.H. and J. Stein-Streilein, *Ocular immune privilege and CD1d-reactive natural killer T cells.* Cornea, 2002. **21**(2 Suppl 1): p. S33-8.
58. Jiang, L., et al., *Splenic CD8+ T cells secrete TGF-β1 to exert suppression in mice with anterior chamber-associated immune deviation.* Graefe's Archive for Clinical and Experimental Ophthalmology, 2009. **247**(1): p. 87-92.
59. Kathryn, P., C.P. W., and N.J. Y., *Role of IFN-γ in the establishment of anterior chamber-associated immune deviation (ACAID)-induced CD8+ T regulatory cells.* Journal of Leukocyte Biology, 2012. **91**(3): p. 475-483.
60. Wilbanks, G.A. and J.W. Streilein, *Characterization of suppressor cells in anterior chamber-associated immune deviation (ACAID) induced by soluble antigen. Evidence of two functionally and phenotypically distinct T-suppressor cell populations.* Immunology, 1990. **71**(3): p. 383-389.

61. Moffatt, S.L., V.A. Cartwright, and T.H. Stumpf, *Centennial review of corneal transplantation.* Clin Exp Ophthalmol, 2005. **33**(6): p. 642-57.
62. Murphy, N., et al., *Mesenchymal stem cell therapy to promote corneal allograft survival: current status and pathway to clinical translation.* Curr Opin Organ Transplant, 2016. **21**(6): p. 559-567.
63. Williams, K.A.K., Miriam C; Galettis, Rachel A; Jones, Victoria J; Mills, Richard Arthur; Coster, Douglas John, *The Australian Corneal Graft Registry 2015 Report.* South Australian Health and Medical Research Institute, 409 p, 2015.
64. Zirm, E.K., *Eine erfolgreiche totale Keratoplastik (A successful total keratoplasty). 1906.* Refract Corneal Surg, 1989. **5**(4): p. 258-61.
65. Boisjoly, H.M., et al., *Effect of factors unrelated to tissue matching on corneal transplant endothelial rejection.* Am J Ophthalmol, 1989. **107**(6): p. 647-54.
66. Dana, M.R. and J.W. Streilein, *Loss and restoration of immune privilege in eyes with corneal neovascularization.* Invest Ophthalmol Vis Sci, 1996. **37**(12): p. 2485-94.
67. Maguire, M.G., et al., *Risk factors for corneal graft failure and rejection in the collaborative corneal transplantation studies. Collaborative Corneal Transplantation Studies Research Group.* Ophthalmology, 1994. **101**(9): p. 1536-47.
68. Qazi, Y. and P. Hamrah, *Corneal Allograft Rejection: Immunopathogenesis to Therapeutics.* Journal of clinical & cellular immunology, 2013. **2013**(Suppl 9): p. 006.
69. Sellami, D., et al., *Epidemiology and risk factors for corneal graft rejection.* Transplant Proc, 2007. **39**(8): p. 2609-11.
70. *The collaborative corneal transplantation studies (ccts): Effectiveness of histocompatibility matching in high-risk corneal transplantation.* Archives of Ophthalmology, 1992. **110**(10): p. 1392-1403.
71. Niederkorn, J.Y., *High risk corneal allografts and why they lose their immune privilege.* Current opinion in allergy and clinical immunology, 2010. **10**(5): p. 493-497.
72. Maguire, M.G., et al., *Risk Factors for Corneal Graft Failure and Rejection in the Collaborative Corneal Transplantation Studies.* Ophthalmology, 1994. **101**(9): p. 1536-1547.
73. Chong, E.-M. and M.R. Dana, *Graft failure IV. Immunologic mechanisms of corneal transplant rejection.* International Ophthalmology, 2008. **28**(3): p. 209-222.
74. Streilein, J.W., *Immunobiology and immunopathology of corneal transplantation.* Chem Immunol, 1999. **73**: p. 186-206.
75. Sano, Y., J.W. Streilein, and B.R. Ksander, *DETECTION OF MINOR ALLOANTIGEN-SPECIFIC CYTOTOXIC T CELLS AFTER REJECTION OF MURINE ORTHOTOPIC CORNEAL ALLOGRAFTS: Evidence That Graft Antigens Are Recognized Exclusively via the "Indirect Pathway"1.* Transplantation, 1999. **68**(7): p. 963-970.
76. Boisgérault, F., et al., *Differential roles of direct and indirect allorecognition pathways in the rejection of skin and corneal transplants.* Transplantation, 2009. **87**(1): p. 16-23.
77. Williams, K.A. and D.J. Coster, *The Immunobiology of Corneal Transplantation.* Transplantation, 2007. **84**(7): p. 806-813.
78. Sano, Y., B.R. Ksander, and J.W. Streilein, *Langerhans Cells, Orthotopic Corneal Allografts, and Direct and Indirect Pathways of T-Cell Allorecognition.* Investigative Ophthalmology & Visual Science, 2000. **41**(6): p. 1422-1431.
79. Huq, S., et al., *Relevance of the Direct Pathway of Sensitization in Corneal Transplantation Is Dictated by the Graft Bed Microenvironment.* The Journal of Immunology, 2004. **173**(7): p. 4464-4469.
80. Yamagami, S. and S. Amano, *Role of Resident Corneal Leukocytes and Draining Cervical Lymph Nodes in Corneal Allograft Rejection.* Cornea, 2003. **22**(7): p. S61-S65.

81. Dana, M.R., Y. Qian, and P. Hamrah, *Twenty-five–Year Panorama of Corneal Immunology: Emerging Concepts in the Immunopathogenesis of Microbial Keratitis, Peripheral Ulcerative Keratitis, and Corneal Transplant Rejection.* Cornea, 2000. **19**(5): p. 625-643.
82. Niederkorn, J.Y., *Immune mechanisms of corneal allograft rejection.* Curr Eye Res, 2007. **32**(12): p. 1005-16.
83. Slegers, T.P., et al., *Effect of macrophage depletion on immune effector mechanisms during corneal allograft rejection in rats.* Invest Ophthalmol Vis Sci, 2000. **41**(8): p. 2239-47.
84. Hegde, S., et al., *CD4+ T-Cell–Mediated Mechanisms of Corneal Allograft Rejection: Role of Fas-Induced Apoptosis.* Transplantation, 2005. **79**(1): p. 23-31.
85. McMenamin, P.G., et al., *Immunomorphologic studies of macrophages and MHC class II-positive dendritic cells in the iris and ciliary body of the rat, mouse, and human eye.* Invest Ophthalmol Vis Sci, 1994. **35**(8): p. 3234-50.
86. Camelo, S., et al., *Local Retention of Soluble Antigen by Potential Antigen-Presenting Cells in the Anterior Segment of the Eye.* Investigative Ophthalmology & Visual Science, 2003. **44**(12): p. 5212-5219.
87. Steptoe, R., P. McMenamin, and P. G. Holt, *Resident tissue macrophages within the normal rat iris lack immunosuppressive activity and are effective antigen-presenting cells*. Vol. 8. 2000. 177-87.
88. Hamrah, P., et al., *Novel Characterization of MHC Class II–Negative Population of Resident Corneal Langerhans Cell–Type Dendritic Cells.* Investigative Ophthalmology & Visual Science, 2002. **43**(3): p. 639-646.
89. Dana, M.R., *Corneal antigen-presenting cells: diversity, plasticity, and disguise: the Cogan lecture.* Invest Ophthalmol Vis Sci, 2004. **45**(3): p. 722-7; 721.
90. Hamrah, P., et al., *Alterations in corneal stromal dendritic cell phenotype and distribution in inflammation.* Archives of Ophthalmology, 2003. **121**(8): p. 1132-1140.
91. Liu, Y., et al., *Draining Lymph Nodes of Corneal Transplant Hosts Exhibit Evidence for Donor Major Histocompatibility Complex (MHC) Class II–positive Dendritic Cells Derived from MHC Class II–negative Grafts.* The Journal of Experimental Medicine, 2002. **195**(2): p. 259-268.
92. Mayer, W.J., et al., *Characterization of Antigen-Presenting Cells in Fresh and Cultured Human Corneas Using Novel Dendritic Cell Markers.* Investigative Ophthalmology & Visual Science, 2007. **48**(10): p. 4459-4467.
93. Yamagami, S. and M.R. Dana, *The critical role of lymph nodes in corneal alloimmunization and graft rejection.* Invest Ophthalmol Vis Sci, 2001. **42**(6): p. 1293-8.
94. Yamagami, S., M.R. Dana, and T. Tsuru, *Draining Lymph Nodes Play an Essential Role in Alloimmunity Generated in Response to High-Risk Corneal Transplantation.* Cornea, 2002. **21**(4): p. 405-409.
95. Yamagami, S., et al., *Early ocular chemokine gene expression and leukocyte infiltration after high-risk corneal transplantation.* Mol Vis, 2005. **11**: p. 632-40.
96. Yamagami, S., M. Isobe, and T. Tsuru, *CHARACTERIZATION OF CYTOKINE PROFILES IN CORNEAL ALLOGRAFT WITH ANTI-ADHESION THERAPY1.* Transplantation, 2000. **69**(8): p. 1655-1659.
97. Yamagami, S., et al., *Differential chemokine gene expression in corneal transplant rejection.* Invest Ophthalmol Vis Sci, 1999. **40**(12): p. 2892-7.
98. He, Y.G., J. Ross, and J.Y. Niederkorn, *Promotion of murine orthotopic corneal allograft survival by systemic administration of anti-CD4 monoclonal antibody.* Investigative Ophthalmology & Visual Science, 1991. **32**(10): p. 2723-2728.

99. Hegde, S. and J.Y. Niederkorn, *The Role of Cytotoxic T Lymphocytes in Corneal Allograft Rejection.* Investigative Ophthalmology & Visual Science, 2000. **41**(11): p. 3341-3347.
100. Yamada, J., B.R. Ksander, and J.W. Streilein, *Cytotoxic T Cells Play No Essential Role in Acute Rejection of Orthotopic Corneal Allografts in Mice.* Investigative Ophthalmology & Visual Science, 2001. **42**(2): p. 386-392.
101. Callanan, D., J. Peeler, and J.Y. Niederkorn, *Characteristics of rejection of orthotopic corneal allografts in the rat.* Transplantation, 1988. **45**(2): p. 437-43.
102. Callanan, D.G., et al., *Histopathology of rejected orthotopic corneal grafts in the rat.* Investigative Ophthalmology & Visual Science, 1989. **30**(3): p. 413-424.
103. Niederkorn, J.Y., et al., *CD4+ T-Cell–Independent Rejection of Corneal Allografts.* Transplantation, 2006. **81**(8): p. 1171-1178.
104. Pepose, J.S., et al., *Composition of cellular infiltrates in rejected human corneal allografts.* Graefes Arch Clin Exp Ophthalmol, 1985. **222**(3): p. 128-33.
105. Yamada, J., et al., *Mice with Th2-Biased Immune Systems Accept Orthotopic Corneal Allografts Placed in "High Risk" Eyes.* The Journal of Immunology, 1999. **162**(9): p. 5247-5255.
106. Beauregard, C., et al., *Cutting Edge: Atopy Promotes Th2 Responses to Alloantigens and Increases the Incidence and Tempo of Corneal Allograft Rejection.* The Journal of Immunology, 2005. **174**(11): p. 6577-6581.
107. Hargrave, S., et al., *Preliminary findings in corneal allograft rejection in patients with keratoconus.* American Journal of Ophthalmology. **135**(4): p. 452-460.
108. Chen, H., et al., *A pathogenic role of IL- 17 at the early stage of corneal allograft rejection.* Transplant Immunology, 2009. **21**(3): p. 155-161.
109. Chen, X., et al., *Neutralization of mouse interleukin-17 bioactivity inhibits corneal allograft rejection.* Mol Vis, 2011. **17**: p. 2148-56.
110. Cunnusamy, K., P.W. Chen, and J.Y. Niederkorn, *IL-17 promotes immune privilege of corneal allografts.* J Immunol, 2010. **185**(8): p. 4651-8.
111. Li, S., et al., *The Balance of Th1/Th2 and LAP+Tregs/Th17 Cells Is Crucial for Graft Survival in Allogeneic Corneal Transplantation.* J Ophthalmol, 2018. **2018**: p. 5404989.
112. Chauhan, S.K., et al., *Levels of Foxp3 in regulatory T cells reflect their functional status in transplantation.* Journal of immunology (Baltimore, Md. : 1950), 2009. **182**(1): p. 148-153.
113. Joffre, O., et al., *Prevention of acute and chronic allograft rejection with CD4+CD25+Foxp3+ regulatory T lymphocytes.* Nat Med, 2008. **14**(1): p. 88-92.
114. San Segundo, D., et al., *Reduced numbers of blood natural regulatory T cells in stable liver transplant recipients with high levels of calcineurin inhibitors.* Transplant Proc, 2007. **39**(7): p. 2290-2.
115. Korczak-Kowalska, G., et al., *The influence of immuosuppressive therapy on the development of CD4+CD25+ T cells after renal transplantation.* Transplant Proc, 2007. **39**(9): p. 2721-3.
116. Kharod-Dholakia, B., et al., *Prevention and treatment of corneal graft rejection: current practice patterns of the Cornea Society (2011).* Cornea, 2015. **34**(6): p. 609-14.
117. Tandon, R., et al., *Intravenous dexamethasone vs methylprednisolone pulse therapy in the treatment of acute endothelial graft rejection.* Eye (Lond), 2009. **23**(3): p. 635-9.
118. Poon, A., et al., *Topical Cyclosporin A in the treatment of acute graft rejection: a randomized controlled trial.* Clin Exp Ophthalmol, 2008. **36**(5): p. 415-21.

119. Cosar, C.B., et al., *Topical cyclosporine in pediatric keratoplasty.* Eye Contact Lens, 2003. **29**(2): p. 103-7.
120. Rumelt, S., et al., *Systemic cyclosporin A in high failure risk, repeated corneal transplantation.* Br J Ophthalmol, 2002. **86**(9): p. 988-92.
121. Dhaliwal, J.S., B.F. Mason, and S.C. Kaufman, *Long-term Use of Topical Tacrolimus (FK506) in High-risk Penetrating Keratoplasty.* Cornea, 2008. **27**(4): p. 488-493.
122. Joseph, A., et al., *Tacrolimus immunosuppression in high-risk corneal grafts.* Br J Ophthalmol, 2007. **91**(1): p. 51-5.
123. Sloper, C.M., R.J. Powell, and H.S. Dua, *Tacrolimus (FK506) in the management of high-risk corneal and limbal grafts.* Ophthalmology, 2001. **108**(10): p. 1838-44.
124. Reinhard, T., et al., *Systemic mycophenolate mofetil avoids immune reactions in penetrating high-risk keratoplasty: preliminary results of an ongoing prospectively randomized multicentre study.* Transpl Int, 2005. **18**(6): p. 703-8.
125. Reis, A., et al., *Mycophenolate mofetil versus cyclosporin A in high risk keratoplasty patients: a prospectively randomised clinical trial.* Br J Ophthalmol, 1999. **83**(11): p. 1268-71.
126. Birnbaum, F., et al., *Immunosuppression with cyclosporine A and mycophenolate mofetil after penetrating high-risk keratoplasty: a retrospective study.* Transplantation, 2005. **79**(8): p. 964-8.
127. Birnbaum, F., et al., *Mycophenolate mofetil (MMF) following penetrating high-risk keratoplasty: long-term results of a prospective, randomised, multicentre study.* Eye (Lond), 2009. **23**(11): p. 2063-70.
128. Steinman, R.M. and Z.A. Cohn, *Identification of a novel cell type in peripheral lymphoid organs of mice. I. Morphology, quantitation, tissue distribution.* J Exp Med, 1973. **137**(5): p. 1142-62.
129. Banchereau, J. and R.M. Steinman, *Dendritic cells and the control of immunity.* Nature, 1998. **392**(6673): p. 245-52.
130. Merad, M., et al., *The dendritic cell lineage: ontogeny and function of dendritic cells and their subsets in the steady state and the inflamed setting.* Annu Rev Immunol, 2013. **31**: p. 563-604.
131. Pulendran, B., *The Varieties of Immunological Experience: Of Pathogens, Stress, and Dendritic Cells.* Annu Rev Immunol, 2015.
132. Shortman, K. and Y.J. Liu, *Mouse and human dendritic cell subtypes.* Nat Rev Immunol, 2002. **2**(3): p. 151-61.
133. Iwasaki, A. and R. Medzhitov, *Regulation of adaptive immunity by the innate immune system.* Science, 2010. **327**(5963): p. 291-5.
134. Pulendran, B., *Modulating vaccine responses with dendritic cells and Toll-like receptors.* Immunol Rev, 2004. **199**: p. 227-50.
135. Pulendran, B., K. Palucka, and J. Banchereau, *Sensing pathogens and tuning immune responses.* Science, 2001. **293**(5528): p. 253-6.
136. Banchereau, J., et al., *Immunobiology of dendritic cells.* Annu Rev Immunol, 2000. **18**: p. 767-811.
137. Hammer, G.E. and A. Ma, *Molecular control of steady-state dendritic cell maturation and immune homeostasis.* Annu Rev Immunol, 2013. **31**: p. 743-91.
138. Satpathy, A.T., et al., *Re(de)fining the dendritic cell lineage.* Nat Immunol, 2012. **13**(12): p. 1145-54.
139. Shortman, K. and S.H. Naik, *Steady-state and inflammatory dendritic-cell development.* Nat Rev Immunol, 2007. **7**(1): p. 19-30.
140. Wu, L. and Y.J. Liu, *Development of dendritic-cell lineages.* Immunity, 2007. **26**(6): p. 741-50.

141. Mildner, A. and S. Jung, *Development and function of dendritic cell subsets.* Immunity, 2014. **40**(5): p. 642-56.
142. Ishikawa, F., et al., *The developmental program of human dendritic cells is operated independently of conventional myeloid and lymphoid pathways.* Blood, 2007. **110**(10): p. 3591-660.
143. Baranov, M.V., et al., *Podosomes of dendritic cells facilitate antigen sampling.* J Cell Sci, 2014. **127**(Pt 5): p. 1052-64.
144. Crespo, H.J., J.T. Lau, and P.A. Videira, *Dendritic cells: a spot on sialic Acid.* Front Immunol, 2013. **4**: p. 491.
145. Norbury, C.C., *Drinking a lot is good for dendritic cells.* Immunology, 2006. **117**(4): p. 443-51.
146. Raker, V.K., M.P. Domogalla, and K. Steinbrink, *Tolerogenic Dendritic Cells for Regulatory T Cell Induction in Man.* Front Immunol, 2015. **6**: p. 569.
147. Giannoukakis, N., et al., *Phase I (safety) study of autologous tolerogenic dendritic cells in type 1 diabetic patients.* Diabetes Care, 2011. **34**(9): p. 2026-32.
148. Hilkens, C.M.U. and J.D. Isaacs, *Tolerogenic dendritic cell therapy for rheumatoid arthritis: where are we now?* Clinical and Experimental Immunology, 2013. **172**(2): p. 148-157.
149. Hogan, P.G., R.S. Lewis, and A. Rao, *Molecular Basis of Calcium Signaling in Lymphocytes: STIM and ORAI.* Annual review of immunology, 2010. **28**: p. 491-533.
150. Baine, I., B.T. Abe, and F. Macian, *Regulation of T-cell tolerance by calcium/NFAT signaling.* Immunol Rev, 2009. **231**(1): p. 225-40.
151. Akbari, O., R.H. DeKruyff, and D.T. Umetsu, *Pulmonary dendritic cells producing IL-10 mediate tolerance induced by respiratory exposure to antigen.* Nat Immunol, 2001. **2**(8): p. 725-31.
152. Hsu, P., et al., *IL-10 Potentiates Differentiation of Human Induced Regulatory T Cells via STAT3 and Foxo1.* The Journal of Immunology, 2015. **195**(8): p. 3665-3674.
153. Wakkach, A., et al., *Characterization of dendritic cells that induce tolerance and T regulatory 1 cell differentiation in vivo.* Immunity, 2003. **18**(5): p. 605-17.
154. Travis, M.A., et al., *Loss of integrin alpha(v)beta8 on dendritic cells causes autoimmunity and colitis in mice.* Nature, 2007. **449**(7160): p. 361-5.
155. Kurts, C., et al., *The peripheral deletion of autoreactive CD8+ T cells induced by cross-presentation of self-antigens involves signaling through CD95 (Fas, Apo-1).* J Exp Med, 1998. **188**(2): p. 415-20.
156. Izawa, T., et al., *Fas-independent T-cell apoptosis by dendritic cells controls autoimmune arthritis in MRL/lpr mice.* PLoS One, 2012. **7**(12): p. e48798.
157. Wu, J. and A. Horuzsko, *Expression and function of immunoglobulin-like transcripts on tolerogenic dendritic cells.* Hum Immunol, 2009. **70**(5): p. 353-6.
158. Keir, M.E., L.M. Francisco, and A.H. Sharpe, *PD-1 and its ligands in T-cell immunity.* Curr Opin Immunol, 2007. **19**(3): p. 309-14.
159. Nguyen, L.T. and P.S. Ohashi, *Clinical blockade of PD1 and LAG3--potential mechanisms of action.* Nat Rev Immunol, 2015. **15**(1): p. 45-56.
160. Laurent, S., et al., *CTLA-4 is expressed by human monocyte-derived dendritic cells and regulates their functions.* Hum Immunol, 2010. **71**(10): p. 934-41.
161. Maldonado, R.A. and U.H. von Andrian, *How tolerogenic dendritic cells induce regulatory T cells.* Advances in immunology, 2010. **108**: p. 111-165.
162. Mellor, A.L. and D.H. Munn, *IDO expression by dendritic cells: tolerance and tryptophan catabolism.* Nat Rev Immunol, 2004. **4**(10): p. 762-74.
163. Hill, J.A., et al., *Retinoic acid enhances Foxp3 induction indirectly by relieving inhibition from CD4+CD44hi Cells.* Immunity, 2008. **29**(5): p. 758-770.

164. Kryczanowsky, F., et al., *IL-10-Modulated Human Dendritic Cells for Clinical Use: Identification of a Stable and Migratory Subset with Improved Tolerogenic Activity.* J Immunol, 2016. **197**(9): p. 3607-3617.
165. Min, W.P., et al., *Dendritic cells genetically engineered to express Fas ligand induce donor-specific hyporesponsiveness and prolong allograft survival.* J Immunol, 2000. **164**(1): p. 161-7.
166. Beriou, G., A. Moreau, and M.C. Cuturi, *Tolerogenic dendritic cells: applications for solid organ transplantation.* Curr Opin Organ Transplant, 2012. **17**(1): p. 42-7.
167. Marin, E., M.C. Cuturi, and A. Moreau, *Tolerogenic Dendritic Cells in Solid Organ Transplantation: Where Do We Stand?* Front Immunol, 2018. **9**: p. 274.
168. Terness, P., et al., *Inhibition of allogeneic T cell proliferation by indoleamine 2,3-dioxygenase-expressing dendritic cells: mediation of suppression by tryptophan metabolites.* J Exp Med, 2002. **196**(4): p. 447-57.
169. O'Flynn, L., et al., *Donor bone marrow-derived dendritic cells prolong corneal allograft survival and promote an intragraft immunoregulatory milieu.* Mol Ther, 2013. **21**(11): p. 2102-12.
170. Takenaka, M.C. and F.J. Quintana, *Tolerogenic dendritic cells.* Seminars in immunopathology, 2017. **39**(2): p. 113-120.
171. Ryan, S.O. and B.A. Cobb, *Roles for major histocompatibility complex glycosylation in immune function.* Semin Immunopathol, 2012. **34**(3): p. 425-41.
172. Saito, Y., et al., *Calreticulin functions in vitro as a molecular chaperone for both glycosylated and non-glycosylated proteins.* EMBO J, 1999. **18**(23): p. 6718-29.
173. Bergeron, J.J., et al., *The role of the lectin calnexin in conformation independent binding to N-linked glycoproteins and quality control.* Adv Exp Med Biol, 1998. **435**: p. 105-16.
174. Sola, R.J. and K. Griebenow, *Effects of glycosylation on the stability of protein pharmaceuticals.* J Pharm Sci, 2009. **98**(4): p. 1223-45.
175. Schauer, R., *Sialic acids as regulators of molecular and cellular interactions.* Current Opinion in Structural Biology, 2009. **19**(5): p. 507-514.
176. Varki, A. and P. Gagneux, *Multifarious roles of sialic acids in immunity.* Ann N Y Acad Sci, 2012. **1253**: p. 16-36.
177. Zhuo, Y. and S.L. Bellis, *Emerging role of alpha2,6-sialic acid as a negative regulator of galectin binding and function.* J Biol Chem, 2011. **286**(8): p. 5935-41.
178. van Kooyk, Y. and G.A. Rabinovich, *Protein-glycan interactions in the control of innate and adaptive immune responses.* Nat Immunol, 2008. **9**(6): p. 593-601.
179. Crocker, P.R., J.C. Paulson, and A. Varki, *Siglecs and their roles in the immune system.* Nat Rev Immunol, 2007. **7**(4): p. 255-266.
180. Videira, P.A., et al., *Surface alpha 2-3- and alpha 2-6-sialylation of human monocytes and derived dendritic cells and its influence on endocytosis.* Glycoconj J, 2008. **25**(3): p. 259-68.
181. Cabral, M.G., et al., *The phagocytic capacity and immunological potency of human dendritic cells is improved by alpha2,6-sialic acid deficiency.* Immunology, 2013. **138**(3): p. 235-45.
182. Crespo, H.J., et al., *Effect of sialic acid loss on dendritic cell maturation.* Immunology, 2009. **128**(1 Suppl): p. e621-31.
183. Harduin-Lepers, A., et al., *The human sialyltransferase family.* Biochimie, 2001. **83**(8): p. 727-37.
184. Garrett, W.S., et al., *Developmental control of endocytosis in dendritic cells by Cdc42.* Cell, 2000. **102**(3): p. 325-34.

185. Nayak, J.V., et al., *Phagocytosis induces lysosome remodeling and regulated presentation of particulate antigens by activated dendritic cells.* J Immunol, 2006. **177**(12): p. 8493-503.
186. Platt, C.D., et al., *Mature dendritic cells use endocytic receptors to capture and present antigens.* Proceedings of the National Academy of Sciences, 2010. **107**(9): p. 4287-4292.
187. de la Rosa, G., et al., *Migration of human blood dendritic cells across endothelial cell monolayers: adhesion molecules and chemokines involved in subset-specific transmigration.* J Leukoc Biol, 2003. **73**(5): p. 639-49.
188. Patel, K.D., et al., *Neutrophils use both shared and distinct mechanisms to adhere to selectins under static and flow conditions.* J Clin Invest, 1995. **96**(4): p. 1887-96.
189. Sperandio, M., *Selectins and glycosyltransferases in leukocyte rolling in vivo.* FEBS J, 2006. **273**(19): p. 4377-89.
190. Julien, S., et al., *Sialyl-Lewis(x) on P-selectin glycoprotein ligand-1 is regulated during differentiation and maturation of dendritic cells: a mechanism involving the glycosyltransferases C2GnT1 and ST3Gal I.* J Immunol, 2007. **179**(9): p. 5701-10.
191. Pendl, G.G., et al., *Immature mouse dendritic cells enter inflamed tissue, a process that requires E- and P-selectin, but not P-selectin glycoprotein ligand 1.* Blood, 2002. **99**(3): p. 946-956.
192. Silva, Z., et al., *Sialyl Lewisx-dependent binding of human monocyte-derived dendritic cells to selectins.* Biochem Biophys Res Commun, 2011. **409**(3): p. 459-64.
193. Laszik, Z., et al., *P-selectin glycoprotein ligand-1 is broadly expressed in cells of myeloid, lymphoid, and dendritic lineage and in some nonhematopoietic cells.* Blood, 1996. **88**(8): p. 3010-21.
194. Boog, C.J., et al., *Specific immune responses restored by alteration in carbohydrate chains of surface molecules on antigen-presenting cells.* Eur J Immunol, 1989. **19**(3): p. 537-42.
195. Stamatos, N.M., et al., *LPS-induced cytokine production in human dendritic cells is regulated by sialidase activity.* J Leukoc Biol, 2010. **88**(6): p. 1227-39.
196. Friedenstein, A.J., I.I. Piatetzky-Shapiro, and K.V. Petrakova, *Osteogenesis in transplants of bone marrow cells.* Journal of Embryology and Experimental Morphology, 1966. **16**(3): p. 381-390.
197. Wei, X., et al., *Mesenchymal stem cells: a new trend for cell therapy.* Acta Pharmacol Sin, 2013. **34**(6): p. 747-754.
198. Bartholomew, A., et al., *Mesenchymal stem cells suppress lymphocyte proliferation in vitro and prolong skin graft survival in vivo.* Exp Hematol, 2002. **30**(1): p. 42-8.
199. Di Nicola, M., et al., *Human bone marrow stromal cells suppress T-lymphocyte proliferation induced by cellular or nonspecific mitogenic stimuli.* Blood, 2002. **99**(10): p. 3838-43.
200. Jiang, X.X., et al., *Human mesenchymal stem cells inhibit differentiation and function of monocyte-derived dendritic cells.* Blood, 2005. **105**(10): p. 4120-6.
201. Li, Y.-P., et al., *Human Mesenchymal Stem Cells License Adult CD34⁺ Hemopoietic Progenitor Cells to Differentiate into Regulatory Dendritic Cells through Activation of the Notch Pathway.* The Journal of Immunology, 2008. **180**(3): p. 1598-1608.
202. Nauta, A.J., et al., *Mesenchymal Stem Cells Inhibit Generation and Function of Both CD34⁺-Derived and Monocyte-Derived Dendritic Cells.* The Journal of Immunology, 2006. **177**(4): p. 2080-2087.
203. Aggarwal, S. and M.F. Pittenger, *Human mesenchymal stem cells modulate allogeneic immune cell responses.* Blood, 2005. **105**(4): p. 1815-22.

204. Beyth, S., et al., *Human mesenchymal stem cells alter antigen-presenting cell maturation and induce T-cell unresponsiveness.* Blood, 2005. **105**(5): p. 2214-9.
205. Maccario, R., et al., *Interaction of human mesenchymal stem cells with cells involved in alloantigen-specific immune response favors the differentiation of CD4+ T-cell subsets expressing a regulatory/suppressive phenotype.* Haematologica, 2005. **90**(4): p. 516-25.
206. Ramasamy, R., et al., *Mesenchymal stem cells inhibit dendritic cell differentiation and function by preventing entry into the cell cycle.* Transplantation, 2007. **83**(1): p. 71-6.
207. Uccelli, A., L. Moretta, and V. Pistoia, *Mesenchymal stem cells in health and disease.* Nat Rev Immunol, 2008. **8**(9): p. 726-36.
208. Bouchlaka, M.N., et al., *Human Mesenchymal Stem Cell-Educated Macrophages Are a Distinct High IL-6-Producing Subset that Confer Protection in Graft-versus-Host-Disease and Radiation Injury Models.* Biol Blood Marrow Transplant, 2017. **23**(6): p. 897-905.
209. Eggenhofer, E. and M.J. Hoogduijn, *Mesenchymal stem cell-educated macrophages.* Transplant Res, 2012. **1**(1): p. 12.
210. Hu, Y., et al., *Mesenchymal Stem Cell-Educated Macrophages Ameliorate LPS-Induced Systemic Response.* Mediators Inflamm, 2016. **2016**: p. 3735452.
211. Kim, J. and P. Hematti, *Mesenchymal stem cell-educated macrophages: a novel type of alternatively activated macrophages.* Exp Hematol, 2009. **37**(12): p. 1445-53.
212. Maggini, J., et al., *Mouse bone marrow-derived mesenchymal stromal cells turn activated macrophages into a regulatory-like profile.* PLoS One, 2010. **5**(2): p. e9252.
213. Benichou, G., et al., *Natural killer cells in rejection and tolerance of solid organ allografts.* Curr Opin Organ Transplant, 2011. **16**(1): p. 47-53.
214. Spaggiari, G.M., et al., *Mesenchymal stem cell-natural killer cell interactions: evidence that activated NK cells are capable of killing MSCs, whereas MSCs can inhibit IL-2-induced NK-cell proliferation.* Blood, 2006. **107**(4): p. 1484-90.
215. Spaggiari, G.M., et al., *Mesenchymal stem cells inhibit natural killer-cell proliferation, cytotoxicity, and cytokine production: role of indoleamine 2,3-dioxygenase and prostaglandin E2.* Blood, 2008. **111**(3): p. 1327-33.
216. Scozzi, D., et al., *The Role of Neutrophils in Transplanted Organs.* Am J Transplant, 2017. **17**(2): p. 328-335.
217. Augello, A., et al., *Bone marrow mesenchymal progenitor cells inhibit lymphocyte proliferation by activation of the programmed death 1 pathway.* Eur J Immunol, 2005. **35**(5): p. 1482-90.
218. Corcione, A., et al., *Human mesenchymal stem cells modulate B-cell functions.* Blood, 2006. **107**(1): p. 367-72.
219. Glennie, S., et al., *Bone marrow mesenchymal stem cells induce division arrest anergy of activated T cells.* Blood, 2005. **105**(7): p. 2821-7.
220. Traggiai, E., et al., *Bone marrow-derived mesenchymal stem cells induce both polyclonal expansion and differentiation of B cells isolated from healthy donors and systemic lupus erythematosus patients.* Stem Cells, 2008. **26**(2): p. 562-9.
221. Rasmusson, I., et al., *Mesenchymal stem cells stimulate antibody secretion in human B cells.* Scand J Immunol, 2007. **65**(4): p. 336-43.
222. Franquesa, M., et al., *Human adipose tissue-derived mesenchymal stem cells abrogate plasmablast formation and induce regulatory B cells independently of T helper cells.* Stem Cells, 2015. **33**(3): p. 880-91.
223. Luk, F., et al., *Inflammatory Conditions Dictate the Effect of Mesenchymal Stem or Stromal Cells on B Cell Function.* Front Immunol, 2017. **8**: p. 1042.
224. Newell, K.A., et al., *Identification of a B cell signature associated with renal transplant tolerance in humans.* J Clin Invest, 2010. **120**(6): p. 1836-47.

225. Sagoo, P., et al., *Development of a cross-platform biomarker signature to detect renal transplant tolerance in humans.* J Clin Invest, 2010. **120**(6): p. 1848-61.
226. Liu, C., et al., *B lymphocyte-directed immunotherapy promotes long-term islet allograft survival in nonhuman primates.* Nat Med, 2007. **13**(11): p. 1295-8.
227. Cho, K.A., et al., *Mesenchymal stem cells ameliorate B-cell-mediated immune responses and increase IL-10-expressing regulatory B cells in an EBI3-dependent manner.* Cell Mol Immunol, 2017.
228. Fan, L., et al., *Interaction between Mesenchymal Stem Cells and B-Cells.* International Journal of Molecular Sciences, 2016. **17**(5): p. 650.
229. Yoshioka, S., et al., *CCAAT/enhancer-binding protein beta expressed by bone marrow mesenchymal stromal cells regulates early B-cell lymphopoiesis.* Stem Cells, 2014. **32**(3): p. 730-40.
230. Mauri, C. and A. Bosma, *Immune regulatory function of B cells.* Annu Rev Immunol, 2012. **30**: p. 221-41.
231. Franquesa, M., et al., *Immunomodulatory effect of mesenchymal stem cells on B cells.* Front Immunol, 2012. **3**: p. 212.
232. Le Texier, L., et al., *Long-term allograft tolerance is characterized by the accumulation of B cells exhibiting an inhibited profile.* Am J Transplant, 2011. **11**(3): p. 429-38.
233. Chabannes, D., et al., *A role for heme oxygenase-1 in the immunosuppressive effect of adult rat and human mesenchymal stem cells.* Blood, 2007. **110**(10): p. 3691-4.
234. Meisel, R., et al., *Human bone marrow stromal cells inhibit allogeneic T-cell responses by indoleamine 2,3-dioxygenase-mediated tryptophan degradation.* Blood, 2004. **103**(12): p. 4619-21.
235. Rasmusson, I., et al., *Mesenchymal stem cells inhibit lymphocyte proliferation by mitogens and alloantigens by different mechanisms.* Exp Cell Res, 2005. **305**(1): p. 33-41.
236. Ren, G., et al., *Mesenchymal stem cell-mediated immunosuppression occurs via concerted action of chemokines and nitric oxide.* Cell Stem Cell, 2008. **2**(2): p. 141-50.
237. Sato, K., et al., *Nitric oxide plays a critical role in suppression of T-cell proliferation by mesenchymal stem cells.* Blood, 2007. **109**(1): p. 228-34.
238. Tse, W.T., et al., *Suppression of allogeneic T-cell proliferation by human marrow stromal cells: implications in transplantation.* Transplantation, 2003. **75**(3): p. 389-97.
239. Zappia, E., et al., *Mesenchymal stem cells ameliorate experimental autoimmune encephalomyelitis inducing T-cell anergy.* Blood, 2005. **106**(5): p. 1755-61.
240. Okazaki, T., et al., *A rheostat for immune responses: the unique properties of PD-1 and their advantages for clinical application.* Nat Immunol, 2013. **14**(12): p. 1212-8.
241. Davies, L.C., et al., *Mesenchymal Stromal Cell Secretion of Programmed Death-1 Ligands Regulates T Cell Mediated Immunosuppression.* Stem Cells, 2017. **35**(3): p. 766-776.
242. Krampera, M., et al., *Role for interferon-gamma in the immunomodulatory activity of human bone marrow mesenchymal stem cells.* Stem Cells, 2006. **24**(2): p. 386-98.
243. Ren, G., et al., *Species variation in the mechanisms of mesenchymal stem cell-mediated immunosuppression.* Stem Cells, 2009. **27**(8): p. 1954-62.
244. Chinnadurai, R., et al., *IDO-Independent Suppression of T Cell Effector Function by IFN-γ-Licensed Human Mesenchymal Stromal Cells.* J Immunol, 2014.
245. Prevosto, C., et al., *Generation of CD4+ or CD8+ regulatory T cells upon mesenchymal stem cell-lymphocyte interaction.* Haematologica, 2007. **92**(7): p. 881-8.

246. English, K., et al., *Cell contact, prostaglandin E(2) and transforming growth factor beta 1 play non-redundant roles in human mesenchymal stem cell induction of CD4+CD25(High) forkhead box P3+ regulatory T cells.* Clin Exp Immunol, 2009. **156**(1): p. 149-60.
247. Chen, W., et al., *Conversion of peripheral CD4+CD25- naive T cells to CD4+CD25+ regulatory T cells by TGF-beta induction of transcription factor Foxp3.* J Exp Med, 2003. **198**(12): p. 1875-86.
248. Fu, S., et al., *TGF-beta induces Foxp3 + T-regulatory cells from CD4 + CD25 - precursors.* Am J Transplant, 2004. **4**(10): p. 1614-27.
249. Ryan, J.M., et al., *Interferon-gamma does not break, but promotes the immunosuppressive capacity of adult human mesenchymal stem cells.* Clin Exp Immunol, 2007. **149**(2): p. 353-63.
250. English, K., et al., *IFN-γ and TNF-α differentially regulate immunomodulation by murine mesenchymal stem cells.* Immunology Letters, 2007. **110**(2): p. 91-100.
251. Baratelli, F., et al., *Prostaglandin E2 induces FOXP3 gene expression and T regulatory cell function in human CD4+ T cells.* J Immunol, 2005. **175**(3): p. 1483-90.
252. Engela, A.U., et al., *On the interactions between mesenchymal stem cells and regulatory T cells for immunomodulation in transplantation.* Frontiers in Immunology, 2012. **3**: p. 126.
253. Nemeth, K., et al., *Bone marrow stromal cells attenuate sepsis via prostaglandin E2-dependent reprogramming of host macrophages to increase their interleukin-10 production.* Nat Med, 2009. **15**(1): p. 42-49.
254. Ge, W., et al., *Regulatory T-cell generation and kidney allograft tolerance induced by mesenchymal stem cells associated with indoleamine 2,3-dioxygenase expression.* Transplantation, 2010. **90**(12): p. 1312-20.
255. Glenn, J.D. and K.A. Whartenby, *Mesenchymal stem cells: Emerging mechanisms of immunomodulation and therapy.* World J Stem Cells, 2014. **6**(5): p. 526-39.
256. Kolf, C.M., E. Cho, and R.S. Tuan, *Mesenchymal stromal cells. Biology of adult mesenchymal stem cells: regulation of niche, self-renewal and differentiation.* Arthritis Res Ther, 2007. **9**(1): p. 204.
257. Le Blanc, K., et al., *Treatment of severe acute graft-versus-host disease with third party haploidentical mesenchymal stem cells.* Lancet, 2004. **363**(9419): p. 1439-41.
258. Le Blanc, K., et al., *Mesenchymal Stem Cells for Treatment of Severe Acute Graft-Versus-Host Disease.* Blood, 2006. **108**(11): p. 2918.
259. Lazarus, H.M., et al., *Cotransplantation of HLA-identical sibling culture-expanded mesenchymal stem cells and hematopoietic stem cells in hematologic malignancy patients.* Biol Blood Marrow Transplant, 2005. **11**(5): p. 389-98.
260. Griffin, M.D., et al., *Concise review: adult mesenchymal stromal cell therapy for inflammatory diseases: how well are we joining the dots?* Stem Cells, 2013. **31**(10): p. 2033-41.
261. Oh, J.Y., et al., *The anti-inflammatory and anti-angiogenic role of mesenchymal stem cells in corneal wound healing following chemical injury.* Stem Cells, 2008. **26**(4): p. 1047-55.
262. Roddy, G.W., et al., *Action at a distance: systemically administered adult stem/progenitor cells (MSCs) reduce inflammatory damage to the cornea without engraftment and primarily by secretion of TNF-alpha stimulated gene/protein 6.* Stem Cells, 2011. **29**(10): p. 1572-9.
263. Jia, Z., et al., *Immunomodulatory effects of mesenchymal stem cells in a rat corneal allograft rejection model.* Exp Eye Res, 2012. **102**: p. 44-9.

264. Oh, J.Y., et al., *Intravenous mesenchymal stem cells prevented rejection of allogeneic corneal transplants by aborting the early inflammatory response.* Mol Ther, 2012. **20**(11): p. 2143-52.
265. Treacy, O., et al., *Mesenchymal stem cell therapy promotes corneal allograft survival in rats by local and systemic immunomodulation.* Am J Transplant, 2014. **14**(9): p. 2023-36.
266. Duijvestein, M., et al., *Pretreatment with interferon-gamma enhances the therapeutic activity of mesenchymal stromal cells in animal models of colitis.* Stem Cells, 2011. **29**(10): p. 1549-58.
267. Ko, J.H., et al., *Mesenchymal stem/stromal cells precondition lung monocytes/macrophages to produce tolerance against allo- and autoimmunity in the eye.* Proceedings of the National Academy of Sciences, 2016. **113**(1): p. 158-163.
268. Fuentes-Julián, S., et al., *Adipose-Derived Mesenchymal Stem Cell Administration Does Not Improve Corneal Graft Survival Outcome.* PLoS ONE, 2015. **10**(3): p. e0117945.
269. Omoto, M., et al., *Mesenchymal Stem Cells Home to Inflamed Ocular Surface and Suppress Allosensitization in Corneal TransplantationMSCs Suppress Corneal Alloimmunity.* Investigative Ophthalmology & Visual Science, 2014. **55**(10): p. 6631-6638.
270. Gerlach, J.Q., M. Kilcoyne, and L. Joshi, *Microarray evaluation of the effects of lectin and glycoprotein orientation and data filtering on glycoform discrimination.* Analytical Methods, 2014. **6**(2): p. 440-449.
271. Gerlach, J.Q., et al., *Urinary nanovesicles captured by lectins or antibodies demonstrate variations in size and surface glycosylation profile.* Nanomedicine (Lond), 2017. **12**(11): p. 1217-1229.
272. Tilney, N.L., *Patterns of lymphatic drainage in the adult laboratory rat.* Journal of Anatomy, 1971. **109**(Pt 3): p. 369-383.
273. Banchereau, J., et al., *Immunobiology of Dendritic Cells.* Annu Rev Immunol, 2000. **18**(1): p. 767-811.
274. Steinman, R.M. and M.D. Witmer, *Lymphoid dendritic cells are potent stimulators of the primary mixed leukocyte reaction in mice.* Proc Natl Acad Sci U S A, 1978. **75**(10): p. 5132-6.
275. Steinman, R.M. and J. Idoyaga, *Features of the dendritic cell lineage.* Immunol Rev, 2010. **234**(1): p. 5-17.
276. Woltman, A.M., et al., *The effect of calcineurin inhibitors and corticosteroids on the differentiation of human dendritic cells.* Eur J Immunol, 2000. **30**(7): p. 1807-12.
277. Obreque, J., et al., *Autologous tolerogenic dendritic cells derived from monocytes of systemic lupus erythematosus patients and healthy donors show a stable and immunosuppressive phenotype.* Immunology, 2017.
278. Zhuang, D., et al., *Effect of calcineurin inhibitors on posaconazole blood levels as measured by the MVista microbiological assay.* Antimicrob Agents Chemother, 2008. **52**(2): p. 730-1.
279. van Kooten, C., et al., *Handbook of experimental pharmacology "dendritic cells": the use of dexamethasone in the induction of tolerogenic DCs.* Handb Exp Pharmacol, 2009(188): p. 233-49.
280. García-González, P., et al., *A short protocol using dexamethasone and monophosphoryl lipid A generates tolerogenic dendritic cells that display a potent migratory capacity to lymphoid chemokines.* Journal of Translational Medicine, 2013. **11**: p. 128-128.

281. Nikolic, T. and B.O. Roep, *Regulatory multitasking of tolerogenic dendritic cells - lessons taken from vitamin d3-treated tolerogenic dendritic cells.* Front Immunol, 2013. **4**: p. 113.
282. Unger, W.W., et al., *Induction of Treg by monocyte-derived DC modulated by vitamin D3 or dexamethasone: differential role for PD-L1.* Eur J Immunol, 2009. **39**(11): p. 3147-59.
283. Wilckens, T. and R. De Rijk, *Glucocorticoids and immune function: unknown dimensions and new frontiers.* Immunol Today, 1997. **18**(9): p. 418-24.
284. Piemonti, L., et al., *Glucocorticoids affect human dendritic cell differentiation and maturation.* J Immunol, 1999. **162**(11): p. 6473-81.
285. Bosma, B.M., et al., *Dexamethasone transforms lipopolysaccharide-stimulated human blood myeloid dendritic cells into myeloid dendritic cells that prime interleukin-10 production in T cells.* Immunology, 2008. **125**(1): p. 91-100.
286. Emmer, P.M., et al., *Dendritic cells activated by lipopolysaccharide after dexamethasone treatment induce donor-specific allograft hyporesponsiveness.* Transplantation, 2006. **81**(10): p. 1451-9.
287. Gordon, J.R., et al., *Regulatory dendritic cells for immunotherapy in immunologic diseases.* Front Immunol, 2014. **5**: p. 7.
288. Moreau, A., et al., *Tolerogenic dendritic cell therapy in organ transplantation.* Transplant International, 2016: p. n/a-n/a.
289. Amon, R., et al., *Glycans in immune recognition and response.* Carbohydr Res, 2014. **389**: p. 115-22.
290. Gleeson, P.A., *The sweet side of immunology: glycobiology of the immune system.* Immunol Cell Biol, 2008. **86**(7): p. 562-3.
291. Collins, B.E., et al., *Masking of CD22 by cis ligands does not prevent redistribution of CD22 to sites of cell contact.* Proc Natl Acad Sci U S A, 2004. **101**(16): p. 6104-9.
292. Pilatte, Y., J. Bignon, and C.R. Lambre, *Sialic acids as important molecules in the regulation of the immune system: pathophysiological implications of sialidases in immunity.* Glycobiology, 1993. **3**(3): p. 201-18.
293. Grauer, O., et al., *Analysis of maturation states of rat bone marrow-derived dendritic cells using an improved culture technique.* Histochem Cell Biol, 2002. **117**(4): p. 351-62.
294. Stax, A.M., et al., *Induction of donor-specific T-cell hyporesponsiveness using dexamethasone-treated dendritic cells in two fully mismatched rat kidney transplantation models.* Transplantation, 2008. **86**(9): p. 1275-82.
295. Horibe, E.K., et al., *Rapamycin-conditioned, alloantigen-pulsed dendritic cells promote indefinite survival of vascularized skin allografts in association with T regulatory cell expansion.* Transpl Immunol, 2008. **18**(4): p. 307-18.
296. Taieb, A., et al., *Intrinsic ability of GM+IL-4 but not Flt3L-induced rat dendritic cells to promote allogeneic T cell hyporesponsiveness.* Clin Immunol, 2007. **123**(2): p. 176-89.
297. Lord, P., et al., *Minimum information about tolerogenic antigen-presenting cells (MITAP): a first step towards reproducibility and standardisation of cellular therapies.* PeerJ, 2016. **4**: p. e2300.
298. Cao, Y., et al., *Glucocorticoid receptor translational isoforms underlie maturational stage-specific glucocorticoid sensitivities of dendritic cells in mice and humans.* Blood, 2013. **121**(9): p. 1553-1562.
299. Yorke, S.C., *The application of N-acetylmannosamine to the mammalian cell culture production of recombinant human glycoproteins.* Chemistry in New Zealand, 2013(January 2013): p. 18-20.

300. van Gelder, T., R.H. van Schaik, and D.A. Hesselink, *Pharmacogenetics and immunosuppressive drugs in solid organ transplantation.* Nat Rev Nephrol, 2014. **10**(12): p. 725-31.
301. Behnam Sani, K. and B. Sawitzki, *Immune monitoring as prerequisite for transplantation tolerance trials.* 2017. **189**(2): p. 158-170.
302. Starr, S.P., *Immunology Update: Long-Term Care of Solid Organ Transplant Recipients.* FP Essent, 2016. **450**: p. 22-27.
303. Jonuleit, H., et al., *Induction of interleukin 10-producing, nonproliferating CD4(+) T cells with regulatory properties by repetitive stimulation with allogeneic immature human dendritic cells.* J Exp Med, 2000. **192**(9): p. 1213-22.
304. Levings, M.K., et al., *Differentiation of Tr1 cells by immature dendritic cells requires IL-10 but not CD25⁺CD4⁺ Tr cells.* Blood, 2005. **105**(3): p. 1162-1169.
305. Kretschmer, K., et al., *Inducing and expanding regulatory T cell populations by foreign antigen.* Nat Immunol, 2005. **6**(12): p. 1219-1227.
306. Moreau, A., et al., *Tolerogenic dendritic cell therapy in organ transplantation.* Transpl Int, 2017. **30**(8): p. 754-764.
307. Xia, C.Q., et al., *Dexamethasone induces IL-10-producing monocyte-derived dendritic cells with durable immaturity.* Scand J Immunol, 2005. **62**(1): p. 45-54.
308. Jenner, J., et al., *Increased alpha2,6-sialylation of surface proteins on tolerogenic, immature dendritic cells and regulatory T cells.* Exp Hematol, 2006. **34**(9): p. 1212-8.
309. Perdicchio, M., et al., *Sialic acid-modified antigens impose tolerance via inhibition of T-cell proliferation and de novo induction of regulatory T cells.* Proc Natl Acad Sci U S A, 2016. **113**(12): p. 3329-34.
310. Cabral, M.G., et al., *The phagocytic capacity and immunological potency of human dendritic cells is improved by α2,6-sialic acid deficiency.* Immunology, 2013. **138**(3): p. 235-245.
311. Silva, M., et al., *Sialic acid removal from dendritic cells improves antigen cross-presentation and boosts anti-tumor immune responses.* Oncotarget, 2016. **7**(27): p. 41053-41066.
312. Julien, S., et al., *Sialyl-Lewis^x on P-Selectin Glycoprotein Ligand-1 Is Regulated during Differentiation and Maturation of Dendritic Cells: A Mechanism Involving the Glycosyltransferases C2GnT1 and ST3Gal I.* The Journal of Immunology, 2007. **179**(9): p. 5701.
313. Gu, X. and D.I. Wang, *Improvement of interferon-gamma sialylation in Chinese hamster ovary cell culture by feeding of N-acetylmannosamine.* Biotechnol Bioeng, 1998. **58**(6): p. 642-8.
314. Werner, R.G., K. Kopp, and M. Schlueter, *Glycosylation of therapeutic proteins in different production systems.* Acta Paediatr, 2007. **96**(455): p. 17-22.
315. Korchagina, E., et al., *Toward creating cell membrane glyco-landscapes with glycan lipid constructs.* Carbohydr Res, 2012. **356**: p. 238-46.
316. Korchagina, E.Y.H., S.M. Biochemistry Moscow, *Synthetic glycolipid-like constructs as tools for glycobiology research, diagnostics, and as potential therapeutics.* Springer (Pleiades Publishing), 2015.
317. Constantino, J., et al., *Dendritic cell-based immunotherapy: a basic review and recent advances.* Immunol Res, 2017. **65**(4): p. 798-810.
318. Shimizu, K., et al., *Systemic DC Activation Modulates the Tumor Microenvironment and Shapes the Long-Lived Tumor-Specific Memory Mediated by CD8+ T Cells.* Cancer Res, 2016. **76**(13): p. 3756-66.
319. Pan, J., et al., *Dexamethasone inhibits the antigen presentation of dendritic cells in MHC class II pathway.* Immunol Lett, 2001. **76**(3): p. 153-61.

320. Shi, Y., et al., *Mesenchymal stem cells: a new strategy for immunosuppression and tissue repair.* Cell Res, 2010. **20**(5): p. 510-8.
321. Dominici, M., et al., *Minimal criteria for defining multipotent mesenchymal stromal cells. The International Society for Cellular Therapy position statement.* Cytotherapy, 2006. **8**(4): p. 315-7.
322. Krampera, M., et al., *Bone marrow mesenchymal stem cells inhibit the response of naive and memory antigen-specific T cells to their cognate peptide.* Blood, 2003. **101**(9): p. 3722-3729.
323. Tipnis, S., C. Viswanathan, and A.S. Majumdar, *Immunosuppressive properties of human umbilical cord-derived mesenchymal stem cells: role of B7-H1 and IDO.* Immunol Cell Biol, 2010. **88**(8): p. 795-806.
324. Chinnadurai, R., et al., *IDO-independent suppression of T cell effector function by IFN-gamma-licensed human mesenchymal stromal cells.* J Immunol, 2014. **192**(4): p. 1491-501.
325. Fan, H., et al., *Pre-treatment with IL-1β enhances the efficacy of MSC transplantation in DSS-induced colitis.* Cellular and Molecular Immunology, 2012. **9**(6): p. 473-481.
326. Saparov, A., et al., *Preconditioning of Human Mesenchymal Stem Cells to Enhance Their Regulation of the Immune Response.* Stem Cells International, 2016. **2016**: p. 3924858.
327. Cuerquis, J., et al., *Human mesenchymal stromal cells transiently increase cytokine production by activated T cells before suppressing T-cell proliferation: effect of interferon-gamma and tumor necrosis factor-alpha stimulation.* Cytotherapy, 2014. **16**(2): p. 191-202.
328. Li, H., et al., *Interferon-gamma and tumor necrosis factor-alpha promote the ability of human placenta-derived mesenchymal stromal cells to express programmed death ligand-2 and induce the differentiation of CD4(+)interleukin-10(+) and CD8(+)interleukin-10(+)Treg subsets.* Cytotherapy, 2015. **17**(11): p. 1560-71.
329. Prasanna, S.J., et al., *Pro-inflammatory cytokines, IFNgamma and TNFalpha, influence immune properties of human bone marrow and Wharton jelly mesenchymal stem cells differentially.* PLoS One, 2010. **5**(2): p. e9016.
330. Jin, P., et al., *Interferon-gamma and Tumor Necrosis Factor-alpha Polarize Bone Marrow Stromal Cells Uniformly to a Th1 Phenotype.* Sci Rep, 2016. **6**: p. 26345.
331. Kfoury, Y. and D.T. Scadden, *Mesenchymal cell contributions to the stem cell niche.* Cell Stem Cell, 2015. **16**(3): p. 239-53.
332. Le Blanc, K. and L.C. Davies, *Mesenchymal stromal cells and the innate immune response.* Immunol Lett, 2015. **168**(2): p. 140-6.
333. Le Blanc, K., et al., *Mesenchymal stem cells inhibit and stimulate mixed lymphocyte cultures and mitogenic responses independently of the major histocompatibility complex.* Scand J Immunol, 2003. **57**(1): p. 11-20.
334. Bernardo, M.E. and W.E. Fibbe, *Mesenchymal stromal cells: sensors and switchers of inflammation.* Cell Stem Cell, 2013. **13**(4): p. 392-402.
335. Slegers, T.P., et al., *Macrophages play a role in the early phase of corneal allograft rejection in rats.* Transplantation, 2004. **77**(11): p. 1641-6.
336. Slegers, T.P., et al., *Effect of local macrophage depletion on cellular immunity and tolerance evoked by corneal allografts.* Curr Eye Res, 2003. **26**(2): p. 73-9.
337. Niederkorn, J.Y. and D.F. Larkin, *Immune privilege of corneal allografts.* Ocul Immunol Inflamm, 2010. **18**(3): p. 162-71.
338. Chang, J., et al., *NF-kappaB inhibits osteogenic differentiation of mesenchymal stem cells by promoting beta-catenin degradation.* Proc Natl Acad Sci U S A, 2013. **110**(23): p. 9469-74.

339. Kleinovink, J.W., et al., *PD-L1 immune suppression in cancer: Tumor cells or host cells?* Oncoimmunology, 2017. **6**(7): p. e1325982.
340. Li, T., et al., *PD-1/PD-L1 costimulatory pathway-induced mouse islet transplantation immune tolerance.* Transplant Proc, 2015. **47**(1): p. 165-70.
341. Tanaka, K., et al., *PDL1 Is Required for Peripheral Transplantation Tolerance and Protection from Chronic Allograft Rejection.* Journal of immunology (Baltimore, Md. : 1950), 2007. **179**(8): p. 5204-5210.
342. Garcia-Diaz, A., et al., *Interferon Receptor Signaling Pathways Regulating PD-L1 and PD-L2 Expression.* Cell Rep, 2017. **19**(6): p. 1189-1201.
343. Nakajima, M., et al., *Mesenchymal Stem Cells Overexpressing Interleukin-10 Promote Neuroprotection in Experimental Acute Ischemic Stroke.* Mol Ther Methods Clin Dev, 2017. **6**: p. 102-111.
344. Sangiorgi, B. and R.A. Panepucci, *Modulation of Immunoregulatory Properties of Mesenchymal Stromal Cells by Toll-Like Receptors: Potential Applications on GVHD.* Stem Cells Int, 2016. **2016**: p. 9434250.
345. Wang, C., et al., *Interleukin-10-Overexpressing Mesenchymal Stromal Cells Induce a Series of Regulatory Effects in the Inflammatory System and Promote the Survival of Endotoxin-Induced Acute Lung Injury in Mice Model.* DNA Cell Biol, 2018. **37**(1): p. 53-61.
346. Gao, F., et al., *Mesenchymal stem cells and immunomodulation: current status and future prospects.* Cell Death Dis, 2016. **7**: p. e2062.
347. Kapranov, N.M., et al., *Effect of Priming of Multipotent Mesenchymal Stromal Cells with Interferon gamma on Their Immunomodulating Properties.* Biochemistry (Mosc), 2017. **82**(10): p. 1158-1168.
348. Polchert, D., et al., *IFN-gamma activation of mesenchymal stem cells for treatment and prevention of graft versus host disease.* Eur J Immunol, 2008. **38**(6): p. 1745-55.
349. Kudlik, G., et al., *Mesenchymal stem cells promote macrophage polarization toward M2b-like cells.* Exp Cell Res, 2016. **348**(1): p. 36-45.
350. Qiu, X., et al., *Mesenchymal stem cells and extracellular matrix scaffold promote muscle regeneration by synergistically regulating macrophage polarization toward the M2 phenotype.* Stem Cell Res Ther, 2018. **9**(1): p. 88.
351. Vasandan, A.B., et al., *Human Mesenchymal stem cells program macrophage plasticity by altering their metabolic status via a PGE2-dependent mechanism.* Sci Rep, 2016. **6**: p. 38308.
352. Casiraghi, F., N. Perico, and G. Remuzzi, *Mesenchymal stromal cells to promote solid organ transplantation tolerance.* Curr Opin Organ Transplant, 2013. **18**(1): p. 51-8.
353. Casiraghi, F., N. Perico, and G. Remuzzi, *Mesenchymal stromal cells for tolerance induction in organ transplantation.* Hum Immunol, 2017.
354. Bunnell, B.A., et al., *Adipose-derived stem cells: isolation, expansion and differentiation.* Methods, 2008. **45**(2): p. 115-20.
355. Guilak, F., et al., *2010 Nicolas Andry Award: Multipotent adult stem cells from adipose tissue for musculoskeletal tissue engineering.* Clin Orthop Relat Res, 2010. **468**(9): p. 2530-40.
356. Ren, Y., et al., *Isolation, expansion, and differentiation of goat adipose-derived stem cells.* Res Vet Sci, 2012. **93**(1): p. 404-11.
357. Ding, D.C., et al., *Human umbilical cord mesenchymal stem cells: a new era for stem cell therapy.* Cell Transplant, 2015. **24**(3): p. 339-47.
358. Kadle, R.L., et al., *Microenvironmental cues enhance mesenchymal stem cell-mediated immunomodulation and regulatory T-cell expansion.* PLoS One, 2018. **13**(3): p. e0193178.

359. Luz-Crawford, P., et al., *Mesenchymal stem cells generate a CD4+CD25+Foxp3+ regulatory T cell population during the differentiation process of Th1 and Th17 cells.* Stem Cell Res Ther, 2013. **4**(3): p. 65.
360. Casiraghi, F., et al., *Localization of Mesenchymal Stromal Cells Dictates Their Immune or Proinflammatory Effects in Kidney Transplantation.* American Journal of Transplantation, 2012. **12**(9): p. 2373-2383.
361. Bai, L., et al., *Human bone marrow-derived mesenchymal stem cells induce Th2-polarized immune response and promote endogenous repair in animal models of multiple sclerosis.* Glia, 2009. **57**(11): p. 1192-203.
362. Batten, P., et al., *Human mesenchymal stem cells induce T cell anergy and downregulate T cell allo-responses via the TH2 pathway: relevance to tissue engineering human heart valves.* Tissue Eng, 2006. **12**(8): p. 2263-73.
363. Fiorina, P., et al., *Immunomodulatory function of bone marrow-derived mesenchymal stem cells in experimental autoimmune type 1 diabetes.* J Immunol, 2009. **183**(2): p. 993-1004.
364. English, K., *Mechanisms of mesenchymal stromal cell immunomodulation.* Immunol Cell Biol, 2013. **91**(1): p. 19-26.
365. Klinker, M.W., et al., *Morphological features of IFN-γ–stimulated mesenchymal stromal cells predict overall immunosuppressive capacity.* Proceedings of the National Academy of Sciences, 2017. **114**(13): p. E2598-E2607.
366. Galleu, A., et al., *Apoptosis in mesenchymal stromal cells induces in vivo recipient-mediated immunomodulation.* Sci Transl Med, 2017. **9**(416).
367. Leibacher, J., et al., *Human mesenchymal stromal cells undergo apoptosis and fragmentation after intravenous application in immune-competent mice.* Cytotherapy, 2017. **19**(1): p. 61-74.
368. Nemeth, K., et al., *Bone marrow stromal cells attenuate sepsis via prostaglandin E(2)-dependent reprogramming of host macrophages to increase their interleukin-10 production.* Nat Med, 2009. **15**(1): p. 42-9.
369. Griffin, M.D., et al., *Anti-donor immune responses elicited by allogeneic mesenchymal stem cells: what have we learned so far?* Immunol Cell Biol, 2013. **91**(1): p. 40-51.
370. Kerkela, E., et al., *Adenosinergic Immunosuppression by Human Mesenchymal Stromal Cells Requires Co-Operation with T cells.* Stem Cells, 2016. **34**(3): p. 781-90.
371. Zhu, H., et al., *The role of the hyaluronan receptor CD44 in mesenchymal stem cell migration in the extracellular matrix.* Stem Cells, 2006. **24**(4): p. 928-35.
372. Chou, K.J., et al., *CD44 fucosylation on mesenchymal stem cell enhances homing and macrophage polarization in ischemic kidney injury.* Exp Cell Res, 2017. **350**(1): p. 91-102.
373. Kumar, A., et al., *Multiple roles of CD90 in cancer.* Tumour Biol, 2016. **37**(9): p. 11611-11622.
374. Zinöcker, S. and J.T. Vaage, *Rat Mesenchymal Stromal Cells Inhibit T Cell Proliferation but Not Cytokine Production Through Inducible Nitric Oxide Synthase.* Frontiers in Immunology, 2012. **3**: p. 62.
375. Gray, A., et al., *Identification of IL-1beta and LPS as optimal activators of monolayer and alginate-encapsulated mesenchymal stromal cell immunomodulation using design of experiments and statistical methods.* Biotechnol Prog, 2015. **31**(4): p. 1058-70.
376. Noone, C., et al., *IFN-gamma stimulated human umbilical-tissue-derived cells potently suppress NK activation and resist NK-mediated cytotoxicity in vitro.* Stem Cells Dev, 2013. **22**(22): p. 3003-14.

377. Saparov, A., et al., *Preconditioning of Human Mesenchymal Stem Cells to Enhance Their Regulation of the Immune Response.* Stem Cells Int, 2016. **2016**: p. 3924858.
378. Tu, Z., et al., *Mesenchymal stem cells inhibit complement activation by secreting factor H.* Stem Cells Dev, 2010. **19**(11): p. 1803-9.
379. Kong, Q.F., et al., *Administration of bone marrow stromal cells ameliorates experimental autoimmune myasthenia gravis by altering the balance of Th1/Th2/Th17/Treg cell subsets through the secretion of TGF-beta.* J Neuroimmunol, 2009. **207**(1-2): p. 83-91.
380. Braza, F., et al., *Mesenchymal Stem Cells Induce Suppressive Macrophages Through Phagocytosis in a Mouse Model of Asthma.* Stem Cells, 2016. **34**(7): p. 1836-45.
381. Casiraghi, F., et al., *Pretransplant infusion of mesenchymal stem cells prolongs the survival of a semiallogeneic heart transplant through the generation of regulatory T cells.* J Immunol, 2008. **181**(6): p. 3933-46.
382. Li, F. and S.Z. Zhao, *Mesenchymal stem cells: Potential role in corneal wound repair and transplantation.* World J Stem Cells, 2014. **6**(3): p. 296-304.
383. Obermajer, N., et al., *Conversion of Th17 into IL-17A(neg) regulatory T cells: a novel mechanism in prolonged allograft survival promoted by mesenchymal stem cell-supported minimized immunosuppressive therapy.* J Immunol, 2014. **193**(10): p. 4988-99.
384. Hu, C. and L. Li, *Preconditioning influences mesenchymal stem cell properties in vitro and in vivo.* J Cell Mol Med, 2018. **22**(3): p. 1428-1442.
385. Bhatti, F.U., et al., *Vitamin E protects rat mesenchymal stem cells against hydrogen peroxide-induced oxidative stress in vitro and improves their therapeutic potential in surgically-induced rat model of osteoarthritis.* Osteoarthritis Cartilage, 2017. **25**(2): p. 321-331.
386. Wang, J., et al., *CX43 change in LPS preconditioning against apoptosis of mesenchymal stem cells induced by hypoxia and serum deprivation is associated with ERK signaling pathway.* Mol Cell Biochem, 2013. **380**(1-2): p. 267-75.
387. Liu, X., et al., *SDF-1/CXCR4 axis modulates bone marrow mesenchymal stem cell apoptosis, migration and cytokine secretion.* Protein Cell, 2011. **2**(10): p. 845-54.
388. Lu, Z., et al., *Activation and promotion of adipose stem cells by tumour necrosis factor-alpha preconditioning for bone regeneration.* J Cell Physiol, 2013. **228**(8): p. 1737-44.
389. Carrero, R., et al., *IL1beta induces mesenchymal stem cells migration and leucocyte chemotaxis through NF-kappaB.* Stem Cell Rev, 2012. **8**(3): p. 905-16.
390. Sullivan, C.B., et al., *TNFalpha and IL-1beta influence the differentiation and migration of murine MSCs independently of the NF-kappaB pathway.* Stem Cell Res Ther, 2014. **5**(4): p. 104.
391. Martino, M.M., et al., *Inhibition of IL-1R1/MyD88 signalling promotes mesenchymal stem cell-driven tissue regeneration.* Nat Commun, 2016. **7**: p. 11051.
392. Francois, M., et al., *Human MSC suppression correlates with cytokine induction of indoleamine 2,3-dioxygenase and bystander M2 macrophage differentiation.* Mol Ther, 2012. **20**(1): p. 187-95.
393. Xia, W., et al., *Macrophage migration inhibitory factor confers resistance to senescence through CD74-dependent AMPK-FOXO3a signaling in mesenchymal stem cells.* Stem Cell Res Ther, 2015. **6**: p. 82.
394. Blobe, G.C., W.P. Schiemann, and H.F. Lodish, *Role of transforming growth factor beta in human disease.* N Engl J Med, 2000. **342**(18): p. 1350-8.
395. Oshimori, N. and E. Fuchs, *The harmonies played by TGF-beta in stem cell biology.* Cell Stem Cell, 2012. **11**(6): p. 751-64.

396. Carrillo-Galvez, A.B., et al., *Mesenchymal stromal cells express GARP/LRRC32 on their surface: effects on their biology and immunomodulatory capacity.* Stem Cells, 2015. **33**(1): p. 183-95.
397. Patel, S.A., et al., *Mesenchymal stem cells protect breast cancer cells through regulatory T cells: role of mesenchymal stem cell-derived TGF-beta.* J Immunol, 2010. **184**(10): p. 5885-94.
398. Salazar, K.D., S.M. Lankford, and A.R. Brody, *Mesenchymal stem cells produce Wnt isoforms and TGF-beta1 that mediate proliferation and procollagen expression by lung fibroblasts.* Am J Physiol Lung Cell Mol Physiol, 2009. **297**(5): p. L1002-11.
399. Ng, F., et al., *PDGF, TGF-beta, and FGF signaling is important for differentiation and growth of mesenchymal stem cells (MSCs): transcriptional profiling can identify markers and signaling pathways important in differentiation of MSCs into adipogenic, chondrogenic, and osteogenic lineages.* Blood, 2008. **112**(2): p. 295-307.
400. Tang, Y., et al., *TGF-beta1-induced migration of bone mesenchymal stem cells couples bone resorption with formation.* Nat Med, 2009. **15**(7): p. 757-65.
401. Dubon, M.J., et al., *Transforming growth factor beta induces bone marrow mesenchymal stem cell migration via noncanonical signals and N-cadherin.* J Cell Physiol, 2018. **233**(1): p. 201-213.
402. van Zoelen, E.J., et al., *TGFbeta-induced switch from adipogenic to osteogenic differentiation of human mesenchymal stem cells: identification of drug targets for prevention of fat cell differentiation.* Stem Cell Res Ther, 2016. **7**(1): p. 123.
403. Li, D., et al., *Low levels of TGF-beta1 enhance human umbilical cord-derived mesenchymal stem cell fibronectin production and extend survival time in a rat model of lipopolysaccharide-induced acute lung injury.* Mol Med Rep, 2016. **14**(2): p. 1681-92.
404. Fischer, U.M., et al., *Pulmonary passage is a major obstacle for intravenous stem cell delivery: the pulmonary first-pass effect.* Stem Cells Dev, 2009. **18**.
405. Eggenhofer, E., et al., *Mesenchymal stem cells are short-lived and do not migrate beyond the lungs after intravenous infusion.* Frontiers in Immunology, 2012. **3**(297).
406. Alegre, M.L., S. Florquin, and M. Goldman, *Cellular mechanisms underlying acute graft rejection: time for reassessment.* Curr Opin Immunol, 2007. **19**(5): p. 563-8.
407. Ingulli, E., *Mechanism of cellular rejection in transplantation.* Pediatr Nephrol, 2010. **25**(1): p. 61-74.
408. Hippen, B.E., et al., *Association of CD20+ infiltrates with poorer clinical outcomes in acute cellular rejection of renal allografts.* Am J Transplant, 2005. **5**(9): p. 2248-52.
409. Lehnhardt, A., et al., *Nodular B-cell aggregates associated with treatment refractory renal transplant rejection resolved by rituximab.* Am J Transplant, 2006. **6**(4): p. 847-51.
410. Malek, T.R., *The biology of interleukin-2.* Annu Rev Immunol, 2008. **26**: p. 453-79.
411. Malek, T.R. and I. Castro, *Interleukin-2 receptor signaling: at the interface between tolerance and immunity.* Immunity, 2010. **33**(2): p. 153-65.
412. González-Amaro, R., et al., *Is CD69 an effective brake to control inflammatory diseases?* Trends in Molecular Medicine, 2013. **19**(10): p. 625-632.
413. Cibrian, D. and F. Sanchez-Madrid, *CD69: from activation marker to metabolic gatekeeper.* Eur J Immunol, 2017. **47**(6): p. 946-953.
414. Gonzalez-Amaro, R. and M. Marazuela, *T regulatory (Treg) and T helper 17 (Th17) lymphocytes in thyroid autoimmunity.* Endocrine, 2016. **52**(1): p. 30-8.
415. Lieberman, S.M., et al., *Site-specific accumulation of recently activated CD4+ Foxp3+ regulatory T cells following adoptive transfer.* Eur J Immunol, 2012. **42**(6): p. 1429-35.

416. Buckner, J.H. and S.F. Ziegler, *Regulating the immune system: the induction of regulatory T cells in the periphery.* Arthritis Res Ther, 2004. **6**(5): p. 215-22.
417. Han, Y., et al., *CD69+ CD4+ CD25- T cells, a new subset of regulatory T cells, suppress T cell proliferation through membrane-bound TGF-beta 1.* J Immunol, 2009. **182**(1): p. 111-20.
418. Lan, R.Y., et al., *Regulatory T cells: development, function and role in autoimmunity.* Autoimmun Rev, 2005. **4**(6): p. 351-63.
419. Ziegler, S.F., *FOXP3: of mice and men.* Annu Rev Immunol, 2006. **24**: p. 209-26.
420. Amouzegar, A. and S.K. Chauhan, *Effector and Regulatory T Cell Trafficking in Corneal Allograft Rejection.* Mediators Inflamm, 2017. **2017**: p. 8670280.
421. Boisgerault, F., et al., *Role of CD4+ and CD8+ T cells in allorecognition: lessons from corneal transplantation.* J Immunol, 2001. **167**(4): p. 1891-9.
422. Joo, C.K., J.S. Pepose, and P.M. Stuart, *T-cell mediated responses in a murine model of orthotopic corneal transplantation.* Invest Ophthalmol Vis Sci, 1995. **36**(8): p. 1530-40.
423. Benichou, G., et al., *Role of Memory T Cells in Allograft Rejection and Tolerance.* Front Immunol, 2017. **8**: p. 170.
424. Zeng, Y.Q., C. Lu, and Z. Dai, *Editorial: Memory T Cells: Effectors, Regulators, and Implications for Transplant Tolerance.* Front Immunol, 2016. **7**: p. 7.
425. Askar, M., *T helper subsets & regulatory T cells: rethinking the paradigm in the clinical context of solid organ transplantation.* Int J Immunogenet, 2014. **41**(3): p. 185-94.
426. Liu, Z., H. Fan, and S. Jiang, *CD4+ T-cell subsets in transplantation.* Immunological Reviews, 2013. **252**(1): p. 183-191.
427. Amouzegar, A., S.K. Chauhan, and R. Dana, *Alloimmunity and Tolerance in Corneal Transplantation.* J Immunol, 2016. **196**(10): p. 3983-91.
428. Hamrah, P., et al., *Alterations in corneal stromal dendritic cell phenotype and distribution in inflammation.* Arch Ophthalmol, 2003. **121**(8): p. 1132-40.
429. Levin LA, A.D., *Ocular Disease: Mechanisms and Management.* Saunders, 2010: p. 65–73.
430. Kaplan, M.H., *Th9 cells: differentiation and disease.* Immunol Rev, 2013. **252**(1): p. 104-15.
431. Chauhan, S.K., et al., *Autoimmunity in Dry Eye is due to Resistance of Th17 to Treg Suppression.* Journal of immunology (Baltimore, Md. : 1950), 2009. **182**(3): p. 1247-1252.
432. Yoshida, S., et al., *Anti-Type V Collagen Lymphocytes that Express IL-17 and IL-23 Induce Rejection Pathology in Fresh and Well-Healed Lung Transplants.* American Journal of Transplantation, 2006. **6**(4): p. 724-735.
433. Claerhout, I., et al., *Role of natural killer cells in the rejection process of corneal allografts in rats.* Transplantation, 2004. **77**(5): p. 676-82.
434. Schwartzkopff, J., et al., *NK cell depletion delays corneal allograft rejection in baby rats.* Mol Vis, 2010. **16**: p. 1928-35.
435. Coster, D.J., C.F. Jessup, and K.A. Williams, *Mechanisms of corneal allograft rejection and regional immunosuppression.* Eye, 2009. **23**: p. 1894.
436. Derynck, R. and R.J. Akhurst, *Differentiation plasticity regulated by TGF-beta family proteins in development and disease.* Nat Cell Biol, 2007. **9**(9): p. 1000-4.
437. Massague, J., S.W. Blain, and R.S. Lo, *TGFbeta signaling in growth control, cancer, and heritable disorders.* Cell, 2000. **103**(2): p. 295-309.
438. Zhang, Y.E., *Non-Smad pathways in TGF-β signaling.* Cell Research, 2008. **19**: p. 128.
439. Schmierer, B. and C.S. Hill, *TGFβ–SMAD signal transduction: molecular specificity and functional flexibility.* Nature Reviews Molecular Cell Biology, 2007. **8**: p. 970.

440. Meisel, R., et al., *Human bone marrow stromal cells inhibit allogeneic T-cell responses by indoleamine 2,3-dioxygenase–mediated tryptophan degradation.* Blood, 2004. **103**(12): p. 4619-4621.
441. Yagi, H., et al., *Mesenchymal Stem Cells: Mechanisms of Immunomodulation and Homing.* Cell transplantation, 2010. **19**(6): p. 667-679.
442. Kerkelä, E., *Reply: Adenosine Producing Mesenchymal Stromal Cells.* STEM CELLS, 2017. **35**(6): p. 1649-1650.
443. Dang, S., et al., *Autophagy regulates the therapeutic potential of mesenchymal stem cells in experimental autoimmune encephalomyelitis.* Autophagy, 2014. **10**(7): p. 1301-15.
444. Kudo, A., *Periostin in fibrillogenesis for tissue regeneration: periostin actions inside and outside the cell.* Cell Mol Life Sci, 2011. **68**(19): p. 3201-7.
445. Elliott, C.G., S.S. Kim, and D.W. Hamilton, *Functional significance of periostin in excisional skin repair: is the devil in the detail?* Cell Adh Migr, 2012. **6**(4): p. 319-26.
446. Blotnick, S., et al., *T lymphocytes synthesize and export heparin-binding epidermal growth factor-like growth factor and basic fibroblast growth factor, mitogens for vascular cells and fibroblasts: differential production and release by CD4+ and CD8+ T cells.* Proceedings of the National Academy of Sciences, 1994. **91**(8): p. 2890-2894.
447. Watkins, D.J., et al., *Heparin-binding EGF-Like Growth Factor Protects Mesenchymal Stem Cells.* The Journal of surgical research, 2012. **177**(2): p. 359-364.
448. Rietscher, K., et al., *Growth Retardation, Loss of Desmosomal Adhesion, and Impaired Tight Junction Function Identify a Unique Role of Plakophilin 1 In Vivo.* J Invest Dermatol, 2016. **136**(7): p. 1471-1478.
449. Rath, M., et al., *Metabolism via Arginase or Nitric Oxide Synthase: Two Competing Arginine Pathways in Macrophages.* Frontiers in Immunology, 2014. **5**: p. 532.
450. Rodriguez, P.C., A.C. Ochoa, and A.A. Al-Khami, *Arginine Metabolism in Myeloid Cells Shapes Innate and Adaptive Immunity.* Frontiers in Immunology, 2017. **8**: p. 93.
451. Rimar, D., et al., *[the Role of Semaphorin 7a in Systemic Sclerosis].* Harefuah, 2017. **156**(7): p. 418-421.
452. Xie, J. and H. Wang, *Semaphorin 7A as a potential immune regulator and promising therapeutic target in rheumatoid arthritis.* Arthritis Research & Therapy, 2017. **19**: p. 10.
453. Albright, R.A., et al., *ENPP1-Fc prevents mortality and vascular calcifications in rodent model of generalized arterial calcification of infancy.* Nat Commun, 2015. **6**: p. 10006.
454. Riese, D.J. and R.L. Cullum, *Epiregulin: Roles in Normal Physiology and Cancer.* Seminars in cell & developmental biology, 2014. **0**: p. 49-56.
455. Allard, B., et al., *The ectonucleotidases CD39 and CD73: Novel checkpoint inhibitor targets.* Immunological Reviews, 2017. **276**(1): p. 121-144.
456. Sakata, D., C. Yao, and S. Narumiya, *Prostaglandin E₂, an Immunoactivator.* Journal of Pharmacological Sciences, 2010. **112**(1): p. 1-5.
457. Singer, N.G. and A.I. Caplan, *Mesenchymal stem cells: mechanisms of inflammation.* Annu Rev Pathol, 2011. **6**: p. 457-78.
458. Kalinski, P., *Regulation of immune responses by prostaglandin E2.* J Immunol, 2012. **188**(1): p. 21-8.
459. Houlihan, D.D., et al., *Isolation of mouse mesenchymal stem cells on the basis of expression of Sca-1 and PDGFR-alpha.* Nat Protoc, 2012. **7**(12): p. 2103-11.
460. Li, Y., et al., *Flk-1(+)Sca-1(-) mesenchymal stem cells: functional characteristics in vitro and regenerative capacity in vivo.* Int J Clin Exp Pathol, 2015. **8**(9): p. 9875-88.
461. Cortes, J.R., et al., *Maintenance of immune tolerance by Foxp3+ regulatory T cells requires CD69 expression.* J Autoimmun, 2014. **55**: p. 51-62.

462. Josefowicz, S.Z., L.F. Lu, and A.Y. Rudensky, *Regulatory T cells: mechanisms of differentiation and function.* Annu Rev Immunol, 2012. **30**: p. 531-64.
463. Domogalla, M.P., et al., *Tolerance through Education: How Tolerogenic Dendritic Cells Shape Immunity.* Front Immunol, 2017. **8**: p. 1764.
464. Lemoine, S., et al., *Human T cells induce their own regulation through activation of B cells.* J Autoimmun, 2011. **36**(3-4): p. 228-38.
465. Wang, R.X., et al., *Interleukin-35 induces regulatory B cells that suppress autoimmune disease.* Nat Med, 2014. **20**(6): p. 633-41.
466. Li, S., et al., *A naturally occurring CD8+CD122+ T-cell subset as a memory-like Treg family.* Cellular And Molecular Immunology, 2014. **11**: p. 326.
467. Lu, L.F., et al., *Mast cells are essential intermediaries in regulatory T-cell tolerance.* Nature, 2006. **442**(7106): p. 997-1002.
468. Chang, H.C., et al., *The transcription factor PU.1 is required for the development of IL-9-producing T cells and allergic inflammation.* Nat Immunol, 2010. **11**(6): p. 527-34.
469. Goswami, R., et al., *STAT6-dependent regulation of Th9 development.* J Immunol, 2012. **188**(3): p. 968-75.
470. Yin, X.T., et al., *Anti-IL-17 therapy restricts and reverses late-term corneal allorejection.* J Immunol, 2015. **194**(8): p. 4029-38.
471. Duffy, M.M., et al., *Mesenchymal stem cell inhibition of T-helper 17 cell-differentiation is triggered by cell-cell contact and mediated by prostaglandin E2 via the EP4 receptor.* Eur J Immunol, 2011. **41**(10): p. 2840-51.
472. Zhang, Y.E., *Non-Smad pathways in TGF-β signaling.* Cell research, 2009. **19**(1): p. 128-139.
473. Derynck, R. and Y.E. Zhang, *Smad-dependent and Smad-independent pathways in TGF-beta family signalling.* Nature, 2003. **425**(6958): p. 577-84.
474. Fang, L., et al., *TGF-beta1 induces COX-2 expression and PGE2 production in human granulosa cells through Smad signaling pathways.* J Clin Endocrinol Metab, 2014. **99**(7): p. E1217-26.
475. Rodriguez-Barbero, A., et al., *TGF-beta1 induces COX-2 expression and PGE2 synthesis through MAPK and PI3K pathways in human mesangial cells.* Kidney Int, 2006. **70**(5): p. 901-9.
476. van Poll, D., et al., *Mesenchymal stem cell-derived molecules directly modulate hepatocellular death and regeneration in vitro and in vivo.* Hepatology, 2008. **47**(5): p. 1634-43.
477. Krampera, M., *Mesenchymal stromal cell 'licensing': a multistep process.* Leukemia, 2011. **25**(9): p. 1408-14.
478. Zanjani, E.D., et al., *Homing of human cells in the fetal sheep model: modulation by antibodies activating or inhibiting very late activation antigen-4-dependent function.* Blood, 1999. **94**(7): p. 2515-22.
479. Chen, X., et al., *CD73 Pathway Contributes to the Immunosuppressive Ability of Mesenchymal Stem Cells in Intraocular Autoimmune Responses.* Stem Cells Dev, 2016. **25**(4): p. 337-46.
480. Klebe, S., D.J. Coster, and K.A. Williams, *Rejection and acceptance of corneal allografts.* Curr Opin Organ Transplant, 2009. **14**(1): p. 4-9.
481. Kelly, T.L., D.J. Coster, and K.A. Williams, *Repeat penetrating corneal transplantation in patients with keratoconus.* Ophthalmology, 2011. **118**(8): p. 1538-42.
482. Sinha, R., et al., *Efficacy of topical cyclosporine A 2% in prevention of graft rejection in high-risk keratoplasty: a randomized controlled trial.* Graefes Arch Clin Exp Ophthalmol, 2010. **248**(8): p. 1167-72.

483. Chatel, M.A. and D.F. Larkin, *Sirolimus and mycophenolate as combination prophylaxis in corneal transplant recipients at high rejection risk.* Am J Ophthalmol, 2010. **150**(2): p. 179-84.
484. Cabral, J., et al., *Distinctive Surface Glycosylation Patterns Associated With Mouse and Human CD4(+) Regulatory T Cells and Their Suppressive Function.* Front Immunol, 2017. **8**: p. 987.
485. Li, C.W., et al., *Eradication of Triple-Negative Breast Cancer Cells by Targeting Glycosylated PD-L1.* Cancer Cell, 2018. **33**(2): p. 187-201 e10.
486. Caplan, A.I., *Mesenchymal stem cells.* J Orthop Res, 1991. **9**(5): p. 641-50.
487. Lazarus, H.M., et al., *Ex vivo expansion and subsequent infusion of human bone marrow-derived stromal progenitor cells (mesenchymal progenitor cells): implications for therapeutic use.* Bone Marrow Transplant, 1995. **16**(4): p. 557-64.
488. Fung, M., et al., *Responsible Translation of Stem Cell Research: An Assessment of Clinical Trial Registration and Publications.* Stem Cell Reports, 2017. **8**(5): p. 1190-1201.
489. Galipeau, J. and L. Sensebe, *Mesenchymal Stromal Cells: Clinical Challenges and Therapeutic Opportunities.* Cell Stem Cell, 2018. **22**(6): p. 824-833.
490. Chinnadurai, R., et al., *Cryopreserved Mesenchymal Stromal Cells Are Susceptible to T-Cell Mediated Apoptosis Which Is Partly Rescued by IFNgamma Licensing.* Stem Cells, 2016. **34**(9): p. 2429-42.
491. Schu, S., et al., *Immunogenicity of allogeneic mesenchymal stem cells.* J Cell Mol Med, 2012. **16**(9): p. 2094-103.
492. Rafei, M., et al., *Allogeneic mesenchymal stem cells for treatment of experimental autoimmune encephalomyelitis.* Mol Ther, 2009. **17**(10): p. 1799-803.
493. Cho, P.S., et al., *Immunogenicity of umbilical cord tissue derived cells.* Blood, 2008. **111**.
494. Romieu-Mourez, R., et al., *Regulation of MHC class II expression and antigen processing in murine and human mesenchymal stromal cells by IFN-gamma, TGF-beta, and cell density.* J Immunol, 2007. **179**(3): p. 1549-58.
495. Stagg, J., et al., *Interferon-gamma-stimulated marrow stromal cells: a new type of nonhematopoietic antigen-presenting cell.* Blood, 2006. **107**(6): p. 2570-7.
496. Chan, J.L., et al., *Antigen-presenting property of mesenchymal stem cells occurs during a narrow window at low levels of interferon-gamma.* Blood, 2006. **107**(12): p. 4817-24.
497. Chen, H., et al., *Pre-activation of mesenchymal stem cells with TNF-alpha, IL-1beta and nitric oxide enhances its paracrine effects on radiation-induced intestinal injury.* Sci Rep, 2015. **5**: p. 8718.
498. Broekman, W., et al., *TNF-α and IL-1β-activated human mesenchymal stromal cells increase airway epithelial wound healing in vitro via activation of the epidermal growth factor receptor.* Respiratory Research, 2016. **17**(1): p. 3.
499. Krampera, M., et al., *Immunological characterization of multipotent mesenchymal stromal cells--The International Society for Cellular Therapy (ISCT) working proposal.* Cytotherapy, 2013. **15**(9): p. 1054-61.
500. Fan, H., et al., *Pre-treatment with IL-1beta enhances the efficacy of MSC transplantation in DSS-induced colitis.* Cell Mol Immunol, 2012. **9**(6): p. 473-81.
501. Tran, D.Q., et al., *GARP (LRRC32) is essential for the surface expression of latent TGF-beta on platelets and activated FOXP3+ regulatory T cells.* Proc Natl Acad Sci U S A, 2009. **106**(32): p. 13445-50.
502. Niu, J., et al., *Mesenchymal stem cells inhibit T cell activation by releasing TGF-beta1 from TGF-beta1/GARP complex.* Oncotarget, 2017. **8**(59): p. 99784-99800.

503. Stamler, J.S., D.J. Singel, and J. Loscalzo, *Biochemistry of nitric oxide and its redox-activated forms.* Science, 1992. **258**(5090): p. 1898-902.
504. Spaggiari, G.M., et al., *MSCs inhibit monocyte-derived DC maturation and function by selectively interfering with the generation of immature DCs: central role of MSC-derived prostaglandin E2.* Blood, 2009. **113**(26): p. 6576-83.
505. O'Callaghan, G. and A. Houston, *Prostaglandin E2 and the EP receptors in malignancy: possible therapeutic targets?* Br J Pharmacol, 2015. **172**(22): p. 5239-50.
506. Narumiya, S., Y. Sugimoto, and F. Ushikubi, *Prostanoid receptors: structures, properties, and functions.* Physiol Rev, 1999. **79**(4): p. 1193-226.
507. Martinet, L., et al., *PGE2 inhibits natural killer and gamma delta T cell cytotoxicity triggered by NKR and TCR through a cAMP-mediated PKA type I-dependent signaling.* Biochem Pharmacol, 2010. **80**(6): p. 838-45.
508. Sharma, S., et al., *Tumor cyclooxygenase-2/prostaglandin E2-dependent promotion of FOXP3 expression and CD4+ CD25+ T regulatory cell activities in lung cancer.* Cancer Res, 2005. **65**(12): p. 5211-20.
509. Assis, A.C., et al., *Time-dependent migration of systemically delivered bone marrow mesenchymal stem cells to the infarcted heart.* Cell Transplant, 2010. **19**(2): p. 219-30.
510. Jin, S.Z., et al., *Ex vivo-expanded bone marrow stem cells home to the liver and ameliorate functional recovery in a mouse model of acute hepatic injury.* Hepatobiliary Pancreat Dis Int, 2012. **11**(1): p. 66-73.
511. Kraitchman, D.L., et al., *Dynamic imaging of allogeneic mesenchymal stem cells trafficking to myocardial infarction.* Circulation, 2005. **112**(10): p. 1451-61.
512. Devine, S.M., et al., *Mesenchymal stem cells distribute to a wide range of tissues following systemic infusion into nonhuman primates.* Blood, 2003. **101**(8): p. 2999-3001.
513. Melief, S.M., et al., *Multipotent stromal cells induce human regulatory T cells through a novel pathway involving skewing of monocytes toward anti-inflammatory macrophages.* Stem Cells, 2013. **31**(9): p. 1980-91.
514. Gore, A.V., et al., *Mesenchymal stem cells increase T-regulatory cells and improve healing following trauma and hemorrhagic shock.* J Trauma Acute Care Surg, 2015. **79**(1): p. 48-52; discussion 52.
515. Gore, A.V., et al., *Mesenchymal stem cells enhance lung recovery after injury, shock, and chronic stress.* Surgery, 2016. **159**(5): p. 1430-5.
516. Ko, J.H., et al., *Mesenchymal stem/stromal cells precondition lung monocytes/macrophages to produce tolerance against allo- and autoimmunity in the eye.* Proc Natl Acad Sci U S A, 2016. **113**(1): p. 158-63.
517. Akiyama, K., et al., *Mesenchymal-stem-cell-induced immunoregulation involves FAS-ligand-/FAS-mediated T cell apoptosis.* Cell Stem Cell, 2012. **10**(5): p. 544-55.
518. Ge, W., et al., *Infusion of mesenchymal stem cells and rapamycin synergize to attenuate alloimmune responses and promote cardiac allograft tolerance.* Am J Transplant, 2009. **9**(8): p. 1760-72.
519. Taylor, A.W. and H.J. Kaplan, *Ocular immune privilege in the year 2010: ocular immune privilege and uveitis.* Ocul Immunol Inflamm, 2010. **18**(6): p. 488-92.
520. Niederkorn, J.Y. and J. Mellon, *Anterior chamber-associated immune deviation promotes corneal allograft survival.* Invest Ophthalmol Vis Sci, 1996. **37**(13): p. 2700-7.
521. Sano, Y., S. Okamoto, and J.W. Streilein, *Induction of donor-specific ACAID can prolong orthotopic corneal allograft survival in "high-risk" eyes.* Curr Eye Res, 1997. **16**(11): p. 1171-4.

522. Schmuck, E.G., et al., *Biodistribution and Clearance of Human Mesenchymal Stem Cells by Quantitative Three-Dimensional Cryo-Imaging After Intravenous Infusion in a Rat Lung Injury Model.* Stem Cells Transl Med, 2016. **5**(12): p. 1668-1675.
523. Gargesha, M., et al., *3D biodistribution of pre-treated MSC in mouse model of liver disease using CryoViz™.* The Journal of Immunology, 2016. **196**(1 Supplement): p. 56.2-56.2.